

UNIVERSITY OF OKLAHOMA
GRADUATE COLLEGE

DEVELOPMENT OF A WEB-BASED INFRASTRUCTURE MANAGEMENT
SYSTEM FOR OKLAHOMA'S GENERAL AVIATION AIRPORTS AND
EXPLORING THE USE OF SPECTRAL ANALYSIS OF SURFACE WAVES AND
IMPULSE RESPONSE FOR PAVEMENT HEALTH MONITORING

A DISSERTATION
SUBMITTED TO THE GRADUATE FACULTY
in partial fulfillment of the requirements for the
degree of
Doctor of Philosophy

By

VIVEK KHANNA
Norman, Oklahoma
2007

UMI Number: 3261108



UMI Microform 3261108

Copyright 2007 by ProQuest Information and Learning Company.
All rights reserved. This microform edition is protected against
unauthorized copying under Title 17, United States Code.

ProQuest Information and Learning Company
300 North Zeeb Road
P.O. Box 1346
Ann Arbor, MI 48106-1346

DEVELOPMENT OF A WEB-BASED INFRASTRUCTURE MANAGEMENT
SYSTEM FOR OKLAHOMA'S GENERAL AVIATION AIRPORTS AND
EXPLORING THE USE OF SPECTRAL ANALYSIS OF SURFACE WAVES AND
IMPULSE RESPONSE FOR PAVEMENT HEALTH MONITORING

A DISSERTATION APPROVED FOR THE
SCHOOL OF CIVIL ENGINEERING AND ENVIRONMENTAL SCIENCE

BY



Dr. Gerald Miller, Committee Co-Chair

 4/30/07

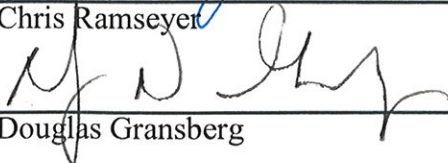
Dr. Michael Mooney, Committee Co-Chair



Dr. K. K. Muraleetharan

 5-5-07

Dr. Chris Ramseyer

 5-4-07

Dr. Douglas Gransberg

DEDICATION

To my dear late father, and my mother and to my dear wife Anuradha who inspired and helped throughout – I could not have completed this without her love, patience and understanding. Honey, I'll take the kids to Soccer practice now!!

Everlasting Quotes from Mahatma Gandhi

- A man is but the product of his thoughts. What he thinks, he becomes.
- First they ignore you, then they laugh at you, then they fight you, then you win.
- There is more to life than simply increasing its speed.
- Live as if you were to die tomorrow. Learn as if you were to live forever.

ACKNOWLEDGEMENTS

I would first like to thank Dr. Michael A. Mooney for giving me a chance to work and lead the Airport Pavement Management Team. I thank him for his leadership, support, and guidance through the initial phase of the project and later in helping me formulate the focus of my dissertation. I have enjoyed working with Dr. Mooney and wish him well in all his endeavors.

I would also like to acknowledge Dr. Gerald A. Miller for his support and guidance to me during the course of this research. Dr. Miller's words of advice in all matters have stood me in good stead.

I would also like to thank the Oklahoma Aeronautics Commission and Dale Williams for actively supporting the Airport Pavement Management Program. Dale's tireless efforts kept the team focused and moving in the right direction. He also provided valuable feedback to the developments undertaken in this research. I respect his engineering ability and professionalism.

I would also like to thank all the students that worked on this project and contributed to making it a model for other states to copy. Noteworthy are Timothy Parsons, Frank Yuan and Charbel Khoury. I am especially grateful to Charbel for his invaluable assistance in leading the project since the summer of 2003. I would also like to acknowledge the hard work of Mike Schmitz in keeping our equipment working.

I thank my late father for his love and teaching. I thank my mother for all her love and support to me in her difficult times. I also thank my wife, Anuradha, for her kind, loving support through this long period. I also thank my children – Dhruv and Prachi, for letting me postpone fun and vacations so that they could call me 'Doctor Dad'.

TABLE OF CONTENTS

ACKNOWLEDGEMENTS.....	iv
TABLE OF CONTENTS.....	v
LIST OF TABLES.....	vii
LIST OF FIGURES.....	viii
ABSTRACT.....	xi
Chapter 1 Introduction to Pavement Management.....	1
1.1 Introduction.....	1
1.1.1 Historical view of PMS development.....	3
1.1.2 Conventional pavement condition assessment.....	6
1.2 Objectives of the current research.....	7
1.3 Overview of conventional and proposed pavement management.....	8
1.3.1 PCI method.....	8
1.4 Dissertation Organization.....	12
1.5 References.....	13
Chapter 2 A Web-Based Pavement Infrastructure Management System.....	19
2.1 Introduction.....	19
2.2 Motivation.....	20
2.3 System Overview and Functionality.....	23
2.3.1 Airport Development Worksheets (ADW).....	24
2.3.2 Online Airport Guide.....	26
2.3.3 Construction Grants Management.....	27
2.3.4 Grant History.....	27
2.3.5 Airport Contact Database.....	28
2.3.6 Network Inventory.....	28
2.4 Pavement Condition Evaluation and Performance Prediction.....	30
2.5 Project and Network Level Planning.....	33
2.6 Benefits of Web-Based IMS.....	34
2.7 Summary and Concluding Remarks.....	38
2.8 References.....	39
Chapter 3 Efficacy of SASW in profiling pavement layers.....	54
3.1 Introduction.....	54
3.2 Objectives of study.....	54
3.3 SASW Background.....	55
3.4 Results.....	60
3.4.1 Comparison of SASW modulus variation with DPI variation and boring logs.....	61
3.4.2 Efficacy of AC surface layer thickness determination.....	65
3.4.3 Efficacy of PCC surface layer thickness determination.....	66
3.5 Conclusions.....	67
3.6 References.....	69
Chapter 4 Exploring AC and PCC Modulus Degradation via SASW for use in Airfield Pavement Management.....	82
4.1 Introduction.....	82
4.2 Summary of Data Collected.....	83
4.3 Modulus Degradation.....	85
4.3.1 Asphalt Pavements.....	90

4.3.2 Portland Cement Concrete Pavements.....	95
4.3.3 Relationship between Modulus Degradation and PCI Degradation	98
4.4 Service life of a GA airport pavement	102
4.5 Conclusions.....	106
4.6 References.....	108
Chapter 5 Use of Impulse Response Testing for Pavement Management.....	134
5.1 Introduction.....	134
5.2 History of the IR Method.....	135
5.3 Overview of the IR Method	138
5.3.1 Data Collection Program.....	140
5.4 Pavement Performance Modeling Approach	142
5.4.1 Asphalt Concrete Pavement Performance Models	147
5.4.2 Portland Cement Concrete Pavement Prediction Models.....	150
5.5 Comparison of IR Stiffness with SASW estimated Modulus.....	152
5.6 Comparison with PCI.....	153
5.7 End of Pavement serviceable life – a comparison between IR Stiffness based models with SASW & PCI based models.....	156
5.8 Conclusions.....	157
5.9 References.....	160
Chapter 6 Conclusions and Recommendations for Future Research.....	180
APPENDIX 1: Sample Calculation of IR Stiffness.....	186
APPENDIX 2: Coefficient of determination of PCI based pavement performance Models	191

LIST OF TABLES

Table 1-1: List of visual distresses in asphalt pavements	16
Table 1-2: List of distresses in concrete pavements	16
Table 2-1: Summary of Network Inventory Data Stored in IMS	42
Table 3-1: Comparison of SASW estimated AC pavement surface layer thickness with core thickness.....	71
Table 3-2: Comparison of SASW estimated PCC pavement surface layer thickness with core thickness.....	71
Table 4-1: Core sizes of AC pavement sections	110
Table 4-2: Core sizes of PCC pavement sections	110
Table 4-3: Guidance for interpretation of r^2	110
Table 4-4: AC pavement family groupings and goodness of regression.....	111
Table 4-5: Significance rank determination of AC regression analysis	112
Table 4-6: PCC pavement family groupings and goodness of regression.....	113
Table 4-7: Significance rank determination of PCC regression analysis	113
Table 4-8: Remaining life Analysis using SASW data with KENPAVE pavement design computer program for AC pavements.....	114
Table 4-9: Remaining life Analysis using SASW data with KENPAVE pavement design computer program for PCC pavements.....	116
Table 4-10: Comparison of Modulus and PCI degradation.....	116
Table 5-1: Core sizes of AC pavement sections	162
Table 5-2: Core sizes of PCC pavement sections	162
Table 5-3: Year-wise number of IR tests performed	162
Table 5-4 PCI based Pavement Performance Models developed by Yuan et al. (2003)	163
Table 5-5: Statistical Results for Family groupings of AC pavements	163
Table 5-6: Statistical Results for Family groupings of PCC pavements	164
Table 5-7: Model selection procedure for family AC (1,1).....	164
Table 5-8: Comparison of efficacy of various grouping techniques for AC pavements	165
Table 5-9: Comparison of efficacy of various grouping techniques for PCC pavements	165
Table 5-10: Length of service life from PCI based models	166
Table 5-11: Predicted and remaining IR stiffness in AC Pavements.....	166
Table 5-12: Predicted and remaining IR stiffness in PCC Pavements.....	166

LIST OF FIGURES

Figure 1-1: Pavement condition decay through the life-cycle of a section (Adapted from Shahin, M.Y., 1994).....	17
Figure 1-2: Pavement sections at Holdenville Municipal Airport.....	18
Figure 2-1: Client-Server architecture of Web-Based IMS.....	43
Figure 2-2: ADW of ADA Municipal with deficiencies noted by Airport Safety Inspector on 09/12/05.....	44
Figure 2-3: Online airport guide page.....	45
Figure 2-4: Construction project information display.....	46
Figure 2-5: Airport grant history for David J. Perry airport.....	47
Figure 2-6: Results of search for contact details using “Oklahoma City” as search string.....	47
Figure 2-7: Network of Oklahoma GA airports.....	48
Figure 2-8: Project-level data options and aerial photograph (Enid Woodring Regional airport).....	48
Figure 2-9: Geotechnical and structural data (Enid Woodring Regional airport).....	49
Figure 2-10: Visual distress and pavement condition index data (Frederick Municipal airport).....	50
Figure 2-11: Hewlett Packard’s tablet PC tc1100 used for real-time pavement condition entry.....	51
Figure 2-12: Pavement condition prediction for Ardmore Downtown Executive airport.....	52
Figure 2-13: Sample network snapshot and future pavement condition forecast.....	53
Figure 3-1: SASW Test Setup.....	72
Figure 3-2: Variation of frequency adjustment factor with temperature for asphalt concrete per Aouad, (24).....	72
Figure 3-3: Results of tests carried out at Thomas Municipal.....	73
Figure 3-4: Results of tests carried out at Mangum’s Scott Field.....	74
Figure 3-5: Results of tests performed at Chandler Municipal.....	75
Figure 3-6: Results of testing at Chickasha Municipal.....	76
Figure 3-7: Results of tests performed at Halliburton Field.....	77
Figure 3-8 Efficacy of AC pavement surface layer thickness determination from SASW testing.....	78
Figure 3-9: Variation of % error in determination of AC pavement thickness using SASW method.....	79
Figure 3-10: Efficacy of PCC pavement surface layer thickness determination from SASW testing.....	80
Figure 3-11: Variation of %error in thickness determination.....	81
Figure 4-1(a): Distribution of AC Core thickness in Oklahoma’s General Aviation airports.....	117
Figure 4-1(b): Distribution of PCC Core thickness in Oklahoma’s General Aviation airports.....	117
Figure 4-2: AC E_{SEIS} as a function of age for family AC(1,1).....	118
Figure 4-3: AC E_{SEIS} decay with age for Family AC(2,1).....	118
Figure 4-4: AC E_{SEIS} deterioration with age for family AC(2,2).....	119
Figure 4-5 AC E_{SEIS} decay with age for family AC(2,5).....	119

Figure 4-6: AC E_{SEIS} degradation with time for family AC(3,1).....	120
Figure 4-7: AC E_{SEIS} deterioration with age for family AC(3,2).....	120
Figure 4-8: AC E_{SEIS} deterioration for family AC(4,2)	121
Figure 4-9: AC E_{SEIS} variation with age for family AC(4,3).....	121
Figure 4-10: AC E_{SEIS} decay with age for family AC(4,4).....	122
Figure 4-11: PCC pavement layer moduli as a function of age for family PCC(1,1).....	122
Figure 4-12: PCC E_{SEIS} deterioration with age for family PCC(2,1).....	123
Figure 4-13: PCC E_{SEIS} decrease with age for family PCC(3,1)	123
Figure 4-14: PCC E_{SEIS} deterioration with age for family PCC(3,2).....	124
Figure 4-15: PCC E_{SEIS} deterioration for family PCC(4,1)	124
Figure 4-16: Comparison of PCI and E_{SEIS} regression for all tested AC pavements.....	125
Figure 4-17: Comparison of PCI and E_{SEIS} degradation for family AC(2,1).....	125
Figure 4-18: Comparison of PCI and E_{SEIS} degradation for family AC(2,2).....	126
Figure 4-19: Comparison of PCI and E_{SEIS} degradation for family AC(2,5).....	126
Figure 4-20: Comparison of PCI and E_{SEIS} degradation for family AC(3,1).....	127
Figure 4-21: Comparison of PCI and E_{SEIS} degradation for family AC(3,2).....	127
Figure 4-22: Comparison of PCI and E_{SEIS} degradation for family AC(4,2).....	128
Figure 4-23: Comparison of PCI and E_{SEIS} degradation for family AC(4,3).....	128
Figure 4-24: Comparison of PCI and E_{SEIS} degradation for family AC(4,4).....	129
Figure 4-25: Comparison of PCI and E_{SEIS} degradation for family PCC(1,1).....	129
Figure 4-26: Comparison of PCI and E_{SEIS} degradation for family PCC(2,1).....	130
Figure 4-27: Comparison of PCI and E_{SEIS} degradation for family PCC(3,1).....	130
Figure 4-28: Comparison of PCI and E_{SEIS} degradation for family PCC(3,2).....	131
Figure 4-29: Comparison of PCI and E_{SEIS} degradation for family PCC(4,1).....	131
Figure 4-30: Variation of E_{SEIS} of pavement sections with PCI for AC pavements.....	132
Figure 4-31: Variation of E_{SEIS} in AC pavements with PCI calculated based on structural distresses alone.....	132
Figure 4-32: Variation of E_{SEIS} of pavement sections with PCI for PCC pavements.....	133
Figure 4-33: Variation of E_{SEIS} in PCC pavements with PCI calculated from Structural distresses alone.....	133
Figure 5-1: Field setup of the Impulse Response test.....	167
Figure 5-2: Time histories for Hammer and Geophone acquired during an IR test	167
Figure 5-3: Velocity and force spectra of acquired signals	168
Figure 5-4: Sample mobility response function from acquired signals	168
Figure 5-5: Calculation of the dynamic stiffness (slope between points A and B)	169
Figure 5-6: Sub-division of Miami Municipal Airport's pavements into branches and sections for Visual Distress Survey	169
Figure 5-7: Decay of k_d with time for family AC(1,1)	170
Figure 5-8: Decay of k_d with time for family AC(2,1)	170
Figure 5-9: k_d degradation for family AC(2,2)	171
Figure 5-10: k_d degradation with pavement age for family AC(2,3).....	171
Figure 5-11: Decay of k_d with pavement age for family AC(2,4)	172
Figure 5-12: Deterioration of k_d with time for family AC(2,5)	172
Figure 5-13: Decay of k_d with time for family AC(2,6)	173
Figure 5-14: Degradation of k_d with pavement age for family AC(2,7).....	173
Figure 5-15: Stiffness decay with pavement age for family AC(3,1).....	174

Figure 5-16: Stiffness decay with time for family AC(3,2).....	174
Figure 5-17: Degradation of k_d with pavement age for family PCC(1,1).....	175
Figure 5-18: Decay of k_d with time observed in pavements grouped in family PCC(2,1)	175
Figure 5-19: Deterioration of k_d with time observed in pavements grouped in family PCC(2,2)	176
Figure 5-20: Decay of k_d with pavement age for family PCC(2,3)	176
Figure 5-21: Variation of k_d with E_{SEIS} for PCC pavements.....	177
Figure 5-22: Variation of k_d with E_{SEIS} for family AC(3,1) pavements	177
Figure 5-23: Variation of k_d with E_{SEIS} for family AC(3,2) pavements	178
Figure 5-24: Variation of k_d with E_{SEIS} for family PCC(1,1) pavements	178
Figure 5-25: Plot of k_d of pavement section with its PCI for AC pavements.....	179
Figure 5-26: Variation of k_d of PCC pavements with PCI.....	179

ABSTRACT

The transportation infrastructure of the United States consumes over 17% of its Gross National product annually and is currently valued at \$1.75 trillion. With the interstate system now 50 years old, the emphasis of the transportation community has shifted from building new assets to maintaining and improving existing assets. Total Expenditures on highways and bridges remain at record levels - \$147.5 billion in 2004.

FHWA advocates the use of transportation asset management rationale in addressing pavement needs and improving customer satisfaction. Transportation asset management is not merely a Pavement Management (PMS) software, it is a decision making process that helps network administrators efficiently allocate limited resources for maximum benefit. The Oklahoma Aeronautics Commission (OAC) felt the need for such a system to efficiently allocate scarce resources at Oklahoma's General Aviation airports.

OAC teamed up with the University of Oklahoma's school of civil engineering and environmental science (CEES); the effort resulted in a web-based infrastructure management system (IMS). A far-cry from the previous "squeaky wheel" system, OAC's web-based IMS presents a vast storehouse of information – visual distresses, PCI ratings, results of nondestructive tests, geotechnical information, to stakeholders .

CEES also felt the need to advance the existing PCI based PMS in use at the time. Accordingly, the Spectral Analysis of Surface Waves (SASW) method and the Impulse Response (IR) method were identified as potential tools for pavement health monitoring. The efficacy of these non-destructive test methods was rigorously investigated. SASW was found to be a potentially valuable tool to characterize pavement sections without

core extractions. Low strain moduli for pavements with asphalt and portland cement concrete surfaces estimated from SASW tests were observed to degrade with time and regression models for this deterioration were prepared and are presented. The ease of testing with the IR method and quick data analysis presents an opportunity for greater spatial coverage of pavements thereby providing a complete picture of the tested site to engineers. It was observed that the pavement section's dynamic stiffness estimated from IR tests degrades with age and regression models capturing this deterioration were prepared.

Chapter 1 Introduction to Pavement Management

1.1 Introduction

The highway infrastructure of the United States consumes 17 percent of its Gross National Product (FHWA, 2006) and has been created over the years at a tremendous cost. Forster (2004) and the Federal Highways Administration (FHWA, 2007) estimate the value of this national transportation infrastructure at \$1.75 trillion. The interstate highway system is now more than five decades old. With this aging, the emphasis of the transportation community has shifted from building new infrastructure assets to maintaining and improving the existing assets. FHWA's online resource center (2007) claims that the total annual capital outlay to preserve and improve the highway system is more than \$139 billion.

There has been a nearly 45% increase in total annual expenditures on highways by Federal, State, and local governments from 1997 to 2004 (FHWA, 2006). In 2004 the total expenditures including funds expended for debt retirement, administration, highway patrol, physical maintenance, and capital expenditures amounted to \$147.5 billion. Capital expenditures alone on highways rose 45.2%, from \$48.4 billion in 1997 to \$70.3 billion in 2004 (FHWA, 2006). Resurfacing, rehabilitation, or reconstruction of existing highways and bridges, consumed 51.8% of the total capital budget in 2004. The net effect of the increase in capital investment and the changed focus of improvement efforts has resulted in a 58% increase in spending on highway and bridge rehabilitation (\$23.0 billion in 1997 to \$36.4 billion in 2004). Investment in construction of new roads and bridges and the widening of existing roads attracted lower funding during this period, rising only 28% from \$21.5 billion in 1997 to \$27.5 billion in 2004 (FHWA, 2006).

Vast sums of money are therefore spent every year towards the maintenance, rehabilitation (MR) and enhancement of this transportation infrastructure that is vital to the economic health of the nation. Despite the healthy increases in governmental spending on highways, the resources deployed to maintain conditions and performance has increased only marginally in current dollars and has actually declined in terms of real dollars. Added to this, escalating global energy prices are fueling large increases in construction costs. It is therefore important to develop tools to aid administrators faced with ever shrinking budgets and greater accountability, in effective utilization of resources to maximize pavement network serviceability.

Pavement management systems (PMS) provide a systems approach to pavement maintenance management. PMS's use sophisticated decision making algorithms to assist in the development of prioritized capital improvement programs (CIP) that lead to optimized pavement condition and maximize network serviceability within the imposed budgetary constraints.

The General Accounting Office (GAO, 1998) in its review of current and future levels of Airport Improvement Program (AIP) funding had this to say –

“The National Priority System, FAA’s primary method for determining which AIP grant applications from individual airports should be funded, establishes a priority rating on the basis of factors such as the purpose and type of the project. Runway rehabilitation projects fare well in this system and are typically funded ahead of most other types of projects. Most applications for such projects received funding in fiscal year 1997, according to FAA officials. However, local FAA officials said that they forward only those applications they are relatively certain will be funded. FAA’s priority system is

not well equipped to determine which proposed rehabilitation projects will deliver the best return for the dollars spent. Waiting to rehabilitate a runway until the pavement has seriously deteriorated can mean that rehabilitation will cost 2 to 3 times as much as it would have if rehabilitation had occurred earlier. The key to identifying the best time to conduct rehabilitation is having comprehensive knowledge of pavement conditions. Currently, fewer than half of the airports in the national system have information systems that will provide this knowledge. Furthermore, when allocating Airport Improvement (AIP) funds, FAA does not evaluate the cost-effectiveness of the rehabilitation projects it approves”.

In its report GAO (1998) recommended that the Federal Aviation Administration (FAA) require all airports in the national airport system (NAS) to submit index ratings on pavement condition on a regular basis and use this information to create a database on pavement conditions for evaluating the cost-effectiveness of project applications and forecasting anticipated pavement needs.

1.1.1 Historical view of PMS development

The concept of pavement management as a tool for maximizing utilization/serviceability of a network of pavements with the deployment of optimal resources dates to the 1960s. Some engineers consider the American Association of State Highway Officials (AASHO) road tests (1956 – 1960) as being the origins of the systems approach to pavement maintenance. As a result of the tests, it was postulated that pavement performance could be described independent of pavement type. In 1966, a study was initiated to arrive at an understanding of the AASHO road tests. Expanding on this study, Hudson (1968) started work on a systems approach to pavement design and

maintenance. Wilkins (1968) led Canadian efforts at developing a systems approach to pavement management. Scrivner (1968) of the Texas transportation Institute presented a systems approach to flexible pavement design.

By the late 1960s, the term “pavement management system (PMS)” had been coined and was in use to describe a systems approach to pavement design and maintenance. One of the earliest attempts to translate the systems concept into a working schema was a result of Texas Department of Transportation’s (TxDOT) Project 123 (Hudson, 1970). This study pioneered development of many of the techniques of pavement management. The National Cooperative Highway Research Program’s (NCHRP) project 1-10 (Hudson, 1973) presented a working methodology for pavement management. The US Army Construction Engineering Research Laboratories (USACERL) with funding from the FAA, American Public Works Association (APWA), Federal Highway Administration (FHWA), US Air Force Engineering and Services Center (AFESC), US Navy and US Army Corps of Engineers (USACOE) released the first version of USACERL’s PMS in 1981.

The PMS concept demonstrated the need as well as the benefit of a systems approach to not only pavement design but to the construction and periodic maintenance of pavements as well. Figure 1-1 reiterates the rationale behind pavement management. It explains that the premise of a systems approach to pavement management is that “for every dollar spent on managed pavements, agencies can save between three to six dollars in reduced pavement maintenance costs”.

The FHWA-University of Texas-HRB conference on structural design of asphalt pavement systems in 1970 made it clear that PMSs were here to stay. The American

Association of State Highway and Transportation Officials (AASHTO) issued their guidelines for pavement management systems in 1985. These guidelines contained minimal suggestions for developing and implementing a PMS. AASHTO (1990) later issued more detailed guidelines in 1990. Then in 2001, AASHTO(2001) issued comprehensive, guidelines identifying the state-of-practice in pavement management. These guidelines provide a good PMS implementation procedure and describe the typical components of a good PMS.

Zimmerman et al. (2000) summarize that PMSs are expected to form a vital part of decision making for managing and maintaining the transportation infrastructure. Pavement managers must address their transportation needs in this era of soaring construction costs and shrinking budgets while at the same time be held to ever greater scrutiny in their efficiency in the expenditure of taxpayer money. As a result, the importance of infrastructure management systems (IMS) to assist with effective allocation of these resources to manage infrastructure assets becomes more critical than ever. The systems approach has created a realization in the stakeholders that the challenge of managing and maintaining existing transportation infrastructure under today's environment is more difficult than the design and construction of the initial system, when there was less scrutiny of public expenditures.

As per Thomas (1995), infrastructure in the United States and the world is aging. Pavement engineers and transportation managers are increasingly aware of the need to assess the condition of this vital asset. However, finite budgets limit the replacement of assets. It is therefore imperative to accurately assess the condition of and damage to transportation infrastructure.

1.1.2 Conventional pavement condition assessment

It is generally accepted that the basic elements of a PMS (AASHTO 1990, Haas et al. 1994, Gendreau and Soriano 1998, Sanford-Bernhardt et al. 2003, Broten and De Sombre 2001) include – a) pavement inventory, b) pavement condition assessment, c) analysis tool to determine pavement needs, d) prioritization matrix/routine for scheduling maintenance and rehabilitation and e) assessment of the impact of funding decisions.

Estimation of pavement condition includes the determination of a) surface distress, b) ride quality or roughness, c) structural capacity and d) surface friction/skid resistance. Traditionally (Gendreau and Soriano 1998, Broten and Zimmerman 1998, Sanford-Bernhardt et al. 2003), agencies have relied upon visual distress surveys to estimate pavement condition using the principles and the procedure described in SHRP-P-338 and ASTM D-5340 to determine a Pavement Condition Index (PCI).

The PCI is a numerical index computed from visual distress surveys. The estimated PCI ranges from ‘100’ for a newly constructed pavement to ‘0’ for a failed pavement. This index was developed to provide both a measure of the structural adequacy and integrity of a pavement section as well as provide an insight into the cause of the experienced distresses in the pavement. The computed PCI of a pavement section also takes into account ride quality/serviceability issues. Therefore, it is difficult to relate a section’s PCI to the structural integrity of the section. The contribution of serviceability to the section’s PCI also makes it difficult to estimate the cause of the various distresses observed i.e. lack of structural adequacy, poor quality of construction, etc.

More and more agencies now estimate structural capacity with non-destructive deflection testing. Coring with boring to collect pavement layer samples is also used (Khanna and Mooney 2002). In the case of roads, highways and commercial service

airports, determination of surface friction is also required. The measurement of friction is normally obtained with either the ASTM locked wheel trailer or a Mu-meter, and now with the Dynamic Friction Tester (DFT). The measured roughness of a pavement is converted into an index such as the International Roughness Index (IRI).

1.2 Objectives of the current research

Oklahoma's air transportation system includes 114 publicly-owned, public-use General Aviation (GA) airports. Of these, 97 GA airports are a part of the national air transportation system (NAS) and are designated as being a part of the national plan for an integrated airport system (NPIAS). In simple terms, these 97 airports are eligible for federal funding. Also, Oklahoma is a large state, ranking 19th of the 50 states in terms of size. A need was felt for a system that would provide decision support to federal (FAA), state (OAC) and local agencies involved in managing Oklahoma's GA airports. It was felt that a web-based IMS would provide the most appropriate solution.

Also, the aviation infrastructure in Oklahoma like in most other states is aging. The average age of AC pavements in the state currently stands at 15.4 years while that of PCC pavements is 32.4 years. Though the GAO (1998) advocated the use of the PCI based PMS to manage airport pavement networks, this was not considered to be the most effective solution based on the failings discussed in the preceding section. There is no well-defined relationship between structural and functional performances (Zaniewski 1991), therefore PCI based PMS's limit the ability to evaluate structural pavement condition and to use structural performance as a project and network level parameter for analysis (Paine 1998). A need and opportunity existed to advance pavement management by adding a mechanistic dimension to PCI. With the increasing use of in-situ

nondestructive testing (NDT) methods coupled with the growth in mechanistic-empirical analysis methodologies, there is a clear need to integrate structural information into PMSs. The current study therefore explores the use of NDT tools to inspect aging aviation infrastructure without impairing its usefulness. The NDT tools explored in the current research include a) the Spectral Analysis of Surface Waves (SASW) method, and b) the Impulse Response (IR) method. The SASW method was used because it could estimate mechanistic pavement design parameters like layer thickness and layer moduli of in-service GA pavements while IR tests could evaluate their dynamic stiffness. A key objective of this study therefore was to investigate if pavement surface layer moduli and dynamic stiffness degrade with time and determine if these mechanistic parameters could be used to characterize pavement condition. If moduli and stiffness did indeed degrade, the current study would evaluate the most suited methodologies to subdivide Oklahoma's network of GA pavements into smaller units with similar modulus and stiffness deterioration.

1.3 Overview of conventional and proposed pavement management

It is important to briefly review the existing/conventional and proposed pavement management procedures.

1.3.1 PCI method

The CERL/APWA's PAVER method presents a system of network identification and definition. The first important task is to identify all pavements that contribute to the serviceability of the network. Once a network has been identified, the network is defined into smaller branches. A branch is a discrete, individual component of an airport pavement that has a distinct function. Thus, airport pavements are grouped into branches

by their function e.g. runways, taxiways and aprons. Because branches can be very large, they may not have consistent characteristics at every discrete location. For this reason, branches are further divided into smaller sections based on structural composition (i.e. thickness and materials), construction history, traffic, environmental conditions, and pavement condition. For example, Figure 1-2 presents the pavement sectioning used for Holdenville Municipal Airport. For the pavement condition survey, the section is broken into representative, randomly selected sample units. Parsons (2002) went a step than the PAVER method and defined an airport as a group of distinct branches and sections.

1.3.1.1 Network Level and Project Level approaches

Before inspection related issues are discussed, it is important to understand the difference between a system-wide or network level approach and a project-level approach that focuses on an individual airport. In network level pavement management, administrative decisions affect programs for the entire system of pavements. This management system considers the needs of the network as a whole and generates decisions for a network-wide program of new construction, maintenance, and rehabilitation. The goal is to optimize the use of funds over the entire system. In project level pavement management, technical decisions are made for specific projects. At this level detailed consideration is given to alternative design, construction, maintenance, and rehabilitation activities for specific projects. Often times, pavement engineers and planners make the mistake of thinking only in terms of individual projects rather than the network. The best or optimal recommendation at the project level may not be the optimal solution for the network.

1.3.1.2 PCI estimation

The estimation of section PCI is accomplished by visual distress surveys of randomly sampled pavement sample units in accordance with ASTM D-5340 and SHRP-P-338. As a result of the survey, the visual distress inventory for the inspected pavements is updated and is used to determine the section PCI. The section PCIs are then used to compute the weighted-average PCI for the branch using the procedure described in ASTM D5340. The branch PCIs are used to compute the weighted average airport PCI (Parsons, 2002). Tables 1-1 and 1-2 list the distresses observed in asphalt and concrete pavements that are used to determine PCI.

1.3.1.3 Pavement Condition Prediction and Maintenance Strategizing

Current and future pavement conditions have typically been based solely upon visually observed distresses in airport pavement management (Gendreau and Soriano 1998, Broten and De Sombre 2001). Future pavement functional performance is predicted by employing suitable regression analysis of PCI data. Oklahoma's web-based IMS employs the family approach developed by Shahin (1994) to classify pavements sections into pavement families based upon similarities of environmental conditions, traffic, pavement structure, pavement use, etc. The PCI and pavement age data collected for a family of similar sections creates a data set spanning PCI values from 100 to 30. The IMS analysis tool uses a polynomial constrained least-squares regression technique to develop performance prediction curves (Yuan and Mooney 2003) for all observed pavement families. This is further described in sections 4.3 and 5.4

Maintenance and rehabilitation (MR) strategies are selected using the "critical PCI procedure" proposed by Shahin and Walther (1990). The procedure was a result of several life-cycle cost analyses and from the dynamic programming network optimization

analysis. Shahin (1994) defines critical PCI as the threshold PCI value below which the rate of PCI deterioration increases significantly. The implementation of this procedure requires the analysis of the life-cycle deterioration model of all pavement sections and preparing a section priority matrix based upon distance of section PCI from its critical PCI.

1.3.1.4 Drawbacks of the PCI/PAVER approach

The PAVER method is the most widely used procedure for pavement management. The MicroPAVER software provides an effective tool for maintaining pavement condition inventory and pavement management. FHWA's (2000) study into the variability in manually collected pavement distress data observed that:

1. Inspector variability for any given distress type/severity level combination is typically large and increases as the distress quantity increases.
2. Total distress group means are generally close to the reference value, while the scatter of individual inspectors is narrower than that for individual distress severity levels. This indicates significant difference in distinguishing severity levels.
3. For closely related distress types, such as fatigue cracking and longitudinal cracking in the wheelpath, compensatory differences between group ratings and reference values were observed, i.e. group ratings indicated a higher quantity of fatigue cracking and a lower quantity of longitudinal cracking as compared to the reference values.
4. The difference between the group mean and the reference value was observed to be less than 6 to 14 PCI points at nine LTPP rater accreditation workshops. The

individual inspector variability was observed to be small when viewed through the composite PCI rating with standard deviation varying from 5 to 8 PCI points in the study.

Other limitations of PCI based PMS observed during the course of the current study include:

1. Deducts assigned to distresses were arbitrarily developed. There is thus no mechanistic rationale for the deduct value curves used in the PAVER method.
2. From a mechanistic point of view, a pavement section's PCI does not provide information about structural adequacy of the pavement section. Some visual distresses do provide insight into structural condition e.g., rutting, alligator cracking in asphalt pavements and linear cracks, and shattered slabs in PCC pavements. Visual distresses mainly provide an assessment of functional pavement performance.

1.4 Dissertation Organization

The dissertation is arranged in five chapters. Chapter one provides a brief introduction to conventional pavement management. Chapter two presents a discussion on efficacy of SASW in profiling pavement layers. Chapter three explores AC and PCC modulus degradation for use in airfield pavement management. Chapter four investigates the use of Impulse Response testing for pavement management. Chapter five presents conclusions based on the research conducted in this study.

1.5 References

- AASHTO, “*Pavement management guide*”, Washington D.C., 1985.
- AASHTO, “*Pavement management guide*”, Washington D.C., 1990.
- AASHTO, “*Pavement management guide*”, Washington D.C., 2001.
- ASTM D5340-04e1, “*Standard Test Method for Airport Pavement Condition Index Surveys*”, ASTM International.
- Broten, M., and De Sombre, R., “*The airfield pavement condition index (PCI) evaluation procedure: Advantages, common misapplications, and potential pitfalls*” Proceedings, 5th Int. Conf. on Managing Pavements, Seattle, (CD-ROM), 2001.
- Broten, M., and Zimmerman, K. “*Basics of airport pavement management.*” Proc., 4th Int. Conf. on Managing Pavements”, Durban, South Africa (CD-ROM), 1998.
- FHWA, “*Variability of pavement distress data from manual surveys*,” Report No, FHWA-RD-00-160, National Technical Information Service, 2000.
- FHWA, “*Status of the Nation's Highways, Bridges, and Transit: 2006 Conditions and Performance Report*”, <http://www.fhwa.dot.gov/policy/2006cpr/hilights.htm>, 2006.
- FHWA, “*Online resource center – Asset Management Guide*”, http://www.fhwa.dot.gov/resourcecenter/teams/finance/fin_1amg.cfm, 2007.
- Forster, J. “*Preventive maintenance: project selection and design*”, Rocky Mountain Asphalt Conference, February 2004.
- General Accounting Office, “*Keeping Nation’s Airport Pavements in Good Condition may require substantially higher Spending*”, GAO/RCED-98-226, Washington D.C., 1998.
- Gendreau, M., and Soriano, P., “*Airport pavement management systems: An appraisal of existing methodologies*”, Transportation Record A, 32(3), pp197–214, 1998.
- Haas, R. Hudson, W.R., and J. Zaniewski, “*Modern Pavement management*”, Krieger Publishing Company, Florida, 1994.
- Hudson, W. R., Finn, F. N., McCullough B.F., Nair, K. and B.A. Vallerga, “*Systems Approach to Pavement Systems Formulation, Performance Definition and Materials Characterization*”, Final Report, NCHRP Project 1-10, Materials Research and Development, Inc., March 1968.

Hudson, W. R., and B. F. McCullough, “*Systems Approach Applied to Pavement Design and Research, Research Report 123-1*”, Center for Transportation Research, The University of Texas at Austin, March 1970.

Hudson, W. R., and McCullough, B. F., “*Flexible pavement design and management, National Cooperative Highway Research Program Report*”, No. 139, 1973.

Khanna, V., and Mooney, M. A. “*Comparison of SASW backcalculated profiles with boring log and DCP data*”, Proc., 2nd Int. Conf. on Application of Geophysical and NDT Methodologies to Transportation Facilities and Infrastructure, Los Angeles, 2002.

Paine, D., “*The incorporation of structural data in a pavement management system*”, Proc., 4th Int. Conf. on Managing Pavements, Durban, South Africa (CD-ROM), 1998.

Parsons, Timothy A., “*Development of an airport pavement history information delivery system (APHIDS)*”, University of Oklahoma, Norman, Oklahoma, 2002.

Sanford-Bernhardt, K.L., Loehr, J.E. and Huaco, D., “*Asset Management Framework for Geotechnical Infrastructure*”, J. Infrastructure Systems, ASCE, 9(3), 107-116, 2003.

Scrivner, F.H., Moore, W.M., and McFarland, W.F., “*A systems approach to the flexible pavement design problem*”, Research Report 32-11, Texas transportation Institute, Texas A&M University, 1968.

Shahin, M.Y. and Walther, J.A., “*Pavement maintenance management for roads and streets using the PAVER system*”, Technical report no. M-90/05, Construction engineering research laboratory, U.S. Army, July 1990.

Shahin, M. Y., “*Pavement management for airports, roads, and parking lots*”, Kluwer Academic, Dordrecht, The Netherlands, 1994.

Strategic Highway Research Program, “*Distress identification manual for the long term pavement performance project*”, SHRP-P-338, Washington D.C., 1993.

Thomas, G., “*Overview of nondestructive technologies*”, Proceedings of the international society for optical engineering, Volume 2457, 5–9, 1995.

Wilkins, E.B., “*Outline of a Proposed Management System for the CGRA Pavement Design and Evaluation Committee*”, Proceedings Canada Good Roads Association, Ottawa, 1968.

Yuan, J., and Mooney, M. A., “*Development of adaptive performance models for Oklahoma Airfield pavement management system*” Transportation Research Record 1853, Transportation Research Board, Washington, D.C., 44–54, 2003.

Zaniewski, J., “Unified *methodology for airport pavement analysis and design*”, Vol. I, State of the Art Technical Report, Federal Aviation Administration, Research and Development Service, Washington, D.C., 1991.

Zimmerman, K.A., Botelho, F. and Clark, D., “*Taking Pavement Management into the Next Millennium, Transportation in the New Millennium: State of the Art and Future Directions*”, Perspectives from Transportation Research Board Standing Committees, Transportation Research Board, 2000.

Table 1-1: List of visual distresses in asphalt pavements

Distress	Name	Cause	Unit	Material
41	Alligator Cracking	Traffic	square feet	AC
42	Bleeding	Other	square feet	AC
43	Block Cracking	Environmental	square feet	AC
44	Corrugation	Other	square feet	AC
45	Depression	Other	square feet	AC
46	Jet Blast	Other	none	AC
47	Reflection Cracking	Environmental	feet	AC
48	L/T Cracking	Environmental	feet	AC
49	Oil Spillage	Other	square feet	AC
50	Patching	Other	square feet	AC
51	Polishing	Other	square feet	AC
53	Rutting	Traffic	square feet	AC
52	Raveling	Environmental	square feet	AC
54	Shoving	Other	square feet	AC
55	Slippage Cracking	Other	square feet	AC
56	Swelling	Other	square feet	AC

Table 1-2: List of distresses in concrete pavements

Distress	Name	cause	units	Material
61	Blowups	Environmental	slabs	PCC
62	Corner Break	Traffic	slabs	PCC
63	Linear Cracking	Traffic	slabs	PCC
64	Durability Cracking	Environmental	slabs	PCC
65	Joint Seal Damage	Environmental	slabs	PCC
66	Small Patch	Other	slabs	PCC
67	Patching	Other	slabs	PCC
68	Popouts	Other	slabs	PCC
69	Pumping	Other	slabs	PCC
70	Scaling	Other	slabs	PCC
71	Settlement	Other	slabs	PCC
72	Shattered Slab	Traffic	slabs	PCC
73	Shrinkage Cracking	Other	slabs	PCC
74	Joint Spalling	Other	slabs	PCC
75	Corner Spalling	Other	slabs	PCC

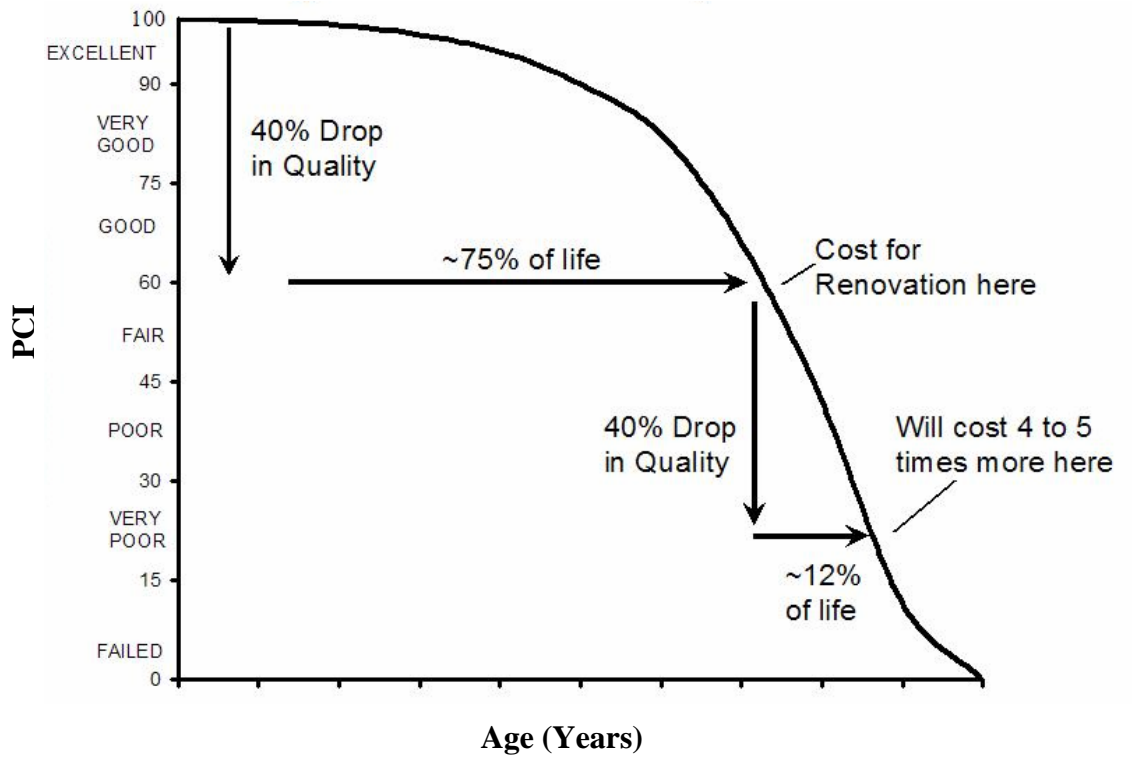


Figure 1-1: Pavement condition decay through the life-cycle of a section (Adapted from Shahin, M.Y., 1994)

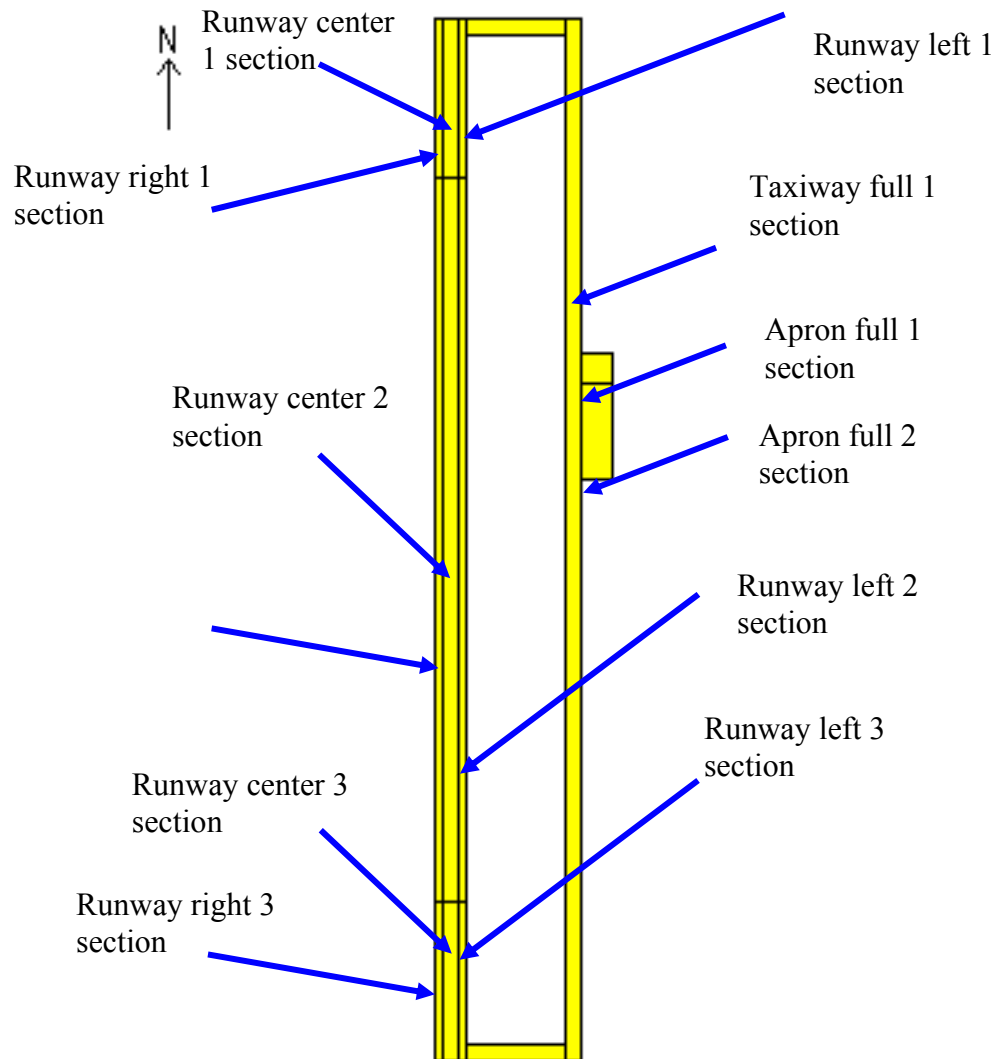


Figure 1-2: Pavement sections at Holdenville Municipal Airport

Chapter 2 A Web-Based Pavement Infrastructure Management System

2.1 Introduction

The demand for a more systems level approach to infrastructure management – engineering the interrelationships between planning, design, construction, maintenance and rehabilitation – has motivated significant advances in the development of management systems for infrastructure, e.g., pavement networks, bridge networks. These Infrastructure Management Systems (IMS) require extensive information engineering, i.e., collecting, archiving, analyzing, processing, forecasting and disseminating information. An IMS must often cater to a broad spectrum of users including engineers, managers, legislators, policy makers, and potentially the general public. The maturation of information technology has facilitated valuable growth in IMS development and deployment to a broad user base (Tsai and Lai, 2002). Ever evolving non-destructive testing methods and discrete sensing continue to improve our knowledge of the local and global integrity of infrastructure. Handheld/portable computing has enabled field data acquisition and data entry. Database and GIS software has enabled simple data entry and elegant data retrieval (Zang and Hudson, 1998), and wireless communication has made possible the remote upload and download of data and information. The rapidly evolving Internet and World Wide Web also provide a powerful platform for information engineering. With major initiatives in web-based digital libraries (NSDL, 2003) and existing prototype web-based management systems in construction, product management, transit, water resources, and national parks (Lam 2002, Liu 2001, Chapman 2003, Wu et

al. 2001) , the ubiquity and agility of the World Wide Web provides a powerful environment for IMS.

This paper describes the development of a web-based IMS, utilizing a flexible shareware open architecture platform to enable remote data entry/access, user directed querying, and information dissemination for a broad spectrum of stakeholders. The web-based system described herein was developed for a network of approximately 81 General Aviation (GA) airport pavements (runways, taxiways, aprons) in Oklahoma. The advances presented here are two fold. First, the traditional functionality of a pavement management system (Haas et al. 1994, AASHTO 2001) has been expanded to incorporate geotechnical and structural capacity data (including nondestructive testing data). Second, web-enabling each system component has provided a de-centralized IMS, promoting remote data upload and data access, and low-cost information delivery to a broad constituency of stakeholders throughout the state. The architecture is described herein together with the various data access/entry and functionality features. Finally, the realized benefits of web-based IMS to the Oklahoma aeronautic stakeholders are presented.

2.2 Motivation

Established in 1963, the Oklahoma Aeronautics Commission (OAC) is a public agency tasked with overseeing the state's aviation needs, serving 114 public-use GA airports, and allocating federal and state funding to 97 National Plan for Integrated Airport System (NPIAS) GA airports. The network of 97 NPIAS GA airports includes over 7.1×10^6 m² of runway, taxiway, and apron pavement. Like many federal, state, and local entities, the OAC must juggle the demands of shifting/growing infrastructure usage,

statewide and regional economic development, and aging infrastructure, often with significant budgetary constraints.

The OAC clearly needed an airport IMS for decision support. The IMS would need to provide not only network wide PMS functionality but also assist in decision making for allocation of resources to non-pavement projects like land acquisition, navigational and approach aids, safety issues etc. Annually, it is estimated that 2/3 of FAA's Airport Improvement Program (AIP) funds go into pavement projects hence a systems approach to managing pavements was required to maximize benefit from the limited resources. Also, an appropriate form of prioritizing the system wide significance of projects was vital to prevent projects not rated by a PMS, i.e. land acquisition, new pavement construction etc, from being overlooked for funding. Consistent with most agencies that oversee airport networks, the OAC has annually prepared a prioritized list of projects selected for funding (network level program planning)—to disperse state and federal funds to NPIAS GA airports. The network level planning approach involves a “from the bottom-up” philosophy where project-level needs are determined and then ranked according to agency decision criteria (described later). At the project level, each GA airport is required to maintain an Airport Development Worksheet (ADW) that details their 20-year plan for infrastructure maintenance, rehabilitation, reconstruction and new construction (hereafter MR). The preparation of each ADW and thus a candidate pool of projects is the responsibility of each GA airport (the OAC does not own any GA airport). Accordingly, each GA airport sponsor plays an important role in the pavement management process. Approximately $\frac{3}{4}$ of the 100 NPIAS GA airports hire consultants to prepare their ADW and preliminary designs. Of the remaining $\frac{1}{4}$, some airport sponsors

use municipal/county engineers and some petition the OAC for assistance. Due to limited funding resources, a typical project in an airport's ADW may have to wait 5 to 7 years before it can expect to be programmed for funding with either state or federal funds. Also, since a project must compete with projects of all other airports in the Oklahoma Airport System (OAS) for merit-based funding, inclusion in the ADW in some cases may not guarantee funding for the project. On account of this and because ADW preparation is not eligible for federal and state funding, coupled with the complexity of designing appropriate remediation strategies for the increasing number of pavement deterioration cases, ADW project scopes and cost estimates tended to be unreliable. And, because of a high turnover in local airport management, many of the smaller GA airports neither have the resources nor trained manpower to update their ADW. Also since state or federal funds could not be guaranteed for a project, ADW preliminary designs were often not based on geotechnical or structural investigations, were often not the appropriate solution, and as a result, cost estimates were significantly different than the actual cost after selection for funding. Further, without structural and geotechnical data and analysis, OAC personnel could not evaluate the integrity of ADW items.

Given the distributed ownership of GA airports (none owned by OAC), airport sponsor responsibility for ADW, and geographic distribution of OAC personnel, effective pavement management required a community and decentralized effort. The deficiencies at the ADW level were undermining any ability to intelligently manage funding for the statewide network of GA airports. To develop comprehensive pavement management, the OAC needed a web-based PMS to foster community involvement in pavement management, and comprehensive geotechnical and structural data for each GA airport to

improve ADW preparation. These two needs coupled with the desire to be integrally involved with the continual development of the PMS in the future, led to the in-house development of the IMS described herein.

2.3 System Overview and Functionality

The success of an IMS depends upon its functionality and ability to meet the demands of the constituents. The improvements to traditional pavement management afforded by web enablement and structural/geotechnical information and tools are presented in the following within the functional framework of the IMS. Though computing capabilities change dramatically over short periods of time, it remains worthwhile to cite the software components utilized to build the IMS. The IMS (<http://apms.aeronautics.ok.gov>) was designed with client-server architecture (Figure 2-1) to enable user access from any geographic location via web browser (e.g., deskbound workstation, handheld or laptop computer, or mobile phone). The network server that facilitates the transfer and formatting of data (input and output), the analysis engine that processes raw data to/from the database and performs project/network level analysis, and the database all reside on a central-office computer. The web-based IMS was built upon the UNIX operating system using RedHat Linux. Apache, an open source HTTP server and the most widely used web server for UNIX and Windows environments (Netcraft, http://news.netcraft.com/archives/web_server_survey.html, March 2007), was employed. The network client and the analysis engine were developed using hypertext preprocessor (PHP), a server-side programming language, to create dynamic maps and graphical data presentation for all users. The database was created using *MYSQL* software, capable of accommodating more than 50 million records and an unlimited number of simultaneous

users. Redhat Linux, PHP and *MYSQL* are each open source and distributed free through the Free Software Foundation (<http://www.gnu.org>). This system could also have been built on a Windows platform; however, the UNIX based components proved to be more stable during development.

2.3.1 Airport Development Worksheets (ADW)

Since Oklahoma has a “channeling legislation” in place, the Commission is tasked with allocation of federal funds in addition to state funds. OAC therefore prepares a three year Capital Improvement Program (CIP) – a list of projects selected for funding - to distribute state and federal funds to Oklahoma airports. The annual CIP projects earmarked for funding are selected from a larger set of candidate rehabilitation, reconstruction, and new construction, land acquisition, navigational aid, safety and routine maintenance projects. Candidate projects are identified by OAC personnel. To be considered for CIP inclusion, candidate projects must be identified in the airport’s development worksheet (ADW).

ADW for every airport included in the OAS can be accessed over the world-wide web at <http://apms.aeronautics.ok.gov/apms.2.0/planning/mainnew.php>. Figure 2-2 presents the ADW for Ada Municipal Airport. As observed in the figure every ADW has a “deficiency box”. The box serves as a tool to highlight deficiencies observed at an airport by OAC staff during routine safety or pavement management inspections and serves to guide local, state and federal capital efforts. Each ADW is delineated into short term (0–5 years), medium term (6–10 years), and long term (11–20 years) planning horizons. The short term entries of each ADW must be accompanied by justification, preliminary designs and cost estimates. The projects selected for funding during

multiyear network level planning are selected from the short term segment of each GA airport's ADW. As observed in Figure 2-2, the ADW details a project's brief description of scope, estimated cost, component affected (i.e. runway, taxiway, apron etc), type of construction (i.e., construction, improvement, lighting etc.), purpose (i.e. safety, environment, standards etc.) as well as its national priority rating (NPR) calculated using Equation (1.1) (FAA, 2000).

$$NPR = (k_5 \times P) \times [(k_1 \times A) + (k_2 \times P) + (k_3 \times C) + (k_4 + T)] \quad (1.1)$$

where:

$$k_1 = 1.00,$$

$$k_2 = 1.40,$$

$$k_3 = 1.00,$$

$$k_4 = 1.20,$$

$$k_5 = 0.25,$$

A= Airport Code (2 to 5 pts.); used to identify the role and size of an airport,

P = Purpose code; identifies the objectives of an airport development project (i.e. reconstruction),

C = component; identifies the physical component for which improvement work is intended (i.e., runway, taxiway), and

T = type; identifies the actual work being done.

Values of the parameters required by Equation (1.1) are stored in the database i.e. airport codes that are calculated from based aircraft data and number of aircraft operations. Others like the 'P', 'C' and 'T' use FAA designated values stored in the database.

A NPR threshold value is established based upon CIP funding requirement and anticipated availability of AIP funds. Using this NPR threshold value with projects included in the short term segment of ADWs, a pool of candidate projects for inclusion in OAC's CIP is developed. Projects that clear the NPR threshold, form an initial pool of CIP candidates that are then subjected to further consideration and scrutiny including PMS recommendations if applicable (i.e. for pavement projects).

FAA maintains a comprehensive, nationwide data repository containing the development needs of all NPIAS airports in the United States. A snapshot of this updated database is taken every two years by FAA and sent to Congress. Upon reviewing this report of nationwide funding needs, Congress decides annual AIP funding levels. The sum of needed capital expenditures in the short term segment of every NPIAS airports' ADW is used to compute the level of Congressional assistance termed as non-primary entitlement funding (NPE). NPE funds amount to 1/5th of the reported short term needs of a GA NPIAS airport subject to a maximum of \$150,000 annually for a location. Over the years, this task of developing and presenting capital needs of Oklahoma's NPIAS GA airports was performed by FAA's Airport Development Office (ADO) without consulting OAC. Since 2005, OAC's ADW database has been used to formulate and then to develop a compatible electronic output. This electronic output is directly uploaded into the NPIAS database by FAA and sent to Congress.

2.3.2 Online Airport Guide

OAC's IMS also includes an online airport guide at the URL <http://apms.aeronautics.ok.gov/apms.2.0/directory/main.php>. Figure 2-3 presents the airport guide for Chickasha Municipal airport. The airport guide page for an airport is

split into two frames. The left frame provides an online version of OAC's airport guide and the right frame seamlessly links over to GCR, Inc.'s website (<http://ww.gcr.com>). GCR is engaged by FAA to maintain records from annual safety inspections at all NPIAS airports. The airport guide includes an aerial photograph that indicates location of the airport's beacon and wind-sock, and provides length, width and end identifier (magnetic bearing) information of the paved and turf runways. It also details communication frequencies for pilots to communicate with the airports traffic control, navigation details like airport elevation, latitude and longitude of the Airports' reference point, brief detail about services available at the airport and the types of navigation and approach aids available. GCR's repository for Chickasha Municipal (Figure 2-3) includes contact details of the airport management as well as details about services and facilities at the airport, based aircraft and aircraft operations, as well as runway information. The IMS is used by OAC to publish a popular, pilot friendly, printed version of Oklahoma's updated Airport Guide.

2.3.3 Construction Grants Management

Figure 2-4 provides a sample of construction grant tracking feature of OAC's IMS. The grant tracker provides details about important milestones in the project at a glance to users. This feature of OAC's IMS is restricted to ordinary users and can only be accessed by authorized users. Though simplistic in form at this time, the tracker has enabled OAC to keep a close watch on construction projects in the state.

2.3.4 Grant History

A complete record of state and federal grants to airports in the OAS is maintained by OAC's IMS. This grant history is available online and can be accessed at the URL

http://apms.aeronautics.ok.gov/apms.2.0/project_history/mainnew.php. Figure 2-5 presents the grant history for the City of Goldsby's David J. Perry airport.

2.3.5 Airport Contact Database

OAC's day to day functioning requires frequent communication with the airports community in Oklahoma. To aid in this, a database dedicated to storage of airport sponsor contact information has been integrated into the IMS. Due to online accessibility, the various branches of OAC can access, input and edit data stored in this database. The database has several helpful features:

- a. Quick look up using search strings like city name etc. (Figure 2-6).
- b. Online access to stored information.
- c. Input/ editing of data requires only very basic computing skills and is performed using a web-browser based interface.
- d. Ability to generate email lists for selected cities.
- e. Mail merge letters used for mass mailing of letters to selected cities.
- f. Mailing labels printout.

2.3.6 Network Inventory

The IMS provides a complete and structured inventory of runway, taxiway, and apron pavement data for 97 GA airports throughout Oklahoma (see Figure 2-7). Note that 81 GA airports are currently housed in the IMS. Consistent with accepted APMS practice, stored data includes construction history, pavement structure, functional classification, surface distress inventory per *ASTM D5340* (extent and severity), traffic information and environmental data (see Table 2-1). This data is referenced to sections— areas of pavement with consistent structure, usage, climatic, and traffic characteristics

(Shahin 1994), and presented to users graphically (see Figure 2-8). The database also maintains comprehensive geotechnical and structural information from each GA airport including data from coring, boring logs, in situ dynamic cone penetration tests, nondestructive testing, and laboratory tests (see Table 2-1). These data are georeferenced to point locations (x, y, z) within the appropriate section.

The geotechnical and structural data maintained in the IMS are summarized as follows:

1. Coring data: Layer thickness of Portland cement concrete (PCC), asphalt concrete (AC), and all overlays.
2. Boring log data: Thickness of each layer (aggregate base, subbase, subgrade) to a depth of approximately 1.5 m; visual classification of geomaterials, groundwater depth if any.
3. Dynamic cone penetration (DCP): An emerging in situ test (*ASTM D6951*) used to profile the penetration resistance versus depth in aggregate base, subbase and subgrade materials to a depth of approximately 1 m. DCP data is correlated to strength (e.g., California bearing ratio) and modulus.
4. Spectral analysis of surface waves (SASW): Nondestructive technique used to profile layer thicknesses and moduli with depth in pavement system (Khanna and Mooney 2002; Nazarian and Stokoe 1986).
5. Impulse response: Nondestructive technique used to quickly attain a composite stiffness of the pavement system at a single location.
6. Laboratory test results (core thickness, Atterberg limits, grain size distribution, soil classification, in situ moisture).

GIS functionality provides clear, accurate, and comprehensive representations of the geotechnical and structural conditions to the various end users involved in project and network level analysis. Figure 2-9 illustrates a plan view of a particular GA airport. Boring log and SASW testing locations are identified, and the pertinent geotechnical and structural data for a selected boring log or test location is provided in graphical form. Figure 2-10 conveys the most recent visual distress data per sample unit and section, as well as pavement condition index (PCI) data (see next section). PCI inspection data is collected using a tablet PC (HP tc1100, Figure 2-11) by field crew connected to the web through mobile broadband internet access and is uploaded to the central database in real time.

2.4 Pavement Condition Evaluation and Performance Prediction

Current and future pavement conditions have typically been based solely upon visually observed distresses in airport pavement management (Gendreau and Soriano 1998, Broten and De Sombre 2001). Although a few surface distresses may provide some insight into structural condition (e.g., rutting, alligator cracking), visual distresses mainly provide an assessment of functional pavement performance (e.g., safety, quality). The incorporation of structural and geotechnical information into an IMS enables capacity analysis and remaining life analysis, provides a better understanding of pavement behavior as a function of traffic loads and the environment, and strengthens the process of selecting appropriate treatment options for pavement sections. After all, the design of a pavement section (reconstruction, rehabilitation, overlay, etc.) is based on structural and geotechnical parameters. Hence, a comprehensive pavement management system should include both functional and structural capabilities.

A structural analysis module was developed within the IMS to perform capacity analysis, remaining life analysis, and pavement section design. The analysis module incorporates structural data directly from the database, namely, pavement layer moduli and thickness, and subgrade strength per DCP correlation (Chen et al. 2001; Livneh et al. 2000). The analysis module is capable of performing both empirical-based pavement analysis and mechanistic-empirical analysis. A finite element structural analysis module was scripted for PCC pavements; the analysis module enables corner and edge loading of multiple single and tandem landing gear configurations, and performs remaining life analysis (Khanna 1992). Structural analysis is performed for individual sections; the properties of a specific section (layer thickness, moduli, strength) are aggregated (if more than one boring log exists in the database per section) and automatically loaded into the analysis module. The Federal Aviation Administration (FAA) layered elastic analysis and design program *LEDFAA* (FAA 2004) is planned to be integrated into the IMS in the future. The IMS also has the ability to conduct empirical analysis and design per conventional FAA methods (FAA 1995).

A common question posed to GA airports and OAC personnel is, “can I land this aircraft here?” There is significant economic incentive for GA airports to utilize (and stretch) the full capacity of the airfield. To assist GA airports, pavement classification number analysis is performed using the structural and geotechnical data per FAA procedure (FAA 1983). In addition, the mechanistic analysis tools are used by OAC personnel to perform scenario analysis for various aircraft (discussed in the next section).

Functional evaluation of airport pavement has very effectively been accomplished through visual survey of surface distresses. The PCI method of evaluating distresses and

quantifying condition has become the defacto functional evaluation procedure used worldwide (Brotten and De Sombre 2001). To this end, the IMS stores and presents individual distress data, and calculates sample unit, section, branch and network PCI per ASTM D5340 (see Figure 2-10).

Functional performance prediction is based on deterministic regression analysis of PCI data. The family approach developed by Shahin (1994) is employed, wherein PCI and pavement age data collected for a family of similar sections create a data set spanning PCI from 100 to 30 and pavement ages from 0 to 30 years for AC pavements and from 0 to 59 years for PCC pavements. The IMS analysis tool uses a polynomial constrained least-squares regression technique to develop performance prediction curves (Yuan and Mooney 2003). Users can modify performance models through user-defined expert opinion regarding the terminal serviceability, terminal life, and expected pavement condition at certain ages. This function allows users to investigate different maintenance scenarios, factor preventive maintenance, and optimize the performance models. The methodology in which the section and family curves are related and adjusted is described elsewhere (Yuan and Mooney 2003).

Project level functional performance prediction can be performed for each branch in the network. For example, Figure 2-12 illustrates the framework in which pavement condition is presented for a GA airport. Visual distress inspection data and age of sections at the time of inspection are used to generate deterioration models. The display presents deterioration of the selected section as well as the pavement family deterioration curve. As new visual distress data are added to the IMS (each GA airport is assessed every 3 years), the performance prediction curves are updated.

2.5 Project and Network Level Planning

The developed IMS serves both project level planning (i.e., individual projects considered in isolation) and network level planning (i.e., numerous projects simultaneously). At the project level, both the functional condition (distress inventory, current and outyear PCI) and structural condition (capacity, remaining life) are provided, as are important data regarding the base layer (e.g., drainage capacity) and subgrade (shrink-swell potential, ground water table). This data coupled with the analysis tools described previously enables users to more accurately decide when pavement sections should be rehabilitated and what treatment or action should be performed. The data and tools used at the project level provide much improved preliminary designs and cost estimates for each GA airport's airport development worksheet that are then used for network level analysis and planning by the OAC.

Consistent with most airport PMSs, the OAC utilizes a bottom-up philosophy to network level planning. Project-level MR needs (provided in the ADWs) are ranked according to agency criteria. The criteria include the priorities recommended by the FAA (in order of importance): safety, preservation, standards, upgrades, and capacity; and the importance of each GA airport based on economic development potential, number of operations, and regional growth. Of course, this process is not immune to political influence, e.g., geographic distribution of projects. Project-level MR needs (and cost) reside within the ADWs in the IMS. Network level IMS tools can assign a factor for FAA priority and then rank the projects. The OAC currently uses the IMS to develop a 3-year network work plan annually; however, the system is capable of n -year planning. Due to the subjectivity of the remaining aforementioned ranking criteria, the final ranking is

performed off-line. Given the bottom-up approach, the improvement in project level MR selection and cost estimating directly improves network level planning.

The system is also capable of functional and structural based network level analysis. Figure 2-13 provides one such “statement of health” for the entire network of airfield pavements based on visual pavement distress and PCI. A statement of health can also be provided at the network level in terms of mechanistic parameters, i.e. pavement moduli degradation (Khanna and Mooney 2002). As MR is performed and branches are re-inspected, pertinent data are loaded into the system’s database.

2.6 Benefits of Web-Based IMS

The IMS has provided a number of benefits to Oklahoma airport pavement management since implementation in 2002. The most significant contribution of the IMS has been observed in project and network level planning activities. Given the role and mission of the OAC, providing a distributed system to share data and tools with GA airport sponsors was viewed as a business requirement. All GA airport sponsors and their consultants are strongly encouraged to utilize the functional and structural/geotechnical data from the IMS to build their ADW entries. Prior to the IMS, ADW entries were rarely predicated upon structural and geotechnical data because site investigation and preliminary design are not eligible for federal and state funding. The use of the IMS translates into GA airports examining the nature and cause of distresses, as well as the existing structural capacity and geotechnical conditions, and then preparing a preliminary MR design predicated upon such findings. OAC personnel perform a quality control check of ADW entries using the data and analysis tools of the IMS. Discrepancies can be addressed before consideration for network level planning. As a result of the web-based

IMS, ADW entries have increased from approximately 1,300 in 2002 to 1,800 in 2004. More importantly, the integrity of ADW entries has improved. For example,

- The City of Muskogee used the IMS to access structural, geotechnical, and visual distress data (present and future) as part of a rehabilitation investigation for their main PCC runway that was exhibiting surface distress. The IMS structural and geotechnical data and analysis revealed no structural deficiency. The IMS was used to design a thin AC overlay (estimated construction cost = \$ 1.8 million) for consideration to restore ride quality rather than the pre-IMS proposed PCC overlay (estimated construction cost = \$6.75 million).
- The City of Goldsby used the IMS to identify weak subgrade underlying the main runway to better understand observed surface distresses. Instead of proposing a standard AC overlay, remaining life analysis recommended a PCC reconstruction design for funding consideration, a more appropriate pavement design for soft subgrade than AC pavement.
- Based solely on observation of fatigue cracking (no use of IMS), Ardmore Municipal Airport requested an AC overlay of their existing AC pavement. The IMS data revealed that no base course and thus no drainage layer was present, and the near surface presence of water. The IMS analysis (2005) recommended a complete reconstruction to include a drainage base course.

GA airports were provided additional resources by Congress in the form of Non-primary entitlement funds under the “Air-21” legislation that came into effect in 2001. Since these funds were provided by Congress to “specific NPIAS airports”, OAC was effectively out of the loop and could not assist Oklahoma’s GA as to maximize their funding potential,

i.e. \$150,000 annually. Based on the well developed ADWs and the IMS's ability to generate ADW output compatible with FAA's NPIAS database, OAC undertook the task to compile the NPIAS needs of Oklahoma's GA airports. Using the extensive airport information available in the IMS and information provided by airport sponsors, OAC was able to complete the NPIAS update in a timely, efficient manner and maximize funding potential of Oklahoma's airports. With this input from OAC, annual NPE funding of Oklahoma airports has increased from \$11.65 million in 2004 to \$14.55 million in 2007 representing a 25% increase.

The structural and geotechnical data stored in the web-based IMS has also enabled OAC staff to efficiently perform structural capacity analysis for GA airports. Due to the economic incentive for GA airports, the OAC receives dozens of requests annually for capacity analysis, e.g., to permit larger aircraft to land. The answer to such requests can have significant economic impact. Recent examples include the analysis of two municipal airport runways in order to operate Boeing-747 aircraft (both cases revealed inadequate support), an analysis of a runway to determine the effect of multiple Gulfstream V operations on pavement health, and an increase in specified capacity of an airport runway based on re-evaluation of capacity analysis.

The IMS has catalyzed organization change within the OAC. Not unlike most industries, the development of software to support innovation in infrastructure management can come from industry, from academia, from government, or from collaborations therein. The pavement management community is replete with agencies that utilize commercial programs (e.g., *MICRO PAVER*, *AIRPAV*, *DSS*, *PAVEMENTVIEW*) and with organizations that have collaborated with academia to

design in-house pavement management systems (White et al. 2005; Tsai and Lai 2002; Falls and Tighe 2003). The commonality among the recent in-house collaborative efforts including the effort presented here is the desire to provide functional advances and the need to customize to agency needs. Equally important, however, is the desire of the agency to integrate IMS development into their mission and culture. IMS functionality continues to grow at a rapid pace, propelled by advances in information technology, sensing technology, and techniques to assess condition, predict future performance, and perform network level planning. To this end, the OAC has adopted a culture of continuous IMS development and improvement. For example, developments underway include the integration of construction management activities into the IMS, the development of improved network-level forecasting and planning using both functional and structural characteristics, the expansion of IMS for public use (e.g., navigation and aircraft approach aids, communication frequencies, weather links, aircraft repair facilities), and the inclusion of other infrastructure management assets (i.e., lighting, buildings).

The web-based IMS has enabled GA airport sponsors and their consultants to play a more effective and active role in project level activities. The number of ADW entries has increased from 1,300 in the year 2002 to 1,800 in 2004, yet the requests for information to OAC have decreased. Consequently, the IMS has enabled the OAC to be more efficient. OAC personnel, and for that matter consultants, can quickly and more efficiently respond to requests for capacity analysis. OAC has also been able to accommodate a much larger portfolio of projects and state/federal funding without an increase in OAC personnel. State and federal funding for Oklahoma airports has more

than doubled, from approximately \$21 million in 2001 to \$48 million in 2003. In effect, OAC has been able to cut, by more than one-half, the ratio of management cost to airport funding.

2.7 Summary and Concluding Remarks

An infrastructure management system was developed to expand upon traditional airport PMS by incorporating structural and geotechnical data and analysis tools, and by distributing data through web enablement to mobilize a broad spectrum of end users. The IMS was developed with off-the-shelf open source software for a network of 100 GA airports in the state of Oklahoma. This expansion has provided numerous benefits, including improved project-level MR treatment selection and cost estimating, improved network level planning, and more balanced emphasis on structural and functional performance rather than just functional performance. Web enablement has placed valuable information in the hands of appropriate airport personnel. A 25% increase in annual NPE funding (\$2.9 million) has come about because of the IMS. Project-level activities by GA airports have increased by more than 30%. The IMS has led to greater efficiency by OAC personnel, as the ratio of management costs to airport funding has been cut by more than 50%. OAC's involvement in the development of the IMS coupled with the rapidly evolving field of infrastructure management has also catalyzed a culture of continuous development within the organization.

2.8 References

AASHTO, “*Pavement management guide*”, Washington D.C., 2001.

ASTM D5340-04e1, “*Standard Test Method for Airport Pavement Condition Index Surveys*”, ASTM International.

ASTM D6951, “Standard test Method for use of the dynamic cone penetrometer in shallow pavement applications”, ASTM International,

Brotten, M., and De Sombre, R. “*The airfield pavement condition index (PCI) evaluation procedure: Advantages, common misapplications, and potential pitfalls.*” Proc., 5th Int. Conf. on Managing Pavements, Seattle (CD-ROM), 2001.

Chapman, A., “*Application of web technology to enhance water system operations.*” Water Supply, 3(1–2), 287–294, 2003.

Chen, D.-H., Wang, J.-N., and Bilyeu, J., “*Application of dynamic cone penetrometer in evaluation of base and subgrade layers.*” Transportation Research Record 1764, Transportation Research Board, Washington, D.C., 1–10, (2001).

Falls, L. C., and Tighe, S., “*Improving LCCA through the development of cost models using the alberta roadway maintenance and rehabilitation analysis application (ROMARA).*” Paper presented, Transportation Research Board, Washington D.C., 2003.

Federal Aviation Administration (FAA), “Standardized method of reporting airport strength.” PCN, Advisory Circular No. AC 5335-5, (<http://www.faa.gov/arp/engineering/index.cfm>), 1983.

Federal Aviation Administration (FAA), “Airport pavement design and evaluation.” Advisory Circular No. AC 150/5320-6D, (<http://www.faa.gov/arp/engineering/index.cfm>), 1995.

Federal Aviation Administration (FAA), “*Airports Capital Improvement Plan – Order 5100.39A*”, http://www.faa.gov/airports_airtraffic/airports/resources/publications/orders/media/AIP_5100_39A.pdf, 2000.

Federal Aviation Administration (FAA), (2004). *Layered elastic pavement design software version 1.3*, (www.faa.gov/arp/engineering/software.cfm).

Gendreau, M., and Soriano, P., “*Airport pavement management systems: An appraisal of existing methodologies.*” Transportation Record A, 32(3), 197–214, 1998.

Haas, R. Hudson, W.R., and J. Zaniewski, “*Modern Pavement management*”, Krieger Publishing Company, Florida, 1994.

Khanna, V., “*Dynamic response of rigid airport pavements subjected to temperature induced warping and multiple aircraft.*” MS thesis, Univ. of Oklahoma, Norman, Oklahoma, 1992.

Khanna, V., and Mooney, M. A., “*Comparison of SASW backcalculated profiles with boring log and DCP data.*” Proc., 2nd Int. Conf. on Application of Geophysical and NDT Methodologies to Transportation Facilities and Infrastructure, Los Angeles, 2002.

Lam, H. F., “*Web-based information management system for construction projects.*” Comput. Aided Civ. Infrastruct. Eng., 17(4), 280–293, 2002.

Liu, D. T. “*A review of web-based product data management systems.*” Comput Ind., 44(3), 251–262, 2003.

Livneh, M., Livneh, N. A., and Ishai, I., “*The Israeli experience with the regular and extended dynamic cone penetrometer for pavement and subsoil-strength evaluation.*” Proc., Nondestructive Testing of Pavements and Backcalculation of Moduli, Vol. 3, ASTM STP 1375, S. D. Tayabji and E. O. Lukanen, eds., American Society for Testing and Materials, West Conshohocken, PA, 2000.

Nazarian, S., and Stokoe, K. H., II., “*In-situ determination of elastic moduli of pavement systems by spectral-analysis-surfacewaves method (theoretical aspects).*” Research Rep. No. 437-2, Center for Transportation Research, The University of Texas at Austin, Austin, TX, 1986.

Shahin, M. Y., “*Pavement management for airports, roads, and parking lots,*” Kluwer Academic, Dordrecht, The Netherlands, 1994.

Tsai, Y., and Lai, J. S., “*Framework and strategy for implementing an information technology-based pavement management system.*” Transportation Research Record 1816, Transportation Research Board, Washington, D.C., 56–64, 2002.

White, G. C., Muench, S. T., Mahoney, J. P., Turkiyyah, G. M., Sivaneswaran, N., and Pierce, L. M., “*PMSView: A web-enabled pavement management system.*” Proc., 6th Int. Conf. on Managing Pavements, Queensland, Australia, in press, 2005.

Wu, M.-L., Lin, Y.-F., Yang, J.-J., and Chung, C.-A., “*National park management using self-developed and web-based geographic information systems.*” Proc., Int. Geoscience and Remote Sensing Symp., 5, 2483–2485, 2001.

Yuan, J., and Mooney, M. A., “*Development of adaptive performance models for Oklahoma Airfield pavement management system.*” Transportation Research Record 1853, Transportation Research Board, Washington, D.C., 44–54, 2003.

Zang, Z., and Hudson, W. R., "*Development of an integrated infrastructure management system.*" Proc., 4th Int. Conf. on Managing Pavements, Durban, South Africa, 1348–1362, 1998.

Table 2-1: Summary of Network Inventory Data Stored in IMS

	Data Type	Information Provided	Referenced to
Planning	ADW/NPIAS needs data	20 year airport development plan	Airport
	Airport guide & Safety information	Airport information for the flying public i.e. communication frequencies, navigational details, services available	Airport
	Grant history	Details of state and federal airport development grants	Airport
	Construction tracker	Construction project monitoring for OAC oversight	
	Airport sponsor contact address	Contact details, i.e. mailing addresses, telephone and email addresses, email lists, mail merge letters with mailing label print out	Airport
Engineering	Visual distress	Individual distresses, PCI	Section
	Coring & boring	Thickness of pavements, base, and each subgrade soil layer; Atterberg limits, grain size distribution, in-situ moisture content, soil classification	Point location
	SASW	Pavement layer thickness and low-strain elastic moduli of each layer	Point location
	Impulse response	Pavement section stiffness and pavement layer mobility	Section
	DCP	Penetration resistance of soils (correlation to modulus, shear strength)	Point location

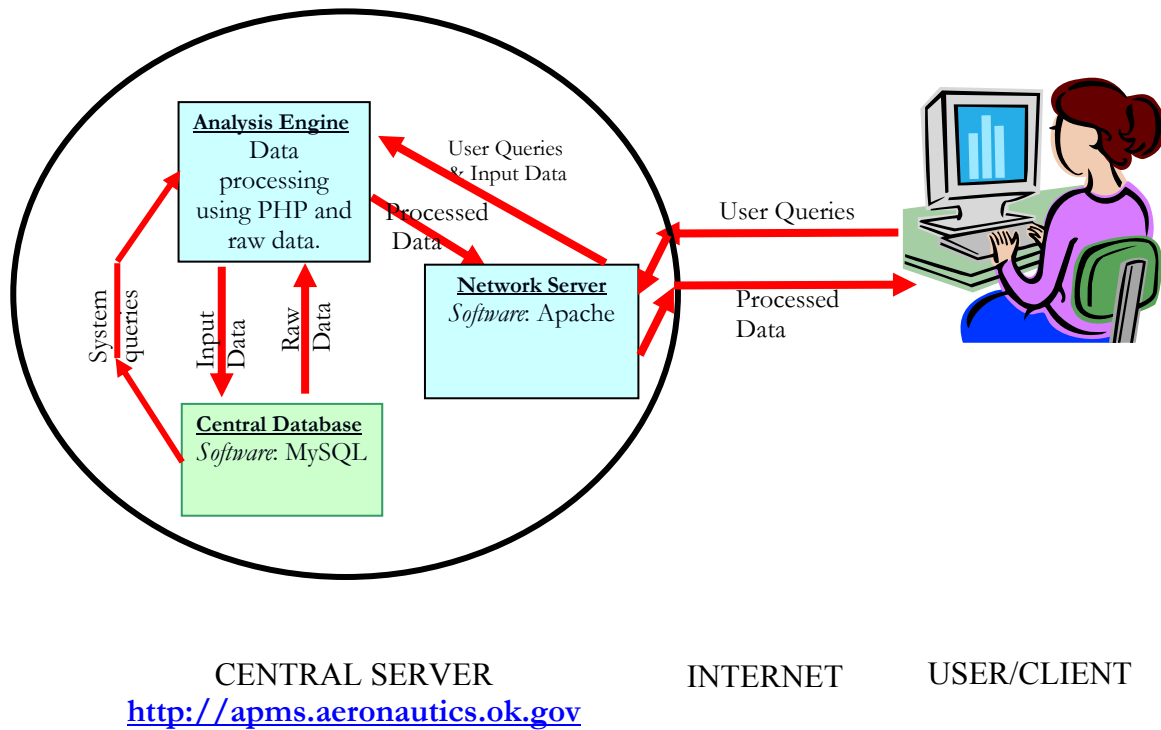


Figure 2-1: Client-Server architecture of Web-Based IMS

Airport Development Worksheet								
DEVELOPMENT BY TIME PERIOD								
DAC Home	APMS Home	Printer friendly	Edit Worksheet	Airport	Ada Municipal	Select by Airport		
Airport: Ada Municipal			City: Ada		NPIAS No: 40-0001			
ARC: B-II			ARC Future: B-II		Classification: RB			
Airport Deficiencies								
09-12-05								
1. Moderate to severe cracking, spalling, deterioration of all pavement surfaces. (RD)								
2. Soft and depressed areas on taxiways, especially TW "A".								
3. Non-standard markings on RW31 end. (RD)								
4. Tall grass within RW13/31 Safety areas.								
5. Two lighting fixtures missing on RW17/35.								
6. Two PAPI lamps OTS on RW17 end.								
7. Unmarked PLINE on RW17 end. (RD)								
8. No protective barrier around fuel pumps.								
RD = RECURRING DEFICIENCYs								
SI = SAFETY ISSUE.								
No.	Project Description	Addendum	Runway	Project cost	Object Code	Airport Comp	Const Type	National Priority
1	Construct Taxiway Re-align and reconstruct parallel taxiways to runway 17/35	-	-	3,315,789	ST	TW	CO	47.1
2	Rehabilitate Taxiway Rehabilitate Taxiway to Runway 17/35	-	-	655,000	RE	TW	IM	63.6
3	Rehabilitate Runway Rehabilitate RW 13/31 (3100 ft x 50 ft)	-	13/31	180,000	RE	RW	IM	67.6
4	Rehabilitate Taxiway Reconstruct Taxiway from TW A to TW B and apron at Hangar D,E, & H; Crack seal, seal coat Ramps at Hangars F,G,C	-	-	250,000	RE	TW	IM	63.6
5	Rehabilitate Taxiway Reconstruct & re-align TWs B&C	-	-	220,000	RE	TW	IM	63.6
6	Acquire Easement For Approaches Acquire land & easements, S. end RW 35	-	-	75,000	ST	LA	SZ	42.0
7	Rehabilitate Access Road Reconstruct entrance roadway	-	-	235,000	OT	GT	AC	21.0
8	Construct Terminal Building Construct new terminal building	-	-	250,000	ST	TE	CO	36.6
9	Update Airport Master Plan Study Update airport action plan, survey for precision approach, update HZO	-	-	75,000	PL	PL	MA	64.0
Time Period: 00-05				Total Cost: \$ 5,255,789	Committed: \$ 3,315,789			
No.	Project Description	Addendum	Runway	Project cost	Object Code	Airport Comp	Const Type	National Priority
1	Rehabilitate Taxiway Reconstruct parallel and connecting TW to RW 13/31 (1770' x 35')	-	-	400,000	RE	TW	IM	63.6
2	Rehabilitate Apron -	-	-	165,000	RE	AP	IM	57.6
3	Construct Apron -	-	-	800,000	CA	AP	CO	52.2
4	Construct Apron Construct aircraft run-up apron	-	-	35,000	ST	AP	CO	42.6
5	Rehabilitate Runway Clean and fill cracks, seal coat, and mark RW 17/35 (6203' x 100')	-	17/35	150,000	RE	RW	IM	67.6
6	Rehabilitate Runway Clean and fill cracks, Seal coat and mark RW 13/31 (3,100' x 50')	-	13/31	75,000	RE	RW	IM	67.6
Time Period: 06-10				Total Cost: \$ 1,625,000	Committed: \$ 0			

Figure 2-2: ADW of ADA Municipal with deficiencies noted by Airport Safety Inspector on 09/12/05

AirportIQ™ 5010 Airport Master Records and Reports

CHICKASHA MUNI Associated City: **CHICKASHA**
18865.*A Location Identifier: **CHK**
Data Effective Date: 03/15/2007 *Provided By: GCR & Associates, Inc.*

General Information **Services & Facilities** **Based Aircraft & Operations** **Runway Information**

CBD to Airport(NM): 03 NW
County: GRADY
REG/ADO: ASW NONE
SECT AERO CHT: DALLAS-FT WORTH
Ownership: PUBLIC
Owner: CITY OF CHICKASHA
Address: CITY HALL 117 N 4TH STREET, CHICKASHA, OK 73018
Phone No: 405-222-6028
Manager: MIKE BRICE
Address: CITY HALL 117 N 4TH STREET, CHICKASHA, OK 73018
Phone No: 405-222-6028
Attendance Schedule: MONTHS: ALL, DAYS: ALL, HOURS: 0800-1700
Airport Use: PUBLIC
Airport Latitude: 35-05-50.4830N ESTIMATED
Airport Longitude: 097-58-03.6890W
Airport Elevation: 1150 ESTIMATED
Acreage: 720
Right Traffic: NO
Non-Commercial Landing Fee: NO
MPIAS/Federal Agreement: NGRPY
FAR 139 Index: 08/09/2005
Last Inspection Date: 08/09/2005

CHICKASHA **CHK** **CHICKASHA MUNICIPAL**

[DAC Home](#) [ADHS Home](#) [Airport Page](#) [Choose another Airport](#)

Communication		Navigation		Services	
TWR	NA	ELEV	1130'	FUEL	100LL, Jet A
GND CON	NA	LAT	35°05'50.483N	REPAIRS	No
UNICOM	123.00	LONG	97°58'03.689W	ATTENDED	Yes
APP/DEP	124.60	VORFO	114.10	AIRPORT	405-222-6006
LIGHTS	MIRL	VORBG	231.00°	CITY	405-222-6028
AMOS FQ	118.175	AMOS	405-574-1016	From City	03 NW

Navigation and Approach Aids			
MDB	VOR	GPS	RNAV
Yes	Yes	Yes	Yes
No	No	No	No
ILS	LOC	ILS	LOC
No	No	No	No

Always check FAA's Airport/Facility Directory for current information. Updated: 08-12-2005

Figure 2-3: Online airport guide page

Construction and Planning Grants Tracking

Airport Details

Sponsor/ Airport	Project No.	ID	Grant Type	Sponsor Share	State Share	FAA Share	Total Cost
Sallisaw Municipal	J5V-06-F		Construction	56610.00	367390.00	300000.00	724000.00

Project Details

Description
Overlay and mark RW 17/35

Important Dates

Grant Appl. Recvd	Comm. Approval	Final Accept.	Audit Recv.	Proj. Closed
00-00-0000	06-08-2006	-	-	-

Comments

09-18-2006 Construction activities started. Contract time is 45 days.
 09-25-2006 Construction Management Program Received.
 10-18-2006 Copies of acceptance test results faxed by Jared Eddy of EST (McAlester). This included
 a) Results of two Gradation and Asphalt Content tests. Air voids, stability and flow test results were not provided
 b) Nuclear density testing was performed though not required for the leveling course.
 11-02-2006 Inspection reports dated 9/18/06 to 10/22/2006 received together. On October 22, 100% of leveling course and 90% of surface course had been placed. A copy of the job mix formula for surface course was provided with the inspection reports. Per inspection reports, work was performed as follows:

Activity	Start Date	End Date
P-101 B Coal Tar removal	09-18-06	09-18-06
P-101 A Milling	100% complete on	10-08-06
P-101 C Crack Filling	100% complete on	10-08-06
P-101 D Patching	75% complete on	10-08-06
P-401 Leveling Course	10-09-06	
a) 948.33 tons		10-09-06
b) 511.20 tons		10-10-06
c) 1095.75		10-11-06
Total laydown described by inspector = 2555.28 tons of P-401 leveling course		
P-630A Geotextile - 33,334 SY	10-13-06	10-15-06
P-401 Asphalt Surface course (2")		10-18-06
a) 1,186.50 tons		10-18-06
b) 1,125.32 tons		10-20-06
c) 1,159.30 tons		10-21-06
d) Tonnage not given - approximately 10% of total		
Total P-401 surface course = approx 3,471.12 tons		IGNORE
e) 593.16 tons		10-23-06

4,064.28 tons		

11-03-2006 Pay request received from City
 11-12-2006 All work on project completed

Figure 2-4: Construction project information display

Airport Development History

[DAC Home](#) | [APMS Home](#) | [Printer friendly](#) | [Edit Worksheet](#) | Airport: David Jay Perry | [Select by Airport](#)

Airport: David Jay Perry **City: Goldsby** **NPIAS No: 40-0066**

FY	Local	State	Federal	Total	Project Description
1968	0	7,500	0	7,500	Preventive maintenance
1969	0	160	0	160	Airport improvements
1972	0	0	56,568	56,568	Construct and mark RW (3,000 x 60); install RW lights, beacon, beacon tower, segmented circle, wind
1973	0	4,410	0	4,410	Improve and extend northwest/southeast RW
1993	5,000	0	0	5,000	Obstruction removal
1993	15,825	15,825	0	31,650	Up front funds for apron reconstruction, construct parallel TW
1994	0	0	0	0	Install self service fuel system
1994	15,814	15,814	284,661	316,289	Reconstruct apron and repair RW
1995	560	2,117	0	2,677	Unicom and anemometer
1996	0	587	0	587	Supplement of FY95 grant
1997	11,548	46,190	0	57,738	Seal coat
2001	4,988	0	44,889	49,877	Design rehabilitation for RW 13/31
2002	0	15,041	0	15,041	Supplemental Grant for RW 13/31 reconstruction
2002	61,722	555,500	0	617,222	Mill 3 inches asphalt and Overlay 6 inches of PCC on Runway 13/31, runway markings and safety featur
2002	0	0	135,111	135,111	Improve Airport drainage, improve drainage in access and hangar areas and taxilanes
2003	0	0	137,045	137,045	Rehabilitate Taxiway and t-hangar taxilanes
2003	1,960	0	37,250	39,210	Conduct Miscellaneous study
2003	3,916	0	74,411	78,327	Rehabilitate Runway
2003	45,012	0	405,111	450,123	Improve Airport Drainage; Rehabilitate Taxiway
TOTAL	166,345	663,144	1,175,046	2,004,535	

Figure 2-5: Airport grant history for David J. Perry airport

[DAC Home](#) | [APMS Home](#) | [Find Address](#) | [Edit Address](#) | [Create Email List](#) | [Create Address Labels](#) | [Mail Merge](#)

Addresses of Airport Managers

City	Airport	Title	First Name	Last Name	Address	State	Zip	Phone	E-Mail	NPE
Oklahoma City	Will Rogers World Airport	The Honorable	Mick	Cornett Mayor of Oklahoma City	200 N. Walker Avenue	OK	73102	405-297-2424	mick.cornett@okc.gov	
Oklahoma City	Wiley Post	General Aviation Manager	Scott	Keith	5915 Phillips J. Rhoads, Room 104	OK	73008	405-789-4061, 623-3008cel	scott.keith@okc.gov	Y
Oklahoma City	Clarence E. Page Municipal Airport	General Aviation Manager	Scott	Keith	5915 Phillips J. Rhoads, Room 104	OK	73008	405-789-4061,623-3008 cel	scott.keith@okc.gov	Y
Oklahoma City	Will Rogers World Airport	City Manager	James D.	Couch	200 N. Walker Avenue	OK	73102	405-297-2345	James.couch@okc.gov	
Oklahoma City	Will Rogers World Airport	Airport Manager	Mark	Kranenburg	7100 Terminal Drive, Room 301	OK	73159	405-680-3260	mark.kranenburg@okc.gov	

Figure 2-6: Results of search for contact details using "Oklahoma City" as search string

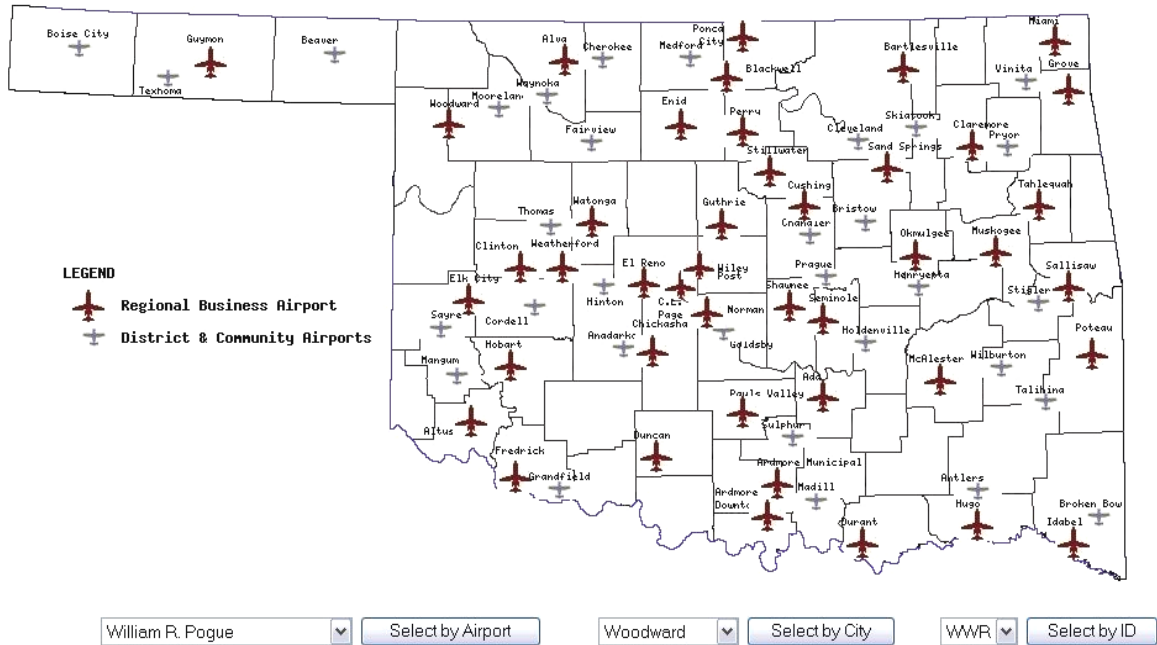


Figure 2-7: Network of Oklahoma GA airports

WDG Enid Woodring Regional, Enid, Oklahoma

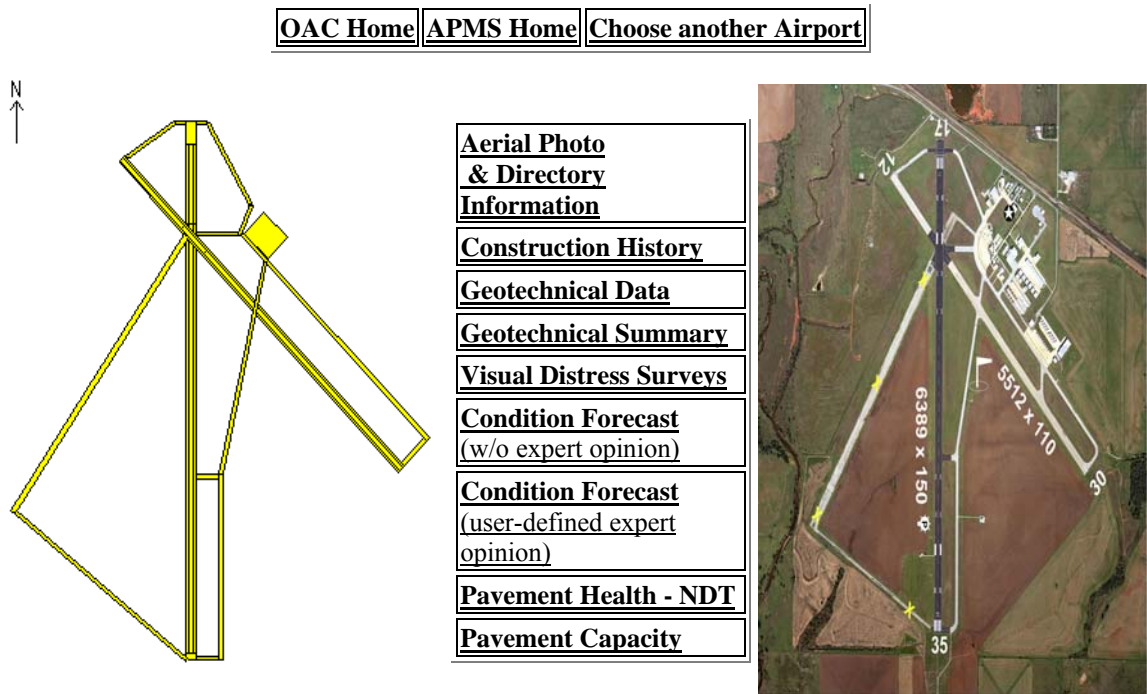


Figure 2-8: Project-level data options and aerial photograph (Enid Woodring Regional airport)

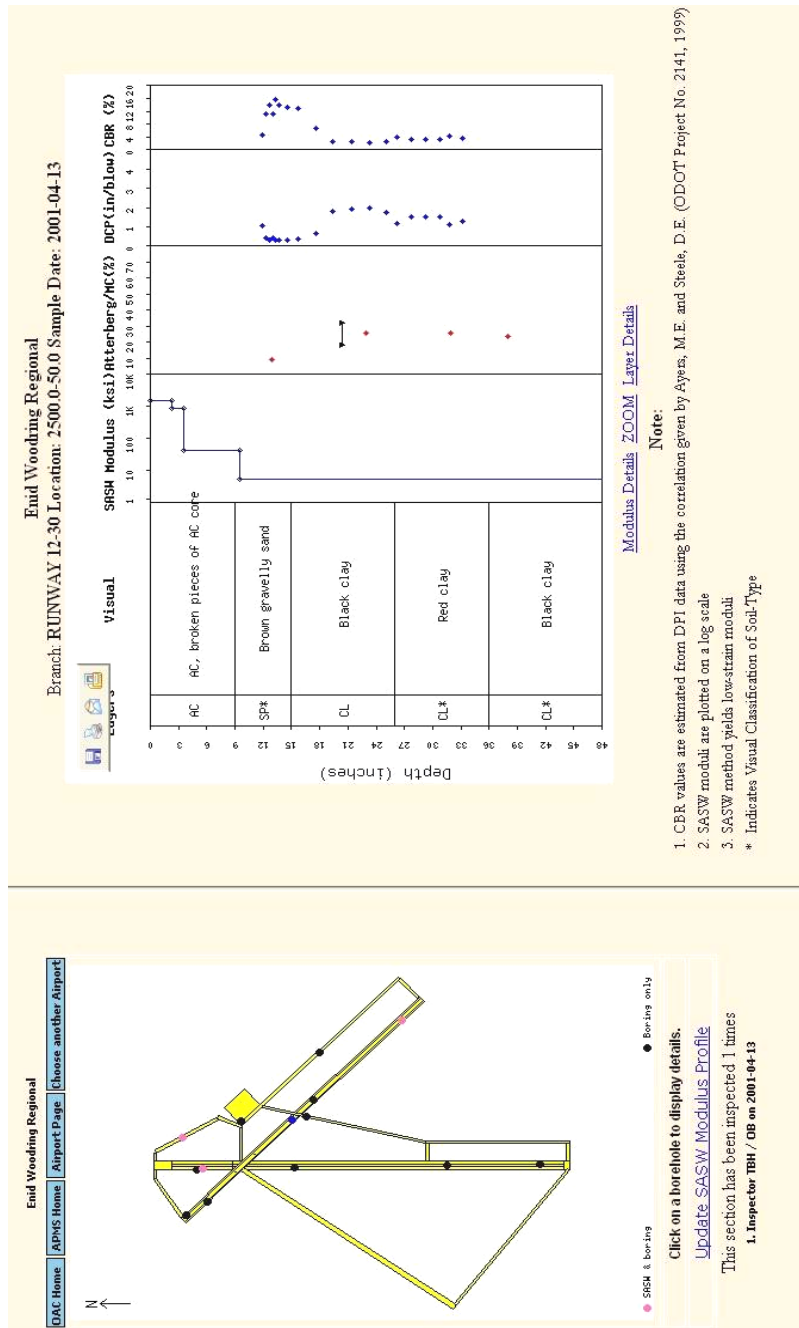


Figure 2-9: Geotechnical and structural data (Enid Woodring Regional airport)

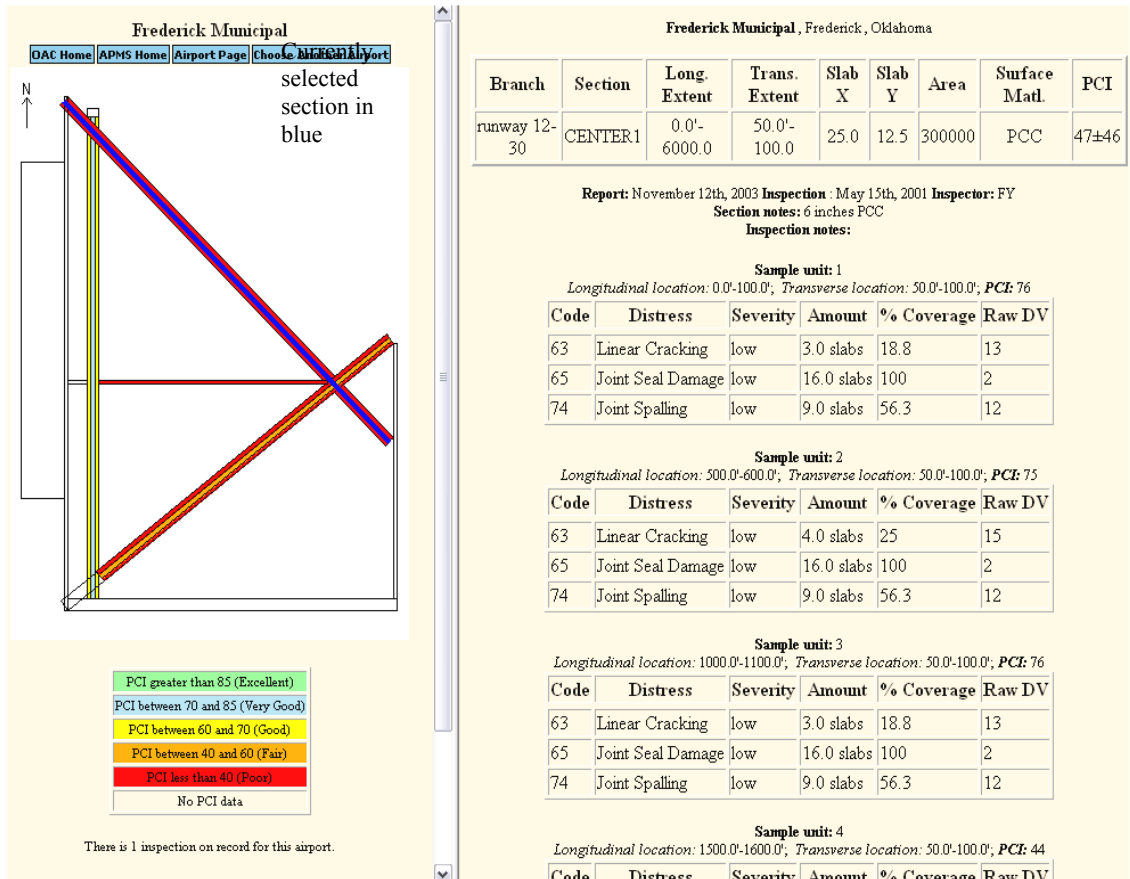


Figure 2-10: Visual distress and pavement condition index data (Frederick Municipal airport)



Figure 2-11: Hewlett Packard's tablet PC tc1100 used for real-time pavement condition entry

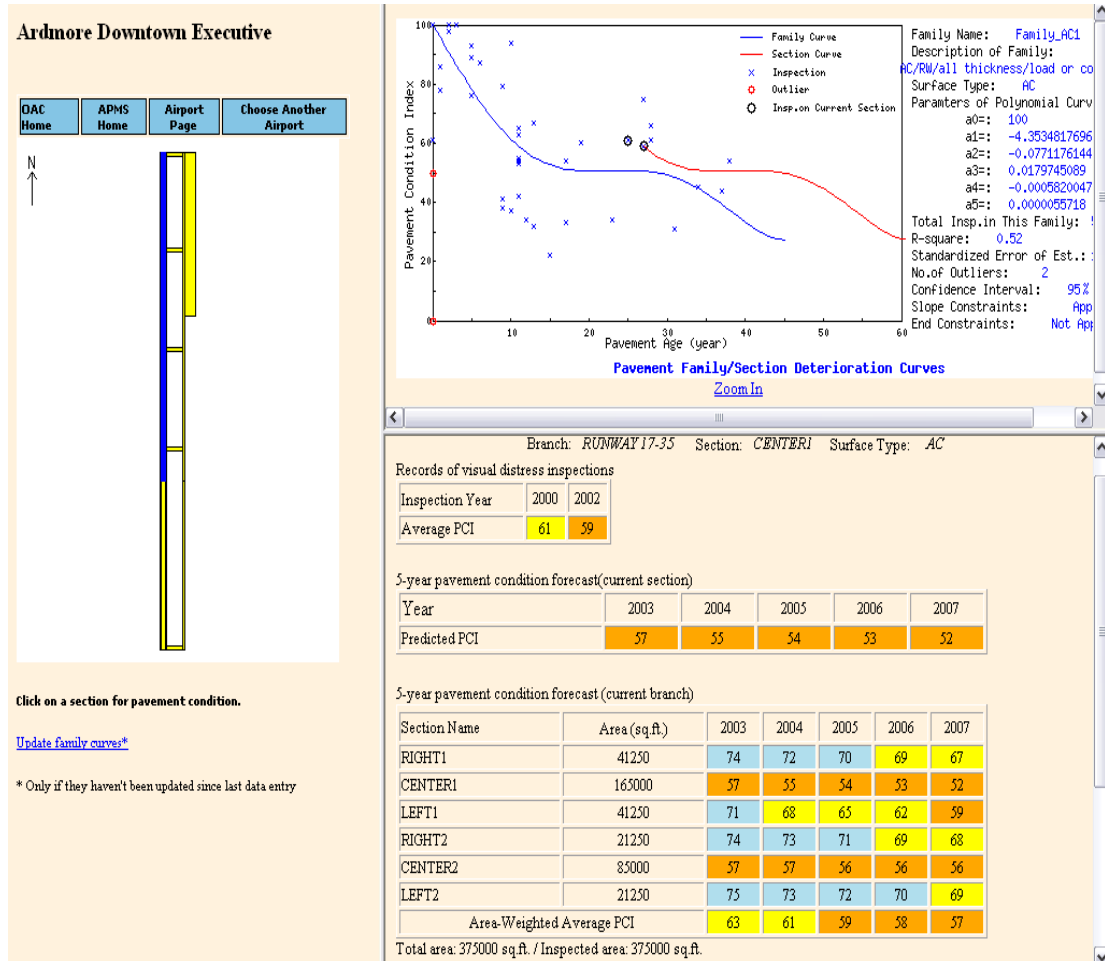


Figure 2-12: Pavement condition prediction for Ardmore Downtown Executive airport

General Information of Airports

Number of Airports: 122
 Number of Inspected Airports: 81
 Total Pavement Area (sq.yds.): 8495468
 Total area of Inspected Sections (sq.yds.): 6547570
 Inspection Coverage: 77%

5-Year Area-Weighted Network PCI Forecasts

Year	Average PCI	Health State
2007	64	Good
2008	62	Good
2009	61	Good
2010	59	Fair
2011	58	Fair

[View 5-Year PCI Forecast Table](#)
 (Inspected Airports only)

[Return](#)

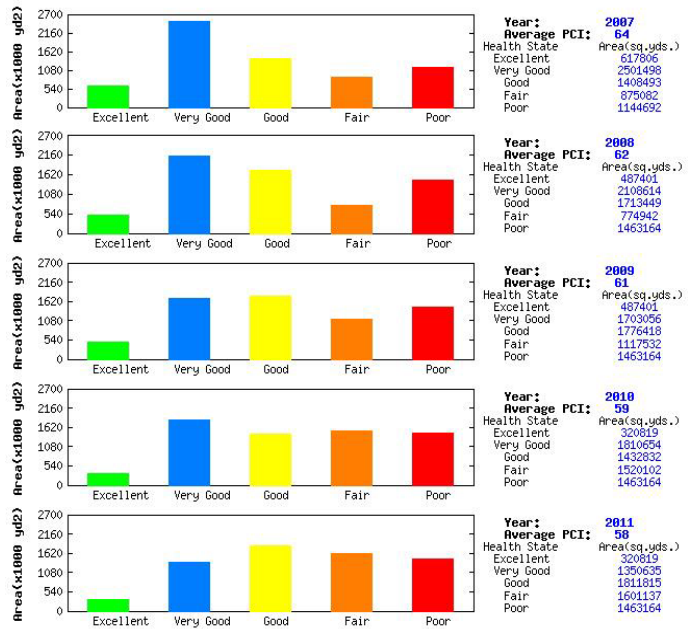


Figure 2-13: Sample network snapshot and future pavement condition forecast

Chapter 3 Efficacy of SASW in profiling pavement layers

3.1 Introduction

Managing an extensive, geographically distributed General Aviation (GA) pavement network (8.5 million sq. yards) with PCI information alone can pose challenges for administrators. The current research seeks to advance pavement management by complementing conventional visual distress based pavement condition with nondestructive testing (NDT) data and an extensive geotechnical database to assist maintenance and rehabilitation (MR) decision making. The inclusion of geotechnical data in a PMS enables stakeholders to better understand causes of pavement distress and devise optimal, most suited solutions.

The Oklahoma Aeronautics Commission's airport Pavement Management System (PMS) includes a comprehensive database of geotechnical information. This online (<http://apms.aeronautics.ok.gov>) database includes conventional geotechnical data like pavement surface layer thickness from core extractions, index properties from tests conducted on soil samples, Dynamic Penetration Index (DPI) variation with pavement depth from Dynamic Cone Penetrometer (DCP) testing. In addition to PCI data from visual distress surveys, the database also includes state-of-the-art NDT information, i.e. results of Spectral Analysis of Surface Waves (SASW) and Impulse Response (IR) testing including pavement layer thicknesses, layer moduli and pavement stiffness.

3.2 Objectives of study

The main driver behind using the SASW method was to provide a reliable, non-destructive determination of mechanistic pavement condition. SASW data could provide

mechanistic inputs like pavement layer thicknesses and layer moduli for use in estimating structural adequacy of pavement sections as well as remaining pavement life. This section examines the efficacy with which SASW estimates layer thicknesses of Oklahoma's General Aviation (GA) airport pavements. SASW's estimates of layer thickness are compared with core extractions, bore logs as well as the result of DCP testing. The current study draws upon SASW tests, DCP tests, core extractions and bore logs at 156 sites with asphalt concrete (AC) surface layer and 52 sites with Portland Cement Concrete (PCC) surface layers. Tests at these locations were conducted from 2000 to 2005. Tests at 25 AC and 3 PCC test sites were performed twice to directly examine possible degradation.

3.3 SASW Background

SASW testing is carried out at extremely low strain levels ranging from $10^{-6}\%$ to $10^{-4}\%$ (Ishihara, 1996). Laboratory testing and FWD testing of pavement materials is carried out at strain levels of $10^{-3}\%$ to $10^{-1}\%$ (Ishihara, 1996, Seed et al, 1970). The SASW method is based on the dispersive character of surface waves propagating in a layered medium. Figure 3-1 illustrates the most commonly used field configuration for the test. The test employs common receivers midpoint (CRMP) geometry where each transducer pair is placed symmetrically about the same imaginary centerline with $d_1 = d_2$ (Sanchez-Salinaro, 1987) as in Figure 3-1. Receiver spacings of 0.25, 0.5, 1, 2, 4, 8 and 16 feet were employed in the current study. Surface waves are generated in the material being tested using the impact from a hammer source. The time series of surface waves recorded by receivers R_1 & R_2 , denoted by $x(t)$ and $y(t)$ respectively, is Fourier-transformed to yield their spectra $X(f)$ and $Y(f)$. In the frequency domain, the transfer

and coherence functions of the recorded signals are computed using Equations (3.1) through (3.4).

$$G_{xx}(f) = X(f) \cdot X^*(f) \quad (3.1)$$

$$G_{yx}(f) = Y(f) \cdot X^*(f) \quad (3.2)$$

$$\psi(f) = \frac{G_{yx}(f)}{G_{xx}(f)} \quad (3.3)$$

$$\gamma^2(f) = \frac{G_{yx}(f) \cdot G_{yx}^*(f)}{G_{xx}(f) \cdot G_{yy}(f)} \quad (3.4)$$

where:

$G_{xx}(f)$ is the auto-power spectrum of receiver R₁,

$G_{yy}(f)$ is the auto-power spectrum of receiver R₂,

$\psi(f)$ is the transfer function of the recorded signals, and

$\gamma^2(f)$ is the coherence function of the recorded signals.

From the phase information of the transfer function and the coherence function for the different receiver spacings, a shear wave velocity versus wavelength profile for the test site is generated using Equations (3.5) through (3.9).

$$\phi_{yx} = \tan^{-1} \left[\frac{\text{Im}(G_{yx})}{\text{Re}(G_{yx})} \right] \quad (3.5)$$

$$t(f) = \frac{\phi_{yx}}{(360 \cdot f)} \quad (3.6)$$

$$V_r(f) = D / t(f) \quad (3.7)$$

$$\lambda_r(f) = V_r(f) / f \quad (3.8)$$

$$V_s = (1.135 - 0.182 \cdot \nu) \cdot V_r \quad (3.9)$$

where:

ϕ_{yx} is the phase shift of the cross power spectrum in degrees at each frequency,

$t(f)$ is the travel time of surface waves at different frequencies from R_1 to R_2 ,

$V_r(f)$ is the surface wave velocity for different frequencies,

$\lambda_r(f)$ is the wavelength of surface waves for different frequencies, and

V_s is the shear wave velocity.

The plot of shear wave velocity with wavelength is commonly referred to as the experimental dispersion curve. The dispersion curve is inverted to obtain the elastic modulus versus depth profile using Equations (3.10) and (3.11).

$$G = \rho \cdot V_s^2 \quad (3.10)$$

$$E_{SEIS} = 2G(1+\nu) \quad (3.11)$$

where:

G is the shear modulus,

E_{SEIS} is the low-strain seismic modulus, and

ν is the poisson's ratio.

The inverted profile is used to compute the forward model, which should approximate the experimental dispersion curve. The forward model is commonly referred to as the theoretical dispersion curve. Inversion and forward modeling is an iterative procedure whereby the forward model is refined and improved, yielding a forward model that is representative of the section being tested (Aouad, 1993). In this study, WINSASW (version 1.23) software based upon the Haskell-Thomson algorithm (1953) was used. SASW data was collected using a portable data acquisition computer manufactured by Olson Engineering (Wheat Ridge, Colorado). The sensors used included uni-axial

accelerometers manufactured by PCB Piezotronics and 4.5 Hz geophones manufactured by Geo Space Corporation. TFS software, provided by Olson Engineering, was used for data acquisition and processing to obtain the transfer function. WINSASW software was used to construct the experimental dispersion curves and to perform the forward modeling.

A number of studies have been performed to assess the ability of SASW to measure layer moduli and thickness. Nazarian et al. (1988) found that backcalculated layer thicknesses differed by 4-20% with those specified in construction drawings. SASW moduli were within 30% of the moduli determined using the FWD. Roesset et al. (1990) concluded that the SASW back-calculated thickness of the AC surface layer matched almost exactly with cores from a test site.

Rix et al. (1990) reported that surface layer modulus for PCC determined by SASW was within 10% of the in-situ value determined from crosshole testing and that of other near-surface layers to about 10–30% of in-situ values. Al-Hunaidi (1991) reported SASW results that over predicted the thickness of aged AC pavement layers by 40%. AC overlay thickness was underpredicted by about 4%. He attributed this to limitations imposed by available transducers. Nazarian et al. (1995) also reported a deviation of 20% in the backcalculation of PCC thickness using the SASW method. Nazarian et al. (1999) reported that for AC layers, in-situ moduli back-calculated by SASW was very close to that determined in the laboratory with seismic methods. For the base and the subgrade, Nazarian et al. (1999) reported good agreement between seismic moduli measured in the field and in the laboratory as long as density and moisture contents of the materials are similar. Nazarian et al. (1999) also conclude that moduli measured with seismic methods

are higher than those obtained from other testing methods such as the resilient modulus and FWD testing. Addo (2000) concluded that AC thickness could be estimated with SASW testing to an accuracy of about 6% if the AC is in a good condition.

Recent advancements in computer hardware and software have helped make data acquisition significantly less challenging. In spite of these advances, an inspector has to rely on personal judgment during field data collection to decide if the acquired signals are acceptable. The shape of the time and frequency domain signals, the coherence between the two receivers and peak amplitude of generated waveforms aid the inspector in signal acquisition. Tawfiq et al. (2002) demonstrate that this may not be enough and that further guidance in defining adequate signals is necessary. They developed an irregularity factor (α) to address this issue and aid in field data collection.

Findings of National Cooperative Highway Research Program's project 10-44a (Hanna, 2002) on the determination of in-situ material properties of asphalt concrete (AC) pavement layers indicate that a) comparable moduli values for AC pavement layers are obtained from FWD and SASW based Seismic Pavement Analyser (SPA) measurements; b) no correlations could be established between the in-situ moduli from FWD or SPA tests and dynamic moduli determined from laboratory testing; c) seismic technology offers advantages over deflection based methods but requires skilled personnel for data-reduction and analysis.

Yuan et al (2005) found that PCC core moduli obtained using ASTM C-469 were approximately 75% of SASW estimated moduli. Asphalt concrete behavior is more complex as asphalt is a viscoelastic material. As such, properties of asphalt are temperature and rate or frequency of loading dependant. Aouad (1993) presented a

scheme for adjustment of the seismic modulus. This consists of first correcting the seismic modulus for temperature. Many relationships exist that recommend means for temperature adjustment. However, a comprehensive model that is universally accepted does not exist. Aouad (1993) used Equation (3.12) to adjust the seismic modulus to a reference temperature of 77°F.

$$\frac{E_t}{E_{77}} = 1.35 - 0.0078(t - 32) \quad (3.12)$$

Where

t is the field temperature during testing, and

E_t is the field estimated SASW modulus and E_{77} the SASW modulus adjusted to 77°F.

Gucunski et al. (2006) developed a similar procedure to correct shear wave velocity of highway pavements in New Jersey for temperature. As described by Aouad (1993) the temperature corrected modulus must also be corrected for the rate of loading. Figure 3-2 illustrates that depending on the pavement temperature, moduli measured with seismic methods should be reduced by a factor of about 3 to 15 to approximate moduli values from FWD testing. All SASW moduli used in the current research were corrected for temperature using Equation (3.12).

3.4 Results

The classification of SASW-estimated modulus profiles into pavement layers was performed using consistent, rational modulus limits for pavement materials. Core thicknesses were reported to the nearest 0.5 inches as the bottom of extracted cores were

“rough” thus these numbers are average values. For both AC and PCC pavements, the error in estimation was computed as in Equation (3.13).

$$\%Error = \frac{t_{SASW} - t_{core}}{t_{core}} \times 100 \quad (3.13)$$

Where,

t_{SASW} = thickness of pavement surface layer estimated using SASW in inches, and

t_{CORE} = thickness of core extracted in inches.

3.4.1 Comparison of SASW modulus variation with DPI variation and boring logs

Figures 3-3, through 3-7, present comparisons using the results of pavement coring, SASW tests and inversion, visual-manual soil classification and laboratory testing, as well as DCP tests.

3.4.1.1 Test sites with AC surface layers

Figure 3-3, 3-4 and 3-5 present data for test sites with for AC pavement surface layers. As presented in the figures, SASW and DCP test data are analyzed to classify the pavement section into pavement layers.

The pavement section at the first test site (Figure 3-3) comprises a 6 inch AC pavement surface layer. The SASW modulus (E_{SEIS}) profile reveals two asphalt layers - a 2.4 inch thick surface layer with a modulus of 600 ksi above a 3.1 inch layer with a modulus of 825 ksi. SASW estimates the modulus of the surface layer to be lower than that of the second asphalt layer. The boring log indicates that the core was retrieved in broken pieces. Thus, at this test site, SASW under estimates total AC layer thickness by about 8%. Figure 3-4 presents results of testing at Mangum’s Scott Field. From the boring log, thickness of the extracted core is taken to be 3.5 inches. The SASW modulus

profile indicates a 3.1 inch thick high modulus (1200 ksi) layer. Thus at this test site SASW under estimates AC pavement surface course thickness by 11%. Figure 3-4 presents results of testing at Chandler Municipal. The boring logs give the thickness of the extracted core as 4.0 inches. SASW results estimate the thickness as 6.0 inches, i.e. an error of 50%.

From the boring log for test site 1 (Figure-3-3) it is observed that there is a 2 inch layer of coarse sandy gravel immediately below the asphalt surface layer. This layer of sandy gravel is supported over silty clay. From the DPI profile in Figure 3-3 a stiff layer extending from the core to a depth of 16 inches is observed. Below this stiff layer, from the increased DPI a softer zone extending from a depth of 16 inches to 27 inches is observed. And immediately below this layer, stiffer soil is indicated by the reduced DPI values recorded from a depth of 27 inches to about 37 inches. DCP test results were not available beyond this depth. The variation of E_{SEIS} with depth exhibits a drastic drop in modulus from 825 ksi to 15 ksi from 5.5 inches to a depth of 35 inches. This is suggestive of a softer zone below the AC surface layer. Below a depth of 35 inches, the modulus increases to about 25 ksi. The boring log provides evidence of three layers below the AC surface layer. DPI variation from DCP tests suggests that soil layers in the structure to a depth of 37 inches could be considered to be three layers. The variation of E_{SEIS} with depth in Figure 3-3 substantiates the existence of only two layers.

From the boring log presented in Figure 3-4, a 5.5 inch thick clayey layer is observed below the AC layer. Below this, a 12 inch layer of silty sand over 15 inches of silty clay and 10 inches of hard clay are observed from the boring log in the figure. DPI data is available from a depth of 9.1 inches to a depth of 37 inches. The low DPI response

from 9.1 inches to 17 inches suggests a stiff soil layer at this depth. From a depth of 17 inches to 34 inches, higher DPI values are observed suggesting the presence of a softer layer of soil. Due to lack of information below 37 inches, increased stiffness of the pavement subgrade is not detected by the DCP though an extrapolation of the DPI trend points towards a stiffer subgrade beyond a depth of about 38 inches. The variation of E_{SEIS} in Figure 3-4 suggests three layers. The first of these layers is suggested to be 6 inches thick with E_{SEIS} of 31 ksi, followed by a layer with lower E_{SEIS} of 16 ksi extending from a depth of 9.1 inches to about 33.1 inches supported over a layer with a higher E_{SEIS} of 24 ksi.

From the boring log in Figure 3-5, 11 inches of clayey sand is observed below the AC layer. Below this 17 inches of clay supported over 16 inches of clayey sand is observed. DPI data is available to a depth of 36 inches. Based on the DPI variation in Figure 3-5, three layers with differing stiffnesses are suggested. Immediately below the AC surface layer, a stiff layer extending from a depth of 5 inches to a depth of 10 inches is observed. Below this, increased DPI suggest a softer layer extending from 10 inches to 30 inches. Below this layer stiffer DPI response is observed. SASW results, i.e., variation of E_{SEIS} with depth, suggests the existence of a single layer, 42 inches thick with a constant E_{SEIS} of 16 ksi.

3.4.1.2 Test sites with PCC surface layers

Figures 3-6 and 3-7 present comparisons as in the previous section for test sites with PCC surface layers. The pavement structure was classified as distinct layers based upon the variation of E_{SEIS} and DPI along the depth of the tested section. The results of this analysis are compared in this section.

Figure 3-6 presents the results of tests performed at Chickasha Municipal. As evidenced by the boring log, a 7 inch PCC core was extracted from the test site. From E_{SEIS} data, a surface layer 3.1 inch thick with a modulus of 6000 ksi over a 6.6 inch layer with a modulus of 2617 ksi is observed. Comparing SASW results with the boring log, it is observed that the PCC thickness is over estimated by 39%. Figure 3-7 presents the results of tests performed at Halliburton Field. A 7 inch PCC core was extracted from the test site. From E_{SEIS} data, a surface PCC layer with total thickness of 8.6 inches is observed. Comparing SASW results with the boring log, it is observed that the PCC thickness is over estimated by 23.4%.

From the boring log presented in Figure 3-6, a 4 inch thick hard silty clay layer is observed immediately below the concrete surface layer. This layer rests over a 37 inch thick clayey layer. DPI data is available from a depth of 8 inches to 37 inches. The initial low DPI response of soil layers from 8 inches to 14 inches indicates a layer of stiff soil. Below this layer based upon the higher DPI response observed, a layer of lower stiffness from 14 inches to 37 inches is inferred. From the variation of E_{SEIS} a 1.2 inch thick layer with a modulus of 152 ksi is observed. Below this layer E_{SEIS} falls to about 24 ksi. SASW results therefore estimate two soil layers 1.2 inches and 37 inches thick while DCP results estimate two layers of soil with thicknesses of 6 inches and 23 inches.

From the boring log presented in Figure 3-7, an 8 inch thick layer of sandy clay is observed immediately below the concrete surface layer. This layer rests over a 3 inch thick silty clayey layer. Below this a 7 inch thick clayey layer over 23 inches of silt clay is reported in the boring log. DPI data is available from a depth of 8 inches to 36 inches. The low initial DPI response from a depth of 8 inches to 14 inches indicates a stiff soil

layer. Below this layer, higher DPI response is observed in the Figure suggesting the presence of a layer of lower stiffness from a depth of 14 inches to 22 inches. Beyond a depth of 22 inches, lower DPI response is observed suggesting a layer of increased stiffness. From the variation of E_{SEIS} a single, 39 inch thick layer, with a modulus of 32 ksi is substantiated. SASW results therefore estimate a single soil layer that is 39 inches thick while DCP results estimate three layers of soil with thicknesses of 6 inches, 8 inches and 14 inches.

3.4.2 Efficacy of AC surface layer thickness determination

Table 3-1, Figure 3-8 and Figure 3-9 present the average % error of SASW based determination of AC pavement t_{SASW} and t_{CORE} . Figure 3-8 includes error bands for 30% error in prediction from the $Y = X$ line. The data in the table and the illustrations in Figures 3-8 and 3-9 indicate that the % error in thickness was the highest for thin AC pavements i.e. nearly 59% for cores less than 2 inches. The error reduces with increasing surface layer thickness. This inference is supported by Figure 3-9 – a plot of % error against core thickness. The error reduced to 4.7% for cores ranging in thickness from 4 inches to 5 inches. From data presented in Table 3-1 and Figures 3-8 and 3-9, it is concluded that for cores less than 6 inches thick, SASW generally over estimated thickness. And, for cores thicker than 6 inches, SASW generally under estimated thickness. From Figure 3-8 it is observed that a linear regression of SASW estimated thicknesses with actual core thicknesses provides a coefficient of determination (r^2) value of 0.41.

The large difference in SASW estimated AC pavement surface layer thickness for core thicknesses less than 3 inches is attributed to the inability of the test equipment to

generate the extremely high frequency stress waves required to sample shallow thicknesses. Over estimation of thickness for cores thicker than 6 inches occurs as the inversion procedure is not sensitive to the change in the velocity of the layer immediately below the surface layer because of the large velocity contrast between the layers. Also, some of the error in estimation of surface layer thickness using SASW results is caused by the error involved in core thickness measurements. For example, an error of 0.5 inches in measuring a core 2 inches thick would cause a 25% error due to the measurement accuracy alone.

Since FAA's pavement design guidelines specify a minimum AC pavement thickness of 3 inches, accuracy of thickness determination for cores thicker than 3 inches is of significance for the current study. The data indicates that for cores thicker than 3 inches, SASW's estimation of pavement surface layer thickness is observed to deviate 2.4% to 14% different from the actual thickness. A weighted average analysis using all data indicated that in general, SASW's determination of AC pavement thickness over estimated extracted core thickness by 4.4%.

3.4.3 Efficacy of PCC surface layer thickness determination

Table 3-2, Figure 3-10 and Figure 3-11, present details about the efficacy of the SASW method in estimating PCC surface layer thicknesses. Figure 3-10 presents a comparison of SASW's estimate of PCC pavement thickness with thickness determination by core extractions. Like Figure 3-8, Figure 3-10 includes error bands for 30% error in prediction from the $Y = X$ line. Table 3-2 and Figure 3-11 depict the variation of error (%) in SASW's estimate of pavement thickness computed using Equation (3.13). From Table 3-2 it is observed that PCC pavement surface thickness is

consistently over estimated by SASW. The determination generally improves with increasing thickness and is worst for core thickness between 6 and 7 inches (Table 3-2, Figure 3-11). A weighted average analysis using all data indicated that in general, SASW method over estimated PCC pavement thickness by 14%.

The difference in SASW estimates for PCC pavements are caused by the limitations of the Haskell-Lemon (1953) algorithm to model sharp deviations in moduli. Over-estimation of PCC surface layer thickness is caused as the inversion procedure is not sensitive to change in the velocity of the layer immediately below the surface layer because of the large velocity contrast between the layers. Also, some of the error in estimation of surface layer thickness using SASW results is caused by the error involved in core thickness measurements as explained in the previous section.

3.5 Conclusions

The SASW method provides a potentially valuable tool for the mechanistic characterization of in-service GA airport pavements. AC pavement thickness was over estimated for pavement sections less than 6 inches thick. Since FAA's pavement design guidelines require a minimum thickness of AC pavements of 3 inches, this does not impact efficacy of the procedure. From the results of the current study it is observed that for AC pavements greater than 3 inches, estimate of pavement thickness from SASW tests deviated from actual by 2.4% to 13.7 %. From a weighed average analysis using data from all tested sections, the estimation of AC pavement thickness from SASW tests was found to over estimate extracted core thickness by 4.4%. PCC pavement thicknesses were consistently over estimated by SASW testing. SASW's estimates of PCC pavement thickness were found to deviate from core sizes by 11.2% to 26.4%. A weighted average

analysis using all data indicated that in general, SASW results over estimated PCC pavement thickness by 14%. Comparison of SASW estimated pavement layer thicknesses with boring logs indicate a lack of SASW's ability to discover soil layer changes.

3.6 References

- Addo, K.O., “*Innovations in Urban Infrastructure: A Non-Destructive Pavement Evaluation Tool for Urban Roads*”, Report NRCC 53. CPWA, 2000
- Al-Hunaidi, O.M., “*Nondestructive profiling of pavement sites using the surface wave method*”, Proc., 44th Canadian Geotechnical Conference, Calgary, Alberta, Canadian Geotechnical Society, 1991, pp. 12-1 – 12-9.
- Aouad, M.F., “*Evaluation of Flexible pavements and subgrades using the spectral analysis of surface waves (SASW) method*”, University of Texas Austin, 1993.
- Gucunski, N., Zaghoul, S. , Maher, A. and Hadidi, R., “*Development of Seasonal Variation Models of Pavement Properties Using Seismic Nondestructive Testing (NDT) Techniques*,” Proceedings of GeoCongress 2006, Atlanta, Georgia, 2006.
- Hanna, A.N., “*Determination of In-situ Material Properties of Asphalt Concrete Pavement Layers from Nondestructive Tests*,” NCHRP Research Results Digest, Number 271, December 2002.
- Haskell, N.A., “*The dispersion of surface waves on multilayered media. Bulletin of Seismological Society of America*,” No. 43, 1953, pp. 14 – 34.
- Ishihara, K., “*Soil Behavior in Earthquake Geotechnics*,” Oxford Science Publications, Oxford, 1996.
- Nazarian, S., Stokoe, K.H. II, and R.C. Briggs, “*Determination of pavement layer thickness and moduli by SASW method*,” Transportation Research Record 1196, Transportation Research Board, National Research Council, Washington D.C., 1988, pp. 133-150.
- Nazarian, S., Baker, M., and K. Crain., “*Determination of pavement layer thickness and moduli by SASW method*,” Transportation Research Record 1505, TRB, National Research Council, Washington D.C., 1995, pp. 1-8.
- Nazarian, S., Yuan, D., and V. Tandon, “*Structural field testing of flexible layers with seismic methods for quality control*,” Transportation Research Record 1654, TRB, National Research Council, Washington D.C., 1999, pp. 1-27.
- Rix, J.R., and K.H. II Stokoe, “*Stiffness profiling of pavement subgrades. In Transportation Research Record 1235*,” TRB, National Research Council, Washington D.C., 1990, pp. 1–9.

Roesset, J.M., Chang, D., and K.H. II Stokoe, “*Modulus and thickness of the pavement surface layer from SASW tests*”, Transportation Research Record 1260, TRB, National Research Council, Washington D.C., 1990, pp. 53-63

Sanchez-Salinaro, I., “*Analytical investigation of seismic methods used for engineering applications*,” Ph.D. Dissertation, University of Texas at Austin, 1987.

Seed, H.B., and I.M. Idriss, “*Soil Moduli and Damping Factors for Dynamic Response Analysis*,” Report EERC 70-10, University of California, 1970.

Tawfiq, K., Armaghani, J. and J. Sobanjo, “*Rational Method for selecting Seismic Waves for Pavement Evaluation*,” Journal of transportation engineering, Vol. 128, No. 6, November 2002.

Yuan, D., Nazarian, S., Perea, A. and Zhang, D., “*Relating seismic modulus to strength parameters of Portland cement concrete*,” Research Report 1700-8, Center for infrastructure systems, University of Texas at El Paso, 2005.

Table 3-1: Comparison of SASW estimated AC pavement surface layer thickness with core thickness

Core Thickness Range	% Error in layer thickness estimation*
1" < Core ≤ 2"	58.9%
2" < Core ≤ 3"	33.5%
3" < Core ≤ 4"	13.7%
4" < Core ≤ 5"	4.7%
5" < Core ≤ 6"	-2.4%
6" < Core ≤ 7"	-10.7%
7" < Core ≤ 8"	-6.9%
8" < Core ≤ 9"	-10.9%
> 9"	-10.2%
ALL CORES	4.4%

* A positive number implies over prediction of core-thickness and a negative number indicates under-prediction of core thickness

Table 3-2: Comparison of SASW estimated PCC pavement surface layer thickness with core thickness

Core Thickness Range	% Accuracy in layer thickness estimation
4" < Core ≤ 6"	12.6%
6" < Core ≤ 7"	26.4%
7" < Core ≤ 8"	20.2%
8" < Core ≤ 9"	21.0%
> 9"	11.2%
ALL Cores	14.0%

* A positive number indicates over-prediction of core-thickness and a negative number indicates under-prediction of core thickness

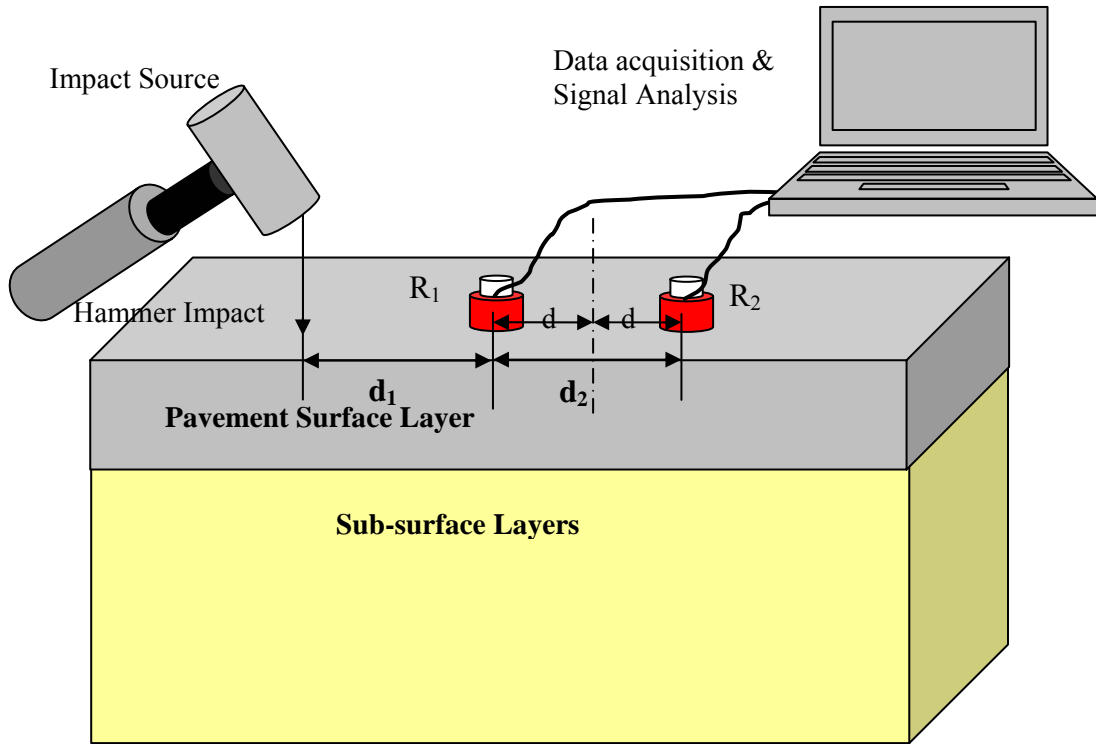


Figure 3-1: SASW Test Setup

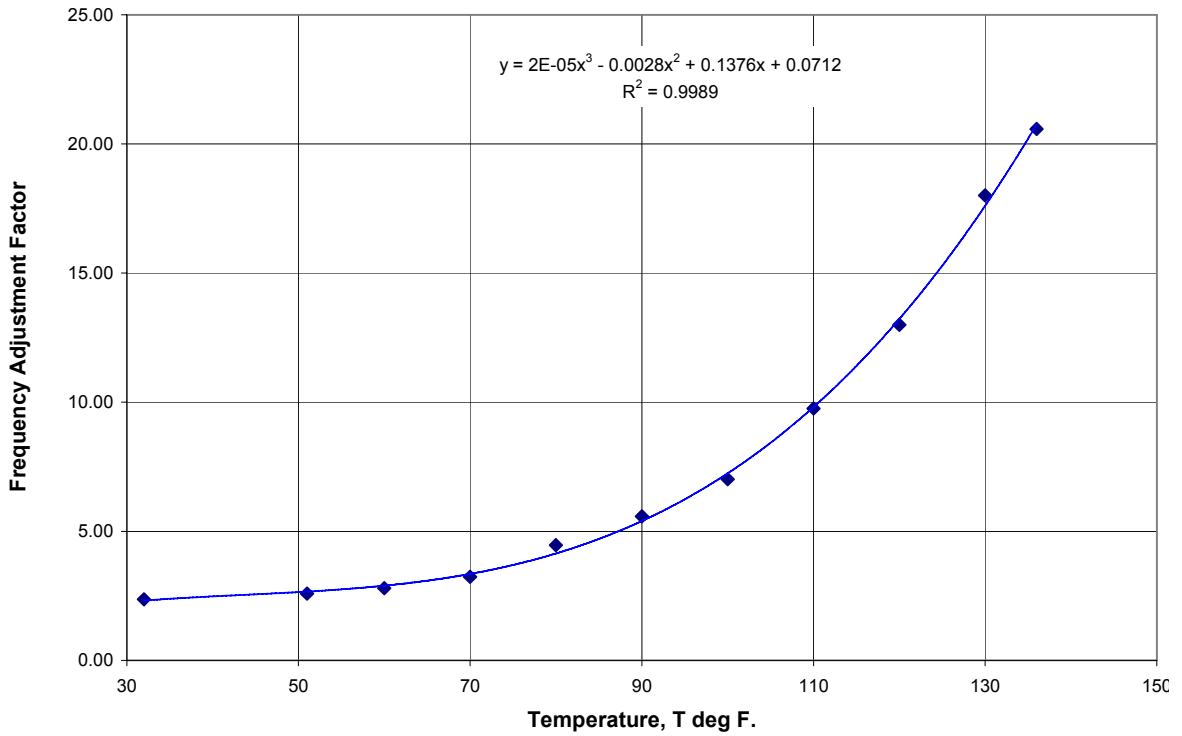


Figure 3-2: Variation of frequency adjustment factor with temperature for asphalt concrete per Aouad, (24)

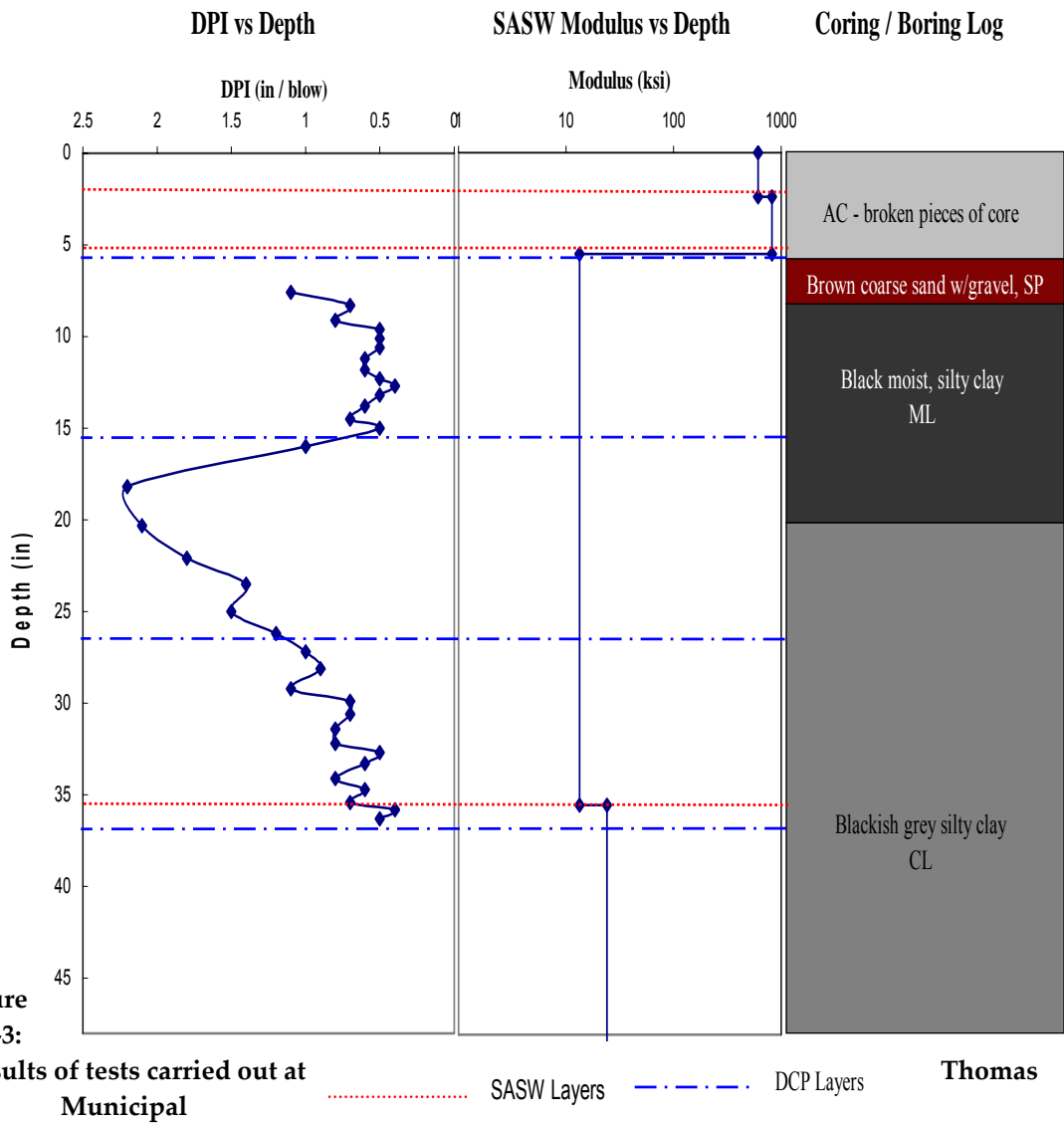


Figure 3-3:
Results of tests carried out at
Municipal

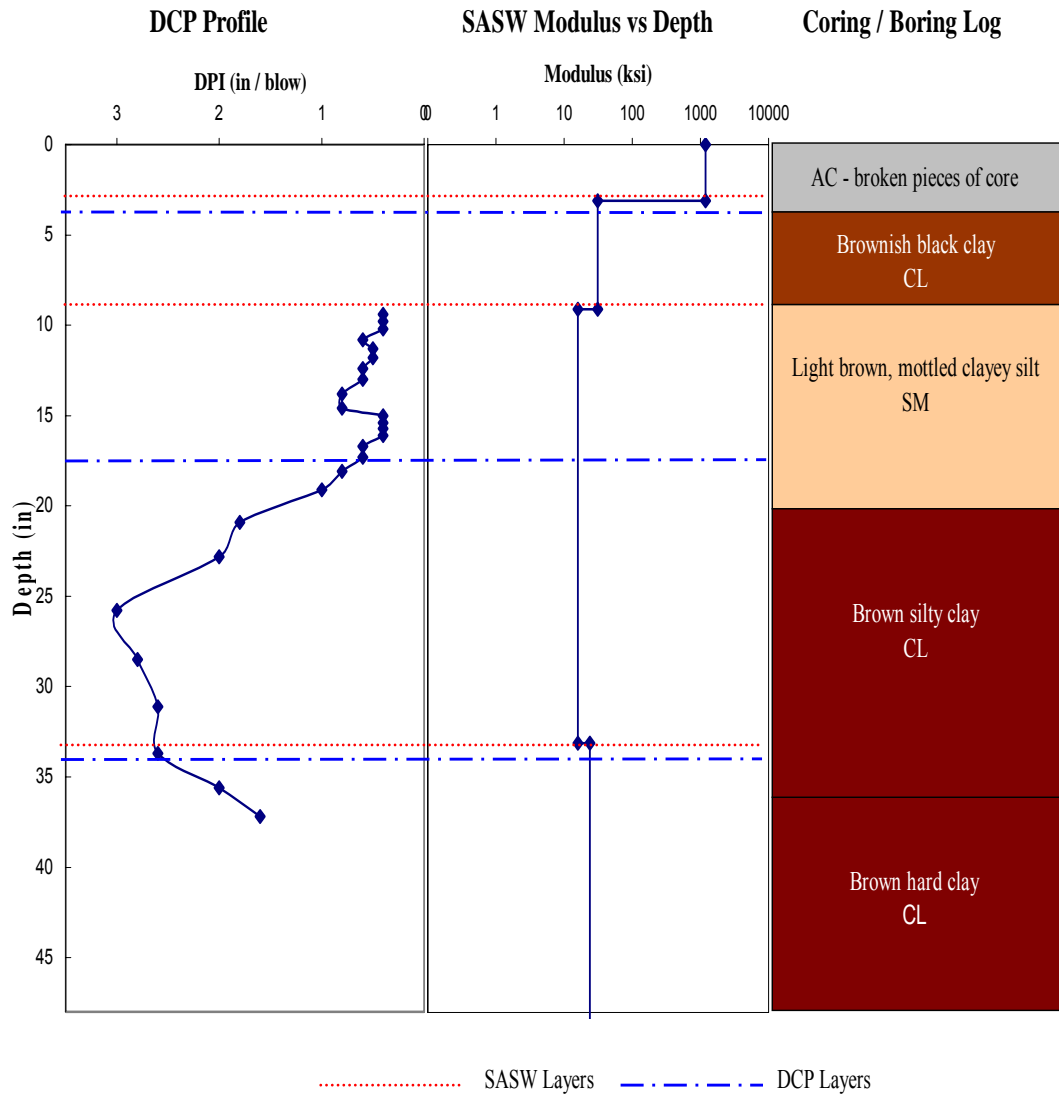


Figure 3-4: Results of tests carried out at Mangum's Scott Field

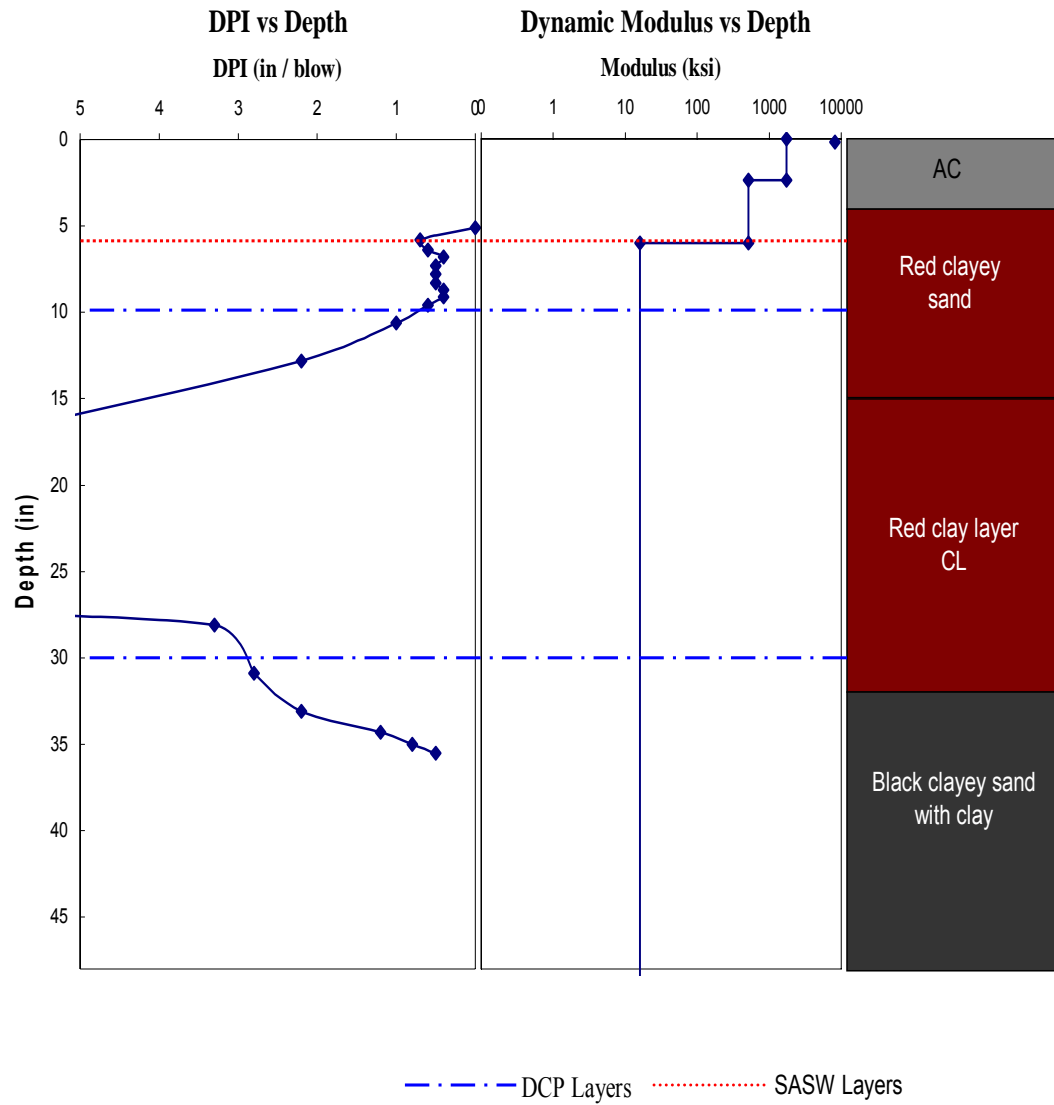


Figure 3-5: Results of tests performed at Chandler Municipal

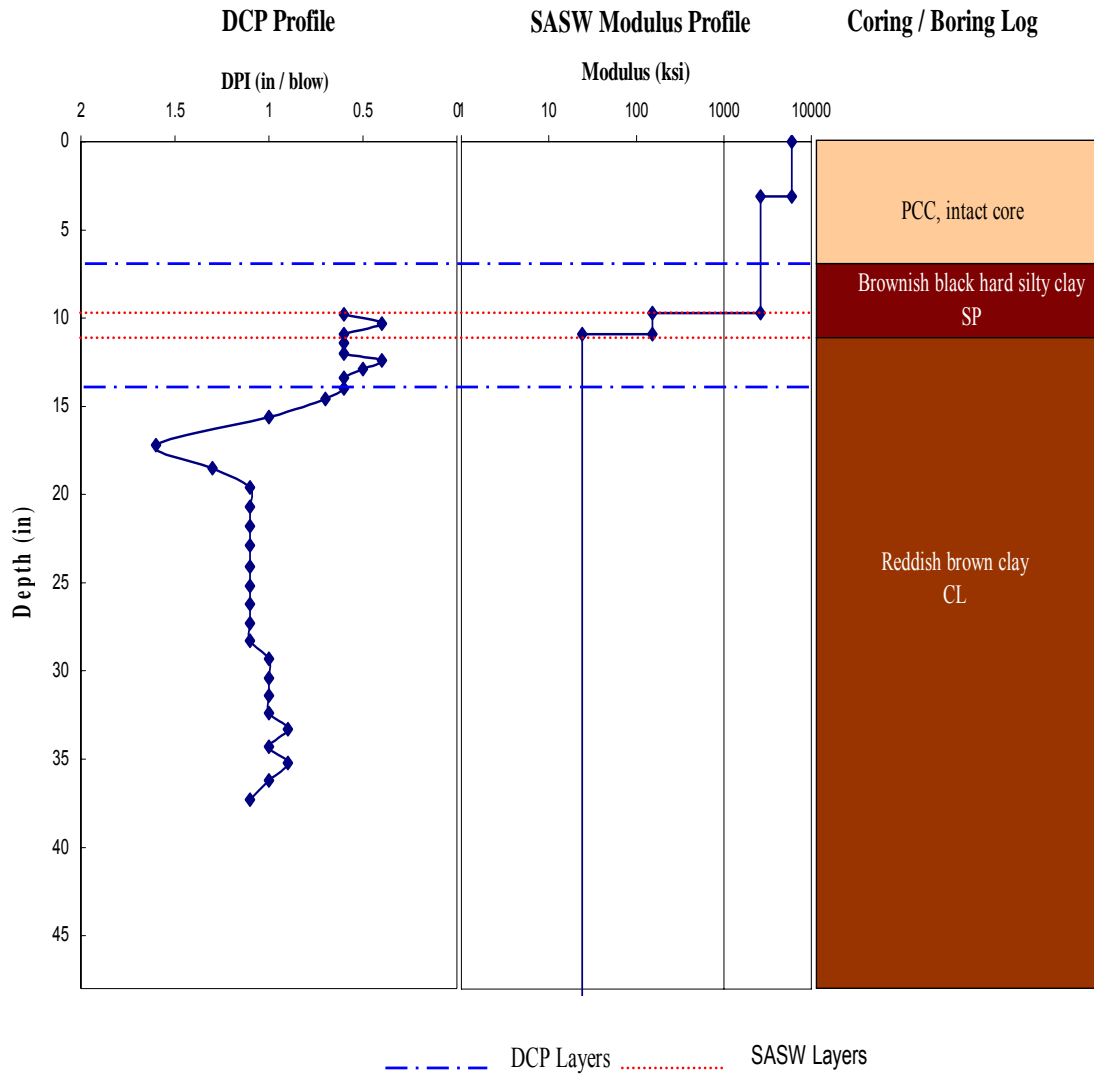


Figure 3-6: Results of testing at Chickasha Municipal

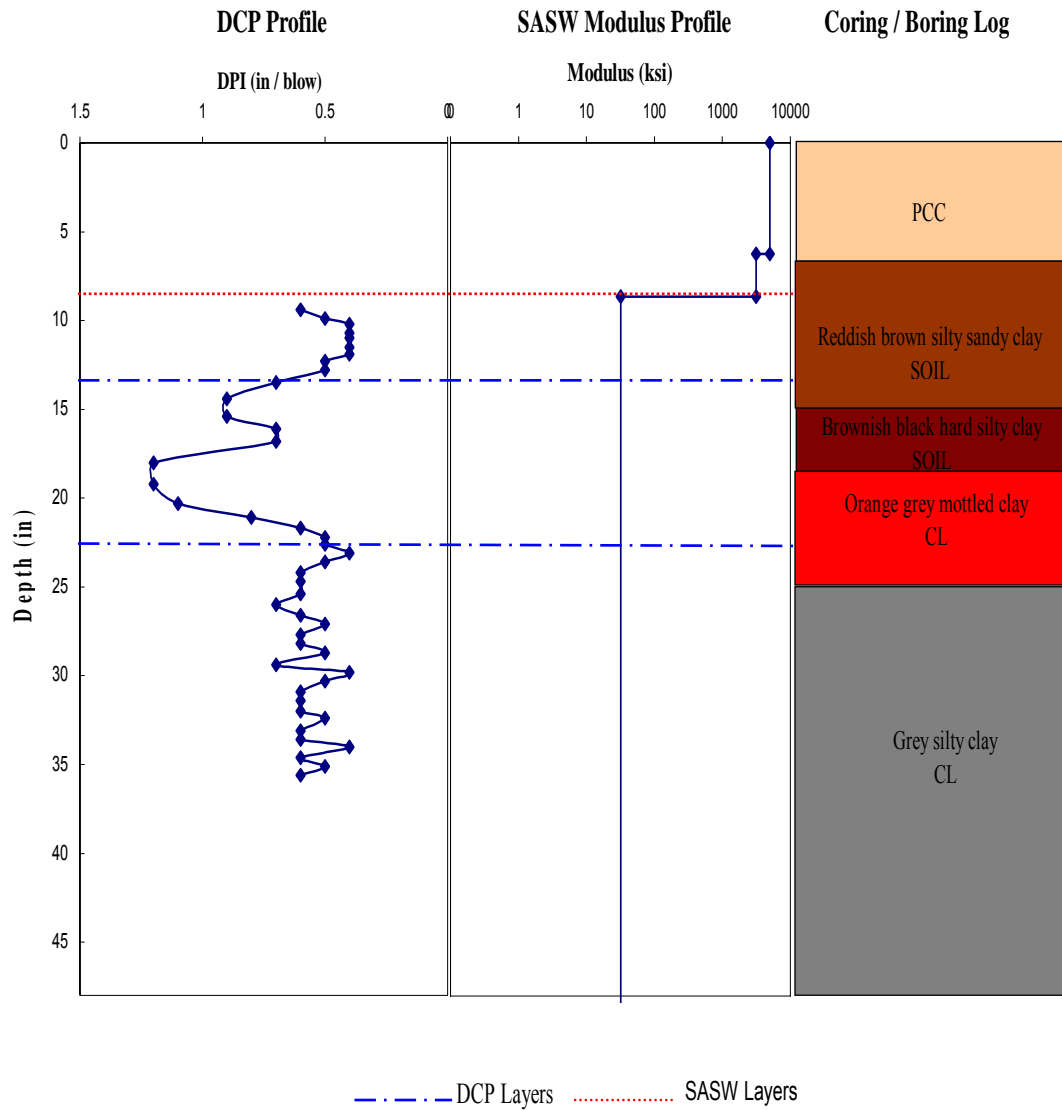


Figure 3-7: Results of tests performed at Halliburton Field

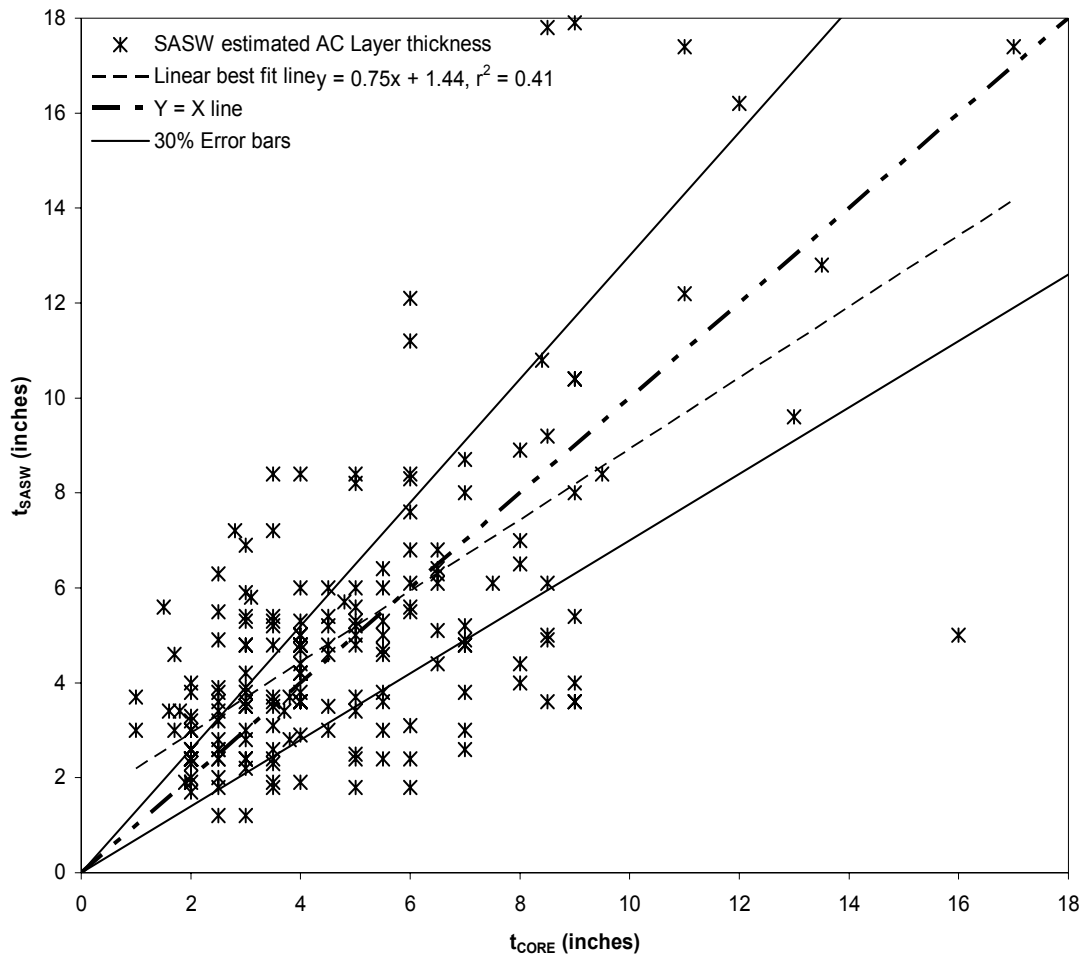


Figure 3-8 Efficacy of AC pavement surface layer thickness determination from SASW testing

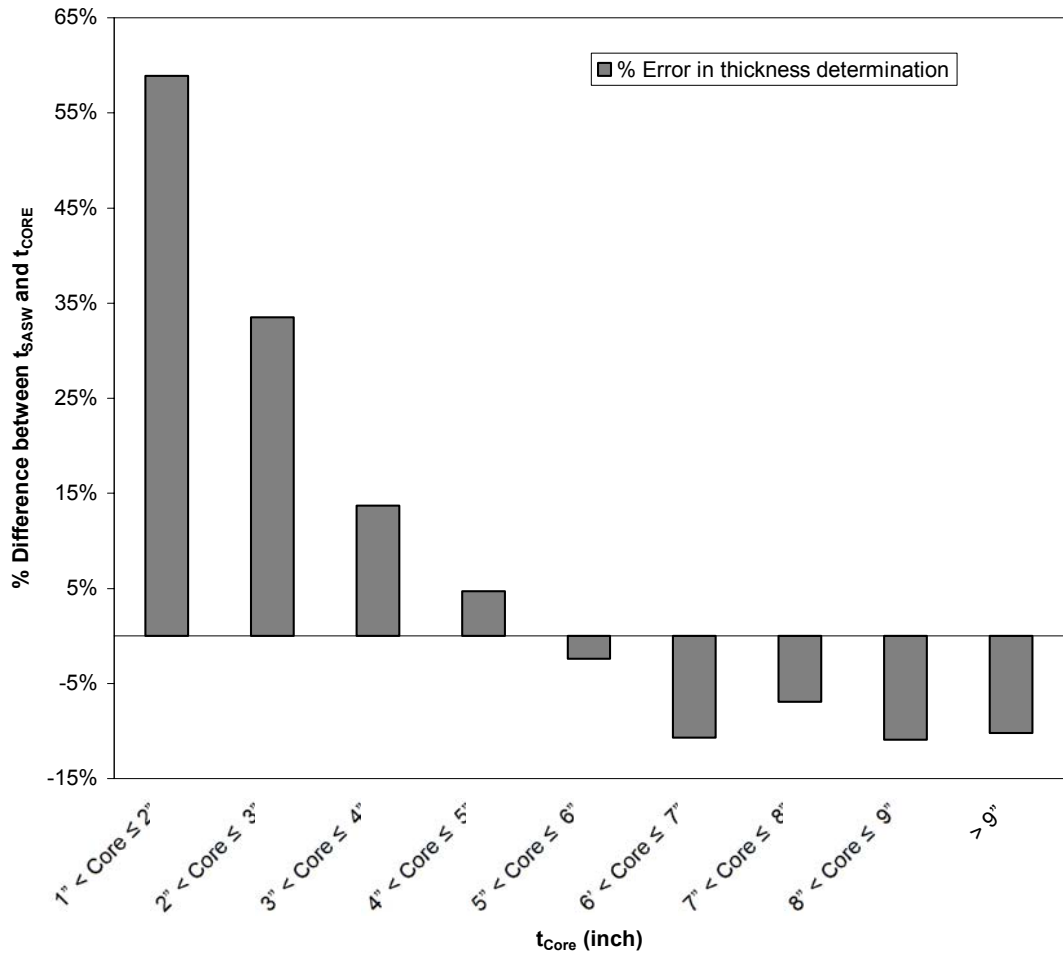


Figure 3-9: Variation of % error in determination of AC pavement thickness using SASW method

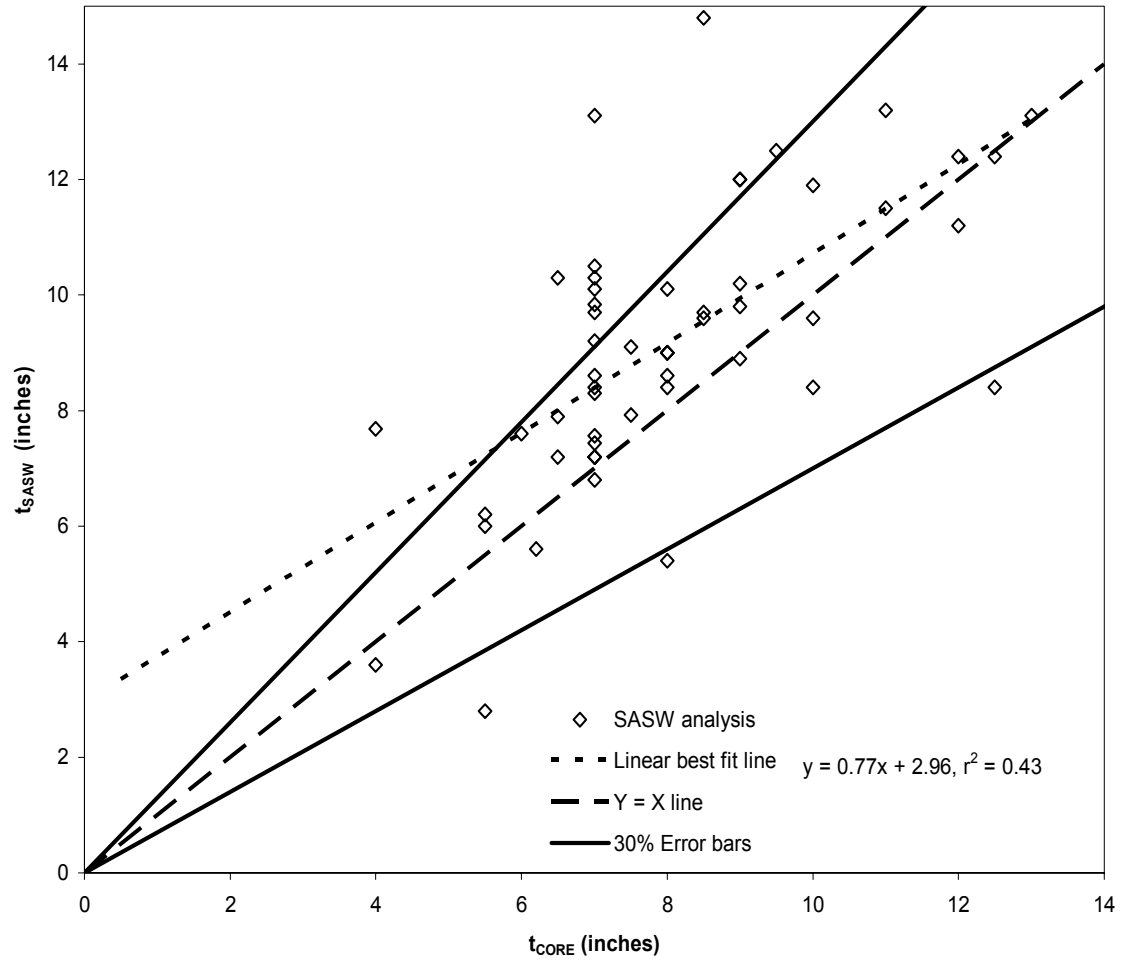


Figure 3-10: Efficacy of PCC pavement surface layer thickness determination from SASW testing

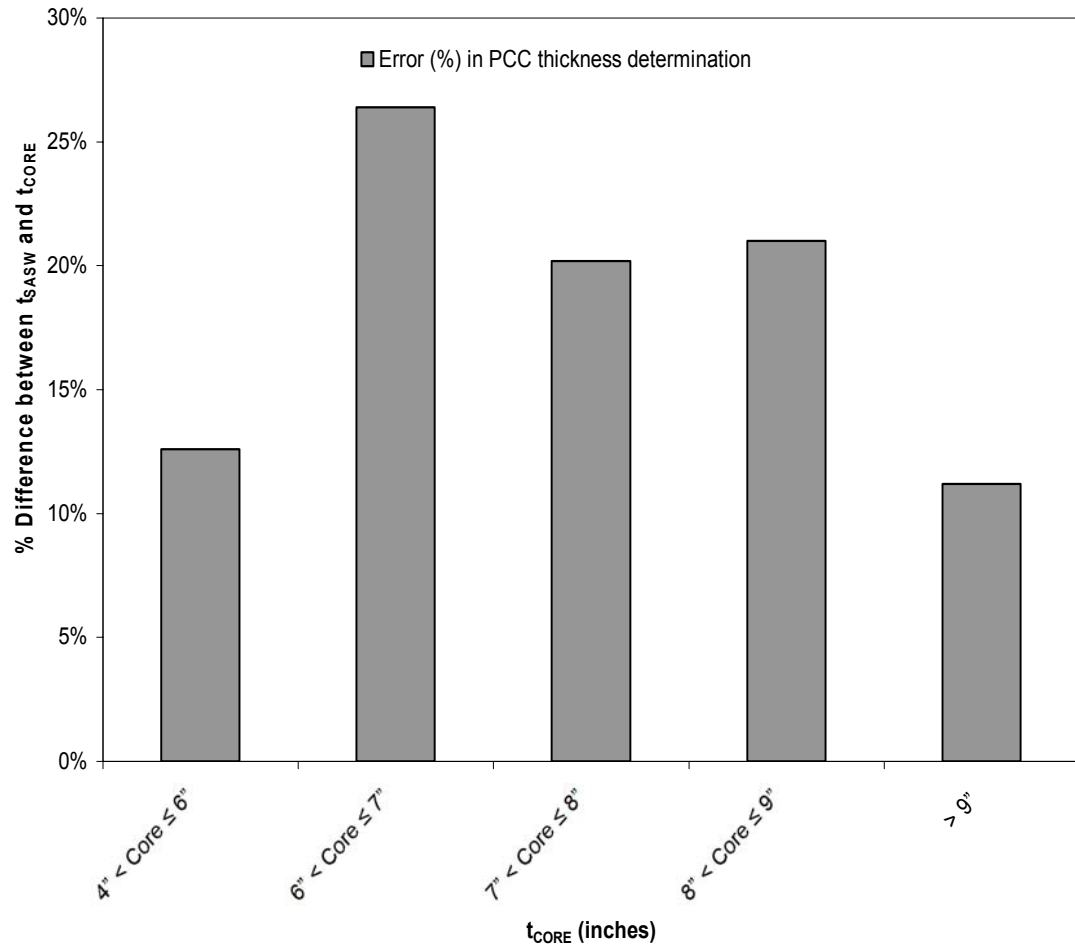


Figure 3-11: Variation of %error in thickness determination

Chapter 4 Exploring AC and PCC Modulus Degradation via SASW for use in Airfield Pavement Management

4.1 Introduction

Current and future pavement conditions in airport PMSs are typically based upon visually observed distresses in airport pavement management (Gendreau and Soriano 1998, Sanford-Bernhardt et al. 2003, Broten and De Sombre 2001). In this approach, performance evaluation and prediction utilize the principles and procedures described in SHRP-P-338 and ASTM D5340 to determine a pavement condition index (PCI). The PCI reflects a range of visually observed distresses, e.g., cracking, rutting, raveling, swelling, patching, scaling, pumping, joint deterioration, settlement, etc. Future pavement functional performance is predicted by employing suitable regression analysis of PCI data using the family approach developed by Shahin (1994) to classify pavement sections into pavement families based upon similarities of environmental conditions, traffic, pavement structure, pavement use, etc. Maintenance and rehabilitation (MR) strategies are selected using the critical PCI procedure (Shahin and Walter 1990), results of several life-cycle cost analyses, and from the dynamic programming network optimization analysis.

The PCI approach measures some distresses that indirectly relate to structural degradation, e.g., cracking, rutting, yet there is no well-defined relationship between structural and functional performance (Zaniewski 1991). Therefore, PCI-based PMSs are generally unable to assess current and future structural performance (Paine 1998). There is a need to advance pavement management by adding a mechanistic dimension. With the

increasing use of in-situ testing methods there is an opportunity to integrate structural and geotechnical data into PMSs.

The current study aims to provide a mechanistic measure of pavement condition using the SASW method. A visual distress based characterization of a pavement's condition presumes that surface distresses can describe what the pavement is experiencing. Based on this assumption a methodology to determine current and future pavement condition using the visually estimated PCI is in use with federal and state agencies. The current study aims to provide a rational, mechanistic measure of pavement condition using the SASW method.

A key objective of this study therefore was to determine if AC and PCC layer moduli degraded with pavement age and if this degradation could be used to characterize pavement condition. Assuming layer moduli did degrade, a second objective aimed to devise the most suited methodology to subdivide Oklahoma's GA airport pavements network into smaller units with similar modulus deterioration characteristics. SASW results provide the additional benefit of providing a damage analysis based, project level estimate of the tested section's remaining life.

The study also sought to evaluate the relationship between modulus degradation and PCI decay and investigate the existence of a correlation between them. In accordance with the objectives of the study, SASW tests and visual distress surveys were conducted at 81 General Aviation (GA) airports in Oklahoma over a 5-year period (2000-2005).

4.2 Summary of Data Collected

The current study draws upon SASW testing and visual distress observation at 156 AC site locations and 52 PCC site locations conducted from 2000 to 2005. Tests at

25 AC and 3 PCC test sites were performed twice to directly examine possible degradation. Test locations included runways, taxiways and aprons. AC pavements tested varied in age from 0 to 47 years and age of PCC pavements tested ranged from 0 to 59 years. Based on coring, AC pavement thicknesses varied from 1 inch to 17 inches thick and PCC thickness varied from 4 inches to 18 inches. Pavement structures also varied in terms of structure, e.g., existence of drainable base course, and in construction history, e.g., overlays, etc. Tables 4-1 and 4-2 summarize the important pavement characteristics. Figures 4-1(a) and 4-1(b) illustrate data presented in the tables.

To enable the effective comparison of modulus degradation and PCI degradation, SASW tests were conducted on various sections consistent with ASTM D5340. Testing on runway sections was given a higher priority. Additional tests conducted at these locations included destructive testing, e.g. coring with boring, and dynamic cone penetration (DCP) testing in the bore hole after extraction of the pavement core. Coring was performed after SASW testing had been completed in-order to maintain undisturbed conditions. Upon extraction of the pavement core and the completion of DCP testing, soil samples to a depth of 4 ft, or auger refusal were recovered using a hand auger. The processed data therefore yielded low-strain elastic moduli (E_{SEIS}) for pavement layers, PCI, Dynamic Penetration Index (DPI) variation with pavement depth from DCP testing, index properties of soil and core thicknesses. The results from SASW testing and PCI were used in conjunction with construction history information for the test sites to develop pavement performance models (PPM).

4.3 Modulus Degradation

Yuan and Mooney's analysis (2003) using PCI data with the family grouping methodology (Shahin, 1994) resulted in the subdivision of Oklahoma's GA airport pavement network into 11 pavement families. In the current study, Yuan and Mooney's methodology as well as additional classification factors were explored. For each classification methodology an identification tag was assigned to the family groupings generated. The tags use a XX (m, n) format, where XX represents the pavement surface type, i.e. AC or PCC, m the trial number (1st trial, 2nd trial etc.), and n the family number of the mth trial.

The following family grouping factors were evaluated:

1. AC(1,1) – All AC pavements were collected in a single family.
2. AC(2,1) through AC(2,6) – AC pavements with similar load resisting thickness and similar type of layers were grouped together. Using collected geotechnical data, the total thickness of “structurally-capable” pavement layers at a test site was estimated, i.e., the total thickness of the surface layer, aggregate or stabilized layer for each tested section. AC pavement sections with total load-resisting thickness less than 10 inches were tagged as thin and those thicker than 10 inches were identified as thick. Further, thick and thin AC pavements with an aggregate base or a stabilized base were grouped into distinct, separate families.
3. AC(3,1) and AC(3,2) – Family groupings were derived using a procedure similar to that in 2 above, i.e. based on similar load resisting thickness of pavement sections. However, in this trial, the existence of aggregate or stabilized base layers was ignored and only the total load resisting thickness was used to generate pavement families.

4. AC(4,1) through AC(4,7) – Family groupings were obtained by applying the procedure devised by Yuan and Mooney (2003) to tested AC pavement sections.
5. AC(5,1) and AC(5,2) – Pavement sections were grouped into families based on similar dominant distresses exhibited. A pavement section was taken to exhibit either dominant load or dominant environmental distresses if greater than 50% of visual distress based deducts were caused by traffic related or environmental distresses, respectively.
6. PCC(1,1) – All tested PCC sections were grouped in a single family.
7. PCC(2,1) through PCC(2,6) – PCC Pavements with similar load resisting thickness and similar make-up of pavement sections were grouped together.
8. PCC(3,1) through PCC(3,4) – Family groupings were obtained by applying Yuan and Mooney’s (2003) analysis to PCC pavements.
9. PCC(4,1) and PCC(4,2) – Like in 5, tested PCC pavement sections were grouped into families based on similarity of observed dominant visual distresses.

The number of pavement families obtained by applying the above and the goodness of regression are summarized in following sections. A constrained multi-degree polynomial regression procedure was employed (Lawson and Hanson 1974) to characterize modulus degradation. The problem formulation in the present study is similar to that used by Yuan and Mooney (2003).

Minimize

$$\|Y_i - A(x_i)\| \tag{4.1}$$

where:

Y_i is E_{SEIS} of the i^{th} pavement section,

$$A(x_i) = a_0 + a_2x^2 + \dots + a_nx^n \quad (4.2)$$

x_i is the age of the i^{th} pavement section, and

n = polynomial regression order.

Subject to a) Slope constraints, i.e. $\frac{\partial Y_i}{\partial x_i} \leq 0$ (4.3)

The value of a_0 in Equation (4.2) is specified by the user. The study uses an outlier detection procedure (Equation 4.5) based on standardized residuals e_i^* evaluation for a 95% confidence interval. The standardized residuals are calculated from the residuals, e_i .

$$e_i = Y_i - \hat{Y}_i \quad (4.4)$$

Where \hat{Y}_i is the fitted/predicted E_{SEIS} of the i^{th} pavement section at age x_i .

$$|e_i^*| \cong \frac{e_i}{s} > 1.96 \quad (4.5)$$

Yuan and Mooney (2003) evaluated the goodness of fit for each family model using the value of the coefficient of determination (r^2), the number of outliers and the square root of the average squared error of prediction called the standardized error of the estimate (SEE).

$$r^2 = 1 - \frac{\sum_i^N (Y_i - \hat{Y}_i)^2}{\sum_i^N (Y_i - \bar{Y})^2} \quad (4.6)$$

where:

N is the number of inspections in the family under evaluation,

\bar{Y} is the mean, and

and Y_i, \hat{Y}_i have meanings as defined previously.

Usually r^2 is interpreted as the percent of the "dependent" variable that is "explained" by the "independent" variable. Thus, $r^2 = 1$ indicates that the fitted model explains all variability in y , while $r^2 = 0$ indicates no 'linear' relationship between the response variable and regressors. An r^2 value of 0.7 may be interpreted to indicate that approximately seventy percent of the variation in the response variable can be explained by the independent variable. The remaining thirty percent is attributed to the scatter, variability in the data.

Cohen (1988), for example, has suggested the interpretations in Table 4-3 for correlations in psychological research. Cohen observes, however, that all such criteria are in some ways arbitrary and should not be observed too rigidly. This is because the interpretation of a correlation coefficient depends on the context and purposes. A correlation of 0.9 may be very low if one is verifying a physical law using high-quality instruments, but may be regarded as very high in the social sciences where there may be a greater contribution from complicating factors.

The standard deviation (SD), SEE, and standard error of measurement (SEM), are commonly used to characterize the goodness-of-fit. These parameters are related, but measure different physical quantities. SD can be characterized as measuring the variability of sample observations, and SEE provides an estimate of the dispersion of the prediction errors for prediction of Y values from X values in a regression analysis. In other words, SEE is a measure of the variability, or scatter, of the observed sample Y values around the regression line. SD can be written as

$$\sigma = \sqrt{V_x} \quad (4.7)$$

SEE is given as

$$SEE = \sqrt{\frac{\sum_{i=1}^n (Y_i - \hat{Y}_i)^2}{n - k - 1}} \quad (4.8)$$

Where

σ is the standard deviation of the family grouping,

k is the polynomial regression order,

n is the number of data points in the data set, and

V_x is the variance of the data = $\frac{1}{(n-1)} \sum_{i=1}^n (Y_i^2 - \bar{Y}^2)$.

Though regression analysts generally like the SEE to be as low as possible, there is no guidance available on how low it should be. Guidance is however, available for the relative standard error (RSE) or the coefficient of residual variability. This is explained in Equation (4.9).

$$RSE = \frac{SEE \times 100}{\bar{Y}} \quad (4.9)$$

Regression analysts desire regression models with RSE lower than 15%. However, this traditional expectation is not observed in pavement data due to the scatter of data points and also due to the difficulty in characterizing such a large object with a few sample points. Therefore, regression models with RSE values lower than 20% are considered adequate.

It is also pertinent to point out that conventional wisdom leads one to expect that increasing values of the coefficient of determination (r^2) will result in lower standard deviation and lower SEE/RSE values. As observed from Equations (4.7) and (4.8), both SD and SEE are computed from the square of the residuals, i.e. square of the difference

in fitted and actual data values. It is expected that with higher correlations, i.e. increasing r^2 , the sum of the residuals ($\sum e_i^2$) will reduce. In the present research, outliers are identified in every regression run. Identification of outliers can impact the sum of residuals and cause SEE to increase with increasing correlations.

Pavement performance models (PPM) were selected in the present study based on combined rankings from a set of regression runs using linear, 2nd order and 3rd order polynomials and assigning ranks for r^2 , RSE and the number of outliers. The PPM with the lowest total rank for all three parameters was selected to model the modulus decay with age of the family being evaluated. While developing PPMs it is important to bear in mind that sample sizes smaller than 30 cannot be adequately approximated by a normal distribution (Mendenhall and Sincich, 2003). It is accepted that for most sampled populations sample sizes of $n \geq 30$ suffice for the normal approximation to be reasonable.

4.3.1 Asphalt Pavements

Figure 4-2 presents the decrease of E_{SEIS} with age using a family grouping composed of all tested AC pavements, i.e. family AC(1,1). The figure includes plots of 1st to 3rd order regression as well as the best-fit equations, r^2 and RSE values and the number of outliers for each. Using the total ranking approach described earlier, the 3rd order model is observed to best represent E_{SEIS} decay with age for the AC pavements tested. In the selected 3rd order model, E_{SEIS} for AC pavements is observed to degrade in an ‘s-shaped’ curve over 37 years. In the first 10 years E_{SEIS} decreases linearly from 2200 ksi to 1250 ksi. From 10 to 25 years, modulus is observed to fall 200 ksi. For pavement age greater than 25 years, the third order model indicates that E_{SEIS} decays at a faster rate than for age between 10 and 25 years. At an age of 37 years a residual modulus of about

60 ksi is observed. The RSE value ranges from 22.9% to 24.6% and r^2 from 0.32 to 0.46 indicating significant scatter in the data.

The high RSE values and low r^2 values of family AC(1,1) reiterate the need to further divide the available test data into smaller units to better characterize variables that influence modulus degradation. The sub-divisions attempted and their key statistical parameters for AC pavements are summarized in Table 4-4.

The first sub-division attempted was based upon the total thickness and type of “structurally-capable” layers in the pavement section. Structurally-capable pavement layers were taken to include the AC surface layers and aggregate or stabilized bases. AC pavements with total thickness of this “structurally capable” section less than 10 inches were classified as thin and those with thickness in excess of 10 inches were classified as thick. This methodology led to division of SASW test data for AC pavements into 6 families (see Table 4-4 for details) – AC(2,1) through AC(2,6). Of these, families AC(2,4) and AC(2,6) included 4 and 6 tests each and are not used for regression analysis. Only 22 SASW tests were performed in pavements grouped into family AC(2,2) and 14 in pavements classified as family AC(2,3). Though the number of tests in each of the above was fewer than 30, regression analysis was performed with the assumption that data was normally distributed. Also, a correlation of modulus decay with pavement age for family grouping AC(2,3) could not be established even with the assumption of normal distribution.

Figure 4-3 depicts the decay of E_{SEIS} with age for pavements grouped into family AC(2,1). The figure presents 1st to 3rd order regression models and includes key regression parameters. A 3rd order polynomial is observed to best fit the data with an r^2 of

0.38, 5 outliers (8.6%) and a RSE under 10%. From the Figure it is observed that the r^2 value for the selected model is not very high and falls in the range of medium significance based on Cohen's (Table 4-3) analysis. Figure 4-4 depicts the deterioration of E_{SEIS} for family AC(2,2) comprising of thin AC pavements with aggregate or gravel bases. Using the ranking procedure described earlier, the 3rd order polynomial was selected to model modulus decay with age. The selected model has a significant r^2 of 0.86, and RSE lower than 15% with 3 Outliers i.e. 13% of the total data. The high correlation validates the assumption that data was normally distributed. Figure 4-5 presents deterioration with age of AC modulus for family AC(2,5) comprising of thick AC pavements with aggregate or gravel bases. The figure shows considerable scatter in the data which is borne out by the high RSE values, in excess of 30% for each model. The 3rd order model provides the best fit with a significant r^2 of 0.59 but with nearly 17% outliers and a high RSE of 30.5%. Though RSE values for family AC(2,5) were higher than expected, the current sub-division methodology could be taken to have met expectations. However, it is pertinent to note that with the current size of the database, 3 of the sub-divisions included fewer than 30 tests.

Using only the total thickness of structurally-capable layers, all tested AC pavements were classified into two families. Figures 4-6 and 4-7 illustrate E_{SEIS} degradation for AC pavements with thickness of the “structurally capable section“ less than 10 inches (i.e. family grouping AC(3,1)) and with thickness greater than 10 inches (i.e. family AC(3,2)), respectively. Figure 4-6 presents 1st to 3rd order regression analysis for the deterioration of E_{SEIS} with age of pavements grouped in family AC(3,1). The 3rd order model ranks highest and is taken to best fit the family data. The selected model has

a significant r^2 of 0.61, 13 outliers or 28% of total data and RSE lower than 20%. The r^2 and RSE values lend credibility to the model even though there are a significant number of outliers. Figure 4-7 presents deterioration of E_{SEIS} observed in thick AC pavements. The r^2 value for the 1st to 3rd order regression models depicted in the figure range from 0.39 to 0.51, with RSE ranging from 27.4% to 32.5%. The linear and 2nd order models have 1 outlier each or 1% of total data. There are 7 outliers or nearly 8% of total data to the 3rd order model. The 3rd order model ranks the highest and is therefore taken to best-fit the test data. This selected model has a significant r^2 and low outliers but high RSE indicative of large scatter.

Since the results of this study may potentially be used for predicting the condition of Oklahoma's GA airport pavements, it is important to investigate the suitability of existing PCI based family groupings devised by Yuan and Mooney (2003) for use with modulus data. As evidenced in Table 4-4, three of the resulting family groupings i.e. AC(4,5), AC(4,6) and AC(4,7) comprising of tests performed on taxiway and apron pavements included fewer than 10 tests each. Regression analysis was not performed for these family groupings. Also, there are fewer than 30 tests in each of family AC(4,2) and AC(4,4). Regression analysis was performed for these family groupings with the assumption that data are normally distributed. Regression results were inconclusive for family AC(4,1).

Figure 4-8 illustrates the decay of E_{SEIS} of AC pavements with age for family AC(4,2). The figure presents results of 1st to 3rd order regression analysis. Large scatter observed in the data is confirmed by RSE values in excess of 28% for each of the three models. The r^2 values for the models shown in the figure range from 0.46 to 0.57 and

there are 0 to 8% outliers. Figure 4-9 presents the result of regression analysis using tests performed on pavements grouped in family AC(4,3). The 3rd order polynomial ranks highest and is selected to model pavement performance for the family grouping. The selected model exhibits a significant r^2 of 0.61, RSE of approximately 15% and 6 outliers (i.e. 16% of total data). Figure 4-10 presents decay with age of AC pavement modulus for family AC(4,4). From the figure large scatter in the data is observed and E_{SEIS} data beyond 20 years of pavement age was not available. The 3rd order polynomial ranks highest and is selected to model pavement performance for this family grouping. The selected model exhibits an r^2 value of 0.36, 4.2% outliers and RSE of 26.7%. Regression results of pavement families obtained using Yuan and Mooney's (2003) sub-division methodology yields significant results. However, regression could not be performed for 4 of the 7 pavement families (Table 4-4).

Family AC(5,1) and AC(5,2) are derived by grouping all AC pavements that exhibit similar dominant visual distress together. From the data it is observed that there is no GA airport pavement in Oklahoma's network with visual, load related dominant distress. Consequently the distribution achieved is identical to that of family AC(1,1) and therefore regression effort was not duplicated.

Table 4-5 presents significance ranks for each family grouping procedure evaluated in this study in an effort to determine the most suited methodology for modulus data. As presented in the table, regression results were ranked for r^2 values, percent outliers, and RSE values. A ranking score was estimated from the sum of these ranks for each case analyzed. Using this rank score, an overall rank for each sub-division methodology was estimated. Using the number of SASW tests in each case, a weighted

rank was calculated for each family grouping methodology. A simple average of ranks for each family grouping methodology was also computed. Table 4-5 presents the significance rank for each sub-division methodology using – a) a simple average, and b) the weighted average. Using ranks based on a simple average, the family grouping procedure based on total thickness of “structurally capable” pavement layers produced the best results with the simplified structure based grouping coming in second. Using a weighted average analysis, family grouping AC(2,x) outperformed the rest. However, all other family groupings were observed to perform equally well and came in joint-second.

4.3.2 Portland Cement Concrete Pavements

In Figure 4-11, E_{SEIS} is observed to degrade over 60 years of pavement life. The figure depicts the decrease of E_{SEIS} with age with all tested PCC pavements grouped into a single family - PCC(1,1). From the figure it is observed that E_{SEIS} of new PCC pavements (approximately 7,000-8,000 ksi) degrades in a generally linear fashion until age 25, at which point it continues to degrade though at a slower rate. 1st through 3rd order polynomial regressions are shown in the figure. The best-fit equations along with r^2 , RSE and number of outliers are shown within each graph. The 3rd order polynomial is determined to best approximate E_{SEIS} data for the family with an r^2 of 0.75, RSE lower than 15% and approximately 13% outliers.

As in the case of AC pavements, data was sub-divided into smaller units to better characterize variables that influence modulus degradation. The sub-divisions attempted and their key statistical parameters are placed in Table 4-6. As a first attempt pavements were divided into families based upon the total thickness of “structurally capable layers” in the pavement section. PCC pavements with thickness of this “structurally capable”

section less than 10 inches were classified as thin and those with thickness in excess of 10 inches were classified as thick. This methodology led to division of SASW test data for PCC pavements into 6 families – PCC(2,1) through PCC(2,6). Only family grouping PCC(2,1) comprising thin PCC pavements with neither an aggregate nor a stabilized base had in excess of 30 SASW tests. Family grouping PCC(2,2) (thin PCC pavements with aggregate base) and family grouping PCC(2,6) (thick PCC pavements with stabilized base) did not include any test data. Families PCC(2,3), PCC(2,4) and PCC(2,5) included fewer than five SASW tests each. Therefore regression could be performed on family grouping PCC(2,1) alone. Figure 4-12 presents the results of the regression analysis performed on family grouping PCC(2,1). A linear model was selected to model the decay of E_{SEIS} with time. The model exhibited an r^2 value of 0.88, lower than 10% RSE and approximately 18% outliers. With the exception of the outliers, there is low scatter in the data, borne out by the low RSE.

Again, as in the case of AC pavements, it is of interest to explore the suitability of Yuan and Mooney's (2003) analysis for family groupings based on visual distress to develop PPMs for modulus decay with age of PCC pavements. As evidenced in Table 4-6, fewer than 5 tests were performed in families PCC(3,3), and PCC(3,4) including taxiway and apron pavements. Regression analysis could not be performed for these family groupings. Although, there are fewer than 30 tests in each of family PCC(3,1) and PCC(3,2), regression analysis was performed with the assumption that data was normally distributed. Figure 4-13 details the results of regression analysis on pavements grouped in family PCC(3,1). The r^2 values ranged from 0.81 to 0.86 for the 1st to 3rd order models presented in the figure. Also, as observed from the figure and Table 4-6, RSE values for

each of the depicted models was lower than 15% and there were 3 to 5 outliers (12% to 20%). The linear model was selected to approximate the family's pavement performance. Figure 4-14 depicts decay of E_{SEIS} with age for pavements grouped in family PCC(3,2). The models exhibit high r^2 , low outliers (8%) and RSE values lower than 15% indicating low scatter of test data. The 3rd order polynomial is selected to model the family's modulus decay with age.

Family PCC(4,1) included PCC pavements that exhibit dominant, visually inferred, environmental distress. Of the 110 PCC pavement sections tested, only 9 sections were classified as exhibiting visually determined, dominant traffic related distress. The sections exhibiting visually inferred, dominant traffic related distress were identified as family PCC(4,2). Since family PCC(4,2) comprised of fewer than the required 30 SASW tests, regression analysis could not be performed for data included in it. Regression was performed for family PCC(4,1). Figure 4-15 presents the results of the regression analysis. A linear model was selected. The model exhibited significant r^2 of 0.82, lower than 15% RSE and approximately 23% outliers. Based on the RSE and r^2 , it is concluded that there is low variability in the data.

Table 4-7 presents significance ranks for each family grouping procedure evaluated in this section in an effort to determine the most suited methodology for modulus data of PCC pavements. As presented in the table, regression runs were ranked for r^2 values, percent outliers, and RSE values. As in the case of AC pavements, significance ranks were determined using a simple average score of family ranks as well as using a weighted average score. From the table it is observed that grouping of all pavements into a single family (family PCC(1,1)) produced the worst results. Pavements

grouped using thickness of “structurally capable” layers - family PCC(2,x), and Yuan and Mooney’s (2003) analysis - family PCC(3,x), were the top performers.

4.3.3 Relationship between Modulus Degradation and PCI Degradation

A comparison between E_{SEIS} degradation and PCI degradation is important to investigate the existence of a correlation between a pavement’s PCI and its structural adequacy. In the previous section, it emerged that family groupings devised on the basis of the total thickness of “structurally-capable” layers in a pavement section produced the best regression results for both AC and PCC pavements. In this section all previously developed regression models for AC and PCC pavements are compared with the PCI degradation models. PCI degradation curves using Yuan and Mooney’s (2003) analysis (available at <http://apms.aeronautics.ok.gov>) were used for the current analysis. Where PCI degradation curves were not available, these were developed using Oklahoma Aeronautics Commission’s (OAC) database of PCI data with the Lawson-Hanson (1974) algorithm. Figures 4-16 through 4-24 present comparisons of E_{SEIS} and PCI decay for AC pavements. Figures 4-25 through 4-29 present the comparison for PCC pavements.

Figure 4-16 presents a comparison of E_{SEIS} degradation with PCI degradation using all tested AC pavements grouped into a single family. The PCI degradation curve was generated using OAC’s database of PCI data and the Lawson-Hanson algorithm (1974). The E_{SEIS} degradation curve exhibits an RSE value of 23.0% compared to PCI degradation’s RSE value of 11.35%. The PCI degradation curve exhibits a significant r^2 while E_{SEIS} degradation has an r^2 value of medium significance. The modulus is estimated to fall from 2200 ksi to 0 in about 37.3 years, while PCI is predicted to reduce to zero between 65 to 70 years.

Figure 4-17 compares E_{SEIS} degradation with PCI degradation for family grouping AC(2,1). The degradation trend observed in both curves is similar with RSE value for E_{SEIS} degradation observed to be lower at 19.7% compared to RSE value of 24.0% for the PCI degradation. Figure 4-18 presents the comparison for family grouping AC(2,2). The E_{SEIS} deterioration model exhibits a lower RSE value (19.7%) compared to that of the PCI curve of 30.7%. The E_{SEIS} model exhibits an r^2 value of large significance (0.86) while the PCI degradation model exhibits an r^2 value of small significance. Figure 4-19 illustrates the E_{SEIS} and PCI degradation curves for family grouping AC(2,5). The PCI curve, generated using OAC's database shows a significant r^2 of 0.93 and an RSE of 8.5%. The trends of PCI and E_{SEIS} degradation are similar though the latter has a lower, yet significant, r^2 of (0.59) with a higher RSE of 30.5% indicating greater scatter in the modulus data.

Figures 4-20 and 4-21 present a comparison of E_{SEIS} and PCI degradation for families AC(3,1) and AC(3,2), respectively. In Figure 4-20, dissimilar trends of E_{SEIS} and PCI decay are observed. E_{SEIS} data exhibits greater scatter (RSE=17.8%), than PCI data (RSE=8.6%). Both E_{SEIS} and PCI fall to zero by about 39 years. Figure 4-21 presents a comparison of PCI and E_{SEIS} deterioration for pavement sections classified as family AC(3,2). From the figure it is observed that PCI degrades by approximately 45% while E_{SEIS} degrades by 64% at the end of 15 years of pavement life. From 15 to 30 years rate of E_{SEIS} decay decreases. From the data, E_{SEIS} is estimated to reach a value of zero modulus at an age of 37 years. The PCI curve on the other hand flattens out beyond the initial sharp decrease.

In the case of families devised using Yuan and Mooney's (2003) analysis, Figures 4-22, 4-23 and 4-24 illustrate similar initial decay of E_{SEIS} with diverging decay from that point onwards. Extrapolating the E_{SEIS} decay model, modulus is estimated to fall to zero at an age of 37.5 years for families AC(4,3) and AC(4,4) and 46 years for family AC(4,2). RSE values for E_{SEIS} degradation vary from 15.5% to 28.4% and from 17.9%-18.3% for PCI degradation, reiterating greater scatter in E_{SEIS} data. Also, r^2 values for E_{SEIS} degradation models are generally lower than those for PCI degradation models.

Figure 4-25 presents a comparison between E_{SEIS} and PCI degradation with age for all tested PCC pavements. The PCI degradation was estimated using OAC's database and Lawson-Hanson's algorithm (1974). The E_{SEIS} degradation curve exhibits an r^2 value of 0.75, interpreted as exhibiting large significance. The PCI degradation also exhibits an r^2 value (0.61) of large significance. RSE values for both data are close indicating comparable scatter. The age at which PCI degrades to zero is estimated as 64 years from the figure, while the age at which E_{SEIS} decays to zero is observed to be about 70 years.

Figure 4-26, depicts a comparison between E_{SEIS} and PCI decay with age for family PCC(2,1) devised using the total thickness of "structurally capable" sections. In the Figure, a linear regression model for E_{SEIS} decay is presented. For both the PCI and E_{SEIS} data, scatter is observed to be comparable and r^2 values are also close. However, the real difference is in the shape of the regression models and the age at which the degradation curves reach a value of zero. Extrapolating the best fit models, PCI value is estimated to degrade to zero at section age of approximately 65 years while E_{SEIS} degrades to zero at an age of about 118 years.

Figure 4-27, depicts a comparison between E_{SEIS} and PCI decay with age for family PCC(3,1) devised using Yuan and Mooney's (2003) analysis. From the Figure, scatter, inferred from RSE values, is observed to be comparable and r^2 values are also close. Extrapolating the best fit models, PCI is estimated to degrade to zero at an age of 65 years while E_{SEIS} is estimated to degrade to zero at an age of about 116 years. Figure 4-28 compares PCI and E_{SEIS} data and their degradation with age for family PCC(3,2). Though the key statistical measures for both data are comparable, the trends of the curves are dissimilar. It is estimated that E_{SEIS} will degrade to zero at an age of 73 years and PCI would degrade to zero by an age of 75 years.

Figure 4-29 compares the selected linear E_{SEIS} decay model for family PCC(4,1) with the 5th order degradation model for PCI devised by Yuan and Mooney (2003). RSE values of the two models are comparable with r^2 for E_{SEIS} degradation (0.79) being slightly higher than the r^2 for PCI degradation (0.64). It is observed that PCI decreases to zero at a pavement age of 68 years while E_{SEIS} is estimated to decrease to zero at an age of 116 years.

Figures 4-30 and 4-31 examine the existence of a correlation between E_{SEIS} and PCI degradation for AC pavements. From Figure 4-30 it is observed that a correlation between SASW based structural adequacy of AC pavements and their visual distress based PCI rating could not be established. This analysis was taken a step further and E_{SEIS} was plotted against PCI computed using structural distresses like alligator cracking and rutting, alone. Figure 4-31 depicts the variation of E_{SEIS} with PCI computed from structural distresses. Again, no correlation is observed to exist between an AC E_{SEIS} and PCI. Figure 4-32 depicts a linear correlation of "medium" significance between E_{SEIS} and

PCI of PCC pavement sections. Figure 4-33 provides a comparison between E_{SEIS} in PCC pavements and their PCI, computed using structural distresses like corner break, linear cracking, and shattered slab. Using the limited data available, it was observed that comparison of E_{SEIS} with PCI from structural distresses alone had no effect on the correlation.

4.4 Service life of a GA airport pavement

From the PCI data (<http://apms.aeronautics.ok.gov>), Yuan and Mooney (2003) estimated the average life of an AC pavement to be 45 years and the average life of a PCC pavement to be approximately 65 years. In sharp contrast to this, FAA's advisory circulars (FAA AC 150/5320-6D) for pavement design require airport pavements to have a minimum 20 year structural life as long as there are no major changes in forecast traffic. FAA's guidelines permit rehabilitation of surface grades and renewal of skid-resistance properties during the pavement life-cycle. Since these permitted rehabilitations cannot alter the load carrying ability of the pavement, its structure must retain the capacity to support the design load for 20 years. Therefore, it is pertinent to investigate whether this "longer life" as estimated by PCI based models is also observed with modulus data.

Using the procedures explained previously for AC pavements, E_{SEIS} can be corrected for the rate of loading to estimate design modulus of pavements. Using this design modulus, it is possible to estimate the remaining life of pavement sections using the following:

For AC pavements, failure criteria for fatigue cracking and rutting (permanent deformation) are given in Equations (4.10) and (4.11) (Huang, 1993).

$$N_f = f_1(\varepsilon_t)^{-f_2}(E_1)^{-f_3} \quad (4.10)$$

$$N_d = f_4(\varepsilon_c)^{-f_5} \quad (4.11)$$

Where:

N_f is the allowable number of load repetitions to prevent fatigue cracking,

N_d is the allowable number of load repetitions to prevent permanent deformation,

ε_t is the tensile strain at the bottom of asphalt layer,

E_1 is the elastic modulus of AC layer,

ε_c is the compressive strain at the top of subgrade,

f_1, f_2, f_3 are constants values of which are given by the Asphalt Institute as, 0.0796, 3.291 and 0.854 respectively, and

f_4, f_5 are constants values of which are given as 1.365×10^{-9} and 4.477 respectively by the Asphalt Institute.

Using N_f and N_d , the damage ratio D_r can be calculate as given in Equation (4.12).

$$D_r = \sum_{i=1}^p \sum_{j=1}^m \frac{n_{ij}}{N_{ij}} \quad (4.12)$$

$$Life = 1/D_r \quad (4.13)$$

In the above,

n_{ij} is the predicted number of load repetitions for load j in period i,

N_{ij} is the allowable number of load repetitions based on Equations (4.10) and (4.11),

p is the number of periods in a year, and

m is the number of load groups.

The Life of the pavement section was evaluated for both fatigue cracking and rutting and the one that is lesser of the two is used.

For PCC pavements, a similar damage analysis procedure is used to determine the life of the pavement section. PCC moduli are estimated from field moduli as described earlier. In the case of PCC pavements, damage is based upon fatigue cracking only. The allowable number of repetitions is estimated as in Equations (4.14a), (4.14b) and (4.14c).

$$\text{For } \frac{\sigma}{S_c} \geq 0.55 : \quad \log N_f = 11.737 - 12.077 \left(\frac{\sigma}{S_c} \right) \quad (4.14a)$$

$$\text{For } 0.45 < \frac{\sigma}{S_c} < 0.55 : \quad N_f = \left(\frac{4.2577}{\frac{\sigma}{S_c} - 0.4325} \right)^{3.268} \quad (4.14b)$$

$$\text{For } \frac{\sigma}{S_c} \leq 0.45 : \quad N_f = \text{unlimited} \quad (4.14c)$$

In the above,

N_f is the allowable number of repetitions,

σ is the flexural stress in slab, and

S_c is the modulus of rupture of concrete.

For PCC pavements a cracking index (CI) is computed similar to D_r in Equation (4.12). Pavement life is estimated as

$$\text{Life} = 1/CI \quad (4.15)$$

Since pavement family groupings include dissimilar pavement sections subjected to different types of aircraft loads and different levels of aircraft operations, using the above procedure to model remaining pavement life at the network level is not feasible. The procedure is however, useful for project-level analysis. Five pavement sections – four AC and one PCC, at varying ages and in different family groupings are studied at the

project level to determine their remaining service life using the procedure outlined above. Results from the analysis are presented in Table 4-8 for AC pavements and in Table 4-9 for PCC pavements.

The first case studied was a section from family grouping AC(2,1). As expected, it is observed that pavement life decreases with the severity of traffic loading. Thus we see that remaining life of Guymon Municipal airport's runway pavement reduces from 32.1 years for a light aircraft (Single Wheel Gear, 12,500 lbs) to 2.1 years for a typical corporate jet aircraft (Dual Wheel Gear, 30,000 lbs). The analysis is performed for aircraft 50,000 operations in each case in Tables 4-8 and 4-9. Changing the number of operations will also impact pavement life. In the case of Alva Regional airport's runway pavement (family AC(2,5)), remaining life decreases from 157 years for light aircraft traffic (Single Wheel Gear, 12,500lbs) to just over 5 years for heavier traffic (Single and Dual Wheel Gear, 30,000 lbs). Similar results are observed for Shawnee Regional airports runway pavement (family AC(2,1) where the remaining life decreases from in excess of 200 years for light aircraft traffic to nearly 18 years for corporate jet traffic. This trend is repeated in Guymon's taxiway pavement where remaining life decreases from 32 years to nearly 2 years for heavier aircraft loads. From the results for pavement evaluation in Table 4-9, West Woodward airport's runway pavement is concluded to be thicker than the loading imposed on it, i.e. over-designed. The remaining life of the pavement is infinite in the three cases evaluated using West Woodward airport's runway pavement data with light and heavy aircraft traffic.

As mentioned earlier, FAA's pavement design procedure requires a 20 year pavement structural life for the same level of aircraft traffic. With FAA's advisory

circular as a guide, and assuming a normal factor of safety of 2 in airport pavement design, a decrease in modulus greater than 50% of the original is taken to signal the need for a major rehabilitation effort like a thick overlay or a total reconstruction of the pavement section. Table 4-10 presents the percentage remaining SASW modulus in AC and PCC pavements with the passage of time. Using FAA's criteria and SASW based pavement deterioration models, service life of family the service life of AC pavements is observed to range from 8.5 years to 30.0 years and for PCC pavements the service life is observed to range from 52.0 to 59.0 years. The pavement life estimated using modulus decay is lower than that estimated using PCI data.

4.5 Conclusions

Data collected and analyzed in the current research validates the main objective of the study – i.e. to investigate if SASW estimated pavement modulus degrades with time. Regression results using E_{SEIS} data yielded r^2 values ranging from 0.36 to 0.86 for AC pavements and from 0.75 to 0.90 for PCC pavements. The values compare well with regression results obtained by other researchers working with PCI data (Appendix 2).

The current research examined different methodologies to classify Oklahoma's GA airport pavements network into rational, similar performing groups or families. From the analysis presented it is observed that the groupings based on thickness of "structurally-capable" layers in a pavement section yielded the best regression results. The modulus and remaining life degradation curves and the modulus data present excellent tools for project level capacity analysis of individual pavement sections. The service life of pavements used in this study is based upon FAA's expectation of pavement life. Using this definition, service life of AC pavements was observed to range from 8.5

years to 30 years for AC pavements and from 52 years to 59 years for PCC pavements. This is lower than the service lives estimated by Yuan and Mooney (2003), i.e. 45 years for AC pavements and 60 years for PCC pavements, based upon PCI decay for Oklahoma's airport pavements.

For AC pavements, an overall correlation between E_{SEIS} and PCI could not be established. No correlation was also observed to exist between E_{SEIS} and PCI computed using only structural distresses in AC pavements. This finding suggests that in AC pavements, visually inferred traffic-related distresses do not correlate with structural failure. In the case of PCC pavements, a correlation of medium significance ($r^2=0.39$) was observed between section PCI and modulus. Since PCI measures several parameters relating to ride quality the low correlations are in line with expectations. The correlation remained unchanged ($r^2=0.41$) when only structural distresses were used. This correlation of medium significance suggests that the identification of structural distresses in PCC pavements is more accurate than for AC pavements.

4.6 References

ASTM D5340-04e1, “*Standard Test Method for Airport Pavement Condition Index Surveys*”, ASTM International.

Brotten, M., and De Sombre, R., “*The airfield pavement condition index (PCI) evaluation procedure: Advantages, common misapplications, and potential pitfalls*”, Proceedings, 5th Int. Conf. on Managing Pavements, Seattle, (CD-ROM), (2001).

Cohen, J. (1988). “*Statistical power analysis for the behavioral sciences (2nd ed.)*”, Hillsdale, NJ: Lawrence Erlbaum Associates. ISBN 0-8058-0283-5.

Federal Aviation Administration, “*Airport Pavement Design and Evaluation*”, Advisory Circular AC 150/5320-6D, Change 4, 2006.

Gendreau, M., and Soriano, P., “*Airport pavement management systems: An appraisal of existing methodologies*,” Transportation Record A, 32(3), pp197–214, 1998.

Haskell, N.A., “*The dispersion of surface waves on multilayered media*,” Bulletin of Seismological Society of America, No. 43, 1953, pp. 14 – 34.

Huang, Y.H., “*Pavement analysis and design*,” Prentice Hall, Inc., New Jersey, 1993.

Lawson, C.L., and Hanson, R.J., Solving least squares problems, Prentice-Hall, Inc., 1974.

Lawson, C.L., and Hanson, R.J., “*Solving least squares problems*”, Prentice-Hall, Inc., 1974.

Mendenhall, W. and T. Sincich, “*A second course in statistics – regression analysis (6th edition)*,” Pearson Education Inc., New Jersey, ISBN 0-13-022323-9, 2003.

Paine, D., The incorporation of structural data in a pavement management system, Proceedings, 4th Int. Conf. on Managing Pavements, Durban, South Africa (CD-ROM), 1998.

Sanford-Bernhardt, K.L., Loehr, J.E. and Huaco, D, Asset Management Framework for Geotechnical Infrastructure, J. Infrastructure Systems, ASCE, 2003, 9(3), 107-116.

Shahin, M.Y. and Walther, J.A., Pavement maintenance management for roads and streets using the PAVER system, Technical report no. M-90/05, Construction engineering research laboratory, U.S. Army, July 1990.

Shahin, M.Y., Pavement Management for Airport Pavements, Roads, and Parking Lots, Kluwer Academic Publishers, Massachusetts, 1994.

Strategic Highway Research Program, Distress identification manual for the long term pavement performance project, SHRP-P-338, Washington D.C. 1993.

Witczak, M.W., Bonaquist, R., Von Quintus, H., and katoush, K, Specimen geometry and aggregate size effects in uniaxial compression and constant height shear tests, Journal of Association of Asphalt Paving Technologist, Volume 69, pp 733-793, 1999.

Yuan, J., and Mooney, M. A. (2003). "Development of adaptive performance models for Oklahoma Airfield pavement management system" Transportation Research Record 1853, Transportation Research Board, Washington, D.C., 44-54.

Zaniewski, J., Unified methodology for airport pavement analysis and design, Vol. I, State of the Art Technical Report, Federal Aviation Administration, Research and Development Service, Washington, D.C., (1991).

Table 4-1: Core sizes of AC pavement sections

Core thickness	No. of Pavement Sections
$t \leq 2''$	26
$2'' < t \leq 3''$	35
$3'' < t \leq 4''$	37
$4'' < t \leq 6''$	43
$6'' < t \leq 8''$	23
$8'' < t \leq 9''$	16
$9'' < t \leq 10''$	2
$t > 10''$	7

Table 4-2: Core sizes of PCC pavement sections

Core thickness	No. of Pavement Sections
$t \leq 6''$	5
$6'' < t \leq 7''$	18
$7'' < t \leq 8''$	8
$8'' < t \leq 10''$	11
$10'' < t \leq 12''$	3
$t > 12''$	4

Table 4-3: Guidance for interpretation of r^2

Correlation	Value of r^2
Small	0.10 to 0.29
Medium	0.30 to 0.49
Large	0.50 to 1.00

Table 4-4: AC pavement family groupings and goodness of regression

<i>Group Factor</i>	<i>Family</i>	<i>Family Description</i>	<i>No. of SASW Tests</i>	<i>Outliers</i>	<i>r²</i>	<i>SEE</i>	<i>RSE (%)</i>
<i>All AC Test sites</i>	<i>AC(1,1)</i>	All AC pavements	139	17 (12.2%)	0.46	304.9	23.0
<i>Thickness of structurally capable layers</i>	<i>AC(2,1)</i>	AC/Thin (no aggregate or stab base)	58	5 (8.6%)	0.38	264.4	19.7
	<i>AC(2,2)</i>	AC/ Thin /Aggregate base/ (no stabilized base)	22	3 (13.6%)	0.86	170.0	14.2
	<i>AC(2,3)</i>	AC/Thin/Stabilized base (no aggregate base)	14	Regression results inconclusive			
	<i>AC(2,4)</i>	AC/Thick (no aggregate or stabilized base)	4	Insufficient Data			
	<i>AC(2,5)</i>	AC/Thick /Aggregate base (no stabilized base)	36	6 (16.7%)	0.59	400.5	30.5
	<i>AC(2,6)</i>	AC/Thick/Stabilized base (no aggregate base)	5	Insufficient Data			
<i>Simplified structure based grouping</i>	<i>AC(3,1)</i>	AC/Thin (sum of thickness of load bearing layers > 10 inches)	92	13 (14.1%)	0.51	361.6	27.4
	<i>AC(3,2)</i>	AC/Thick (sum of thickness of load bearing layers < 10 inches)	47	7 (14.9%)	0.61	234.2	17.8
<i>Classification used for PCI degradation by Yuan (2003)</i>	<i>AC(4,1)</i>	AC/RW/Load & Combined	40	Regression results inconclusive			
	<i>AC(4,2)</i>	AC/RW/ Thin/Environmental	24	2 (8.3%)	0.57	307.7	28.4
	<i>AC(4,3)</i>	AC/RW/Medium/Environmental	39	6 (15.4%)	0.61	207.9	15.5
	<i>AC(4,4)</i>	AC/RW/ Thick /Environmental	24	1 (4.2%)	0.36	344.1	26.7
	<i>AC(4,5)</i>	AC/TW/Environmental	4	Insufficient Data			
	<i>AC(4,6)</i>	AC/TW/Load & Combined	1	Insufficient Data			
	<i>AC(4,7)</i>	AC/AP	7	Insufficient Data			
<i>Dominant distress based grouping</i>	<i>AC(5,1)</i>	AC/Environmental	139	Yields same result as family AC (1,1)			
	<i>AC(5,2)</i>	AC/Load	0	No pavement with dominant load related distress			

Table 4-5: Significance rank determination of AC regression analysis

<i>Family</i>	<i>Rank Outliers</i>	<i>Rank r^2</i>	<i>Rank RSE</i>	<i>Score</i>	<i>Combined Rank</i>	<i>Weighted Average Score</i>	<i>Simple Average Score</i>	<i>Significance Rank*</i>
<i>AC(1,1)</i>	<i>4</i>	<i>7</i>	<i>5</i>	<i>16</i>	<i>6</i>	<i>6.0</i>	<i>6.0</i>	<i>4(2)</i>
<i>AC(2,1)</i>	<i>3</i>	<i>8</i>	<i>4</i>	<i>15</i>	<i>4</i>	<i>5.0</i>	<i>4.7</i>	<i>1(1)</i>
<i>AC(2,2)</i>	<i>5</i>	<i>1</i>	<i>1</i>	<i>7</i>	<i>1</i>			
<i>AC(2,5)</i>	<i>9</i>	<i>4</i>	<i>9</i>	<i>22</i>	<i>9</i>			
<i>AC(3,1)</i>	<i>6</i>	<i>6</i>	<i>7</i>	<i>19</i>	<i>8</i>	<i>6.0</i>	<i>5.0</i>	<i>2(2)</i>
<i>AC(3,2)</i>	<i>7</i>	<i>2</i>	<i>3</i>	<i>12</i>	<i>2</i>			
<i>AC(4,1)</i>	<i>10</i>	<i>10</i>	<i>10</i>	<i>30</i>	<i>10</i>	<i>6.0</i>	<i>5.8</i>	<i>3(2)</i>
<i>AC(4,2)</i>	<i>4</i>	<i>5</i>	<i>8</i>	<i>15</i>	<i>4</i>			
<i>AC(4,3)</i>	<i>3</i>	<i>3</i>	<i>2</i>	<i>13</i>	<i>3</i>			
<i>AC(4,4)</i>	<i>6</i>	<i>9</i>	<i>6</i>	<i>16</i>	<i>6</i>			

Numbers in parentheses represent the significance based upon the weighted average score

Table 4-6: PCC pavement family groupings and goodness of regression

<i>Grouping Rationale</i>	<i>Family</i>	<i>Family Description</i>	<i>No. of SASW Tests</i>	<i>Outliers</i>	<i>r²</i>	<i>SEE</i>	<i>RSE (%)</i>
<i>All PCC test sites</i>	<i>PCC(1,1)</i>	All PCC pavements	47	6 (12.8%)	0.75	565.8	12.5
<i>Thickness of structurally capable layers</i>	<i>PCC(2,1)</i>	PCC/Thin (no aggregate or stabilized base)	39	7 (17.9%)	0.88	423.5	9.0
	<i>PCC(2,2)</i>	PCC/Thin/Aggregate base (no stabilized base)	0	No Data			
	<i>PCC(2,3)</i>	PCC/Thin/Stabilized base (no aggregate base)	1	Insufficient Data			
	<i>PCC(2,4)</i>	PCC/Thick (no aggregate or stabilized base)	3	Insufficient Data			
	<i>PCC(2,5)</i>	PCC/Thick/Aggregate base (no stabilized base)	4	Insufficient Data			
	<i>PCC(2,6)</i>	PCC/Thick/Stabilized Base (no aggregate base)	0	No Data			
<i>Classification used for PCI degradation by Yuan (2003)</i>	<i>PCC(3,1)</i>	PCC/RW/DNF	25	5 (20.0%)	0.86	421.4	8.8
	<i>PCC(3,2)</i>	PCC/RW/WNF	19	2 (10.5%)	0.90	431.4	9.8
	<i>PCC(3,3)</i>	PCC/TW	3	Insufficient Data			
	<i>PCC(3,4)</i>	PCC/AP	0	No Data			
<i>Dominant distress based grouping</i>	<i>PCC(4,1)</i>	PCC/Environmental	38	5 (13.2%)	0.79	485.3	10.9
	<i>PCC(4,2)</i>	PCC/Load	9	Insufficient Data			

Table 4-7: Significance rank determination of PCC regression analysis

<i>Family</i>	<i>Rank Outliers</i>	<i>Rank r²</i>	<i>Rank RSE</i>	<i>Rank Score</i>	<i>Total Rank</i>	<i>Weighted Average Score</i>	<i>Simple Average Score</i>	<i>Significance Rank*</i>
<i>PCC(1,1)</i>	2	5	5	12	5	5.0	5.0	4(4)
<i>PCC(2,1)</i>	4	2	2	8	2	2.0	2.0	1(1)
<i>PCC(3,1)</i>	5	3	1	9	3	2.1	2.0	1(2)
<i>PCC(3,2)</i>	1	1	3	5	1			
<i>PCC(4,1)</i>	3	4	4	11	4	4.0	4.0	3(3)

* Numbers in parentheses represent the significance based upon the weighted average score

Table 4-8: Remaining life Analysis using SASW data with KENPAVE pavement design computer program for AC pavements

<i>Airport</i>	<i>SASW (Top Ranked Family)</i>	<i>Location</i>	<i>Layer</i>	<i>Material</i>	<i>Thick. (in)</i>	<i>Aircraft Load</i>	<i>Design Modulus (ksi)</i>	<i>Age at Test (Yrs)</i>	<i>Balance Life (Yrs)</i>
Guymon Muni.	AC(2,5)	2000-15	Surface	AC	3	SW 12.5 kip	346,936	1	32.1*
			Base	Aggr.	8		53,000		
			Subgrade	Soil			18,800		
Guymon Muni.	AC(2,5)	2000-15	Surface	AC	3	SW 30 kip	346,936	1	1.4*
			Base	Aggr.	8		53,000		
			Subgrade	Soil			18,800		
Guymon Muni.	AC(2,5)	2000-15	Surface	AC	3	DW 30 kip	346,936	1	1.1*
			Base	Aggr.	8		53,000		
			Subgrade	Soil			18,800		
Alva Regnl.	AC(2,1)	500-2	Surface	AC	4.8	SW 12.5 kip	244,184	5	157*
			Base	Aggr.	4		71,900		
			Subgrade	Soil			13,200		
Alva Regnl.	AC(2,1)	500-2	Surface	AC	4.8	SW 30 kip	244,184	5	5.3*
			Base	Aggr.	4		71,900		
			Subgrade	Soil			13,200		
Alva Regnl.	AC(2,1)	500-2	Surface	AC	4.8	DW 30 kip	244,184	5	5.4*
			Base	Aggr.	4		71,900		
			Subgrade	Soil			13,200		

** Pavement sections experienced failure due to rutting of subgrade in simulations*

Table 4-8 (Contd.): Remaining life Analysis using SASW data with KENPAVE pavement design computer program for AC pavements

<i>Airport</i>	<i>SASW Family</i>	<i>Location</i>	<i>Layer</i>	<i>Material</i>	<i>Thick. (in)</i>	<i>Aircraft Load</i>	<i>Design Modulus (ksi)</i>	<i>Age at Test (Yrs)</i>	<i>Balance Life (Yrs)</i>
Shawnee Regnl.	AC(2,1)	5500-98	Surface	AC	5.2	SW 12.5 kip	296,273	6	211.5*
			Base	Aggr	1		74,857		
			Subgrade	Soil			13,200		
Shawnee Regnl.	AC(2,1)	5500-98	Surface	AC	5.2	SW 30.0 kip	296,273	6	17.7**
			Base	Aggr	1		74,857		
			Subgrade	Soil			13,200		
Shawnee Regnl.	AC(2,1)	5500-98	Surface	AC	5.2	DW 30.0 kip	296,273	6	17.7**
			Base	Aggr	1		74,857		
			Subgrade	Soil			13,200		
Guymon Muni. TWY	AC(2,2)	2950-17	Surface	AC	3.5	SW 12.5 kip	177,494	16	32.3**
			Base	Aggr	1.2		76,250		
			Sugrade	Soil			5,076		
Guymon Muni. TWY	AC(2,2)	2950-17	Surface	AC	3.5	SW 30.0 kip	177,494	16	2.9**
			Base	Aggr	1.2		76,250		
			Sugrade	Soil			5,076		
Guymon Muni. TWY	AC(2,2)	2950-17	Surface	AC	4(3.5)	DW 30.0 kip	177,494	16	1.9**
			Base	Aggr	3(1.2)		76,250		
			Sugrade	Soil			5,076		

* Pavement sections experienced failure due to rutting of subgrade in simulations

** Pavement sections experienced fatigue failure in simulations

Table 4-9: Remaining life Analysis using SASW data with KENPAVE pavement design computer program for PCC pavements

<i>Airport</i>	<i>SASW Family</i>	<i>Location Details</i>	<i>Layer</i>	<i>Material</i>	<i>Thick. (in)</i>	<i>Aircraft Load</i>	<i>Design Modulus (ksi)</i>	<i>Age at Test (Yrs)</i>	<i>Balance Life (Yrs)</i>
West Woodward	PCC(2,1)	4000-50; PCC Slabs 15' x 12'	Surface	PCC	11.2	SW 12.5 kip	4,538,550	2	infinite
			Sugrade	Soil			9,400		
West Woodward	PCC(2,1)	4000-50; PCC Slabs 15' x 12'	Surface	PCC	11.2	SW 30 kip	4,538,550	2	infinite
			Sugrade	Soil			9,400.		
West Woodward	PCC(2,1)	4000-50; PCC Slabs 15' x 12'	Surface	PCC	11.2	DW 30 kip	4,538,550	2	infinite
			Sugrade	Soil			9,400		

Table 4-10: Comparison of Modulus and PCI degradation

Family Name	PCI based modeling				SASW based modeling				
	Outliers	r ²	RSE (%)	Age for Zero PCI (yrs)	Outliers	r ²	RSE (%)	Age for Zero Modulus (yrs)	Age at 50% initial Modulus (yrs)
AC(1,1)	21	0.64	11.4	65-70	17	0.46	23.0	37.3	24.0
AC(2,1)	0	0.41	24.0	30.2	5	0.41	19.7	32.0	23.5
AC(2,2)	0	0.24	30.7	Infinite	3	0.86	19.7	37.5	30.5
AC(2,5)	3	0.93	8.5	36.5	6	0.59	30.5	38.4	8.5
AC(3,1)	12	0.49	21.3	Infinite	13	0.51	27.4	37.0	8.5
AC(3,2)	6	0.91	8.6	39.2	7	0.61	17.8	38.6	29.0
AC(4,2)	2	0.74	18.3	66.0	2	0.57	28.4	37.5	23.0
AC(4,3)	5	0.54	17.9	52.5	6	0.61	15.5	46.0	30.0
AC(4,4)	5	0.34	17.9	Infinite	1	0.36	27.3	37.5	10.0
PCC(1,1)	1	0.61	11.4	64.0	6	0.75	12.5	70.0	52.0
PCC(2,1)	0	0.67	10.8	65-70	7	0.88	9.0	118.0	59.0
PCC(3,1)	8	0.85	8.6	65-70	5	0.86	8.8	116.0	58.0
PCC(3,2)	7	0.77	11.3	75.0	2	0.90	9.8	73.5	54.0
PCC(4,1)	1	0.64	10.7	67.5	5	0.79	10.9	116.0	58.0

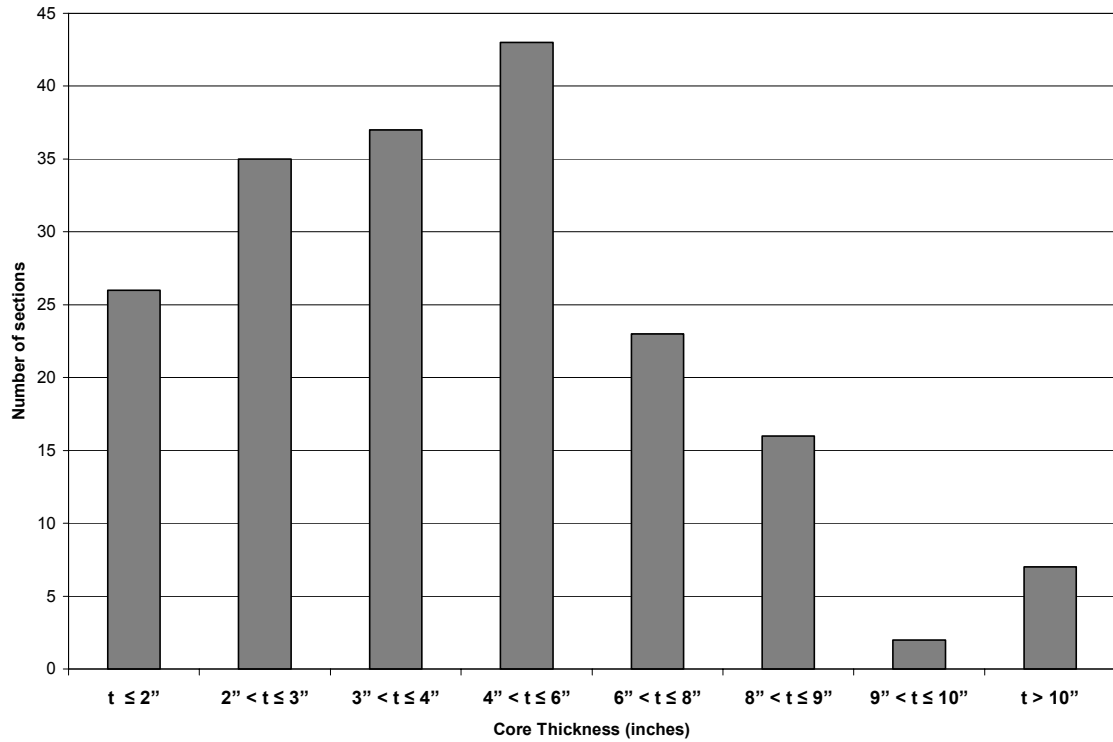


Figure 4-1(a): Distribution of AC Core thickness in Oklahoma's General Aviation airports

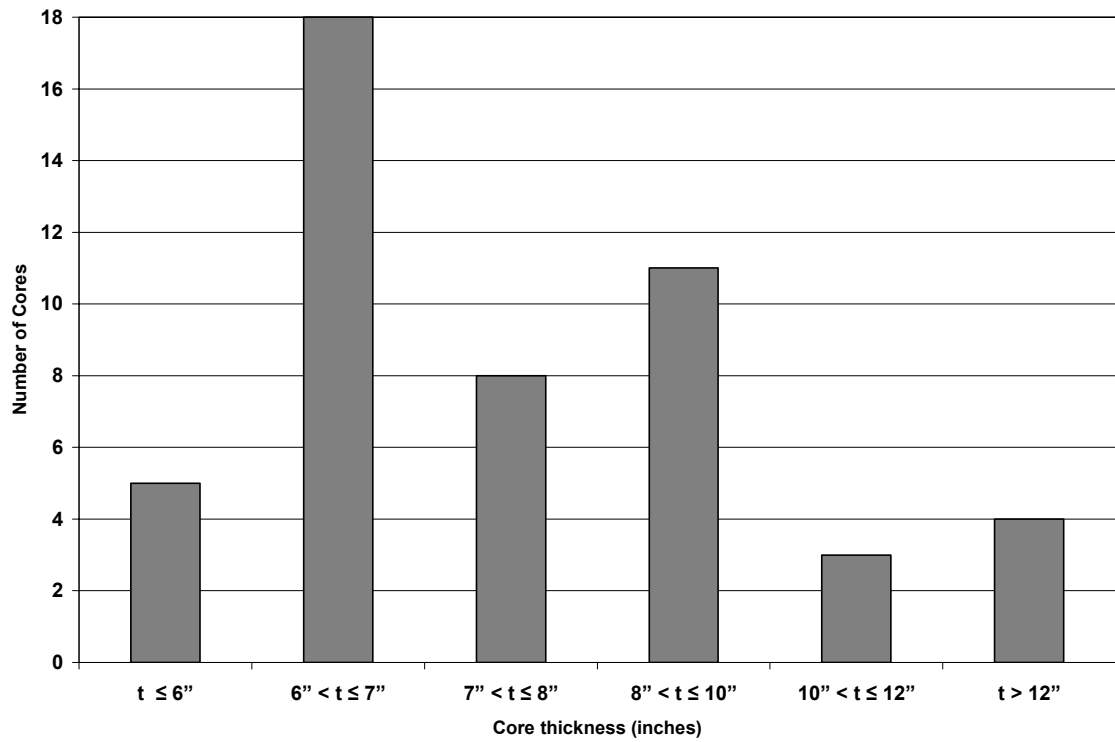


Figure 4-1(b): Distribution of PCC Core thickness in Oklahoma's General Aviation airports

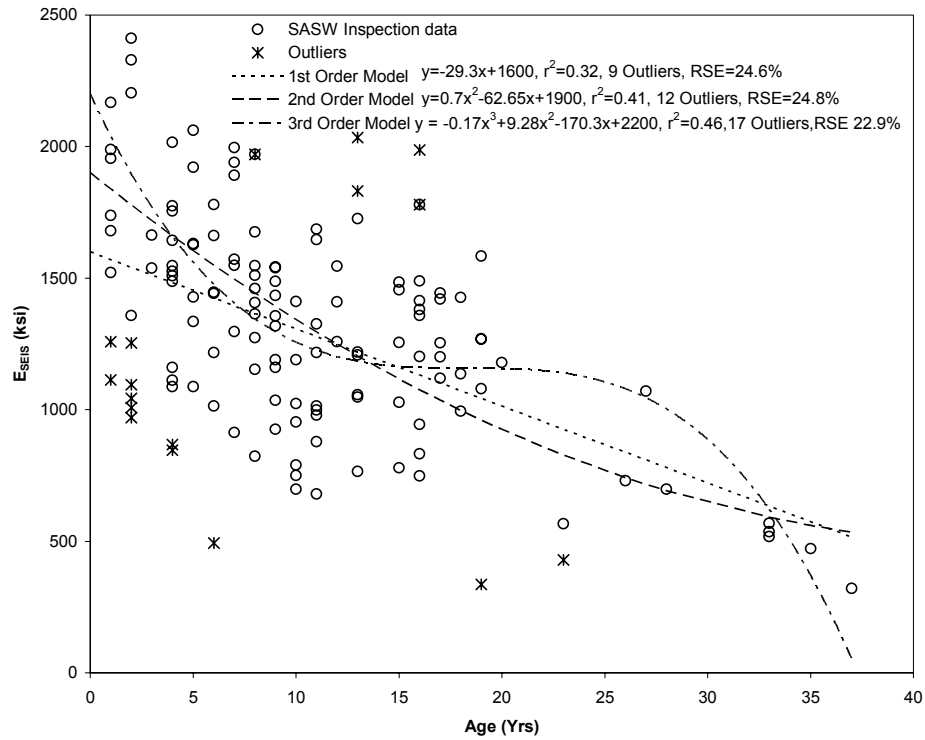


Figure 4-2: AC E_{SEIS} as a function of age for family AC(1,1) (Outliers for selected 3rd Order model shown)

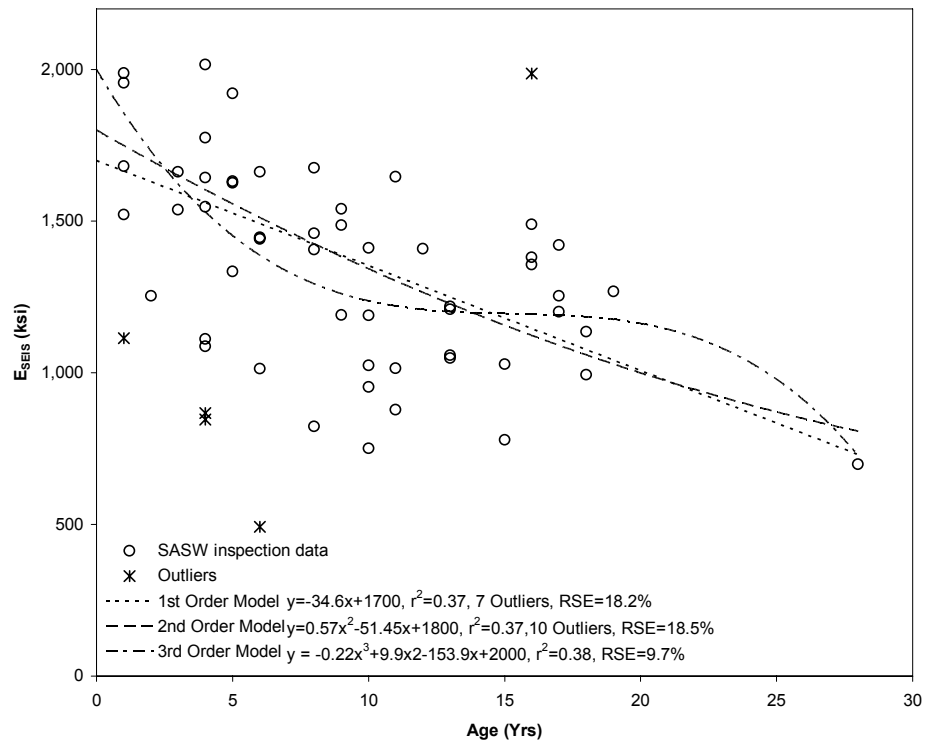


Figure 4-3: AC E_{SEIS} decay with age for Family AC(2,1) (Outliers for 3rd Order model shown)

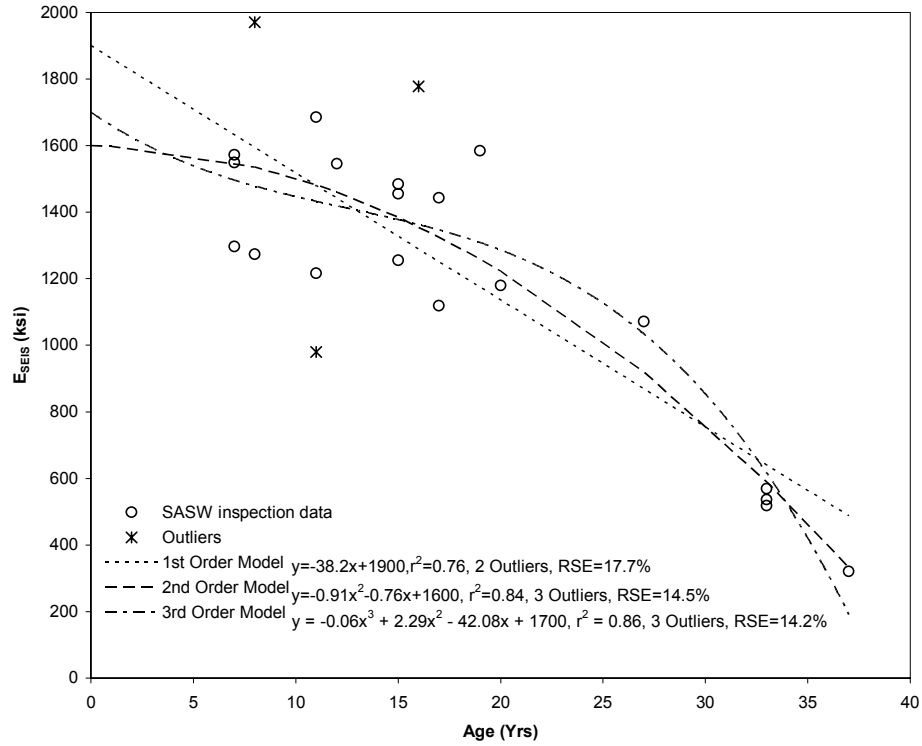


Figure 4-4: AC E_{SEIS} deterioration with age for family AC(2,2) (Outliers from 3rd order model shown)

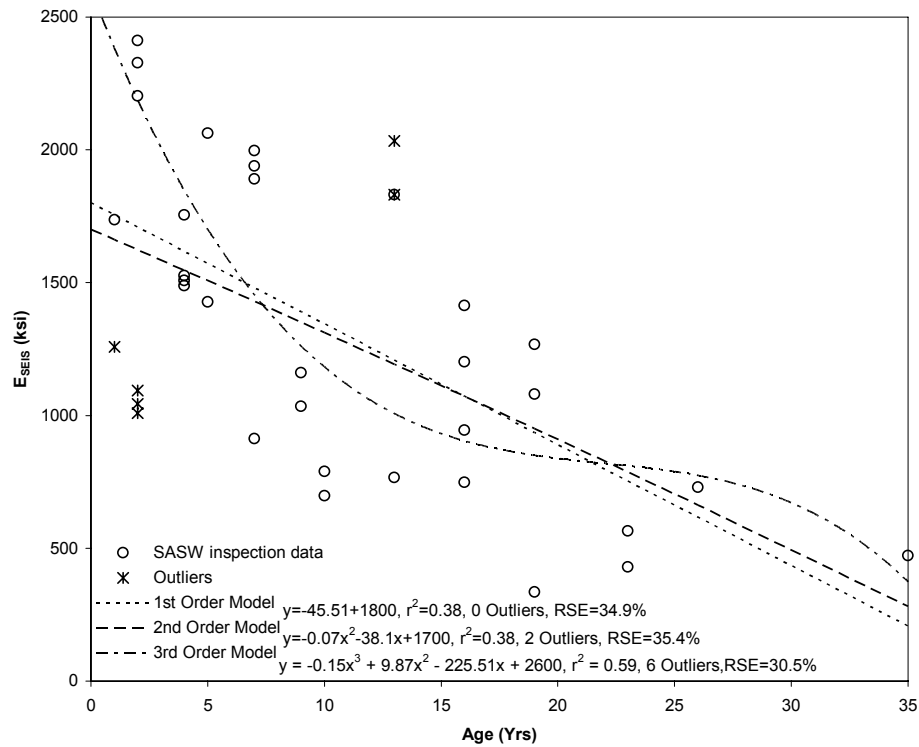


Figure 4-5 AC E_{SEIS} decay with age for family AC(2,5) (Outliers from 3rd order model shown)

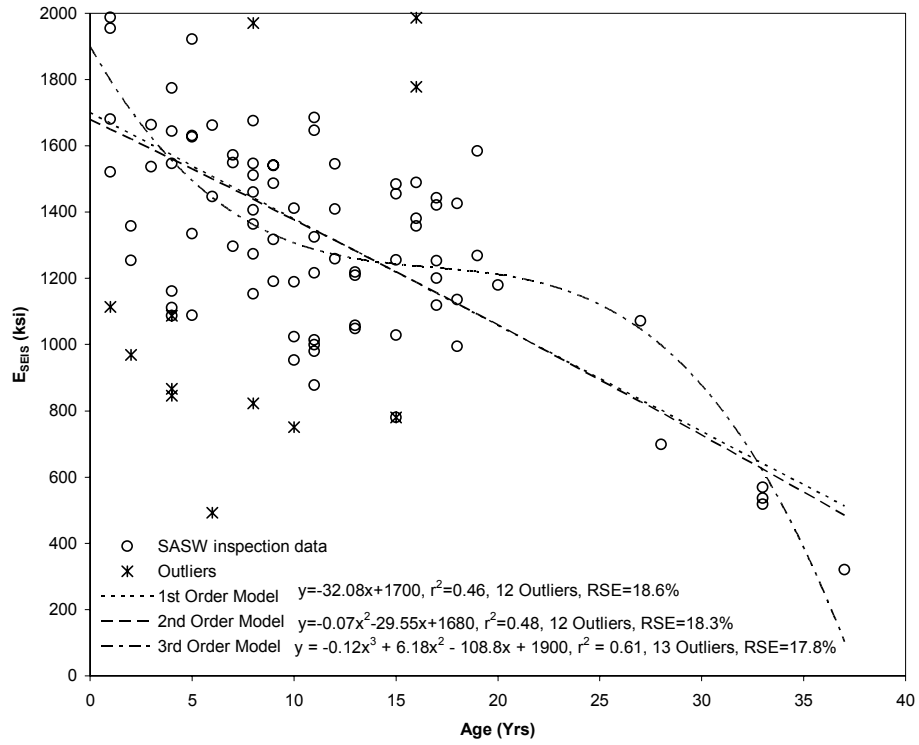


Figure 4-6: AC E_{SEIS} degradation with time for family AC(3,1) (Outliers from 3rd order model shown)

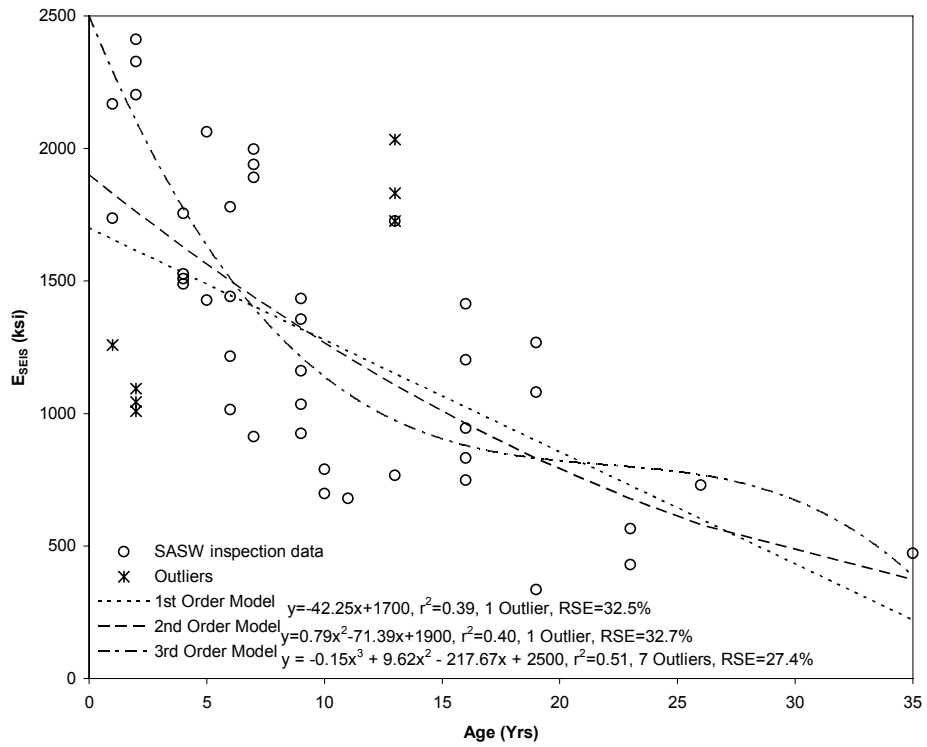


Figure 4-7: AC E_{SEIS} deterioration with age for family AC(3,2), (Outliers from 3rd order model shown)

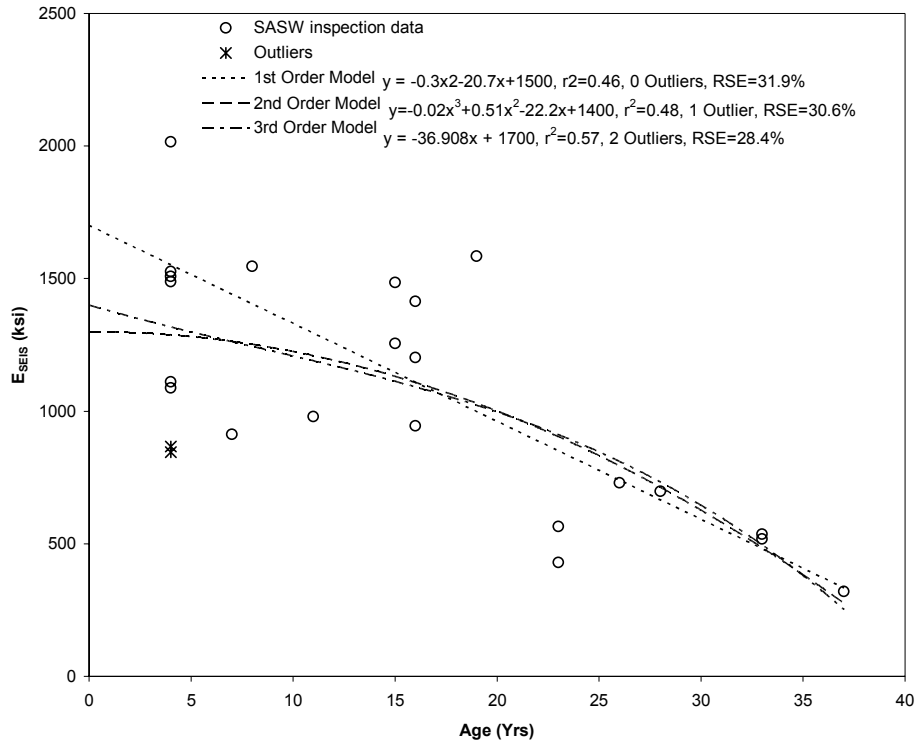


Figure 4-8: AC E_{SEIS} deterioration for family AC(4,2) (Outliers for Linear model shown)

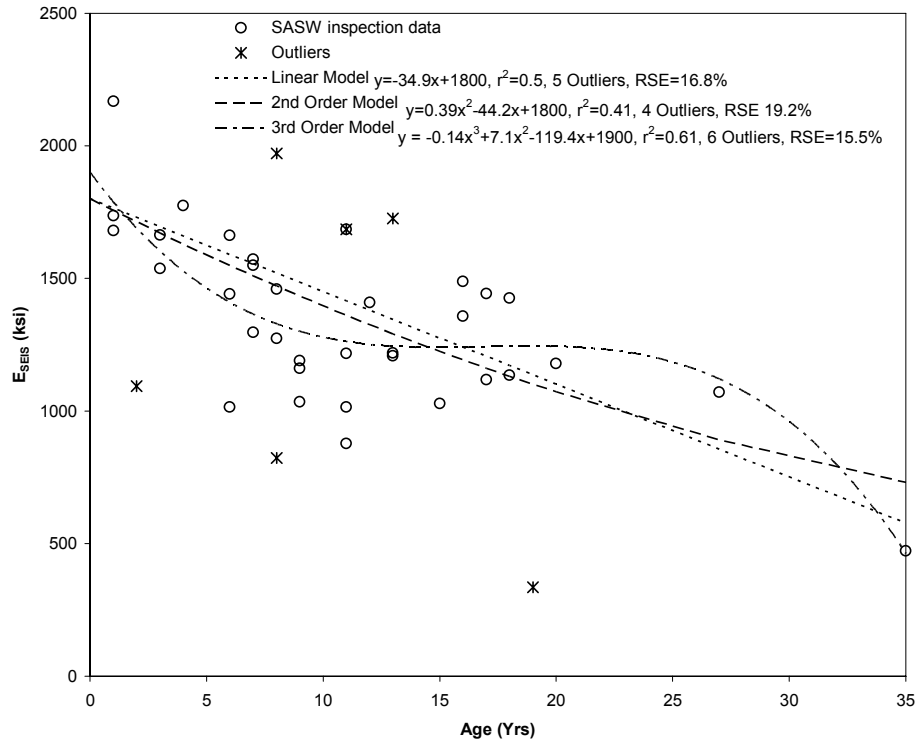


Figure 4-9: AC E_{SEIS} variation with age for family AC(4,3), (Outliers for selected 3rd order model shown)

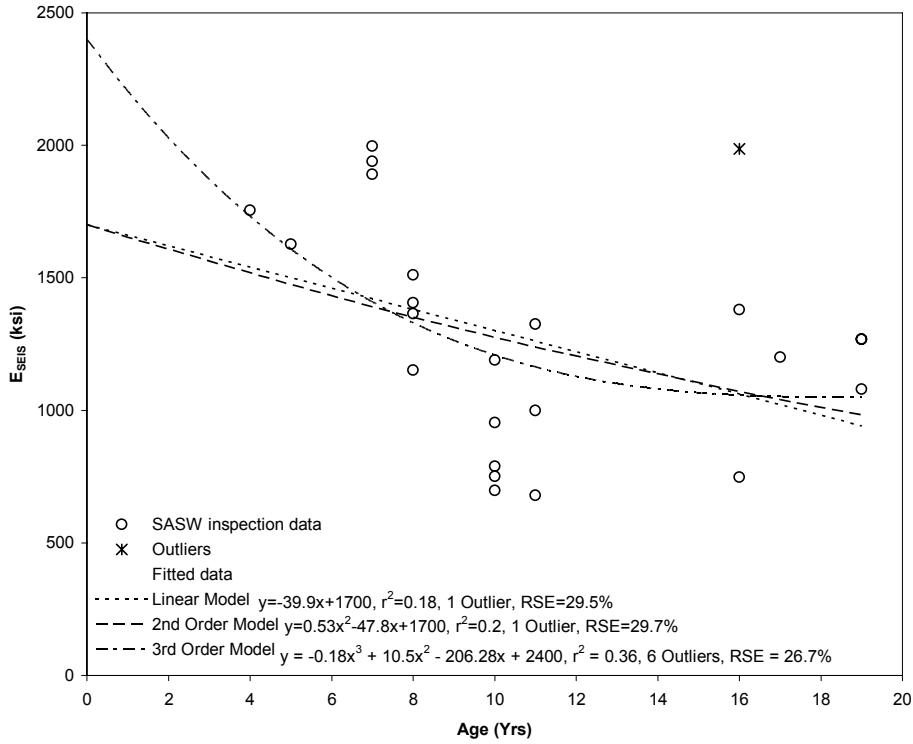


Figure 4-10: AC E_{SEIS} decay with age for family AC(4,4) (Outliers for selected 3rd order model shown)

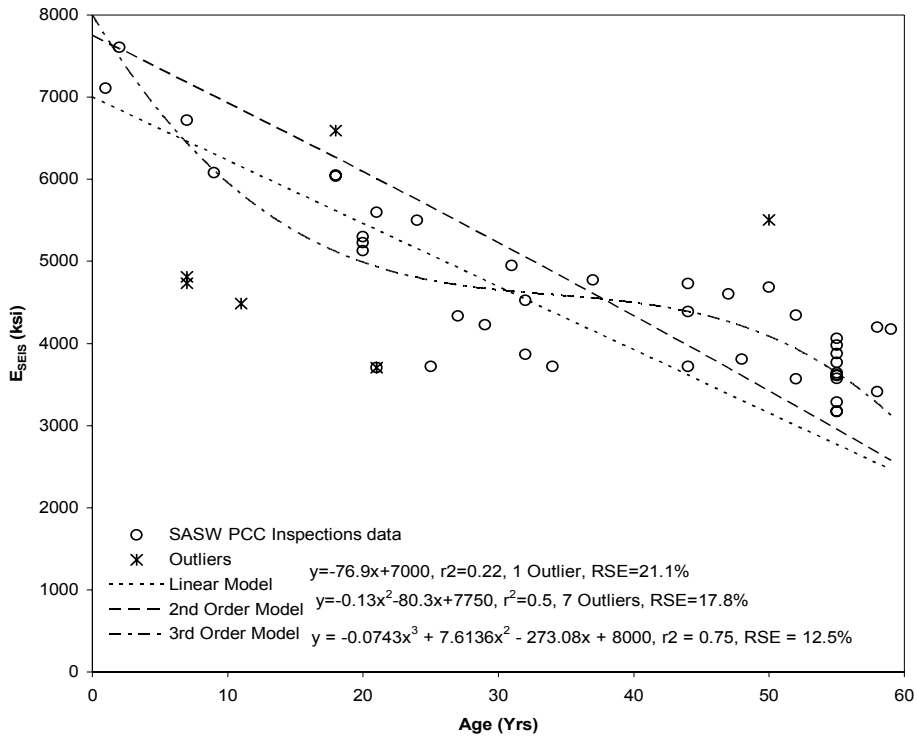


Figure 4-11: PCC pavement layer moduli as a function of age for family PCC(1,1) (Outliers for selected 3rd Order model shown)

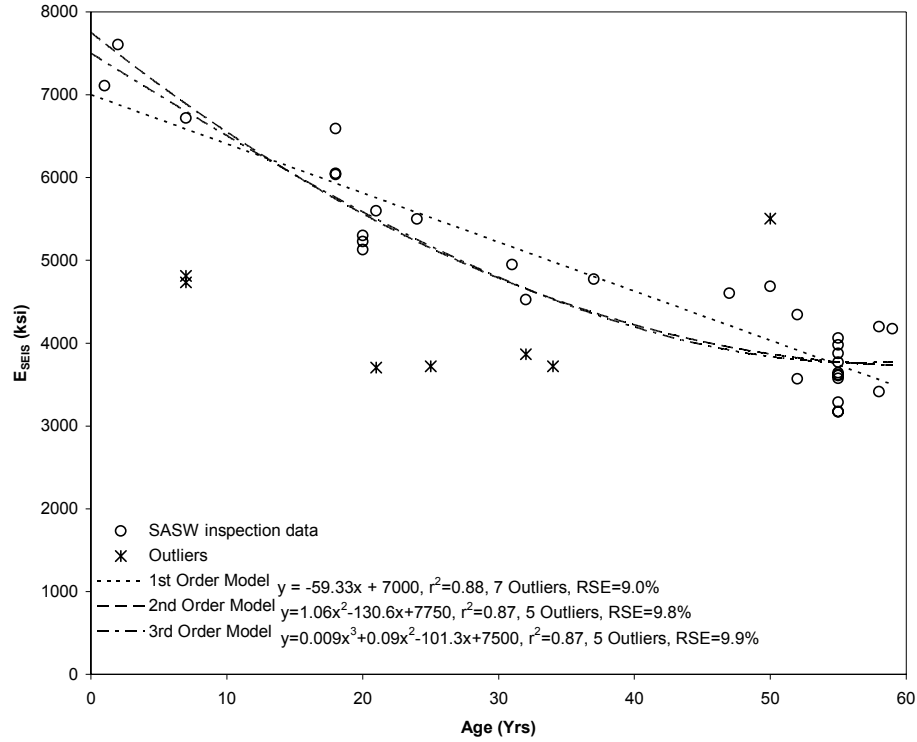


Figure 4-12: PCC E_{SEIS} deterioration with age for family PCC(2,1) (Outliers for selected Linear model shown)

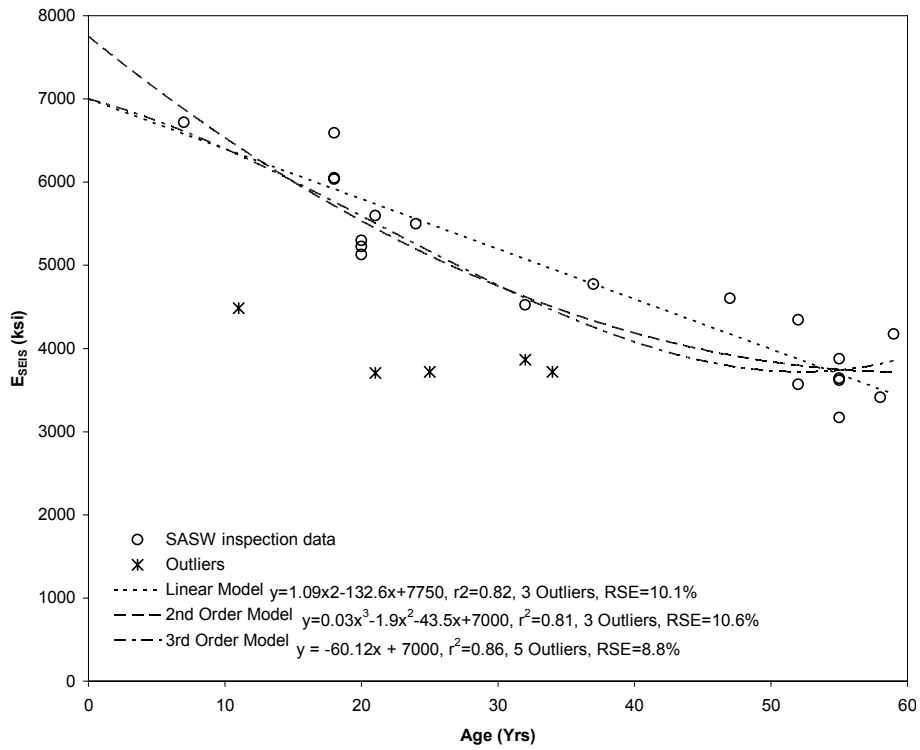


Figure 4-13: PCC E_{SEIS} decrease with age for family PCC(3,1) (Outliers for selected Linear model shown)

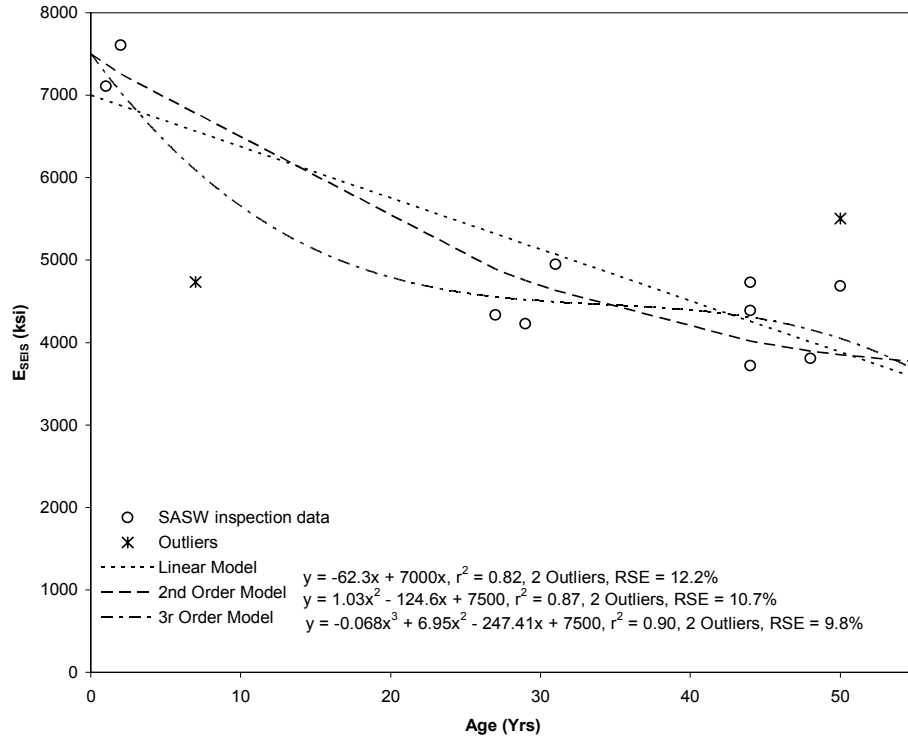


Figure 4-14: PCC E_{SEIS} deterioration with age for family PCC(3,2) (Outliers for selected 3r order model shown)

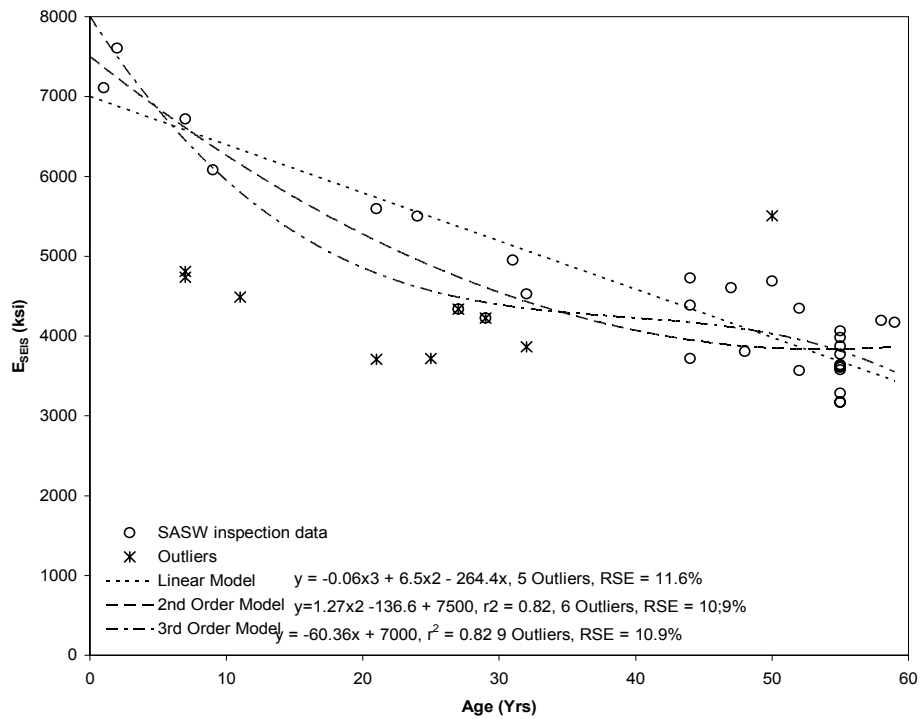


Figure 4-15: PCC E_{SEIS} deterioration for family PCC(4,1); (Outliers for selected Linear order model shown)

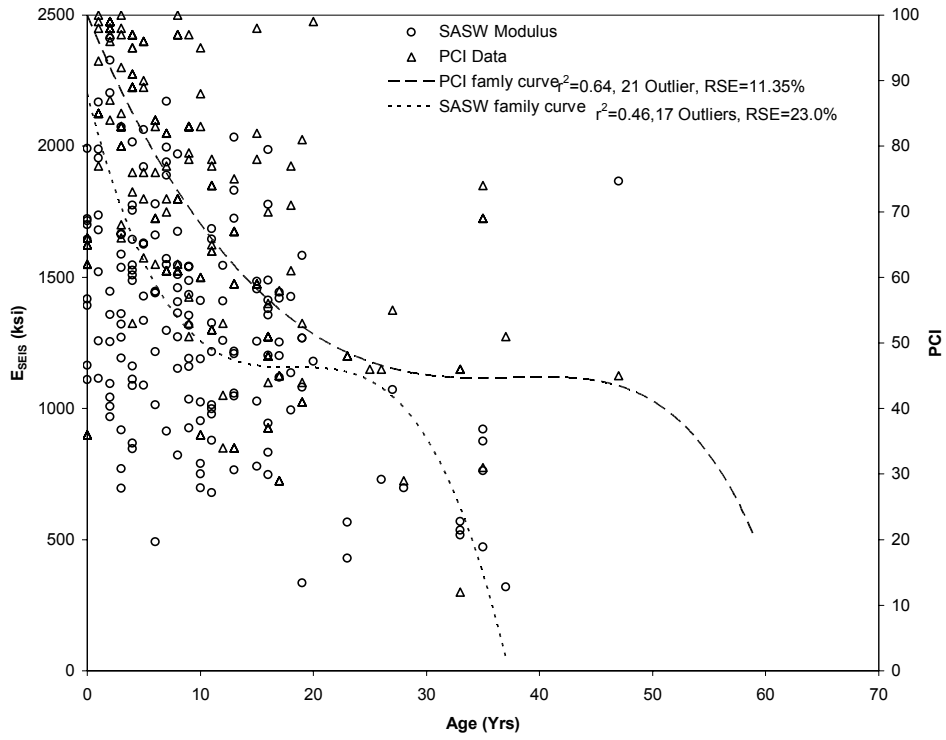


Figure 4-16: Comparison of PCI and E_{SEIS} regression for all tested AC pavements

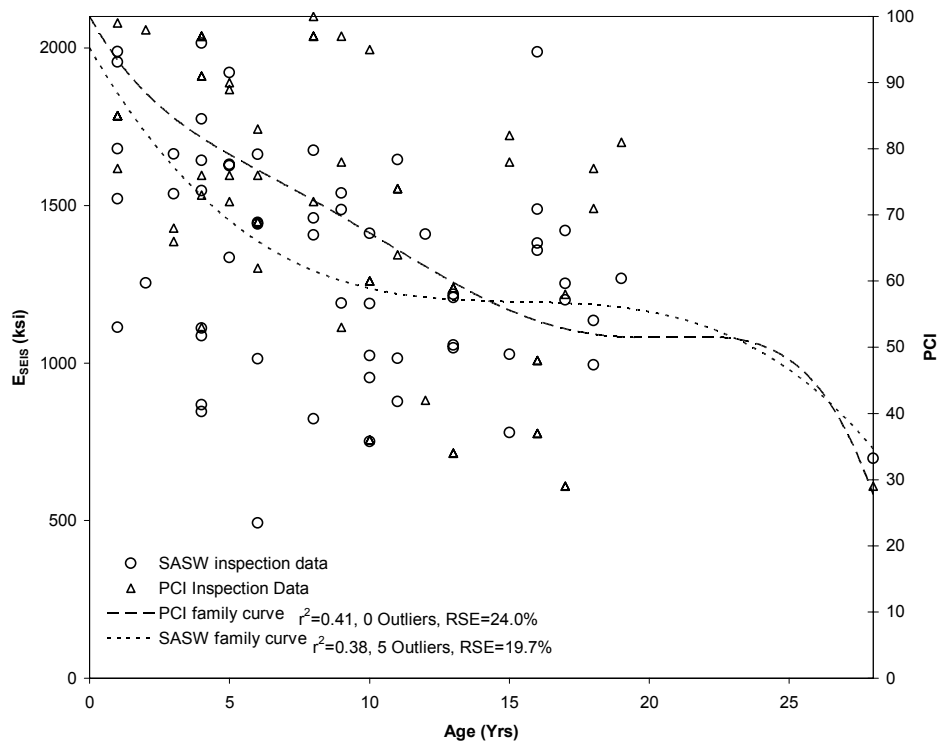


Figure 4-17: Comparison of PCI and E_{SEIS} degradation for family AC(2,1)

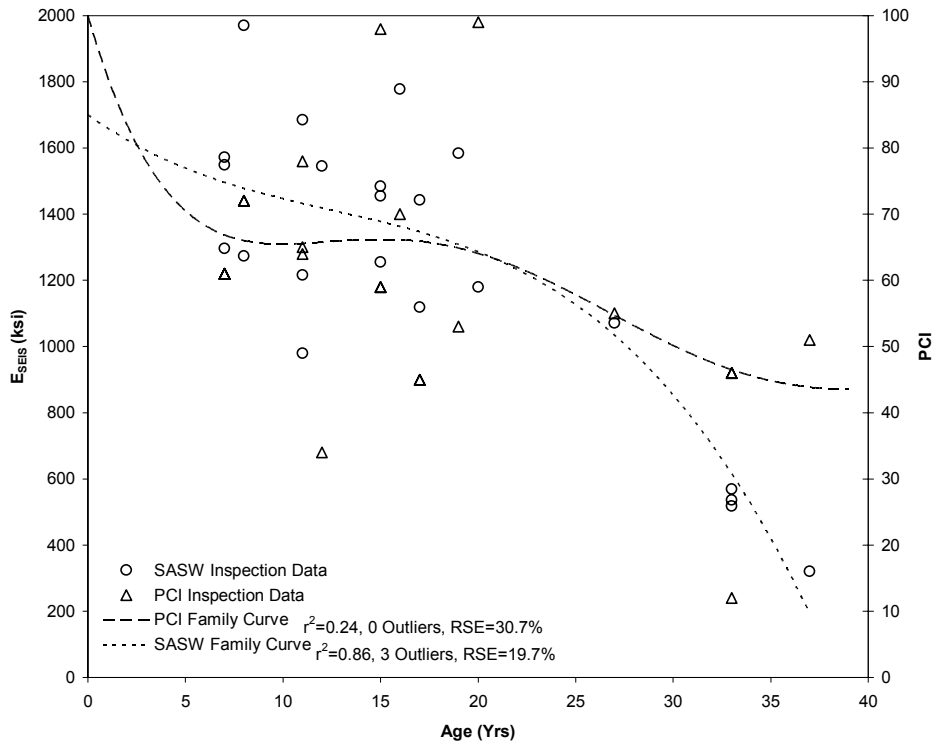


Figure 4-18: Comparison of PCI and E_{SEIS} degradation for family AC(2,2)

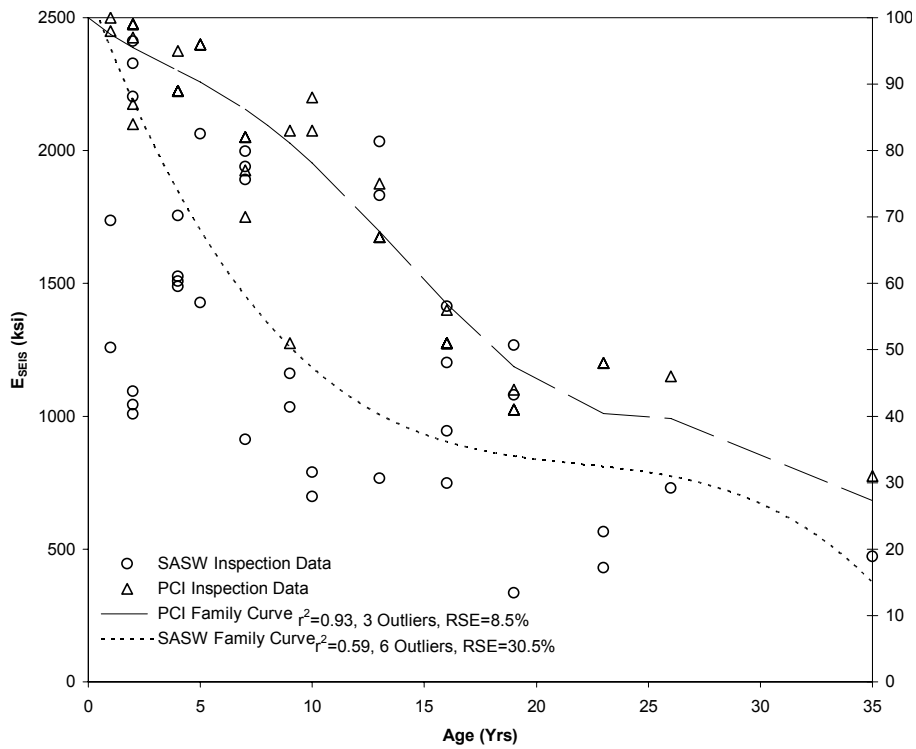


Figure 4-19: Comparison of PCI and E_{SEIS} degradation for family AC(2,5)

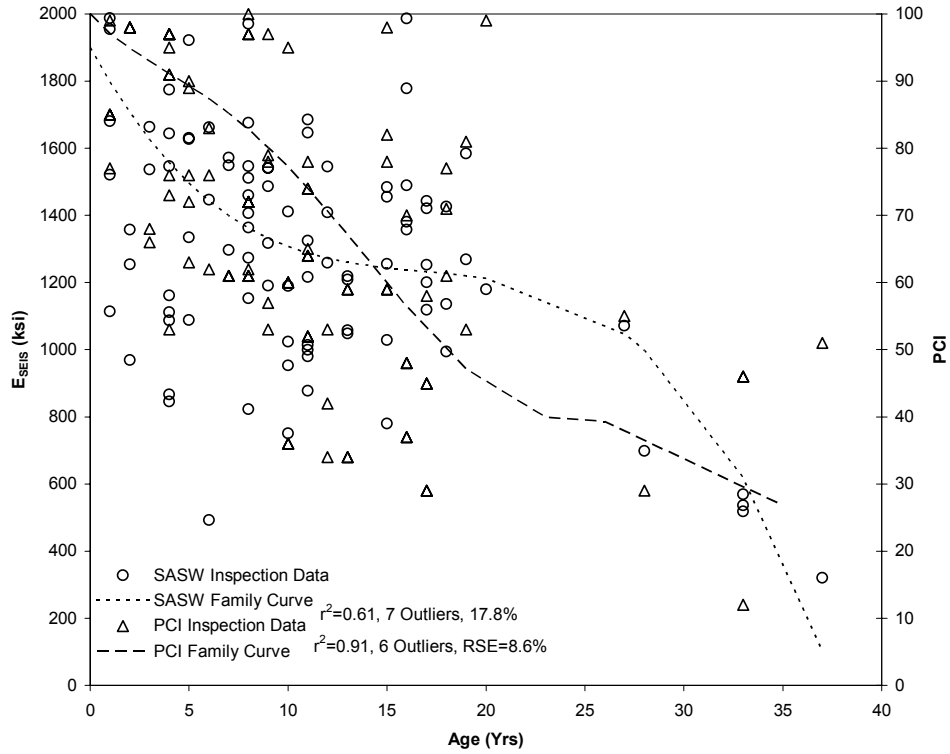


Figure 4-20: Comparison of PCI and E_{SEIS} degradation for family AC(3,1)

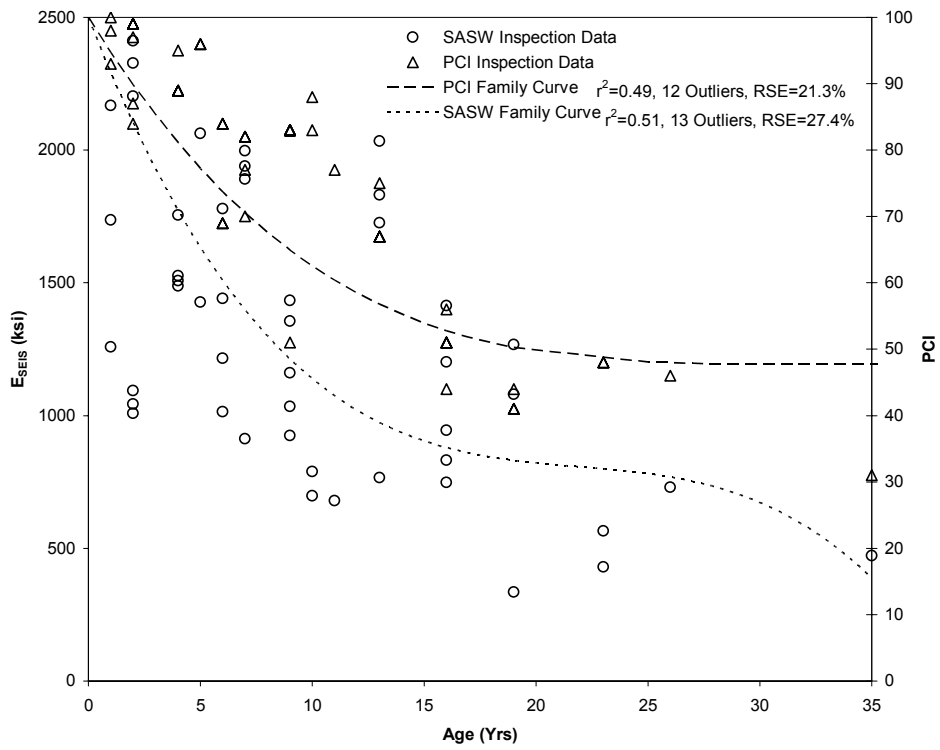


Figure 4-21: Comparison of PCI and E_{SEIS} degradation for family AC(3,2)

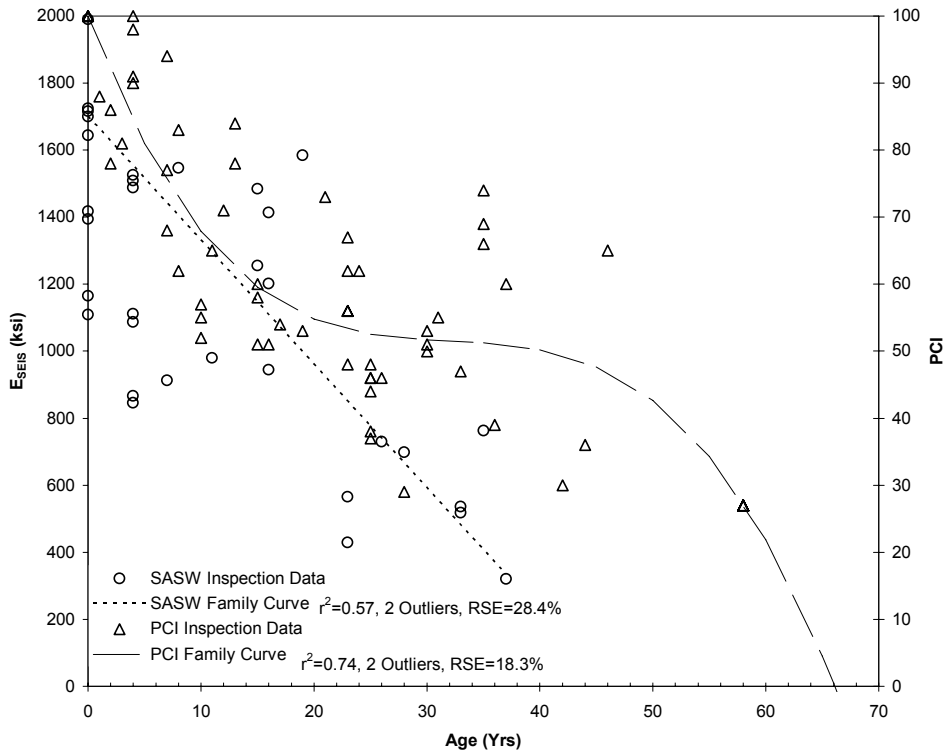


Figure 4-22: Comparison of PCI and E_{SEIS} degradation for family AC(4,2)

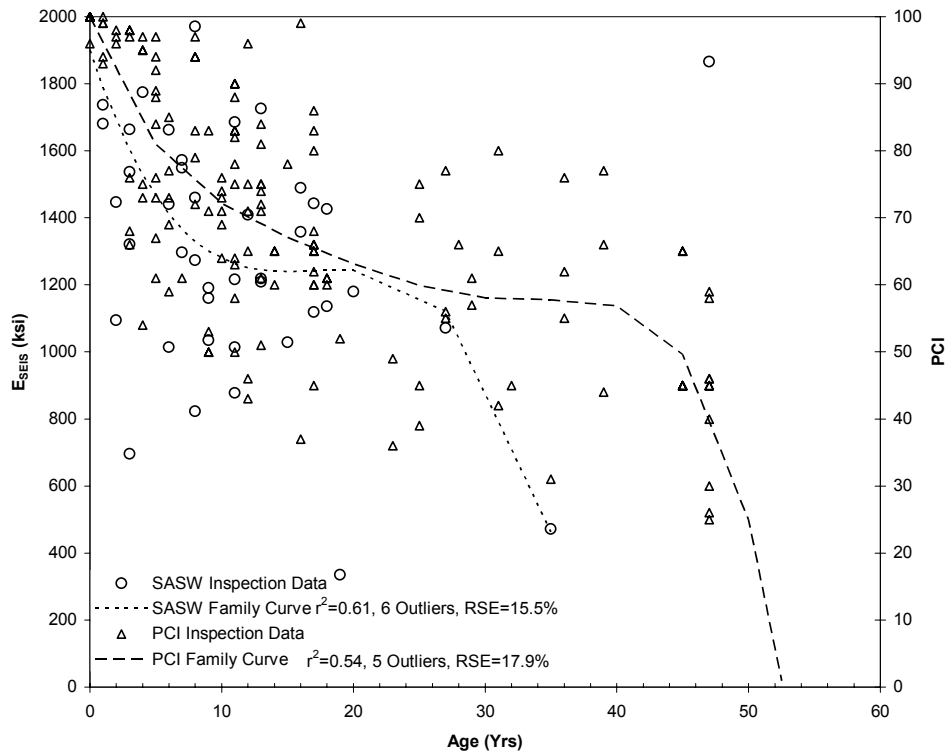


Figure 4-23: Comparison of PCI and E_{SEIS} degradation for family AC(4,3)

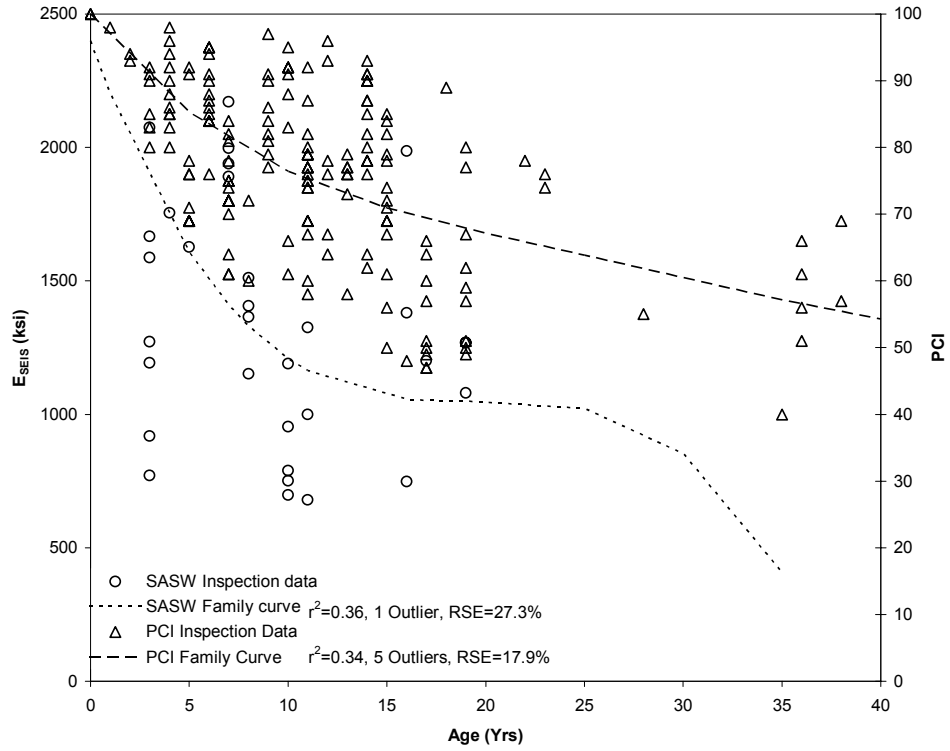


Figure 4-24: Comparison of PCI and E_{SEIS} degradation for family AC(4,4)

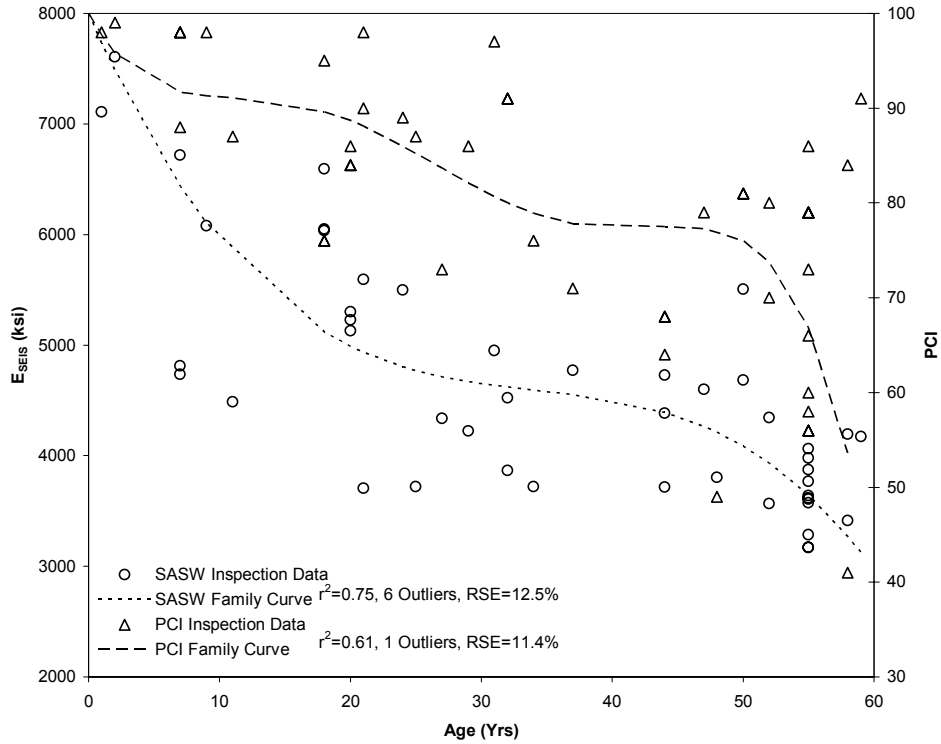


Figure 4-25: Comparison of PCI and E_{SEIS} degradation for family PCC(1,1)

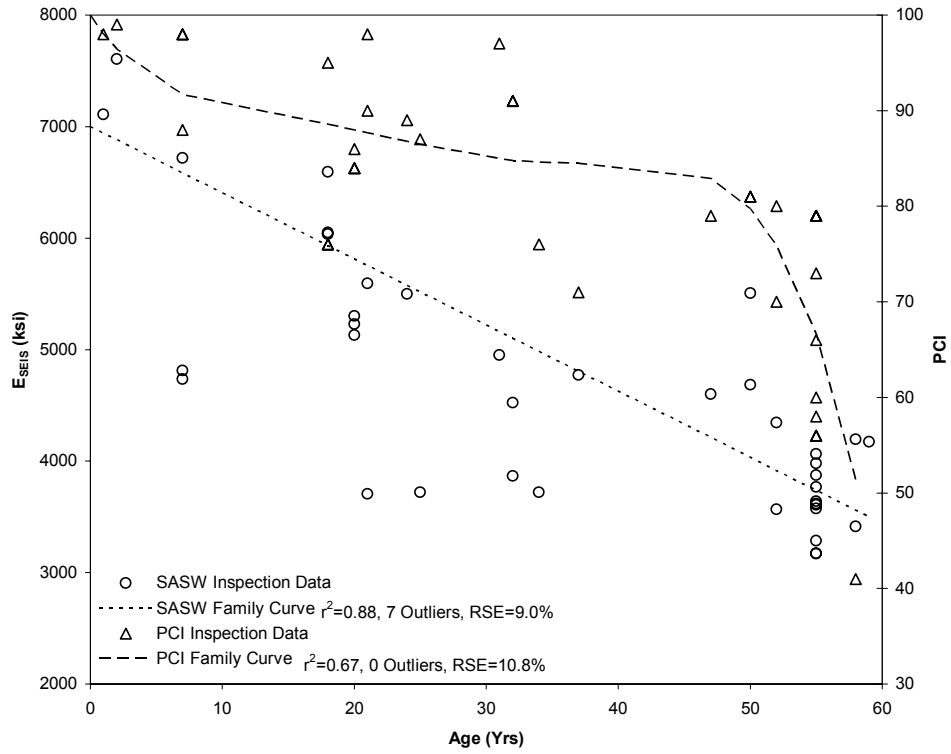


Figure 4-26: Comparison of PCI and E_{SEIS} degradation for family PCC(2,1)

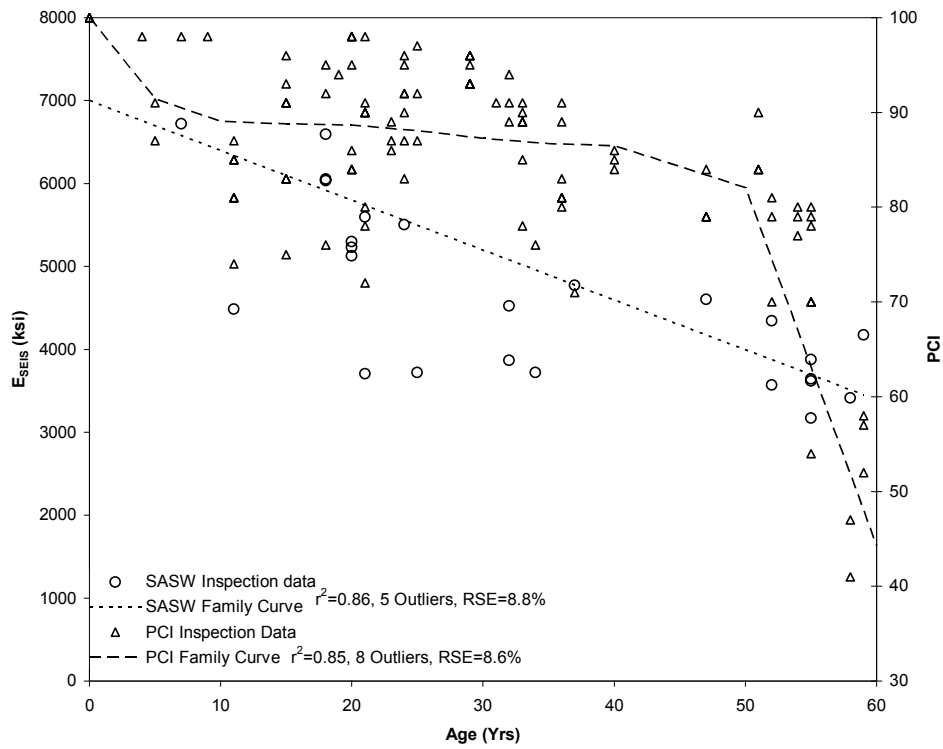


Figure 4-27: Comparison of PCI and E_{SEIS} degradation for family PCC(3,1)

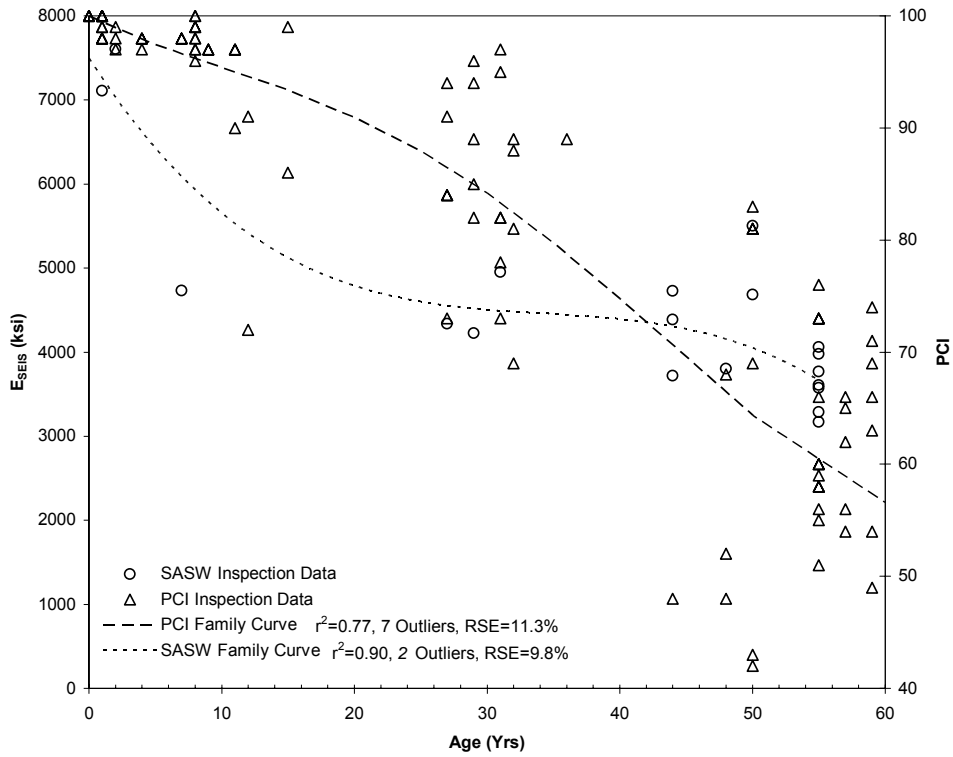


Figure 4-28: Comparison of PCI and E_{SEIS} degradation for family PCC(3,2)

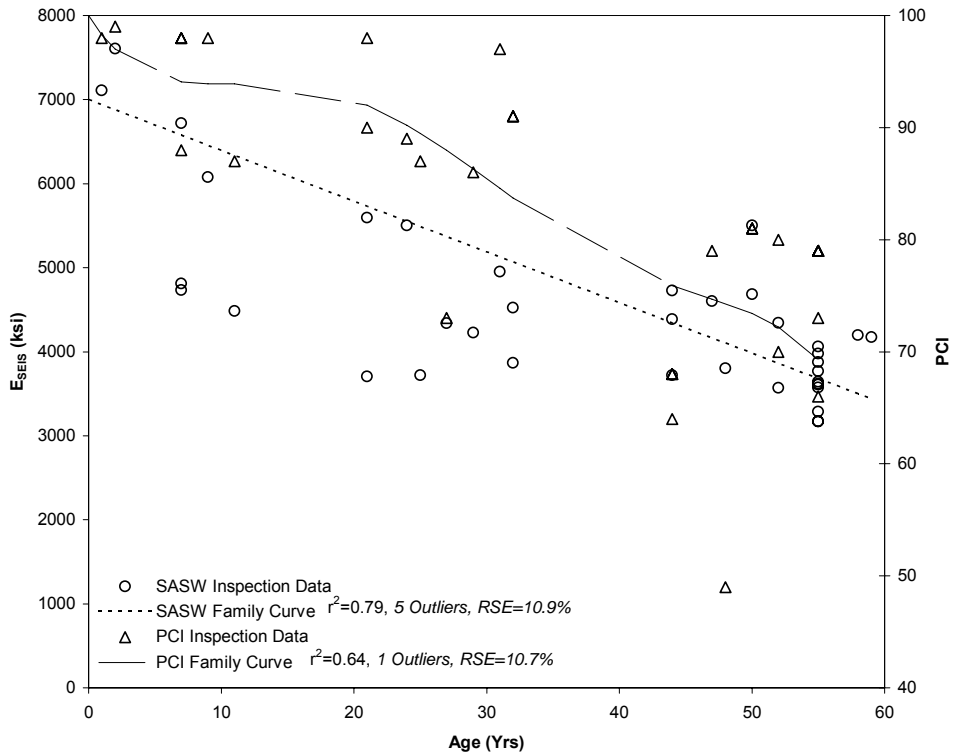


Figure 4-29: Comparison of PCI and E_{SEIS} degradation for family PCC(4,1)

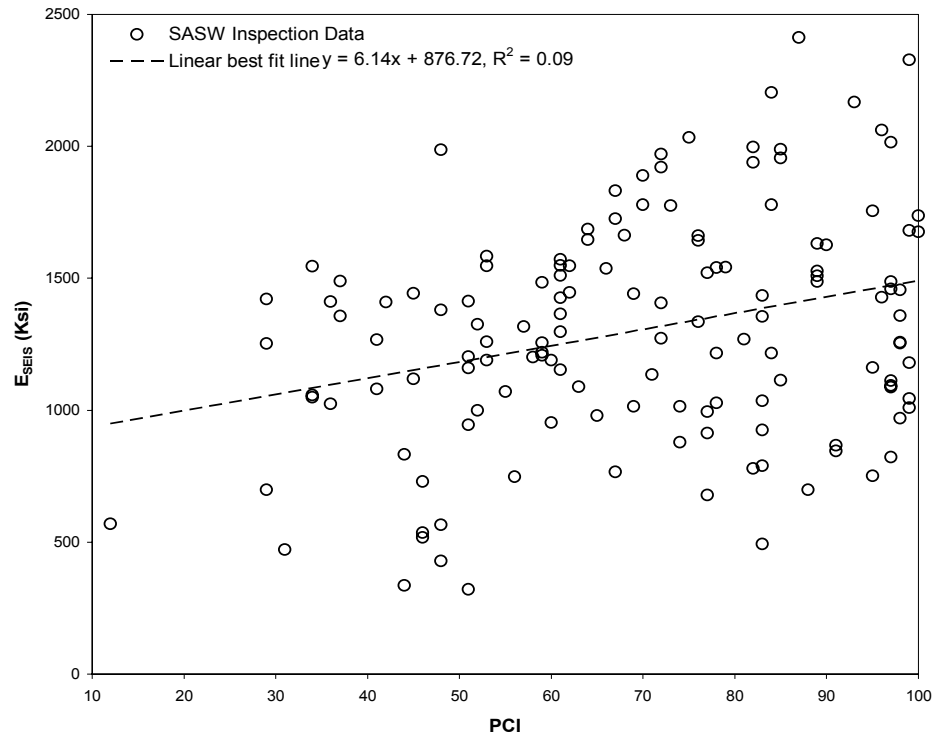


Figure 4-30: Variation of E_{SEIS} of pavement sections with their PCI for AC pavements

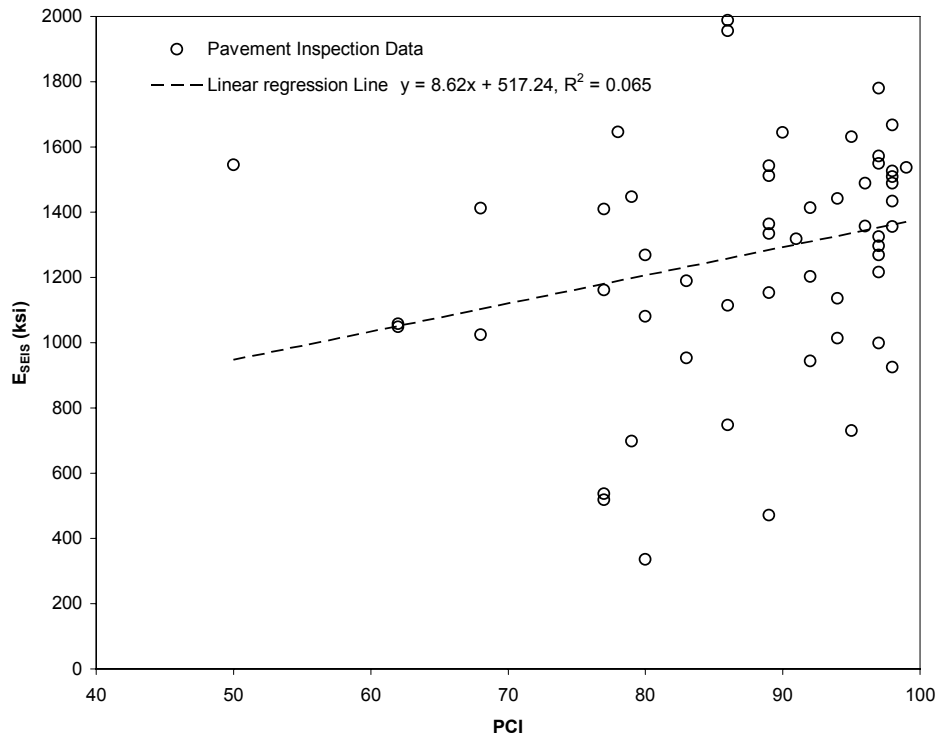


Figure 4-31: Variation of E_{SEIS} in AC pavements with PCI calculated based on structural distresses alone

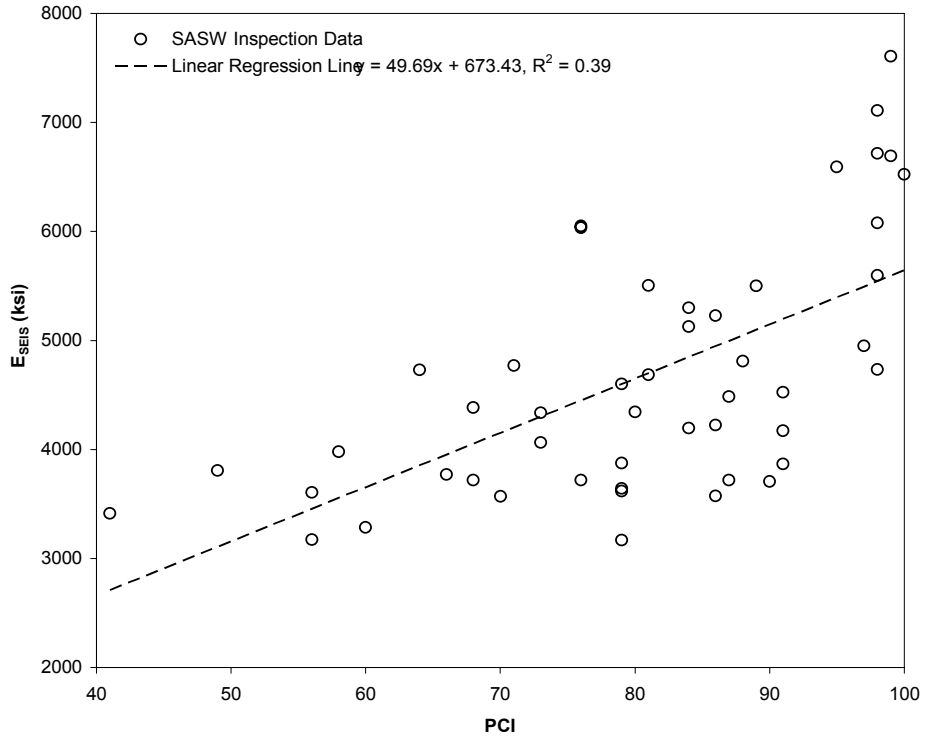


Figure 4-32: Variation of E_{SEIS} of pavement sections with their PCI for PCC pavements

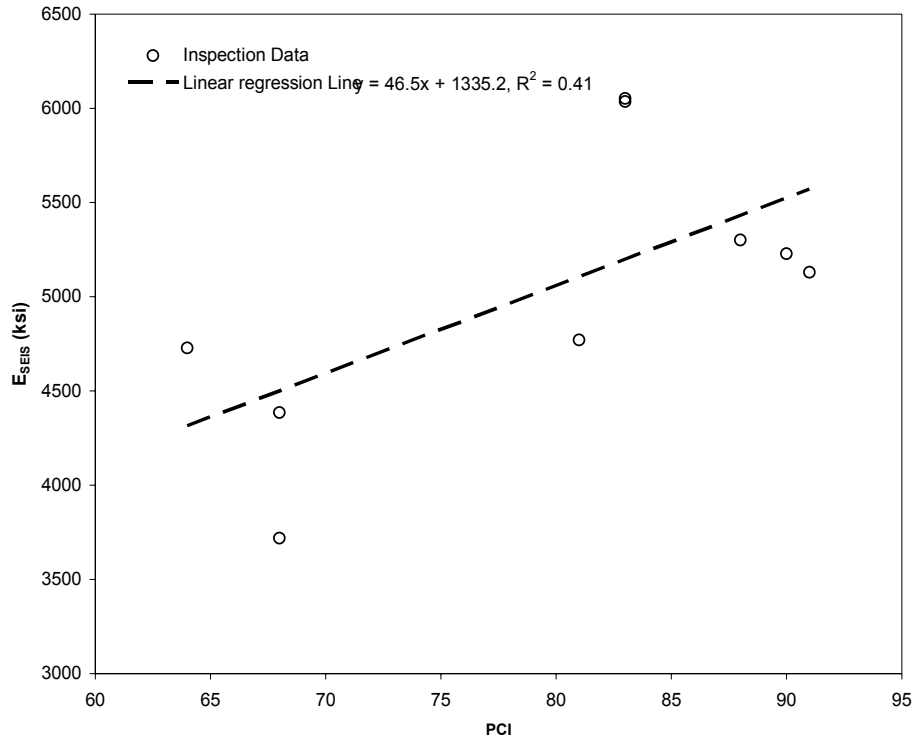


Figure 4-33: Variation of E_{SEIS} in PCC pavements with PCI calculated from Structural distresses alone

Chapter 5 Use of Impulse Response Testing for Pavement Management

5.1 Introduction

A Pavement Condition Index (PCI) based PMS that relies solely on visual condition ratings for pavement condition estimation cannot provide the optimum maintenance selection since it lacks structural information. The current research provides an opportunity to study alternatives to replace or supplement the visually derived PCI. Chapter four presented an evaluation of the Spectral Analysis of Surface Waves (SASW) method for pavement condition monitoring. The current chapter will examine the suitability of the Impulse Response (IR) method for pavement health monitoring. A key motive for this study is the need to improve pavement management with the addition of pavement health monitoring indicators like the dynamic stiffness from IR testing. Owing to the rapid test procedure and ease of data analysis, IR testing presents an opportunity for developing a mechanistic, non-destructive pavement health monitoring tool. In the current study the dynamic stiffness (k_d) measured by IR testing will be evaluated as an indicator of pavement health. It is postulated that k_d can measure the structural adequacy of an airport AC or PCC pavement and that its degradation over time can be modeled using the results of IR testing, a suitable procedure to classify the pavement network into similar family groups and pertinent statistical techniques.

The current study will also examine the existence or lack thereof of a correlation between k_d and the SASW estimated pavement surface layer modulus (E_{SEIS}). The existence of a correlation between k_d and E_{SEIS} of a pavement section would enable

estimation of pavement load-bearing capacity from IR tests. The current study will also investigate the relationship between PCI degradation and the observed stiffness degradation of AC and PCC pavements. A major advantage of IR based structural health models is expected to be their ability to efficiently extrapolate predictions out of the data range and conditions. With refinement of the models over time as the database is enhanced with additional data collection cycles, the error in predicted versus observed pavement health is expected to be minimized. Such performance degradation models would enhance the understanding of the causes of pavement distress and assist in the selection of the most appropriate M&R strategy for the network.

5.2 History of the IR Method

The IR method is also referred to as the transient dynamic response method or the sonic mobility method. It is believed to have been developed from the forced vibration method in France in the early 1960's for evaluating the integrity of cast in place bored piles. Since the 1980's, with advances in portable computers and data acquisition sensors and equipment, the IR method has been applied by researchers to various different problems. Davis and Dunn (1974) used the method to detect defects in piles by comparing their response with the expected response of sound piles. Prommer (1994) described the IR method as a surface reflection method used by researchers for evaluating drilled shafts in a free-head condition. They studied the effectiveness of the IR method on inaccessible shafts and used this to study bridge foundations eliminating the need for costly access tubes as required for the parallel seismic and sonic logging methods. Davis and Hertlein (1995) used the IR method to investigate integrity of ageing concrete chimney stacks and fly ash silos in electricity generating plants. They found the

simplicity of the IR test especially useful because of the large size and tall heights of the structures investigated. They computed the ratio of mean mobility to k_d for test sites along the structure and were able to locate sections with problems like exposed steel reinforcement, areas of concrete delamination and honey-combing. Pederson and Senkowski (1996) undertook research to determine the proper procedures to effectively stabilize the soil beneath plain PCC pavement, the quantity of material needed, and a method of verifying the quality of the stabilization operation for a highway pavement. They successfully used the IR method to map void patterns and to measure the stiffness of PCC slabs. Davis and Hertlein (1996) used the IR method to identify the debonding of concrete overlays on reinforced concrete (RCC) bridge approach slabs at seven different bridge decks on a heavily traveled interstate highway in eastern USA. They found that the k_d estimated from IR testing decreased with increasing severity of overlay debonding and mean mobility increased with decreasing effective layer thickness. Davis et al. (1997) used IR testing along with other nondestructive techniques like parallel seismic testing, ultrasonic pulse velocity, and sonic logging to evaluate concrete radioactive waste tanks for Los Alamos National Laboratory, New Mexico. IR testing was used to study honeycombing and cracking in concrete structural elements. Davis and Kennedy (1998) used IR testing to evaluate the degree of alkali-aggregate reaction (AAR) in concrete drilled shaft foundations for electricity transmission towers. The tested shafts were rated for increasing AAR severity in order to prioritize the maintenance effort. Davis (2005) used IR testing to evaluate the efficiency of tunnel lining grouting programs. The testing measured the average mobility, k_d and the peak/mean mobility ratio also called the void ratio.

Reddy (1992) used a curve-fitting algorithm with the flexibility response curve from IR testing to extract modal parameters like static flexibility and maximum flexibility. Using these extracted parameters, the shear modulus of subgrade and damping ratio of the subgrade could be computed. Reddy concluded that this flexibility based IR testing produced repeatable results and that the method was successful in locating voids greater than twice the thickness of the slab. Nazarian et al. (1994) present the details of the flexibility based IR testing method and presented case studies to demonstrate its use. Again, the procedure showed its robustness in detecting voids underneath rigid pavement. The seismic pavement analyzer (SPA) developed by Nazarian et al. (1995) can rapidly perform IR, Impact-echo (IE), SASW tests, ultrasonic surface wave velocity tests, and ultrasonic body wave velocity tests. The case studies presented include the performance of IR tests with others on AC and PCC pavements. IR testing was used to detect voids and loss of support.

In the case of the AC pavements, SASW and IR stiffness tests were in agreement. Reddy and Nazarian (1996) concluded that elastic modulus and dimensions of the slab have little effect on flexibility while thickness of the slab and the modulus of the subgrade more significantly affect the flexibility spectrum. Gucunski et al. (2001) used IR testing to evaluate pavement undersealing on a section of I-287 in New Jersey. The undersealing operation involved the injection of polyurethane foam under slab joints. IR tests performed before and after injection indicated an increase in subgrade modulus confirming the success of the operation.

Davis (2003) outlined the growth of the IR test in North America in the period 1985 – 2001. He describes that the method has received far less publicity than the Impact

Echo (IE) test. It is stated that IR testing is widely used in Europe and Asia for quality control testing of new piles. In North America, on the other hand, IR testing has expanded into testing of plate-like structures, i.e. pavements, bridge decks and walls. As a result most of the publications about IR testing have focused on the method's application to structural integrity testing rather than pile quality testing.

5.3 Overview of the IR Method

The IR test uses a low-strain hammer impact to send a stress wave through a pavement section. The experimental setup is described in Figure 5-1. At low frequencies (<1 kHz) the pavement surface layer responds to the IR hammer impact in a bending mode. At the interface of the surface layer and the base layer, a portion of this energy is transmitted to the bottom layers and the remainder is reflected to the surface layer. In the case of voids, nearly the entire incident energy is reflected. The load and displacement time histories are recorded and transformed to the frequency domain. The ratio of the resulting velocity spectrum is divided by the force spectrum to obtain a transfer function termed mobility of the element under testing in units of velocity/force. The response graph of mobility plotted against frequency contains information on the condition and the integrity of the pavement in the tested elements as well as the quality of subgrade support, delamination and debonding of overlays, honey combing in concrete etc. The two important parameters derived from this test are: a) k_d and b) Mobility. IR data was collected using a portable data acquisition computer manufactured by Olson Engineering (Wheat Ridge, Colorado) and geophones manufactured by Geo Space Corporation. TFS software was used for data acquisition and processing to obtain the transfer function, mobility and flexibility plots.

The field data collected for AC pavements was corrected for temperature using the relation provided by Aouad (1993) for seismic modulus.

$$\frac{E_t}{E_{77}} = 1.35 - 0.0078(t - 32) \quad (5.1)$$

Where

t is the field temperature during testing, and

E_t is the field estimated SASW modulus and E_{77} the SASW modulus adjusted to 77°F.

The equation is assumed to hold good for AC stiffness from IR tests. Therefore, an equation of the form as in Equation (5.2) was used to correct field stiffness to a reference temperature of 77°F.

$$\frac{K_{dt}}{K_{d77}} = 1.35 - 0.0078(t - 32) \quad (5.2)$$

Where

t is the field temperature during testing, and

k_{dt} is the field estimated stiffness and k_{d77} the stiffness adjusted to 77°F.

Figures 5-2 through 5-5 present a brief insight into the data collection and analysis procedure followed during IR tests. As soon as the hammer is impacted on the test surface, the data acquisition (DAQ) device acquires the response from the load cell in the instrumented hammer and the geophone. The acquired signals are presented in Figure 5-2 (also see Appendix 1). The acquired time-histories from the sensors are then transformed to the frequency domain to get the velocity and force spectra. Figure 5-3 presents the velocity and force spectra for the signals acquired. Mobility, the normalized response of a test surface is obtained as in Equation (5.3).

$$M(f) = V(f)/F(f) \quad (5.3)$$

Where:

f is frequency,

$M(f)$ is the mobility response function,

$V(f)$ is the velocity spectrum obtained by a fast fourier transformation (FFT) of the velocity time history $V(t)$, and

$F(f)$ is the force spectrum obtained by an FFT of the force time history $F(t)$.

Using Equation (5.3) with the spectra obtained previously produces the mobility response function in Figure 5-4. The slope of the mobility response function below 50 Hz defines the compliance or flexibility of the test surface as explained in Equation (5.4).

$$\text{MobilitySlope} = \frac{d(\text{Mobility})}{df} = \frac{d\left(\frac{\text{Vel}}{\text{Force}}\right)}{df} = \frac{\text{displacement}}{\text{Force}} = \text{flexibility} = \frac{1}{k_d} \quad (5.4)$$

As seen from Equation (5.4), dynamic stiffness (k_d) is the inverse of the slope of the 0-50 Hz portion of the mobility response function. Figure 5-5 presents a sample mobility response function collected on an AC pavement with surface temperature estimated to be 91°F. The figure plots the 0-100 Hz portion of the mobility response function. The slope of the mobility response function was estimated between points A and B in the Figure in order to avoid low coherence portions of the signal below 18 Hz. In this case, k_d was computed as 110.1 kip/in after correcting for temperature using Equation (5.2).

5.3.1 Data Collection Program

The industry standard for pavement condition data collection is set by APWA's MicroPAVER software and data collection methodology. This technique is described in greater detail in ASTM D5340 and by Shahin (1994). As detailed in Figure 5-6, this

involves the subdivision of the airport pavement network's inventory of pavements into smaller, consistent units. Using the PAVER method, Oklahoma's airport pavement network was divided into branches based on use, i.e. runways, taxiways and aprons. Each branch was further sub-divided into sections based on traffic patterns (i.e. left edge, right edge and center) and construction history. In a section, test locations were located in a manner to obtain representative data. Test sites were thus located from every 250 ft in a heavily used pavement to every 1000 ft on a less heavily used pavement section. In the course of the testing program spread over six years (2000 – 2006), testing runway sections was given higher importance over taxiways and aprons. Destructive sampling to extract pavement cores and soil samples, Dynamic Cone Penetration (DCP) tests, SASW tests and visual distress surveys to estimate PCI were conducted in addition to IR tests in each section.

The pavement inventory is described in Tables 5-1 and 5-2. Core data was available for 232 AC pavement sections and 74 PCC pavement sections. IR tests were performed in two phases. In the first phase, baseline data was collected and analyzed at about 80 airports. In the second round, a third of the airports were re-visited annually to collect SASW, IR and visual distress data. Core extractions and soil samples collection were performed only in the first phase. Table 5-3 details the year-wise number of IR tests performed. During the data collection program a total of 6,079 IR tests were performed. The average of all IR tests in a pavement section was used to represent the stiffness of that section. Outliers in the data were identified and excluded from the calculation of average k_d . Thus, data from the 6,079 IR test sites were used to develop dynamic stiffness values for a total of 304 asphalt pavement sections and 110 PCC sections. In the first

phase (2000 – 2002) a total of 180 pavement sections were tested. In the second phase (2003 - 2005) 234 sections were tested. In the second phase, inspections at 85 AC sections and 23 PCC sections were repeated.

5.4 Pavement Performance Modeling Approach

A key feature of a PMS is its ability to forecast future pavement condition. This is performed using Pavement Performance Models (PPMs) that model the degradation of pavement condition with age of the section. Conventional PMS's use visual distress based PPMs. One of the objectives of the current study was to investigate the existence of IR stiffness based PPMs. The development of PPMs using the extensive database of IR data requires the grouping of the entire network into “families” of similar pavement sections. Once this is accomplished, IR stiffness database, and construction history information for the network used with appropriate statistical techniques enables the development of PPMs.

Grouping the network of GA airport pavements into pavement families requires identification of factors that contribute to pavement performance. Pavement sections with similar factors are grouped together. Yuan and Mooney (2003) evaluated seven pavement factors for grouping Oklahoma's airfield pavements into pavement families for developing PCI based PPMs. The factors evaluated included:

- a. Surface type – i.e. AC, PCC.
- b. Pavement function – i.e., runway, taxiway or apron.
- c. Construction and maintenance history – i.e. AC (newly constructed asphalt pavement), ACPC (AC overlay over PCC pavement), ACAC (AC overlay over AC pavement), PCAC (PCC overlay over AC pavement).

- d. Nature of dominant pavement distress – traffic, environment or a combination of both.
- e. Climate zone – dry–freeze (DF), wet-Freeze (WF), Dry-no-freeze (DNF) and wet no-freeze (WNF). Oklahoma is divided into DNF and WNF zones that divide the state into eastern and western halves. It is therefore evident that Oklahoma’s Pavements are not subjected to periods of sustained freeze.
- f. Base drainage condition – drainage layer provided or absent.
- g. Pavement thickness – thin AC pavements (≤ 2.5 in.), medium AC pavements (>2.5 in and < 6 in.), thick AC pavements (≥ 6 in.), thin PCC pavements (≤ 6 in.), medium PCC pavements (> 6 in. and < 12 in.) and thick PCC pavements (≥ 12 in.)

This evaluation resulted in the classification of the Oklahoma airfield pavement network into 11 pavement families (Table 5-4). In the current study, Yuan and Mooney’s analysis as well as additional classification factors were evaluated. For each evaluation, families were assigned identification tags using a XX(m, n) format. In the tags XX would either be AC or PCC for the type of pavements being evaluated, ‘m’ the grouping trial number and ‘n’ the family of the mth trial. Thus, family tag AC(2,1) identifies the 1st family grouping of the second trial for AC pavement sections. The following classification factors were evaluated:

- a. AC(1,1) - All AC pavements were classified in a single family.
- b. AC(2,1) to AC(2,7) – The family classification procedure used by Yuan et al.(2003) for classifying AC pavements.

- c. AC(3,1) and AC(3,2) - The total thickness of “structurally capable” layers, i.e. AC, PCC layers, aggregate layers, cement or other treated and stabilized bases., of each section was used to group asphalt pavements only into two families. Sections with load resisting thickness less than 10 inches were identified with the tag AC(3,1) and those with load resisting thickness in excess of 10 inches were identified as AC(3,2).
- d. PCC(1,1) – All PCC pavements were classified in a single family.
- e. PCC(2,1) through PCC(2,3) - The family classification procedure used by Yuan and Mooney (2003) for classifying PCC pavements.

PPMs for the various family groupings were developed using the constrained multi-degree polynomial regression procedure devised by Lawson and Hanson (1974). The Lawson and Hanson procedure was employed by Yuan and Money (2003) for PCI modeling and is extended in the present study to modeling IR data (see Appendix B). The regression problem can be expressed as:

$$Y_i = PCI(x_i) \tag{5.5}$$

where,

Y_i is the PCI of the i^{th} pavement section, and

x_i is the age of the i^{th} pavement section.

The least squares problem can be written as:

Minimize

$$\|Y_i - PCI(x_i)\| \tag{5.6}$$

subject to:

a) The initial value constraint $PCI(0) = 100$ (5.7)

b) Slope constraints, i.e. $\frac{\partial Y_i}{\partial x_i} \leq 0$ (5.8)

c) Optional terminal constraints, and

$$\text{where, } PCI(x_i) = a_0 + a_1x + a_2x^2 + \dots + a_nx^n \quad (5.9)$$

n = polynomial regression order.

The problem formulation in the present study is similar to that used by Yuan and Mooney (2003):

Minimize

$$\|Y_i' - A(x_i)\| \quad (5.10)$$

subject to:

$$\text{a) Slope constraints, i.e. } \frac{\partial Y_i}{\partial x_i} \leq 0 \quad (5.11)$$

where:

Y_i' is the IR dynamic stiffness k_d of the i^{th} pavement section at age ' x_i '

$$A(x_i) = a_0 + a_2x^2 + \dots + a_nx^n, \text{ and} \quad (5.12)$$

n = polynomial regression order.

The value of a_0 in Equation (5.12) is specified by the user. The study uses an outlier detection procedure (Eq. 5.14) based on standardized residuals e_i^* evaluation for a 95% confidence interval. The standardized residuals are calculated from the residuals, e_i .

$$e_i = Y_i' - \hat{Y}_i \quad (5.13)$$

where \hat{Y}_i is the fitted/predicted IR stiffness of the i^{th} pavement section at age x_i .

$$\left| e_i^* \right| \cong \frac{e_i}{s} > 1.96 \quad (5.14)$$

The goodness of fit for each family model was evaluated from the value of the coefficient of determination (r^2) and the square root of the average squared error of prediction called the standardized error of the estimate (SEE).

$$SEE = \sqrt{\frac{\sum_i^k e_i^2}{k - n + 1}} \quad (5.15)$$

where:

k is the total number of IR tests in the current grouping, and

n is the polynomial regression order.

The magnitude of r^2 is interpreted as the proportion of “dependent” variation "explained" by the “independent” variable. Thus, $r^2 = 1$ indicates that the fitted model explains all variability in y , while $r^2 = 0$ indicates no 'linear' relationship between the response variable and regressors. An r^2 value of 0.7 may be interpreted to indicate that approximately seventy percent of the variation in the response variable can be explained by the independent variable. The remaining thirty percent is attributed to the scatter, variability in the data. Cohen (1988), for example, has suggested the interpretations presented in Table 4-3 for correlations in psychological research. However, all such criteria are in some ways arbitrary and should not be observed too strictly. This is because the interpretation of a correlation coefficient depends on the context and purposes. A correlation of 0.9 may be very low if one is verifying a physical law using high-quality instruments, but may be regarded as very high in the social sciences where there may be a greater contribution from complicating factors.

It is expected that increasing values of the coefficient of determination (r^2) will result in lower SEE values. Equation (5.14) explains the reason for this. From the equation, it is evident that SEE is derived using the square of the residuals i.e. square of the difference in fitted and actual data values. It is expected that with higher correlations i.e. increasing r^2 , the sum of the residuals ($\sum e_i^2$) will reduce. In the present research,

outliers are identified with every regression run. Identification of outliers can impact the sum of residuals and cause SEE to go up with increasing correlations.

Though statisticians generally desire the SEE to be as low as possible, there is no clear guidance available on how low it should be. Guidance is however, available for the relative standard error (RSE) or the coefficient of residual variability defined in Equation (5.16).

$$RSE = \frac{SEE \times 100}{\bar{Y}} \quad (5.16)$$

where \bar{Y} is the mean.

Regression analysts prefer models with RSE lower than 15% (Mendenhall and Sincich, 2003). However, this traditional expectation is waived in pavement data due to spatial variability of pavement properties, and also due to the difficulty in characterizing such a large object with a few sample points. Therefore regression models with RSE values lower than 20% are considered adequate in the current study. Tables 5-5 and 5-6 present the key statistical parameters for the classifications attempted.

5.4.1 Asphalt Concrete Pavement Performance Models

Figure 5-7 presents the PPM for family AC(1,1) developed using IR stiffness data from each of the tested 303 sections. From the figure it is observed that k_d decreases with pavement age. From an initial value of 120 kip/in, the dynamic stiffness degrades to approximately 60 kip/in by the end of the first 20 years of pavement life. Based on the best fit line, from 20 to 35 years, k_d decay decelerates. Several models were evaluated and ranked based on the value of the coefficient of determination (r^2), the number of outliers and the value of the standardized error of the estimate. The model with the lowest average of these three ranks was selected to represent the family's condition

deterioration. An example of the ranking system used for model selection is presented in Table 5-7. The model with the lowest average rank is highlighted and selected as the model that best represents the pavement performance for the current data set. In the case of the current data, a third degree polynomial is observed to best model the pavement stiffness degradation though there are 30 outliers to the selected model (Table 5-5). The outliers represent 9.9% of collected data.

Figures 5-8 through 5-14 present the selected regression models using AC pavement inspection data and the family grouping methodology used by Yuan and Mooney (2003). Table 5-4 provides the factors upon which their grouping is based. Key statistical parameters are available in Tables 5-5. Several models were evaluated and the model selected as the PPM was identified using the ranking procedure described in Table 5-7. The polynomial order of selected PPMs is observed to vary from 2nd to 3rd, with values of r^2 ranging from 0.28 to 0.59, SEE values ranging from 13.8 to 26.0, RSE values ranging from 21.8 to 51.7% and there were 0% to 11.3% outliers. Families AC(2,6) and AC(2,7) had fewer than 30 data sets. For these, data were assumed to be normally distributed.

In each of the Figures 5-8 through 5-14, k_d is observed to degrade with pavement age. In Figure 5-8, stiffness of pavements in family AC(2,1) degrades from an initial 110 kip/in to nearly 60 kip/in at the end of the first 20 years of pavement life. The model selected demonstrates a significant correlation, though the high RSE value (30.7%) indicates large scatter in the data. Figure 5-9 presents the regression analysis for pavements in the family AC(2,2). The selected 3rd order polynomial model presented in the figure exhibits slow initial decay of k_d in the first 20 years with about a 28% decrease

in stiffness in the period. Beyond 30 years of pavement life the best fit model suggests accelerated decay of k_d . Regression analysis provides a correlation of medium significance, 10% outliers, and high RSE value (25.0%) indicative of scatter in the data. Figure 5-10 depicts results of regression analysis performed on family AC(2,3). Initial stiffness of 110 kip/in drops to 55 kips/in at the end of 20 years and then degrades very little from 20 to 40 years. Beyond 40 years, further degradation of k_d is observed from the Figure. The analysis yields a significant correlation with a marginally high RSE value of 21.8%. Figures 5-11 and 5-12 present similar deterioration of k_d with pavement age. A correlation of small significance is observed for family AC(2,4) while a correlation of medium significance is observed for family AC(2,5) in Figure 5-12. Each of Figures 5-13 and 5-14 use fewer than 30 data points for regression. Though this is not adequate, data points are assumed to be normally distributed. Regression analysis upon data of both families yields low r^2 values (0.33, 0.37) and high RSE (44.0, 51.7).

Figures 5-15 and 5-16 present the selected regression models for families devised using the total thickness of structurally capable layers in the pavement section. This results in two pavement families labeled AC(3,1) and AC (3,2). AC pavements with total thickness of structurally capable layers less than 10 inches are classified in family AC(3,1) and those thicker than 10 inches are classified as family AC(3,2). A third degree polynomial model is chosen for each family grouping based on the procedure described in Table 5-7. Values of r^2 (Table 5-5) for grouping AC(3,1) was 0.55 and for grouping AC(3,2) it was observed to be 0.50. SEE was estimated at 13.1 for AC(3,1) and 21.7 for AC(3,2). From Table 5-5 and Figures 5-15 and 5-16, it is observed that the number of outliers identified by the regression procedure used, was 11 (9.8%) for grouping AC(3,1)

and 14 (7.4%) for grouping AC(3,2). The RSE value for family AC(3,1) of 19.2% indicated lower scatter than for family AC(3,2) which was observed to exhibit an RSE value of 30.5%.

Table 5-8 details the comparison of the efficacy of the different family grouping methodologies. Family sub-divisions were assigned ranks for value of r^2 , % outliers, SEE and RSE values. Using these ranks the weighted average rank and the simple average rank of the classifying methodology was developed as in Table 5-8. Families devised using the thickness of “structurally-capable” layers in the pavement section outperformed others. Based on these results family groupings AC(3,1) and AC(3,2) are recommended for use in developing IR stiffness based models for Oklahoma’s AC general aviation airport pavements.

5.4.2 Portland Cement Concrete Pavement Prediction Models

Grouping PCC(1,1) included data from all 110 PCC pavement sections that were tested using the IR method. Based on the regression analysis performed, Figure 5-17 presents the selected 3rd order polynomial for decay of dynamic stiffness with pavement age. It is observed that stiffness degrades to less than half its initial value, i.e. from 400 kips/in to 165 kips/in at the end of the first 20 years of pavement life. The rate of decay of dynamic stiffness slows down from 30 to 50 years. The value of r^2 for the best fit model from regression analysis was 0.92, with a SEE of 20.1 and RSE value of 13.4%. There were 9 outliers (8.2%) to the selected model

Though the regression results for family PCC(1,1) are significant, a comparison with the existing PCI based family approach devised by Yuan and Mooney (2003) for Oklahoma’s GA airports was also studied. As observed from Table 5-6, fewer than 30 IR

tests were performed on pavements included in two of the four PCI based families devised by Yuan and Mooney (2003). Regression analysis to study decay of k_d with pavement age could not be performed for family PCC(2,4) since it included only 4 IR tests. From Table 5-6, it is observed that a total of 16 IR tests were performed on pavements included in family PCC(2,3). Regression analysis to study degradation of stiffness with time was performed on IR test results included in this family with the assumption that data were normally distributed. Figures 5-18 through 5-20 illustrate the results of the regression analysis performed. As observed in the figures, regression analysis produced significant results for all PCC families. The r^2 value varied from 0.91 to 0.97, SEE values ranged from 12.6 to 26.1 with RSE values ranging from 9.2 to 13.8%. The low RSE values are indicative of low scatter in the data. The percentage of outliers identified in the analysis ranged from 0% to 8%.

Similar to the analysis for AC pavements, a significance rank was calculated for PCC family groupings. As before, a family's significance rank was estimated from the key parameters of the selected stiffness decay model including magnitude of r^2 , % outliers, SEE and RSE value. The results are presented in Table 5-9. From the table it is observed that the PCI based rankings work well for IR data. However, at present there are insufficient numbers of IR tests on apron pavements. It is therefore recommended that a single family including all PCC sections i.e. family PCC(1,1) be employed to model decay of stiffness with pavement age. Future data collection efforts should aim to increase the number of IR tests on apron pavements so that a common family structure could be shared for PCI and IR stiffness data.

5.5 Comparison of IR Stiffness with SASW estimated Modulus

It is important to understand the basic difference in the test procedures before comparing results from the two test methods. The IR method uses body waves to estimate the stiffness of the material being investigated. The test uses a low-strain impact to generate stress waves through the tested element. The SASW method on the other hand uses surface waves to estimate the low strain Modulus of Elasticity (E_{SEIS}) of the sampled material. In the case of the SASW method, the travel time of surface waves between two receivers placed at a known distance apart is used to compute the surface wave velocity. The surface wave velocity is then used to estimate E_{SEIS} . Since the dynamic stiffness estimated from IR testing and the E_{SEIS} value estimated by SASW are both measures of the ability to resist deformation of the material under investigation, the existence of a correlation between them was explored. In the case of AC pavements, a correlation between k_d and E_{SEIS} was not observed. Figure 5-21 presents a plot of k_d and E_{SEIS} for 33 PCC pavements. In this case the linear best fit line has an r^2 value of about 0.2. Using the guidance for interpretation of r^2 values in Table 4-3, a correlation of “small” significance between dynamic stiffness from IR tests and SASW estimated modulus for PCC pavements is observed. This observation is consistent with the finding of Reddy and Nazarian (1996) that elastic modulus and dimensions of the slab have little effect on flexibility, the inverse of stiffness.

Figures 5-22, through 5-24 illustrate the variation of k_d and E_{SEIS} in AC and PCC pavements. E_{SEIS} data for AC pavement families AC(3,1), AC(3,2) and family PCC(1,1) from Chapter 4 was used in the comparison with k_d data for the same families. In Figure, 5-22, the SASW best fit model estimates a 32% decrease in E_{SEIS} at the end of the first 10 years of pavement life for family AC(3,1).. From the IR best fit model in the figure

nearly identical (30.5%) decay of k_d is observed at the end of the first 10 years of life. Similar scatter in IR data is concluded from the RSE value for the IR model (19.2%) and the RSE value (17.8%) for the SASW model. In Figure 5-23, a sharp decrease of E_{SEIS} and k_d in the first 15 years of pavement life is observed for family AC(3,2). The decrease is approximately 64% for E_{SEIS} and 52% for k_d . Similar scatter in IR data is concluded from the RSE value for the IR model (30.2%) and the RSE value (27.4%) for the SASW model. In Figure 5-24 a comparison of k_d and E_{SEIS} deterioration for all PCC pavements is presented. The best fit model for k_d data shows a steeper decline in the initial 20 years of pavement life, decreasing by approximately 59% as compared to decrease in E_{SEIS} of 37.5% in the same period. The SASW model for PCC pavements exhibits higher scatter in data based on the higher RSE value of 17.8% compared to a RSE value of 13.4% for the IR model.

5.6 Comparison with PCI

It is of interest to explore the existence or lack of a correlation between k_d and PCI. A comparison of k_d with estimated PCI rating of pavement sections is presented in Figures 5-25 and 5-26. In the figures, k_d is plotted against the estimated PCI as well as the PCI computed using observed structural distresses alone. Tables 1-1 and 1-2 list the distress types observed in AC and PCC pavements as well as the cause for the distress. From the tables it is observed that structural distresses in AC pavements include alligator cracking and rutting. For PCC pavements corner breaks, linear cracking and shattered slab are considered to be caused due to structural failure. The PCI of the structurally distressed sections was calculated using the following:

$$PCI_s = 100 - DV_s \quad (5.17)$$

where, PCI_s is the PCI of the pavement section due to structural distresses alone, and DV_s is the total of traffic-related deducts observed in the section.

The PCI based analysis by Yuan and Mooney (2003) determined that only 2.8% of the inspected sections exhibited dominant traffic or load related distresses. Therefore for a meaningful comparison of IR estimated stiffness with structural distresses, only sections with dominant structural distresses were used. This was also necessary as most of the sections exhibiting dominant environmental distress did not report any structural distress, which would lead to their PCI_s being estimated as 100 using Equation (5.14). It is pertinent to note that Yuan and Mooney (2003) used a cut-off deduct percentage of 70% to classify pavement sections as either exhibiting dominant traffic-related or dominant environment related distress. The current study uses a cut-off deduct percentage of 50% to classify a section as exhibiting either dominant structural or dominant environmental distress. Thus, in a structurally distressed pavement section, traffic-related deducts exceeded 50% of the total deducts due to traffic and environmental causes. Using this procedure, structurally distressed sections were identified for AC and PCC pavements. For the current study only those sections that had both PCI and IR test results were used.

Of the 301 AC pavement sections tested using the IR method, both stiffness and PCI data were available for only 192 sections. Of these, 12 sections exhibited dominant structural distress, i.e., 6.25%. Figure 5-25 plots k_d of AC pavement sections with their PCI as well as PCI_s rating. The linear best fit line shows a correlation of small significance ($r^2 = 0.16$) with overall PCI of the section. Figure 5-25 also presents the best fit line for the variation of IR stiffness with PCI from structural distresses alone. From the

figure it is observed that a correlation of ‘small’ significance exists between a section’s stiffness and its overall and structural PCI.

Figure 5-26 plots the variation of IR stiffness with PCI ratings for 110 PCC pavement sections. The linear best fit line exhibits a correlation with an r^2 value of 0.37. Using the methodology described above, there are 10 structurally distressed PCC pavement sections, i.e. about 9.1% of the total number of PCC sections. The figure also plots the variation of IR stiffness with PCI_s estimated as in the case of AC pavements. The linear best fit line exhibits an r^2 value of 0.40. From the guidance provided in Table 4-3, the correlation of IR stiffness with PCI_s ($r^2=0.40$) falls into the category of medium significance.

The low correlation of total or overall PCI with IR stiffness of both AC and PCC pavements is in agreement with the hypothesis that visual distresses alone cannot provide total guidance to pavement managers for maintenance selection. PCI ratings are calculated based upon several different observed distresses and their severity levels. Quite a few of the distresses used to calculate PCI measure surface serviceability and ride quality. Since the PCI rating is made up of environmental and traffic related distresses, the correlation of overall PCI with a structural index like k_d is expected to be low. However, it was expected that a significant correlation would exist between PCI_s and k_d . A small sample size can be a cause of the weak (AC) to medium (PCC) correlations observed. If the sample size is ignored, it could be concluded from the results presented that for AC pavements, distresses recorded as being caused by structural failure of the pavement are attributable to other reasons. In the case of PCC pavements though the correlation with structural distresses is lower than the total PCI, a correlation of medium

significance is observed between stiffness and PCI data. From the results, ignoring the small size of data used, it is observed that for PCC pavements identification of structural distresses is more accurate than in the case of AC pavements.

5.7 End of Pavement serviceable life – a comparison between IR Stiffness based models with SASW & PCI based models

From the PCI data (Table 5-10), Yuan and Mooney observed the average life of an AC pavement to be 45 years and the average life of a PCC pavement to be more than 65 years. FAA's advisory circulars (FAA AC 150/5320-6D) for pavement design require pavements to have a 20 year structural life as long as there are no major changes in forecast traffic. Therefore, the important question is – is this “longer life” actually observed or is it a flaw in the PCI based models? Also, FAA's guidelines only permit rehabilitation of surface grades and renewal of skid-resistance properties. Since these permitted rehabilitations cannot alter the load carrying ability of the pavement, its structure must retain the designed capacity to support the design load for 20 years. The SASW estimated modulus can be used with layer thickness, traffic and pavement design softwares e.g. PCASE, KENPAVE, to determine pavement section structural capacity. IR estimated stiffness on the other hand cannot be used with a pavement design program to directly yield pavement load-bearing capacity. The current study failed to establish a statistically significant correlation between E_{SEIS} and k_d .

Since the stiffness of a pavement section is a direct measure of its capability to resist deformation, k_d is an indirect measure of the pavement's load bearing capacity and as such it can deliver an estimate of remaining pavement life. With FAA's advisory circular as a guide, and assuming a normal factor of safety of 2 in airport pavement

design, an IR stiffness lower than 50% of the initial pavement stiffness is taken to characterize the end of pavement's serviceable life.

Table 5-11 presents the magnitude and percentage of remaining IR stiffness for AC pavements. The magnitude and percentage of remaining IR stiffness of PCC pavements is placed in Table 5-12. From the table it is observed that for family AC(3,1) the stiffness falls below 50% at a pavement age of 30 years. And, at an age of 50 years, only 11.0% of initial pavement stiffness remains. In the case of family AC(3,2) from data presented in Table 5-11, it is observed that stiffness falls below 50% at a section age of 14 years and below 10% at an age of 45 years. Table 5-12 presents the magnitude and percentage of remaining IR stiffness for PCC pavements. For family PCC(1,1) stiffness falls below 50% of the initial value at a pavement age of 15 years and below 10% at the end of 68 years. For family PCC(2,1) IR stiffness falls to 50% of initial value at an age of 15 years and below 10% of the initial value at the end of 75 years. For pavements classified in family PCC(2,2) the magnitude of IR stiffness falls below 50% of the original value at a pavement age of 19 years and below 10% at an age of 66 years. Lastly at ages of 15 and 67 years IR stiffness for pavements included in family PCC(2,3) fall below 50% and 10% of the initial magnitude, respectively.

5.8 Conclusions

From the results of IR tests at 6,079 sites located at 81 general aviation airports in Oklahoma it was determined that the dynamic stiffness estimated from IR testing can be used to capture pavement deterioration of both AC and PCC pavements. Regression results using k_d data yielded r^2 values ranging from 0.28 to 0.59 for AC pavements and from 0.91 to 0.97 for PCC pavements. The values compare well with regression results

obtained by other researchers working with PCI data (Appendix 2). Stiffness degradation with pavement age was modeled using a family approach. For AC pavements, families devised using the total thickness of structurally-capable layers in a pavement section were found to yield the best results. For the two families generated by this approach – family AC(3,1) and family AC(3,2), 3rd order polynomial regression models were selected. These exhibited r^2 values of 0.50 and 0.55 with SEE values of 13.1 and 21.7 and RSE values of 19.2 and 30.7, respectively. The statistical correlations for deterioration models for PCC pavements were higher (r^2 value ranging from 0.92 to 0.97).

Family classifications devised by Yuan and Mooney (2003) were observed to provide the most statistically significant deterioration models for PCC pavements, though regression analysis could not be performed for family PCC(2,4) – apron pavements. Grouping all PCC pavement sections tested into one family – PCC(1,1) yielded a significant r^2 value of 0.92, SEE equal to 20.1, RSE value of 13.4% and 8.2% outliers. Consequently, grouping of all PCC pavements into one family was recommended for use with Oklahoma’s GA airport pavements.

A statistically significant correlation between IR stiffness and SASW estimated modulus for AC pavement could not be established. In the case of PCC pavements a weak correlation was observed between SASW estimated modulus and IR stiffness. This observation confirmed the finding of Reddy and Nazarian (1996) that elastic modulus and dimensions of the PCC slab have little effect on k_d . A comparison of decay trends of k_d and E_{SEIS} revealed that in the first 10 years of life, pavements grouped in family AC(3,1) exhibited identical percentage decline in k_d (30.5%) and E_{SEIS} (32%). In the case of thicker AC pavements, grouped in family AC(3,2), the percentage decline of E_{SEIS} (64%)

in the first 15 years of pavement life was higher than the percentage decline of k_d (52%). For PCC pavements, the percentage decline in k_d in the first 20 years of life was higher (59%) than the percentage decline in E_{SEIS} (37.5%) during the same period.

A correlation of “small” significance was observed between IR stiffness and PCI rating of AC pavement sections. Though the sample used for comparison with structurally distressed sections was small, results suggest that in AC pavements, visually inferred traffic-related distresses do not correlate with structural failure. In the case of PCC pavements a correlation of “large” significance was observed between k_d and PCI ratings ($r^2=0.5$) and a correlation of “medium” significance was observed between k_d and PCI_S . From the results, ignoring the limited size of the database used, it is observed that for PCC pavements visual identification of structural distresses is more accurate than in the case of AC pavements.

k_d cannot be used with pavement design programs or with existing fatigue failure equations to predict estimated remaining pavement life. As observed from the regression models evolved in this study, 10% of the initial stiffness remains at an age of 50 and 45 years for families AC(3,1) and AC(3,2), respectively. For PCC pavements, 90% of the initial stiffness was found to have degraded at age ranging from 66 to 75 years. The results of this analysis are similar to Yuan and Mooney’s (2003) finding for PCI based models i.e. 45 year life for AC pavements and 60 year life for PCC pavements.

5.9 References

ASTM D5340-04e1, “*Standard Test Method for Airport Pavement Condition Index Surveys*”, ASTM International.

Davis, A.G. and C.S. Dunn. “*From Theory to Field Experience with the Nondestructive Vibration Testing of Piles*”. Proc., Institute of Civil Engineers, 1974, pp 867-875

Davis, A.G. and B.H. Hertlein. “*Nondestructive Testing of Concrete Chimneys and other Structures*”. Proc., SPIE 2457, Conference on Nondestructive Evaluation of Aging Structure and Dams, Oakland, CA pp 129-136, 1995.

Davis, A.G., Hertlein, B.H., Lim, M.K., and K.A. Michols. “*Impact-Echo and Impulse Response Stress Wave Methods: Advantages and Limitations for the Evaluation of Highway Pavement Concrete Overlays*”. Proc., SPIE 2946, Conference on Nondestructive Evaluation of Bridges and Highways, Scottsdale, AZ, 1996.

Davis, A.G. and B.H. Hertlein. “*Nondestructive Evaluation of Concrete Radioactive Waste Tanks*”, Journal on Performance of Constructed Facilities, ASCE, 11(4), pp 161-167, 1997.

Davis, A.G. and J. Kennedy, “*Impulse Response Testing to evaluate the degree of Alkali-Aggregate reaction in concrete drilled shaft foundations under electricity transmission towers*”, Conference on Nondestructive evaluations of Utilities and pipelines, Proceeding of SPIE 3398, Paper 21, San Antonio, TX, April 1998.

Davis A.G., “*The Nondestructive Impulse Response test in North America: 1985 – 2001*”, NDT and E International, v36, n 4, June 2003, p 185-193.

Davis, A.G., Lim, M.K. and C.G.Petersen, “*Rapid and economical evaluation of concrete tunnel linings with impulse response radar non-destructive methods*”, NDT&E International, Vol 38, 2005, pp 181-186.

Federal Aviation Administration, “*Airport Pavement Design and Evaluation*”, Advisory Circular AC 150/5320-6D, Change 4, 2006.

Gucunski, N., Maher, A. and H. Jackson, “*Verification of Pavement Undersealing by Impulse Response Method*”, *Proceedings of Matest 2001 – Nondestructive Testing in Environmental Protection Symposium*”, Cavtat, Croatia, September 22-24, 2001, pp 81-86.

Lawson, C.L., and Hanson, R.J., “*Solving least squares problems*”, Prentice-Hall, Inc., 1974.

Mendenhall, W. and T. Sincich, “*A second course in statistics – regression analysis (6th edition)*”, Pearson Education Inc., New Jersey, ISBN 0-13-022323-9, 2003.

Nazarian, S., Baker M.R. and M.K. Crain. “*Determination of Voids under Rigid Pavements using Impulse Response Method*”. ASTM Special Technical Publication 1198, 1994.

Nazarian, S., Baker M.R. and M.K. Crain, “*Use of Seismic Pavement Analyzer in Pavement Evaluation*”, Transportation Research Record 1505, National Research Council, 1995.

Nazarian, S. and S. Reddy, “*Study of Parameters Affecting Impulse response Method*”, Journal of transportation Engineering, Vol 122, no. 4, July 1996, pp 308-315.

Pederson, C.M. and L.J. Senkowski. “*Slab Stabilization of PCC pavements*”, Proc., Annual meeting of the Transportation Research Board, 1996.

Prommer, P.J., “*Evaluation of Inaccessible Drilled Shafts Using the Impulse Response Method*”, MS Thesis, Northwestern University, 1994.

Reddy, S. “*Improved Impulse Response Testing: Theoretical and Practical Validations*”, M.S. Thesis, University of Texas at El-Paso, 1992.

Seed, H.B., and I.M. Idriss. “*Soil Moduli and Damping Factors for Dynamic Response Analysis*”, Report EERC 70-10. University of California, 1970.

Shahin, M.Y., “*Pavement Management for Airport Pavements, Roads, and Parking Lots*”, Kluwer Academic Publishers, Massachusetts, 1994.

Yuan, J., and Mooney, M. A. (2003). “*Development of adaptive performance models for Oklahoma Airfield pavement management system*” Transportation Research Record 1853, Transportation Research Board, Washington, D.C., 44–54.

Yuan, J., “*Development of Adaptive Pavement Performance for the Oklahoma Airfield Pavement Management System*”, MS Thesis, University of Oklahoma, 2002.

Table 5-1: Core sizes of AC pavement sections

Core thickness	No. of Pavement Sections
$t \leq 2.0''$	36
$2.0'' < t \leq 3.0''$	46
$3.0'' < t \leq 4.0''$	40
$4.0'' < t \leq 6.0''$	48
$6.0'' < t \leq 8.0''$	27
$8.0'' < t \leq 10.0''$	22
$10.0'' < t \leq 12.0''$	9
$t > 12.0''$	9

Table 5-2: Core sizes of PCC pavement sections

Core thickness	No. of Pavement Sections
$t \leq 6.0''$	7
$6.0'' < t \leq 7.0''$	26
$7.0'' < t \leq 8.0''$	12
$8.0'' < t \leq 10.0''$	14
$t > 10.0''$	14

Table 5-3: Year-wise number of IR tests performed

	Phase 1		2003		2004		2005	
No. of IR Tests	2,033		1285		649		2112	
No. of Sections with IR Tests	AC	PCC	AC	PCC	AC	PCC	AC	PCC
	136	44	85	25	40	4	43	37

Table 5-4 PCI based Pavement Performance Models developed by Yuan et al. (2003)

Family Name	Family Description	Number of Points	Outliers	r ²	Polynomial Order used in PPM
AC1	AC/RW/Load & Combined	47	3	0.53	5 th
AC2	AC/RW/Environmental/thin	37	2	0.83	5 th
AC3	AC/RW/environment/medium	64	0	0.48	5 th
AC4	AC/RW/environment/thick	79	1	0.50	5 th
AC5	AC/TW/environment	50	3	0.71	5 th
AC6	AC/TW/Load & combined	32	2	0.78	5 th
AC7	AC/AP	51	4	0.68	5 th
PCC1	PCC/RW/DNF	54	1	0.79	5 th
PCC2	PCC/RW/DNF	56	3	0.78	5 th
PCC3	PCC/TW	39	3	0.80	5 th
PCC4	PCC/AP	25	1	0.56	5 th

Legend:- **AC**- Asphalt Concrete; **PCC** – Portland Cement Concrete; **RW** – Runway pavement; **TW** – Taxiway pavement; **AP** – Apron pavement; **DNF** – Dry, No freeze zone; **WNF** – wet, no freeze zone; **environment** – Pavements with dominant environmental distresses; **Load** – Pavements with dominant Load related distresses; **Combined** – Pavements exhibiting a mix of traffic related and environment related distresses with neither dominating.

Table 5-5: Statistical Results for Family groupings of AC pavements

Family Name	Family Particulars	Sections with IR tests	Polynomial Order of regression Model	r ²	Outliers		Std. Error of est. SEE	RSE (%)
					No.	%		
AC(1,1)	All AC pavements	303	3 rd	0.46	30	9.9	18.8	26.9
AC(2,1)	AC/RW/Load & Combined	64	2 nd	0.51	3	4.7	22.7	30.7
AC(2,2)	AC/RW/Environmental/thin	30	3 rd	0.49	3	10.0	13.81	25.0
AC(2,3)	AC/RW/environment/medium	62	3 rd	0.59	7	11.3	14.2	21.8
AC(2,4)	AC/RW/environment/thick	82	3 rd	0.28	3	3.7	19.2	23.1
AC(2,5)	AC/TW/environment	35	3 rd	0.49	3	8.6	21.1	28.8
AC(2,6)	AC/TW/Load & combined	15	3 rd	0.37	0	0.0	26.0	44.0
AC(2,7)	AC/Apron	15	3 rd	0.33	0	0.0	24.8	51.7
AC(3,1)	Thickness of structural layers less than 10 inches	112	3 rd	0.55	11	9.8	13.1	19.2
AC(3,2)	Thickness of structural layers greater than 10 in.	189	3 rd	0.50	14	7.4	21.7	30.2

Table 5-6: Statistical Results for Family groupings of PCC pavements

Family Name	Family Particulars	Number of Sections with IR tests	Polynomial Order of regression Model	r ²	Outliers		Std. Error of est. (SEE)	RSE (%)
					No.	%		
PCC(1,1)	All PCC pavements	110	3 rd	0.92	9	8.2	20.1	13.4
PCC(2,1)	PCC/RW/DNF	50	3 rd	0.94	4	8.0	12.6	9.2
PCC(2,2)	PCC/RW/DNF	38	3 rd	0.97	3	7.9	16.7	10.9
PCC(2,3)	PCC/TW	16	3 rd	0.91	0	0	26.1	13.8
PCC(2,4)	PCC/Apron	4	Insufficient Data					

Table 5-7: Sample model selection procedure

a0	n	r ²	Rank	No. of Outliers	Rank	SEE	Rank	Average Rank	Final Rank
80	1	0.28	8	37	9	20.1	2	6.3	7
90	1	0.29	7	35	6	20.3	4	5.7	6
100	1	0.26	10	28	2	22.4	8	6.7	8
80	2	0.28	9	38	10	20.1	3	7.3	9
90	2	0.3	5	36	8	20.1	1	4.7	3
100	2	0.32	3	30	3	21.3	6	4.0	2
100	3	0.31	4	32	5	20.8	5	4.7	3
120	3	0.33	2	27	1	21.8	7	3.3	1
140	3	0.34	1	31	4	22.5	9	4.7	3
150	3	0.3	6	35	7	23.2	10	7.7	10

Table 5-8: Comparison of efficacy of various grouping techniques for AC pavements

Family Name	Weight	Rank r ²	Rank Outliers	Rank SEE	Rank RSE	Avg. Score	Rank	Weighted Avge. Rank	Simple Avge.	Efficacy
AC(1,1)	301	7	8	18.8	5	9.7	7	9.7	9	3
AC(2,1)	64	3	4	22.7	8	9.4	5	8.8	5.9	2
AC(2,2)	30	5	9	13.8	4	7.9	3			
AC(2,3)	62	1	10	14.2	2	6.8	2			
AC(2,4)	82	10	3	19.2	3	8.8	4			
AC(2,5)	35	6	6	21.1	6	9.8	8			
AC(2,6)	15	8	1	26	9	11.0	9			
AC(2,7)	15	9	1	24.8	10	11.2	10			
AC(3,1)	112	2	7	13.1	1	5.8	1	8.1	3.0	1
AC(3,2)	189	4	5	21.7	7	9.4	5			

Table 5-9: Comparison of efficacy of various grouping techniques for PCC pavements

Family Name	Weight	Rank r ²	Rank Outliers	Rank SEE	Rank RSE	Avg. Score	Rank	Weighted avge. Score	Simple Avge. Score	Efficacy
PCC(1,1)	110	3	4	3	3	3.25	2	3.3	3.3	2.0
PCC(2,1)	64	2	3	1	1	1.75	1	2.0	1.3	1.0
PCC(2,2)	44	1	2	2	2	1.75	1			
PCC(2,3)	18	4	1	4	4	3.25	2			

Table 5-10: Length of service life from PCI based models

Family Name	Service life from PCI deterioration models
AC(2,1)	38
AC(2,2)	47
AC(2,3)	48
AC(2,4)	infinite
AC(2,5)	47
AC(2,6)	29
AC(2,7)	35
PCC(2,1)	60
PCC(2,2)	infinite
PCC(2,3)	76
PCC(2,4)	59

Table 5-11: Predicted and remaining IR stiffness in AC Pavements

Age	AC(3,1)		AC(3,2)	
	Stiffness	% of a0	Stiffness	% of a0
10	73.2	69.7	79.3	58.7
15	65.0	61.9	64.5	47.8
20	59.9	57.1	55.3	41.0
25	56.5	53.8	49.5	36.7
30	53.2	50.7	44.7	33.1
35	48.6	46.3	38.8	28.7
40	41.1	39.1	29.3	21.7
45	29.3	27.9	14.0	10.4
50	11.6	11.0		

Table 5-12: Predicted and remaining IR stiffness in PCC Pavements

Age	PCC(1,1)		PCC(2,1)		PCC(2,2)		PCC(2,3)	
	Stiffness	% of a0						
10	248.0	62.0	249.4	62.3	266.2	65.6	249.4	62.4
20	164.6	41.2	161.9	40.5	190.9	47.7	168.9	42.2
30	128.4	32.1	120.4	30.1	154.1	38.5	135.4	33.9
40	117.6	29.4	107.9	27.0	135.9	34.0	126.0	31.5
50	110.8	27.7	107.2	26.8	116.1	29.0	117.7	29.4
60	86.4	21.6	101.2	25.3	74.9	18.7	87.6	21.9
70	22.7	5.7	72.8	18.2	-	-	12.7	3.2
75	-	-	44.9	11.2	-	-	-	-

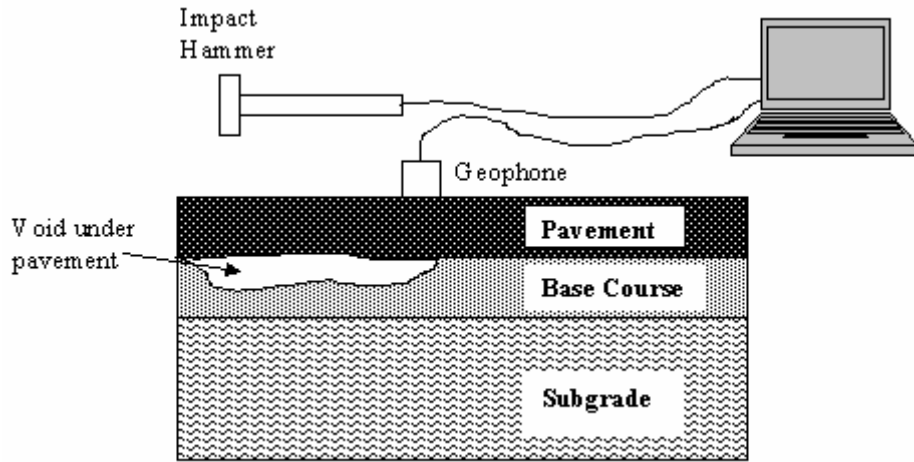


Figure 5-1: Field setup of the Impulse Response test

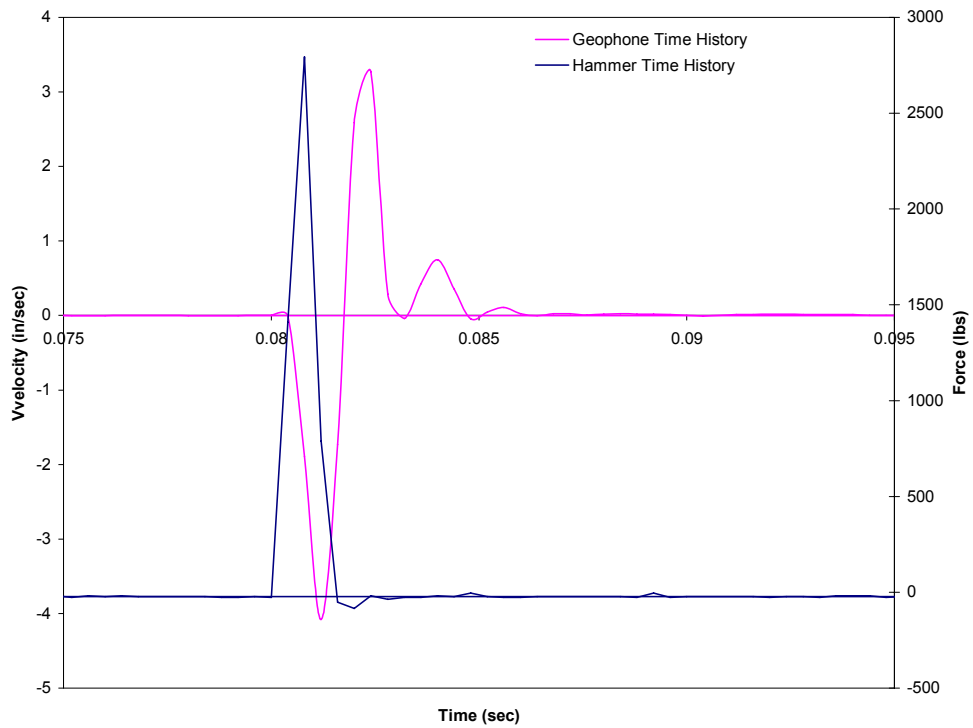


Figure 5-2: Time histories for Hammer and Geophone acquired during an IR test

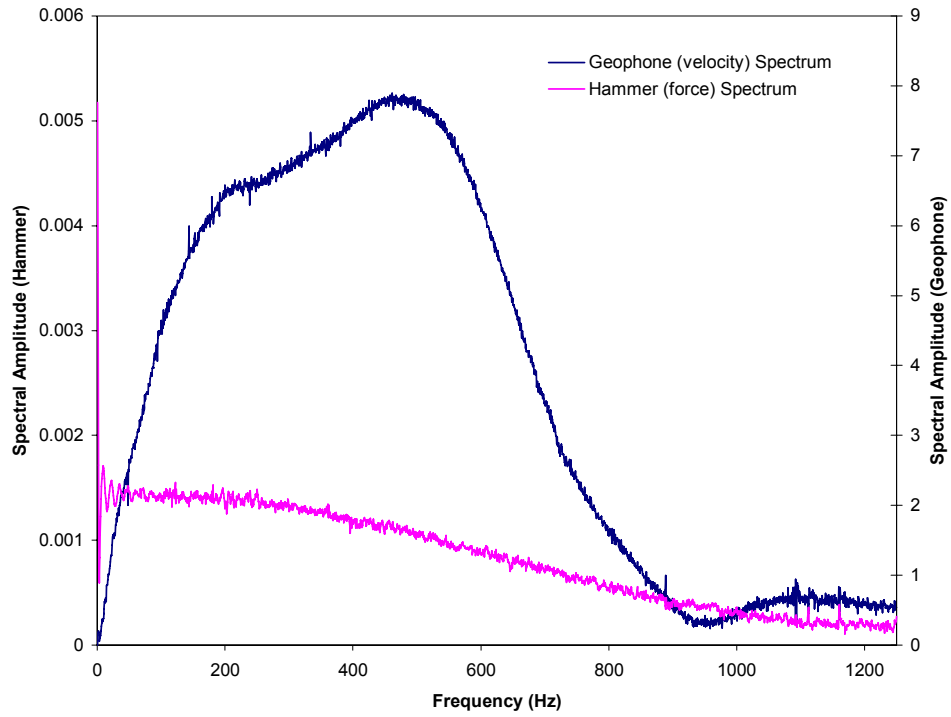


Figure 5-3: Velocity and force spectra of acquired signals

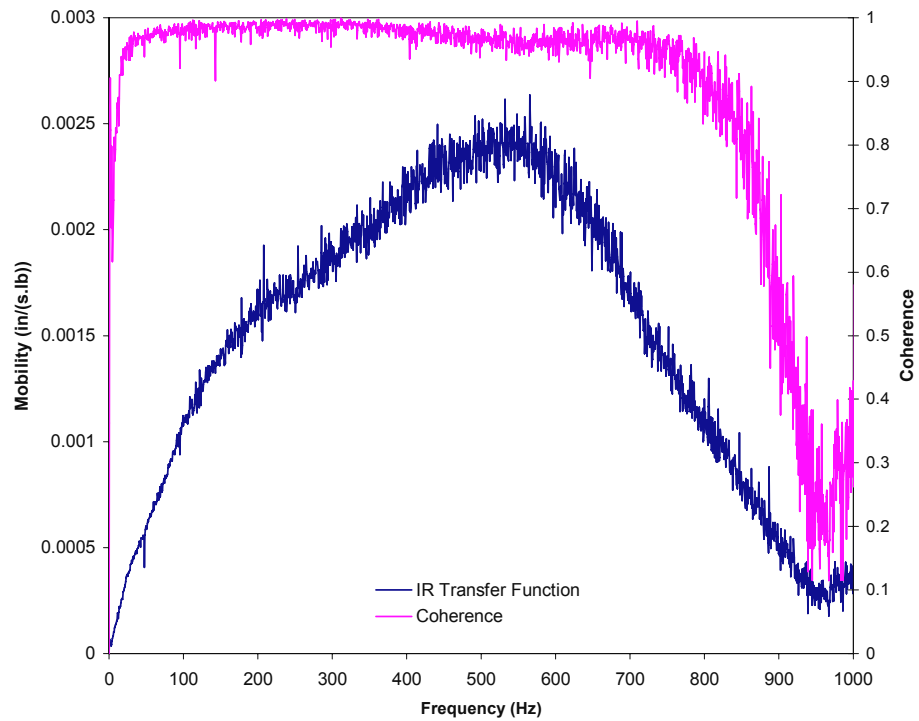


Figure 5-4: Sample mobility response function from acquired signals

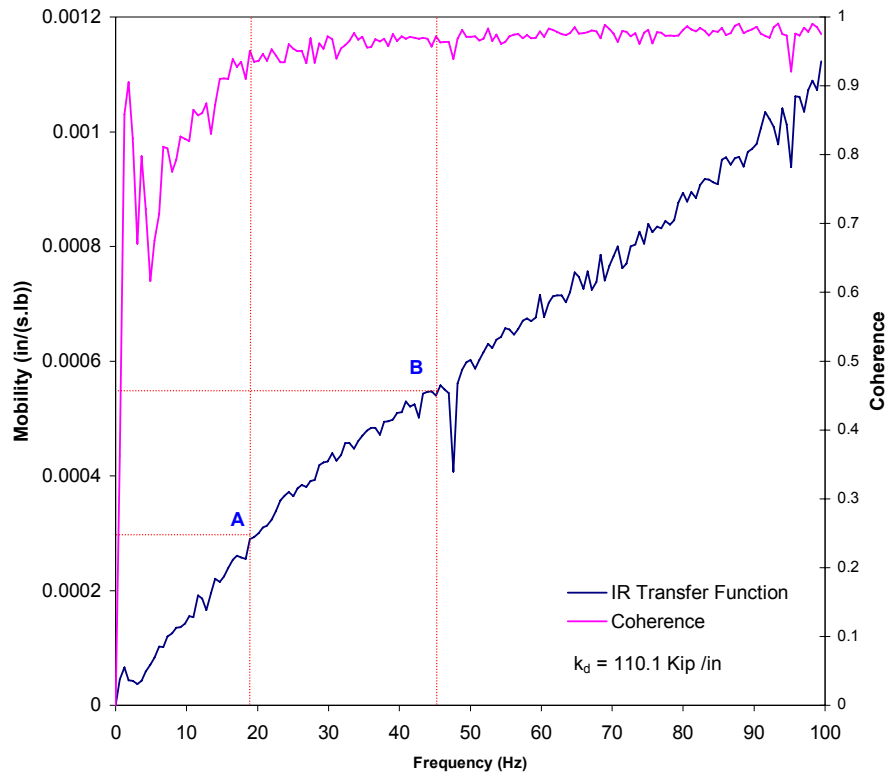


Figure 5-5: Calculation of the dynamic stiffness (slope between points A and B)

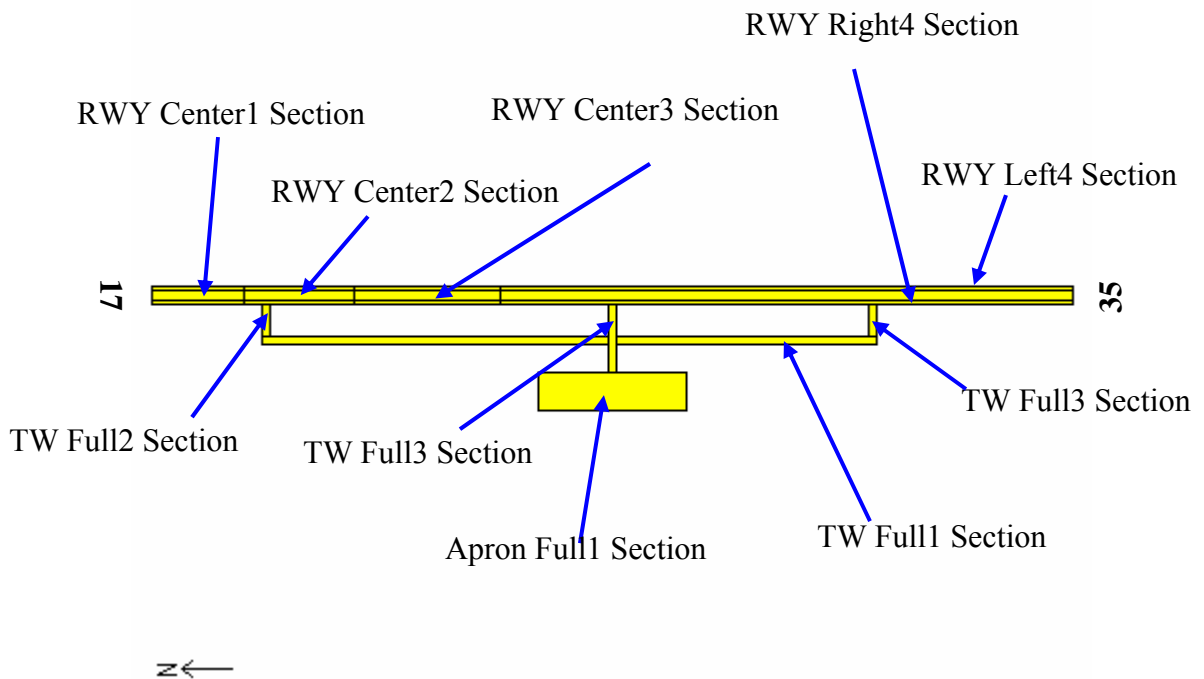


Figure 5-6: Sub-division of Miami Municipal Airport's pavements into branches and sections for Visual Distress Survey

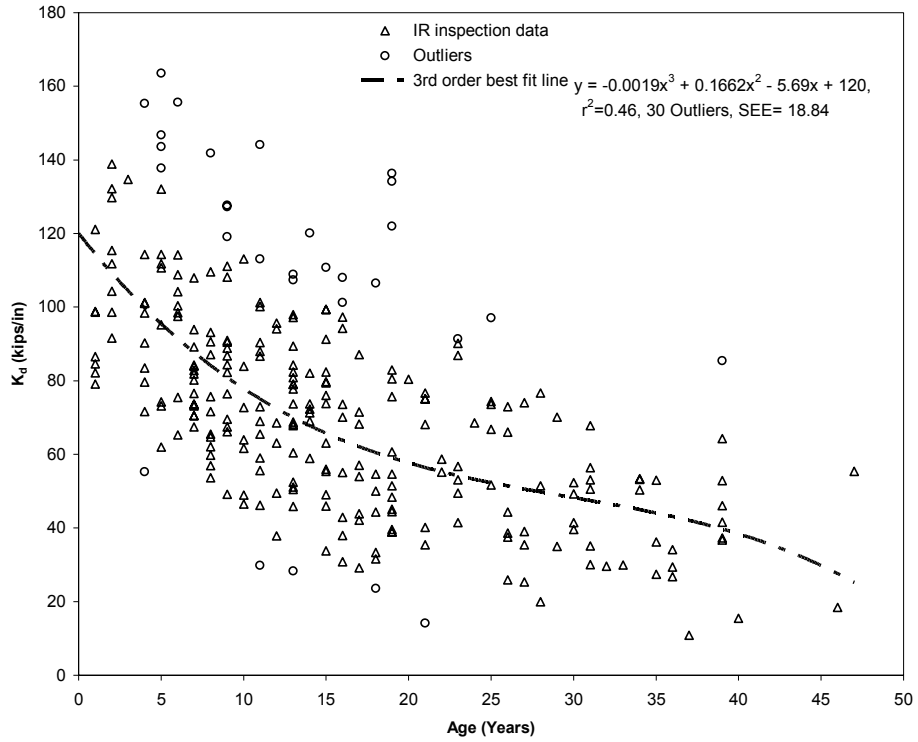


Figure 5-7: Decay of k_d with time for family AC(1,1)

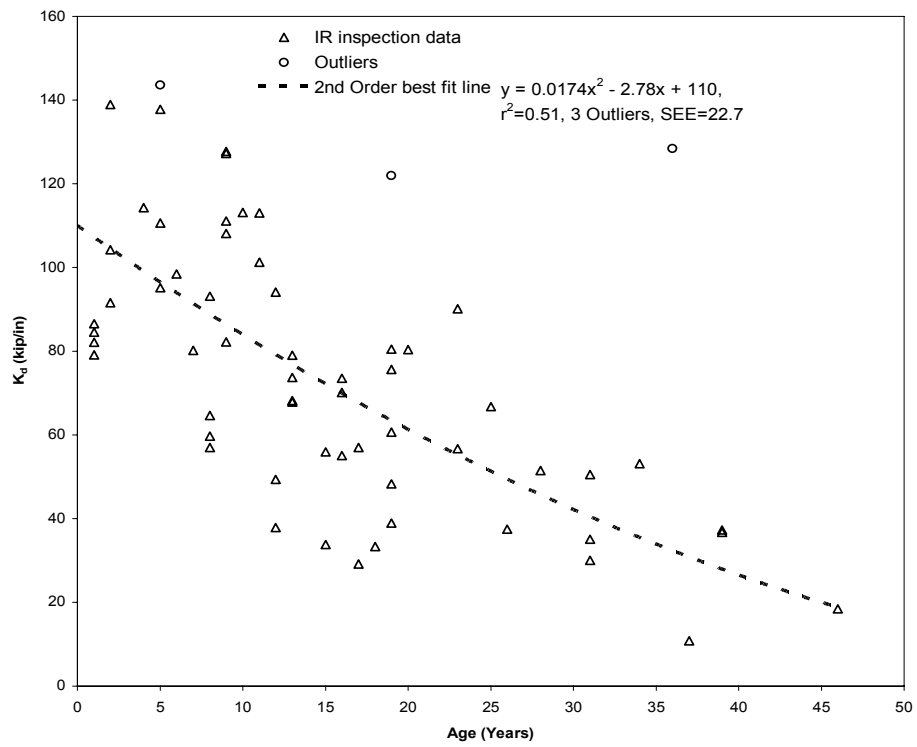


Figure 5-8: Decay of k_d with time for family AC(2,1)

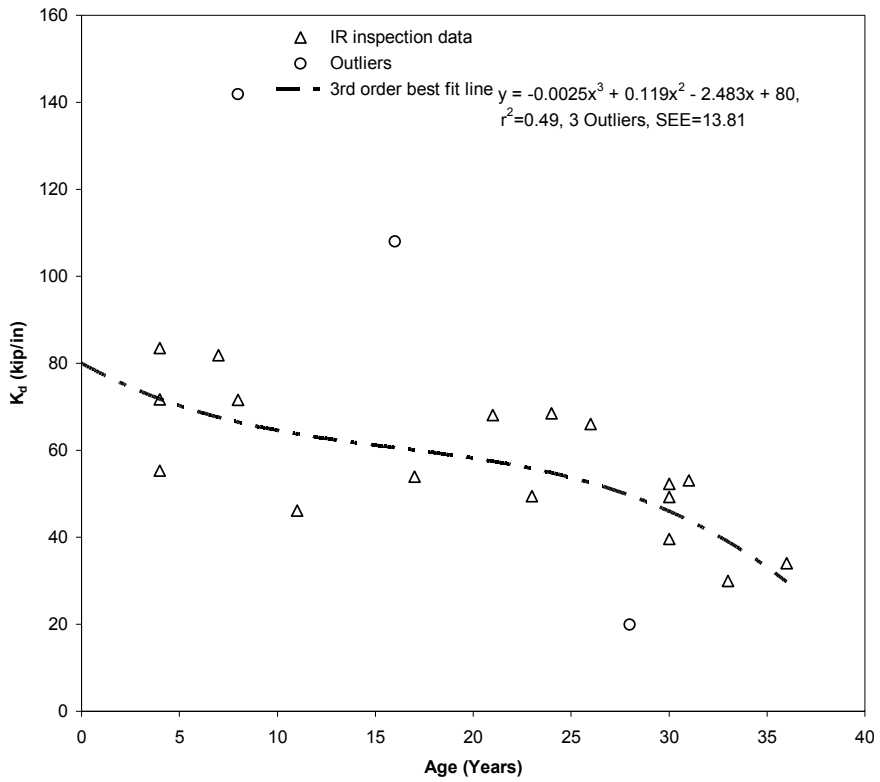


Figure 5-9: k_a degradation for family AC(2,2)

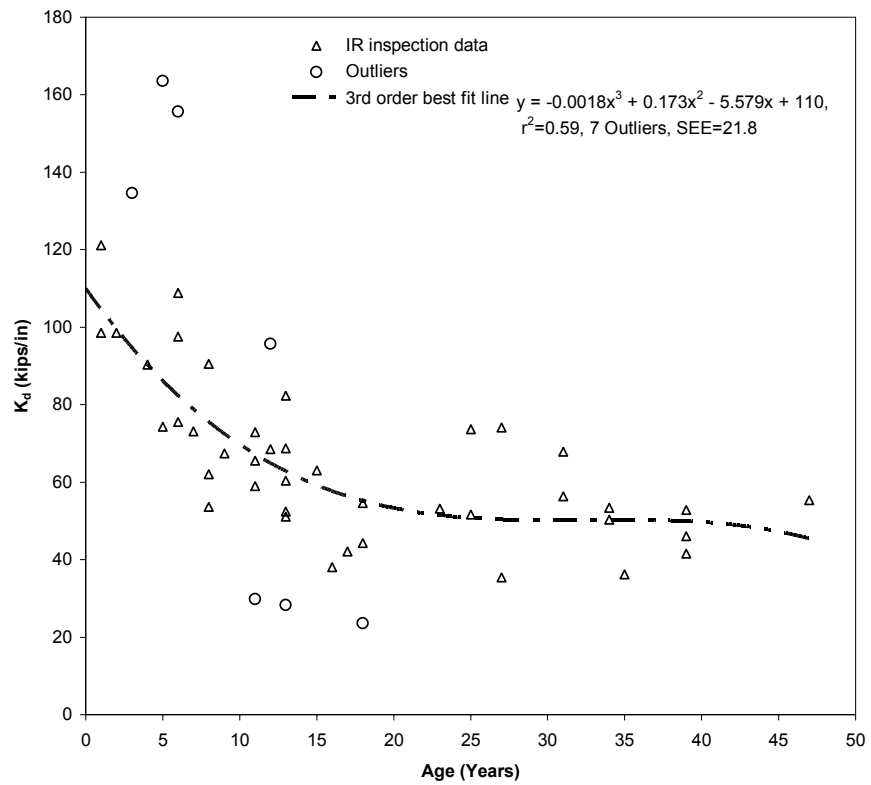


Figure 5-10: k_a degradation with pavement age for family AC(2,3)

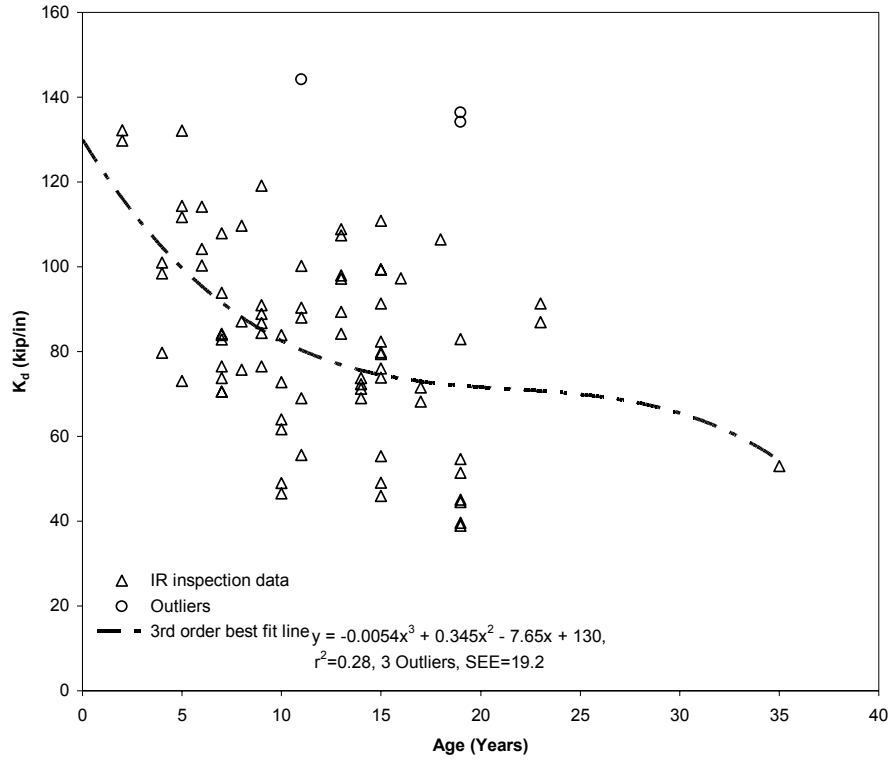


Figure 5-11: Decay of k_d with pavement age for family AC(2,4)

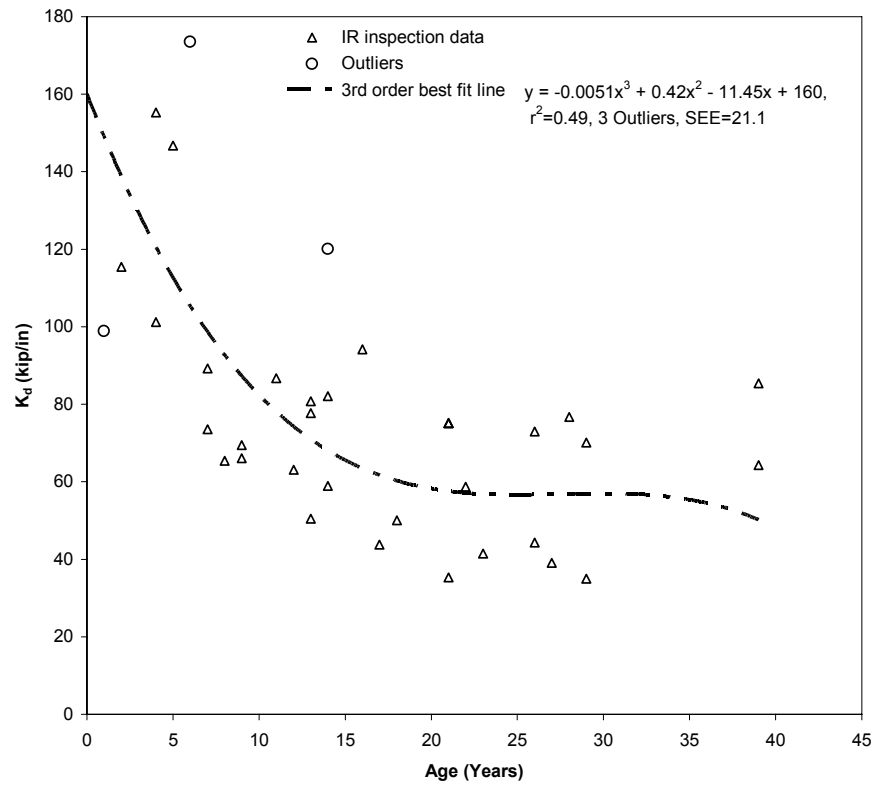


Figure 5-12: Deterioration of k_d with time for family AC(2,5)

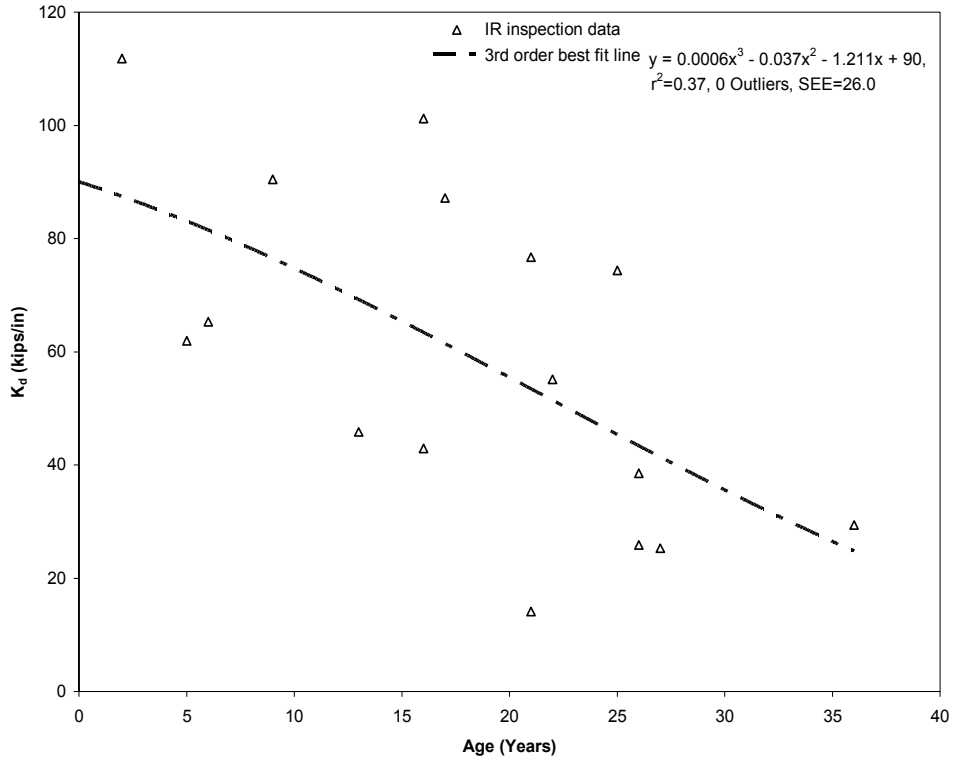


Figure 5-13: Decay of k_a with time for family AC(2,6)

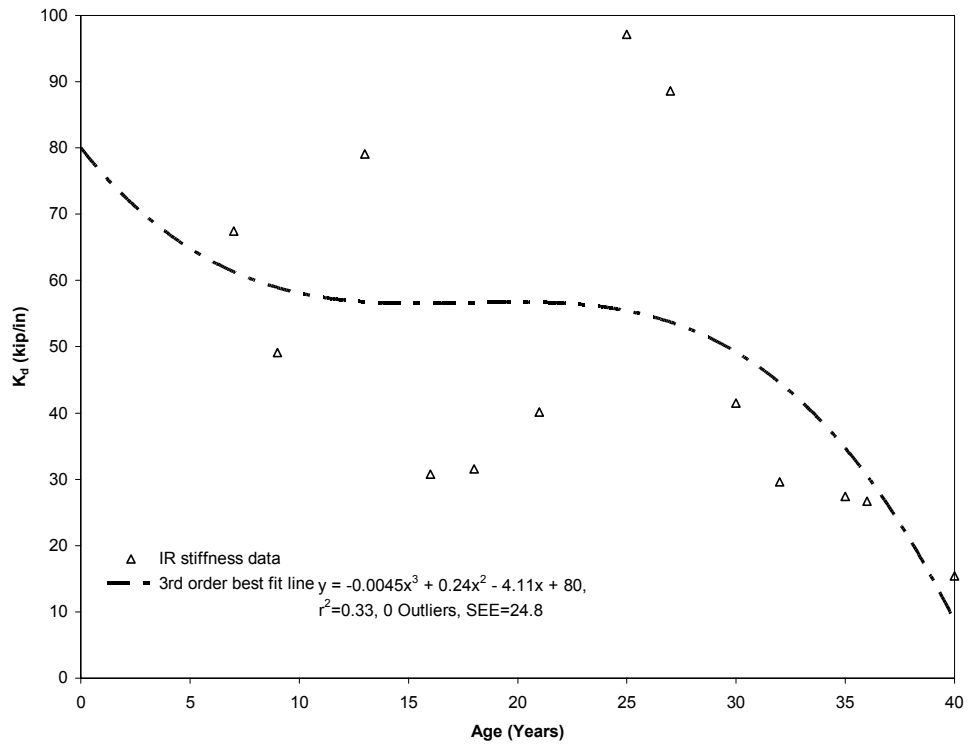


Figure 5-14: Degradation of k_a with pavement age for family AC(2,7)

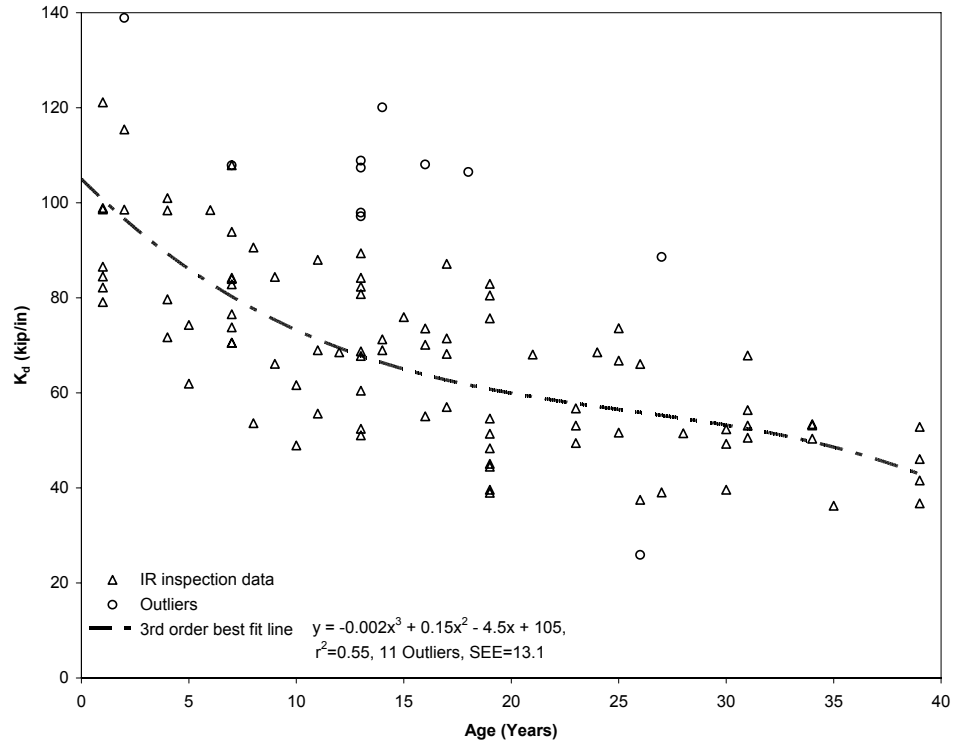


Figure 5-15: Stiffness decay with pavement age for family AC(3,1)

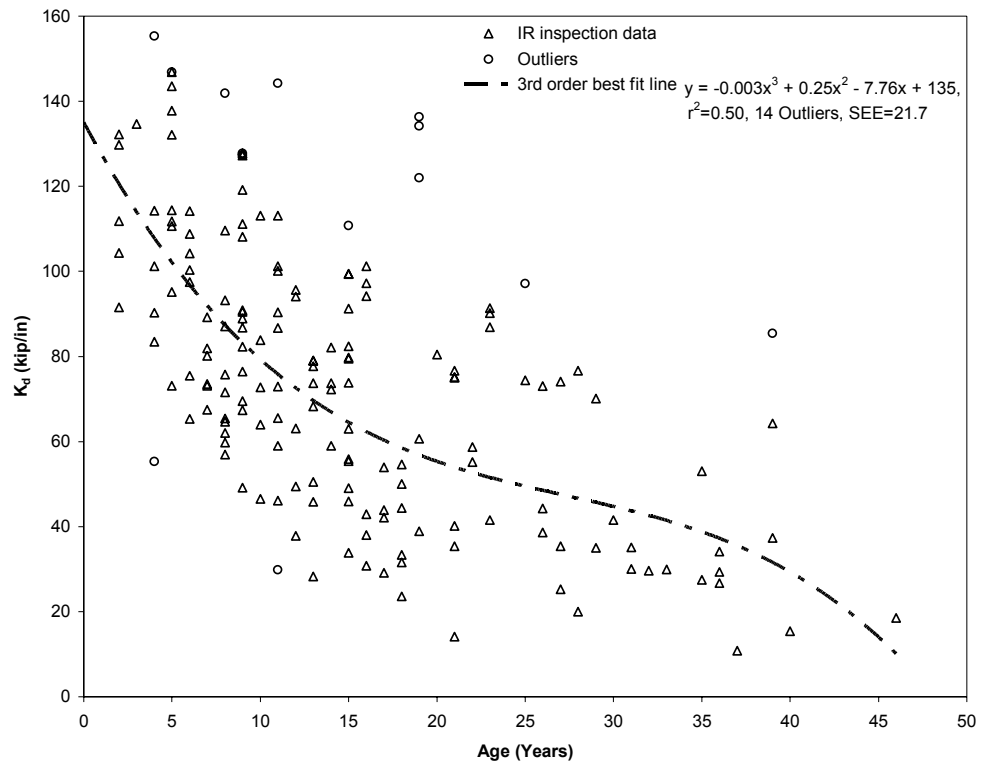


Figure 5-16: Stiffness decay with time for family AC(3,2)

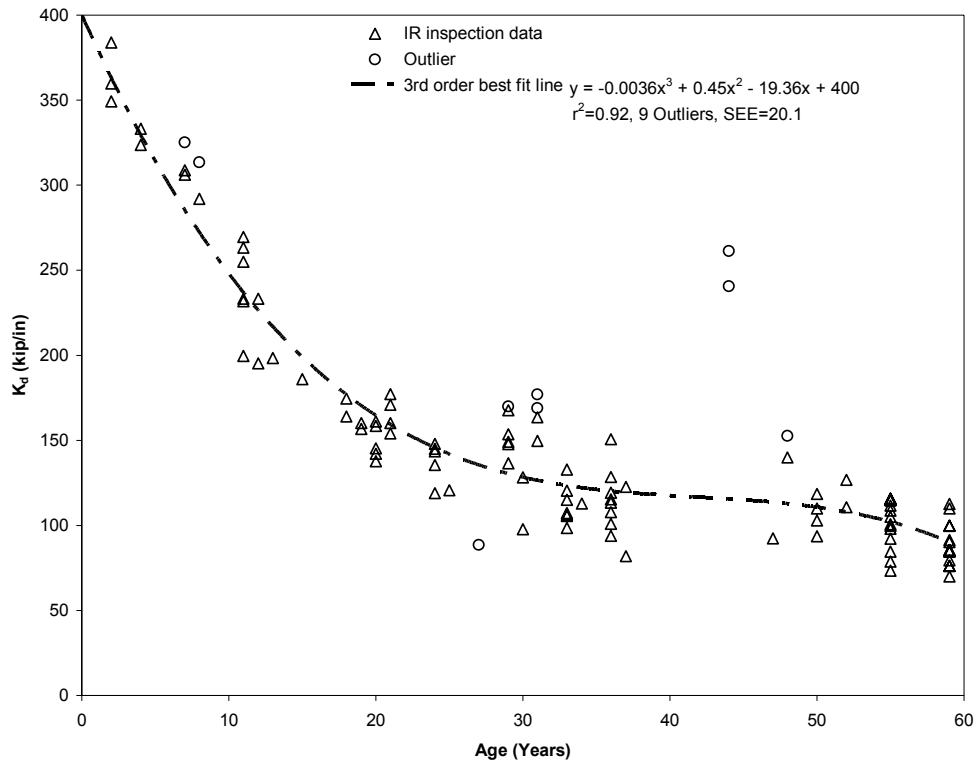


Figure 5-17: Degradation of k_d with pavement age for family PCC(1,1)

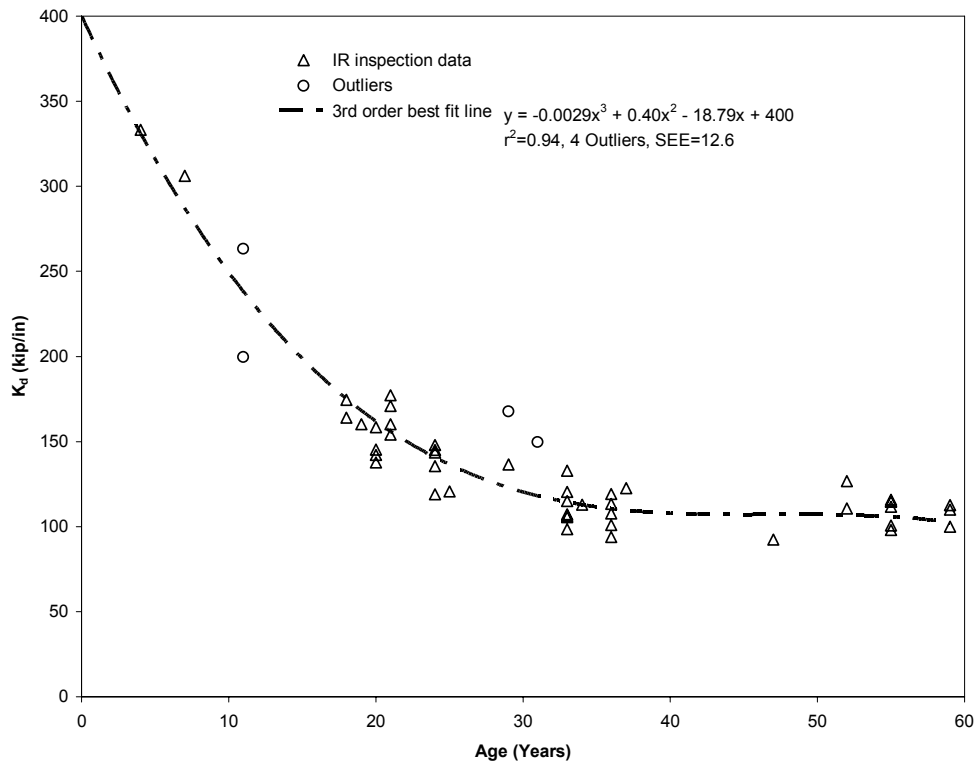


Figure 5-18: Decay of k_d with time observed in pavements grouped in family PCC(2,1)

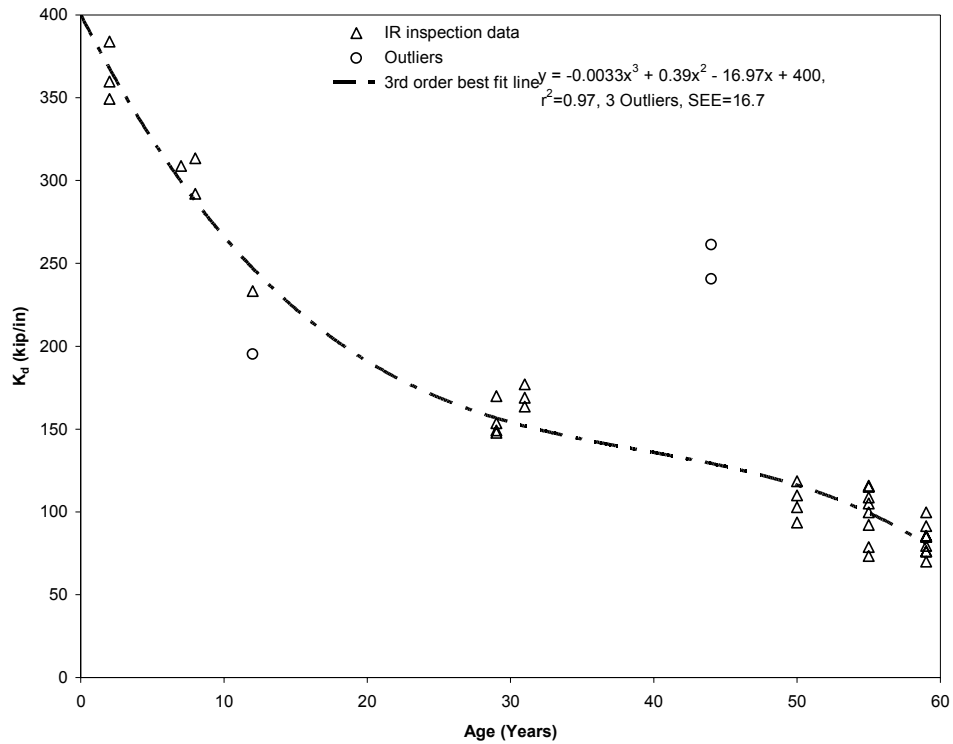


Figure 5-19: Deterioration of k_a with time observed in pavements grouped in family PCC(2,2)

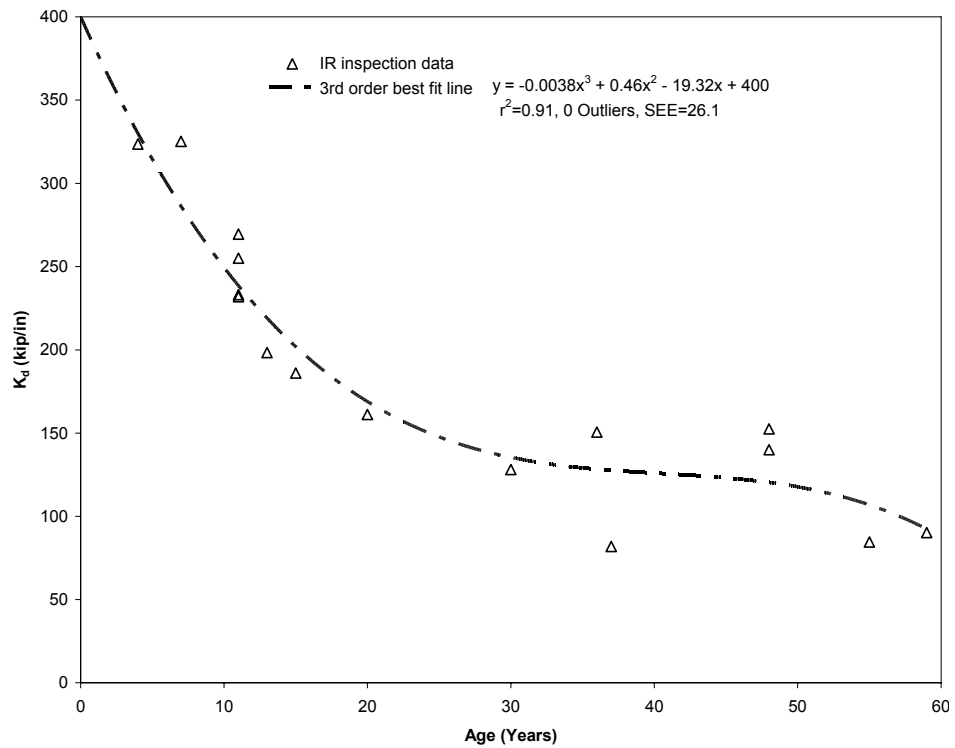


Figure 5-20: Decay of k_a with pavement age for family PCC(2,3)

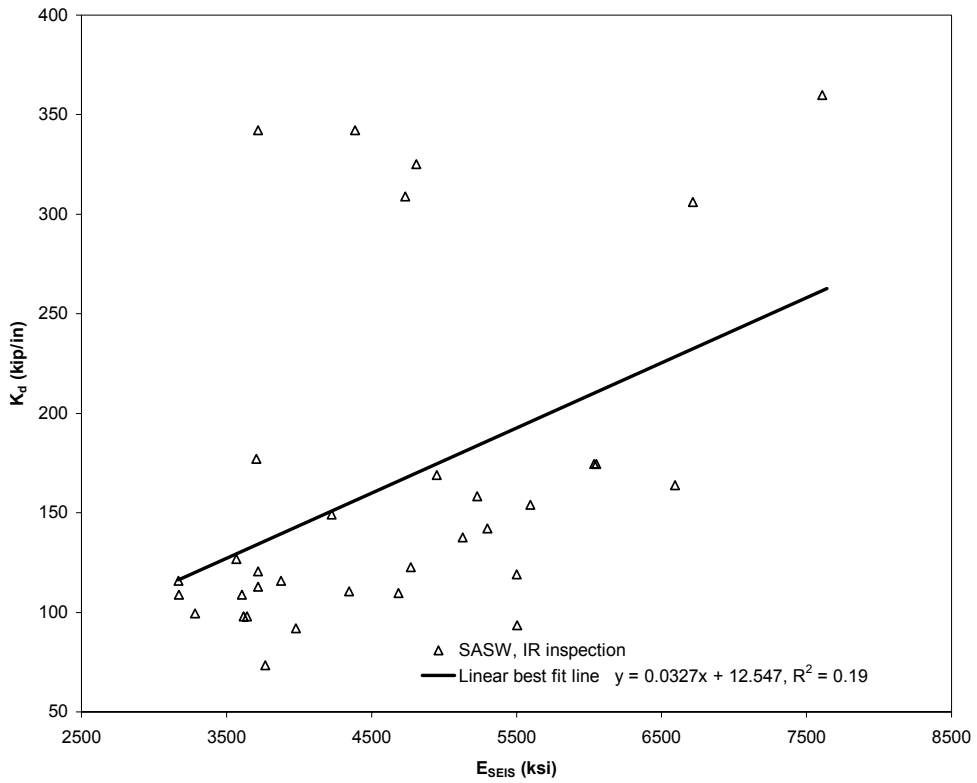


Figure 5-21: Variation of k_d with E_{SEIS} for PCC pavements

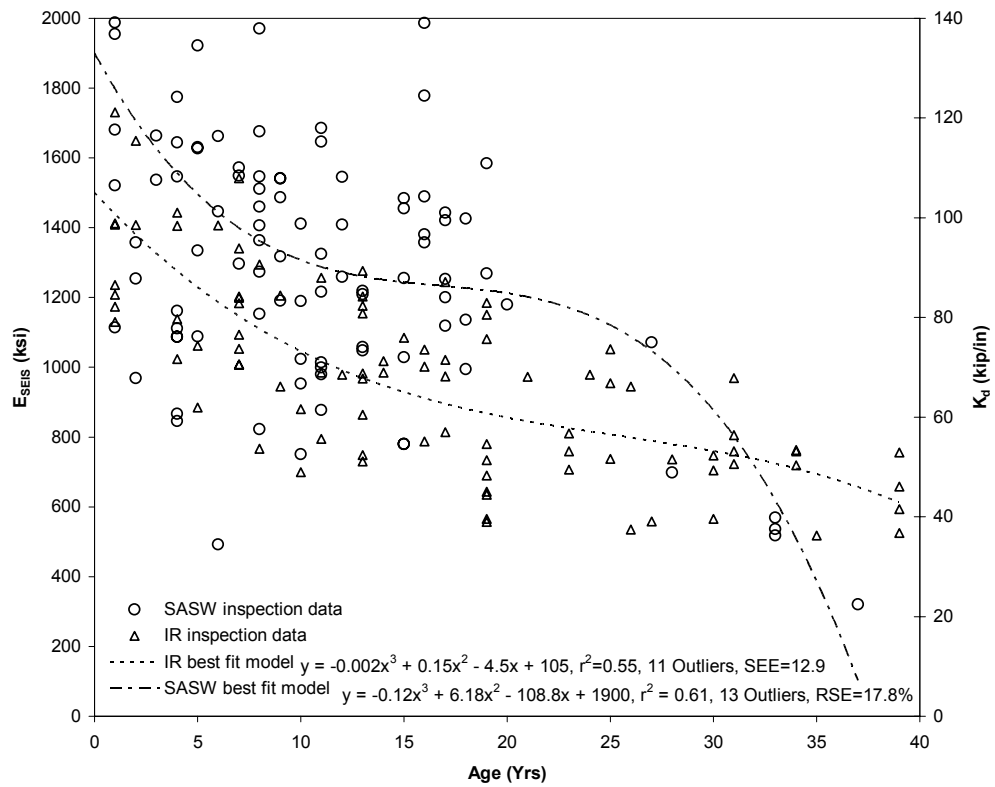


Figure 5-22: Variation of k_d with E_{SEIS} for family AC(3,1) pavements

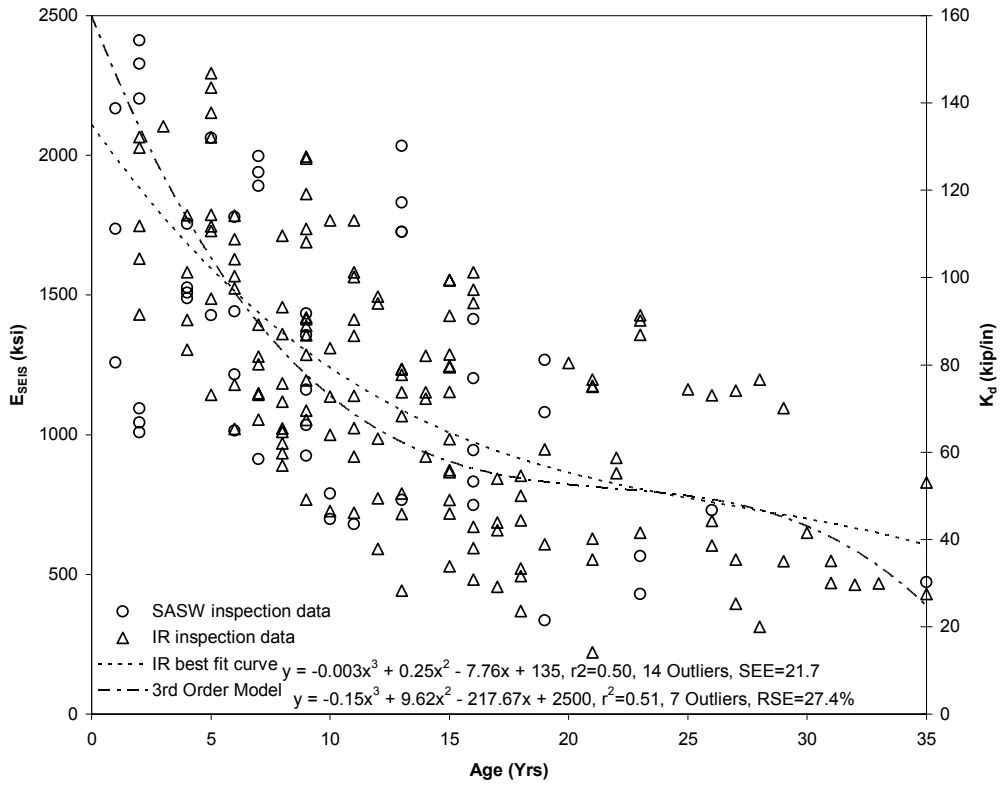


Figure 5-23: Variation of k_d with E_{SEIS} for family AC(3,2) pavements

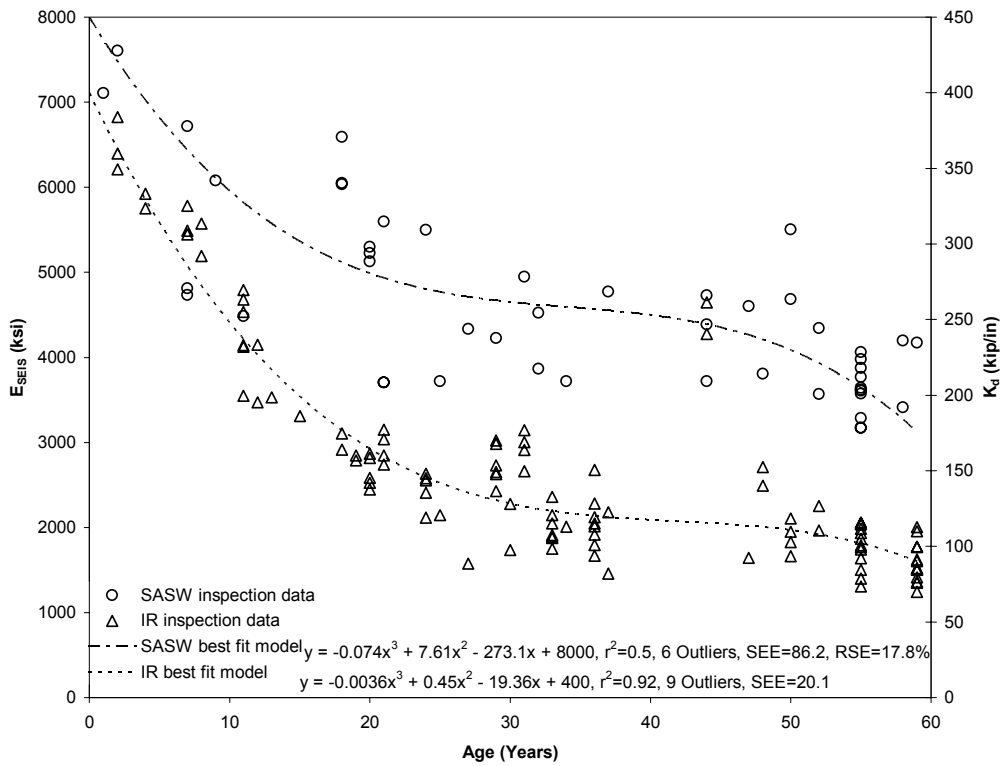


Figure 5-24: Variation of k_d with E_{SEIS} for family PCC(1,1) pavements

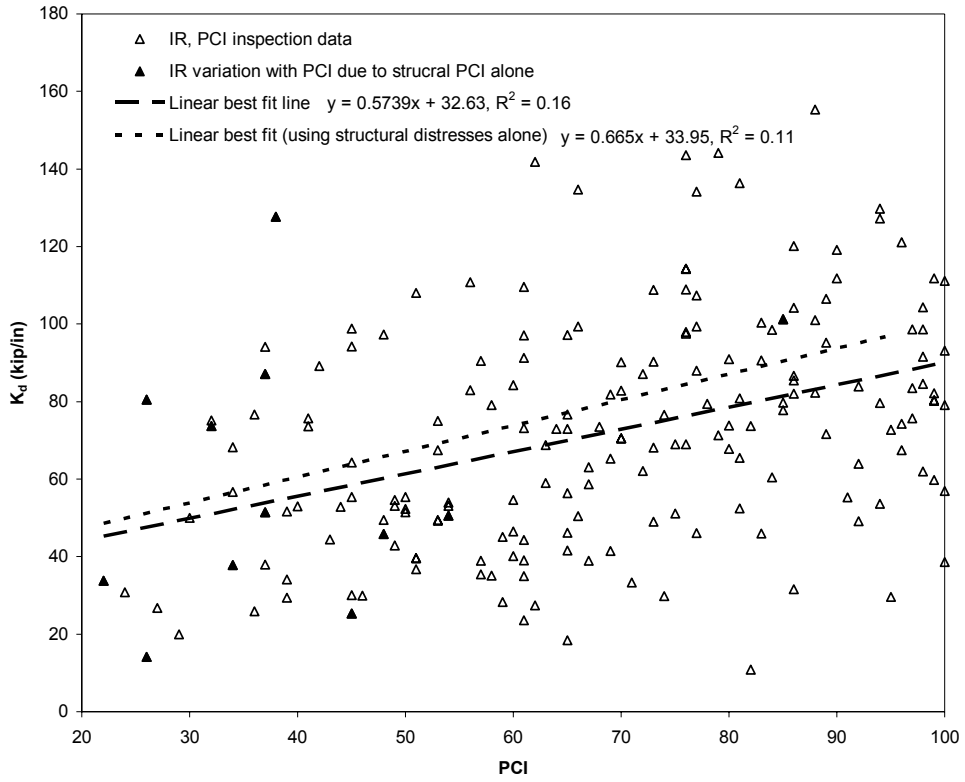


Figure 5-25: Plot of k_d of pavement section with its PCI for AC pavements

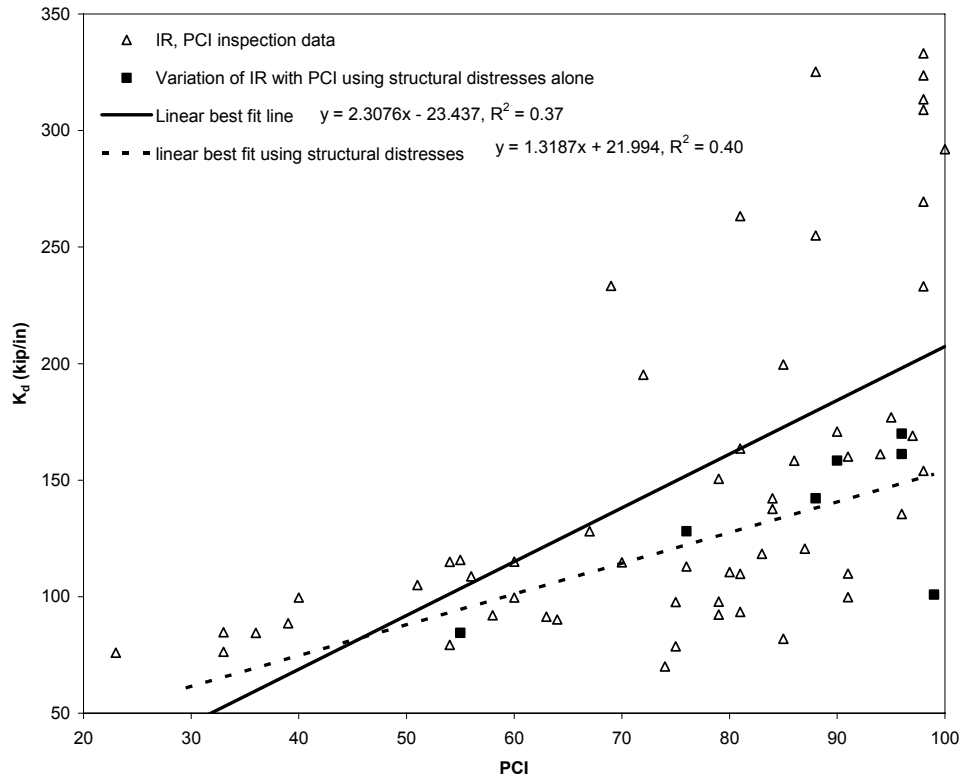


Figure 5-26: Variation of k_d of PCC pavements with PCI

Chapter 6 Conclusions and Recommendations for Future Research

Conventional airport pavement management systems are based upon visual-distress based pavement PCIs. APWA/CERL's MicroPAVER software is the industry leader and uses a family approach to break down large networks comprising of millions of square yards of AC and PCC pavements into smaller, consistent sections that exhibit similar PCI decay with time. The deterioration models for PCI are thus based on an average performance of the sections that make up a pavement family. These decay or degradation models predict the future condition of pavement sections and enable pavement managers to develop cost-effective and most suited MR solutions, thereby maximizing network utilization. A pavement section's PCI, however, does not provide accurate, actionable information about structural integrity of the pavement section since the index also factors in distresses that impact ride quality and safety. Some visual distresses do provide limited insight into structural condition, e.g., rutting, alligator cracking in AC pavements and linear cracks, and shattered slabs in PCC pavements; however, visual distresses mainly provide an assessment of functional pavement performance.

The focus of the research presented here was twofold- a) the development of an IMS for OAC, and b) to study the efficacy of two NDT procedures – SASW and IR, to add a mechanistic dimension to visually estimated PCI thereby providing actionable structural information to pavement engineers.

The IMS developed for OAC has helped streamline its operations and has also greatly benefited the state of Oklahoma. The IMS includes the innovative inclusion of

geotechnical data that is of tremendous use to OAC for its capital planning and to airport sponsors in preparing preliminary designs. The integration of ADWs into the IMS has enabled OAC to present the needs of the state's 97 NPIAS airports to FAA literally at the touch of a button. Since 2005, OAC has taken over the task of updating the NPIAS needs database for Oklahoma's NPIAS airports from FAA. This effort and the use of the IMS has helped increase annual Federal funding for these airports by 25% (\$2.9 million) annually. Additionally, ADWs in the IMS present national priority ratings for projects included in them. These priority ratings combined with the network wide PCI information of pavements, help OAC prepare a disciplined, justifiable CIP for Oklahoma's GA airports.

SASW was found to be a potentially valuable tool to characterize pavement sections without core extractions. AC pavement thickness was over estimated for pavement sections less than 6 inches thick. Since FAA's pavement design guidelines require a minimum thickness of AC pavements of 3 inches, this does not impact efficacy of the procedure. From the results of the current study it is observed that for AC pavements greater than 3 inches, estimate of pavement thickness from SASW tests deviated from actual by 2.4% to 13.7 %. From a weighed average analysis using data from all tested sections, the estimation of AC pavement thickness from SASW tests was found to over estimate extracted core thickness by 4.4%. PCC pavement thicknesses were consistently over estimated by SASW testing. SASW's estimates of PCC pavement thickness were found to deviate from core sizes by 11.2% to 26.4%. A weighted average analysis using all data indicated that in general, SASW results over estimated PCC pavement thickness by 14%. Comparison of SASW estimated pavement layer thicknesses

with boring logs indicate a lack of SASW's ability to discover changes in soil layer changes.

Chapter 4 explored the validity of the hypothesis that modulus of a pavement section, AC or PCC, degrades over time. Results presented in the chapter validate this hypothesis. AC and PCC moduli (E_{SEIS}) were observed to degrade with time and regression models for this deterioration were presented in the chapter. The regression results, i.e. coefficient of determination (r^2) for the current analysis using E_{SEIS} data compare favorably with results obtained by other researchers working with PCI data (Appendix 2). The modulus and remaining life degradation curves and the E_{SEIS} data present excellent tools for project level capacity analysis of individual pavement sections. The chapter also investigates the suitability of using PCI based pavement family classifications with E_{SEIS} data. From the results it was observed that an approach based upon the thickness of structurally-capable layers i.e., layers that add to the pavement section's load bearing capacity, provided the best regression results for decay of E_{SEIS} with time. Service life of AC pavement sections was found to be significantly lower than the estimate of pavement life from PCI decay models for both AC and PCC pavements.

Also, for AC pavements, an overall correlation between E_{SEIS} and PCI could not be established. This finding suggests that in AC pavements, visually inferred traffic-related distresses do not correlate with structural failure. In the case of PCC pavements, a correlation of medium significance ($r^2=0.39$) was observed between section PCI and E_{SEIS} . Since PCI measures several parameters relating to ride quality the low correlations are in line with expectations. The correlation remained unchanged ($r^2=0.41$) when only structural distresses were used. This correlation of medium significance suggests that the

identification of structural distresses in PCC pavements is more accurate than for AC pavements.

A major drawback with using the SASW method for pavement health monitoring is the requirement of skilled man-power for both data collection and analysis. The IR method on the other hand requires little skill in data collection and analysis. The ease of testing and quick data analysis presents an opportunity for greater spatial coverage of pavements thereby providing a complete picture of the tested site to engineers. Chapter 5 presents a study into the use of IR estimated dynamic stiffness (k_d) for pavement health monitoring. As in the case of E_{SEIS} , it was postulated that k_d degrades with a pavement sections age. Results presented in the Chapter validate the hypothesis. Regression results, i.e. coefficient of determination (r^2), for decay of k_d with time for the current analysis compare favorably with results obtained by other researchers working with PCI data (Appendix 2). A correlation between E_{SEIS} and k_d for AC pavements could not be established. For PCC pavements, a correlation of “small” significance ($r^2 = 0.19$) was observed between E_{SEIS} and k_d .

A correlation of “small” significance was observed between k_d and PCI rating of AC pavement sections. Though the sample size used for comparison with structurally distressed sections was small, results suggest that in AC pavements, visually inferred traffic-related distresses do not correlate with structural failure. In the case of PCC pavements a correlation of “large” significance was observed between k_d and PCI ratings ($r^2=0.5$) and a correlation of “medium” significance was observed between k_d and PCI_S . From the results, ignoring the limited size of the database used, it is observed that for

PCC pavements visual identification of structural distresses is more accurate than in the case of AC pavements.

Based on the findings in this research, E_{SEIS} and k_d were found to be suitable for inclusion in a PMS as pavement health monitoring tools. It is therefore recommended that future research should explore the efficacy of a mechanistic PMS. In such a PMS, E_{SEIS} and k_d could potentially add a mechanistic component to the visual distress based PCI ratings. A structural index devised based upon either E_{SEIS} or k_d could provide a structural integrity rating for a pavement section while PCI would provide a serviceability rating. A composite rating could be developed as in Equation (6.1).

$$PCI_M = (a \cdot PCI) + (b \cdot SN) \quad (6.1)$$

where,

PCI_M = Composite, mechanistic PCI developed using PCI and either E_{SEIS} or k_d based structural rating. Like the current PCI, the PCI_M would also range from 100 (newly constructed pavement) to 0 (pavement at the end of its life),

a = a weighting factor to be developed based on the importance of serviceability and ride quality to pavement condition rating,

SN = A structural rating developed from the E_{SEIS} or k_d values, and

b = a weighting factor to be developed on the basis of the importance of structural integrity and adequacy to pavement condition rating.

Agencies responsible for maintaining pavement networks could select either the SASW or IR method for structural health monitoring. PCI_M values and their deterioration with time would be used to select MR strategies for the network. Since this new index would directly measure structural integrity using either E_{SEIS} or k_d , it is expected that such

a PMS could help in optimizing network utility by improved MR selection. This improved MR selection would also lead to improved capital planning and improved fiscal management.

APPENDIX 1: Sample Calculation of IR Stiffness

A sample of IR stiffness calculation and the variation with age is presented here. Data from IR tests conducted at Guymon Municipal Airport runway at on 08/09/2000 and 06/24/2003 is presented.

1. Test conducted on 08/09/2003: The test was conducted at location 5500-55 on the runway with a surface temperature of 116 °F. Figure A.1 presents the velocity and force spectra and Figure A.2 illustrates the mobility response and Figure A.3 presents in the mobility plot from 0 Hz to 100 Hz.

Avoiding the zones of low coherence, the slope of the mobility curve below the 50 Hz portion is estimated as:

$$MobilitySlope = \frac{Mobility_B - Mobility_A}{Freq_B - Freq_A} = \frac{0.00111452 - 0.0004126}{49.4385 - 18.3105} = 2.2549 \times 10^{-5}$$

. Using Equation (5.4),

$$k_d = \frac{1}{MobilitySlope}$$

$$k_d = \frac{1}{2.2549 \times 10^{-5}} = 44.4 \text{ kip/in}$$

Applying the correction for temperature

$$k_d = \frac{44.4}{(1.35 - 0.0078(116 - 32))} = 63.9 \text{ kip/in}$$

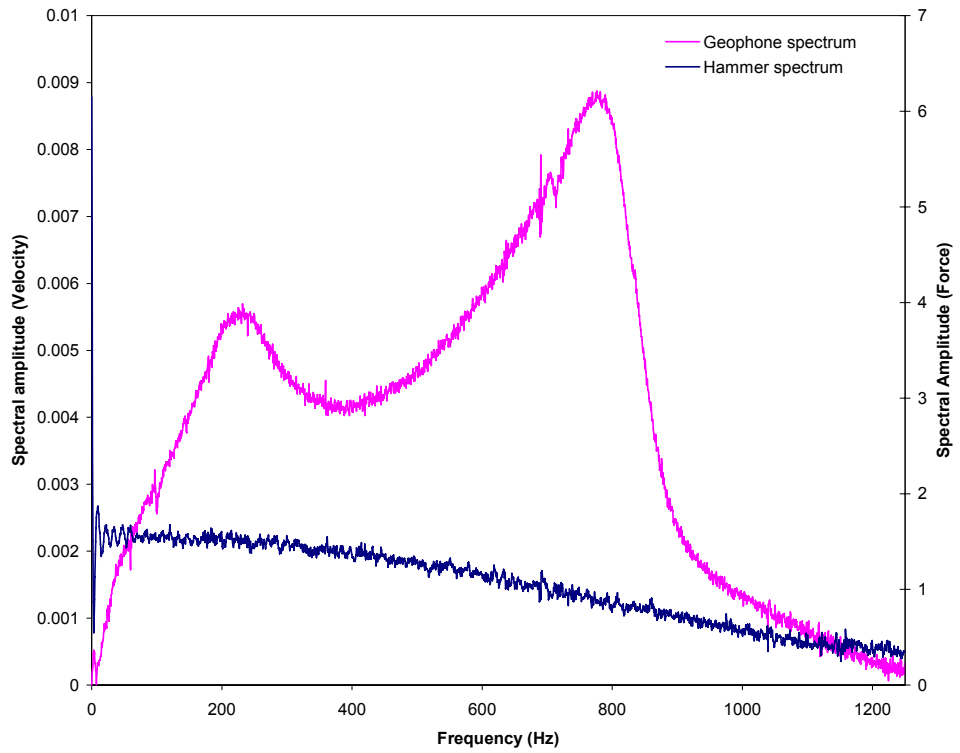


Figure A1- 1: Velocity and force spectra of acquired signals (2000)

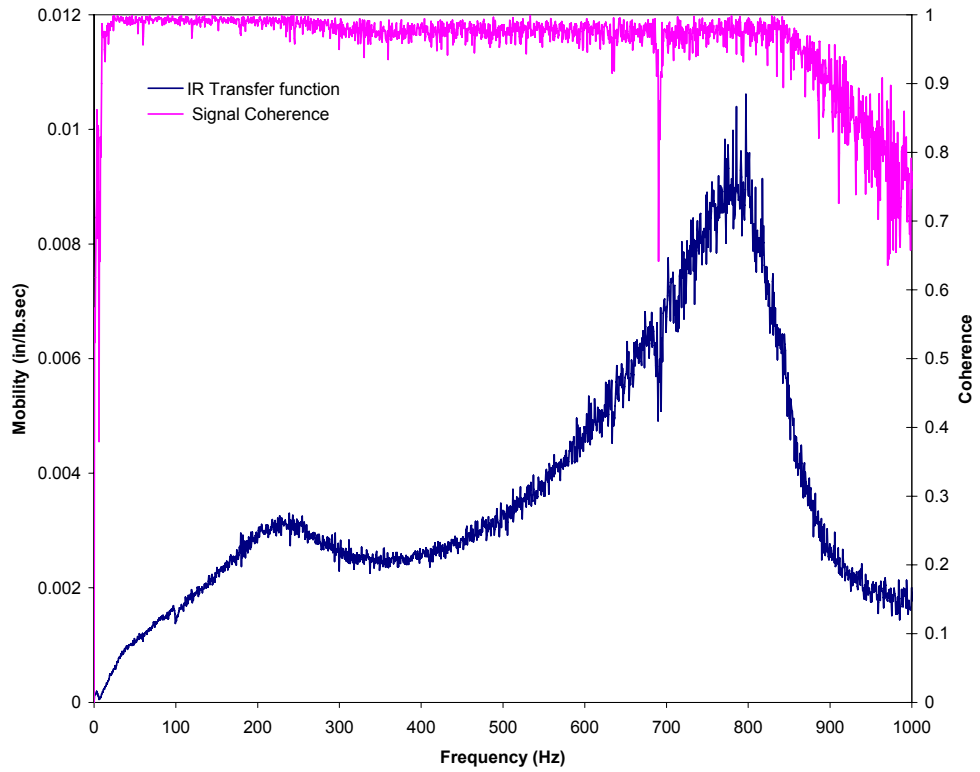


Figure A1- 2: Velocity and force spectra of acquired signals (2003)

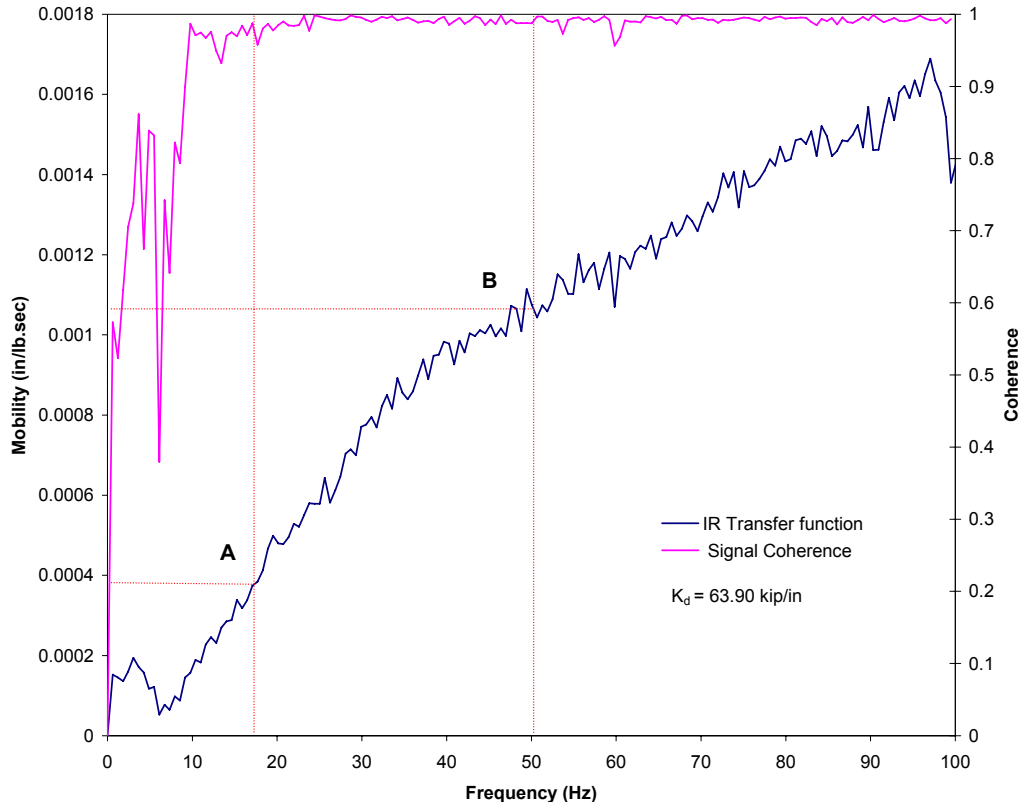


Figure A1- 3: Mobility response from 0Hz to 100 Hz

2. Test conducted on 06/24/2003: The test was conducted at location 5500-50 on the runway with a surface temperature of 91 °F. Figure A.1 presents the velocity and force spectra and Figure A.2 illustrates the mobility response and Figure A.3 presents in the mobility plot from 0Hz to 100 Hz.

Avoiding the zones of low coherence, the slope of the mobility curve below the 50 Hz portion is estimated as :

$$MobilitySlope = \frac{Mobility_B - Mobility_A}{Freq_B - Freq_A} = \frac{0.0005507 - 0.00025793}{46.3687 - 17.7002} = 1.02058 \times 10^{-5}$$

. Using Equation (5.4),

$$k_d = 1 / MobilitySlope$$

$$k_d = \frac{1}{1.0258 \times 10^{-5}} = 97.98 \text{ kip/in}$$

Applying the correction for temperature

$$k_d = \frac{97.98}{(1.35 - 0.0078(116 - 32))} = 110.1 \text{ kip/in}$$

From the results it is observed that stiffness increased from the previous measurement in the year 2000. This happened because the pavement was reconstructed in 2002 and therefore the increase in IR stiffness is a good check on its ability.

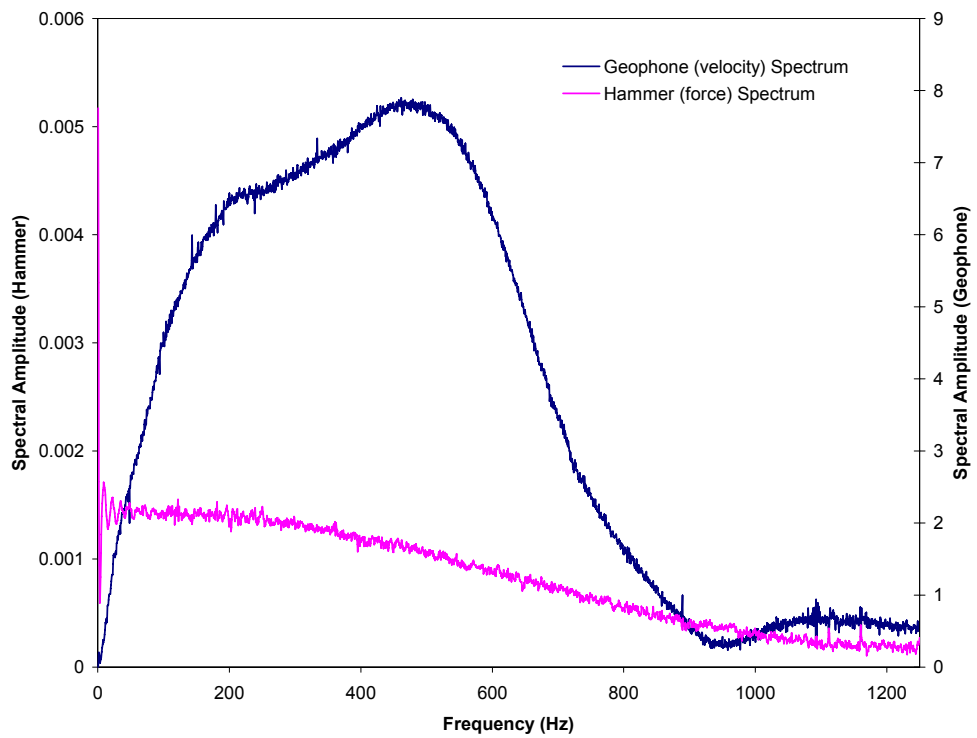


Figure A1- 4: Velocity and force spectra of acquired signals (2003)

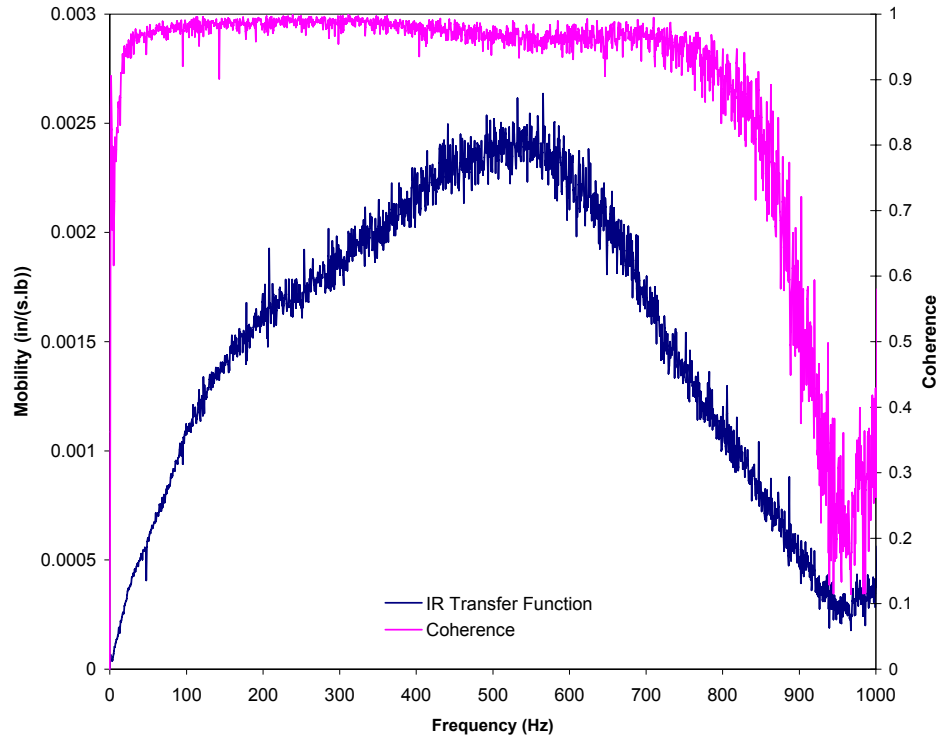


Figure A1- 5: Velocity and force spectra of acquired signals (2003)

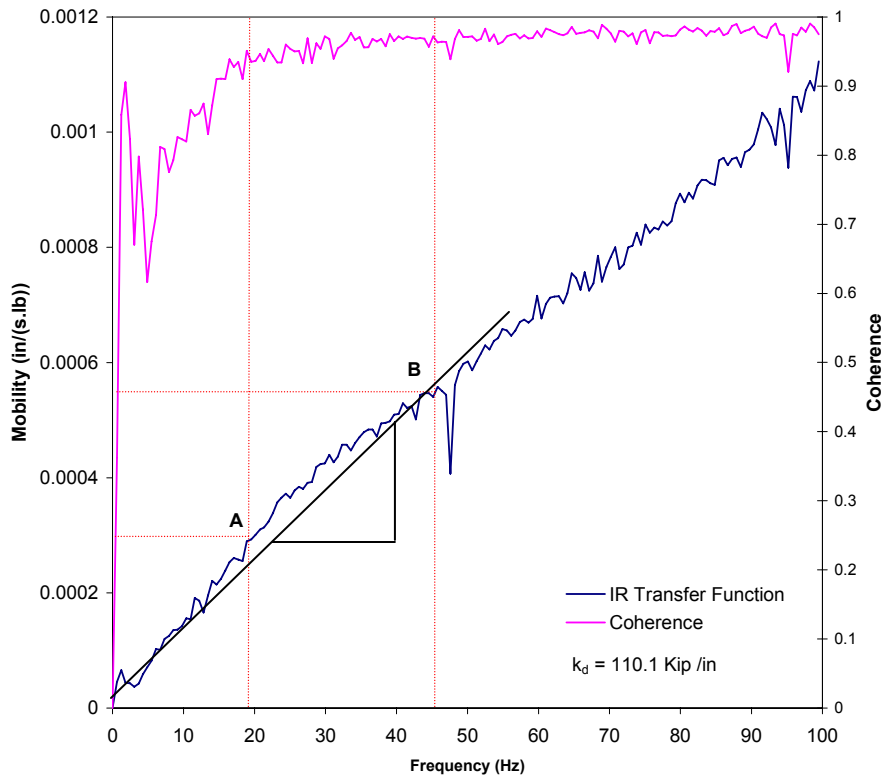


Figure A1- 6: Mobility response from 0Hz to 100 Hz

APPENDIX 2: Coefficient of determination of PCI based pavement performance Models

Usually r^2 is interpreted as the proportion of response variation "explained" by the regressors in the model. Thus, $r^2 = 1$ indicates that the fitted model explains all variability in y , while $r^2 = 0$ indicates no 'linear' relationship between the response variable and regressors. An r^2 value of 0.7 may be interpreted to indicate that approximately seventy percent of the variation in the response variable can be explained by the independent variable. The remaining thirty percent is attributed to the scatter, variability in the data.

In the current study Table 4-3 is taken to interpret the significance of the correlation. The criteria listed in the table however, are in some ways arbitrary and should not be observed too strictly. This is because the interpretation of r^2 depends on the context and purposes. A correlation of 0.9 may be very low if one is verifying a physical law using high-quality instruments, but may be regarded as very high in the social sciences where there may be a greater contribution from complicating factors.

During PCI, SASW and IR surveys a portion of the total area of GA airport pavements are inspected. In the case of PCI surveys, 20% of the runway pavements and 15% of the taxiway pavements are inspected. SASW tests were performed once in every section of the airport. In the case of IR tests, multiple tests were performed in every section. The performance models assume that the surveys performed are adequate to represent the pavements of the airport inspected. Pavements are complex systems. And therefore this assumption may affect the coefficient of determination of performance models developed from these surveys.

Table A2-1 presents r^2 values obtained by researchers for pavement performance models using PCI data.

A2- 1: Coefficient of Determination for pavement performance models using PCI data obtained by researchers

1. No.	2. Source	3. Pavement Type	4. r^2
1	OAC (Yuan and Mooney)	AC	0.48 – 0.83
2	OAC (Yuan and Mooney)	PCC	0.56 – 0.80
3	Florida DOT (Yang et al.)	AC	0.65
4	Florida DOT (Yang et al.)	PCC	0.72
5	Pennsylvania DOT (Chen et al.)	AC	0.30 – 0.71
6	Nevada DOT (Sebaaly et al.)	AC	0.48 – 0.83
7	South Korea (Suh et al)	PCC	0.53 – 0.76

Reference

Chen, X., Hudson, S., Cumberland, G., and E. Perrone, “*Pavement performance modeling program for Pennsylvania*”, Transportation Research Record 1508, Transportation Research Board, Washington, D.C., 1-8.

J. J. Lu, J. Yang, and M. Gunaratne, “*Pavement surface performance forecasting by neuron network models – an application to Florida highway network*”, Research Project Sponsored by FDOT, Tampa, Florida.

Sebaaly, P., Venukanthan, S., Siddharthan, R., Hand, A., and J. Epps, “*Development of pavement network optimization system (development of pavement performance analyses and procedures)*”, Research Report No. 1198-1, Nevada department of transportation, October, 2000

Suh, Y., Park, D., and K. Jeong, “*Development of deterioration prediction models for airfield rigid pavements*”, Transportation Research record 1788, Transportation Research Board, National Research Council, Washington D.C., 1988, pp. 132-137.

Yuan, J., and Mooney, M. A. (2003). “*Development of adaptive performance models for Oklahoma Airfield pavement management system*” Transportation Research Record 1853, Transportation Research Board, Washington, D.C., 44–54.